IDENTIFYING THE EFFECT OF IRON CHELATION ON HUMAN CD4+ T CELLS

Tewari, Damini

Awarding institution:
King's College London

KING'S College LONDON

University of London

IDENTIFYING THE EFFECT OF IRON CHELATION ON HUMAN CD4+ T CELLS

Damini Tewari

A thesis submitted to King's College London, University of London in part fulfillment of the requirements for the degree of Doctor of Philosophy

King's College London

April 2015

ABSTRACT

The importance of iron in physiological and metabolic pathways is well established in the literature. However, the literature is equally rife with studies highlighting the association of iron with cellular toxicities such as production of Reactive Oxygen Species and even the growth of intra-cellular pathogens. This study was based on the observation that in conditions of chronic inflammation, such as Rheumatoid Arthritis, cellular sequestration of iron leads to increased cell proliferation and tissue damage. The inability of the human body to physiologically excrete this excess iron highlights the need to develop a cheap yet effective iron chelator.

Results indicate that CP655, an HPO iron chelator, specifically targets human CD4+ T cells and causes significant inhibition of proliferation of the cells along with significantly inhibiting production of inflammatory cytokine such as IFN-γ and IL-17. A microarray conducted on stimulated human CD4+ T cells demonstrated that the genes most significantly modulated by iron chelation were those encoding for cell cycle regulators and inhibitors of DNA replication, hence preventing cell proliferation, as indicated by the *in-vitro* data. This was validated by cell cycle analysis. Finally, mechanistic experiments revealed that the chelator may be causing an up-regulation of the cell cycle inhibitor protein CDKN1A (p21) as one of its molecular mechanism of action.

Since the depletion of iron can cause dysregulation of several cellular pathways, some of the other potential mechanisms suggested in this study include the reduction in STAT5 phosphorylation following CP655 treatment and inhibition of T cell Receptor downstream signaling molecules.

In conclusion, this study demonstrates that intracellular iron has the ability to modulate CD4+ T cell responses and indicates that the use of novel iron chelators could prove to have therapeutic potential for RA and other diseases driven by excessive T cell proliferation.

ACKNOWLEDGEMENTS

This thesis represents the most important accomplishment of my career so far which would not have been accomplished without the help, guidance and encouragement of my supervisors, Dr. Helen Collins and Dr. Stephen Thompson. I am extremely grateful to them for providing me the opportunity to fulfil my dream and for their faith in my abilities. I would like to whole heartedly express my gratitude to them for all their patience, trust and support over the past few years.

I thank my committee members, Prof. Andrew Cope, Prof. Andrew McKie and Dr. Stuart Neil for their guidance. Thank you to my lab members specially Ahmad Gazali, Katie-Lloyd Jones and Frank Kaiser for constantly helping me learn and grow as a scientist. I would like to sincerely thank Dr. Susan John and Dr. David Cousins for their help and advice throughout this project.

I would also like to express my sincere gratitude to King's College London for funding my PhD and for providing me an excellent environment to hone my skills and personality,

Even though a few lines are not sufficient to express how I feel, I would like to thank my parents and my sister for letting me dream and helping my dreams come true. Their love and support has been my strength throughout the past few years. A special thank you to my grandfather, Prof. P.C.Gururani and grandmother, Indira Gururani. Last but not the least, I would like to thank my fiancé, Ankit Gaur, who has supported me, in every way possible, throughout these past few years. I owe everything I have achieved so far to these people.

DECLARATION

I declare that I have personally prepared this report and that the work described is my own unless otherwise stated. All sources of information have been acknowledged by means of references.

Damini Tewari

April 2015

TABLE OF CONTENTS

LIST OF FIGURES

LIST OF TABLES

LIST OF ABBREVIATIONS

$\cdot O_2$	Superoxide
µg/lt	microgram per litre
µl/lt	microlitre per litre
^3H	Tritiated Thymidine
ACD	Anaemia of Chronic Diseases
AI	Anaemia of Inflammation
ANAPC1	Anaphase Promoting Complex 1
ANOVA	Analysis of Variance
AP1	Activator Protein 1
APC	Antigen Presenting Cells
ASK1	Apoptosis-Signal Regulating Kinase1
BMP	Bone Morphogenetic Protein
BSA	Bovine Serum Albumin
CACNB4	Calcium Channel, Voltage-dependent, beta 4 subunit
CD	Cluster of Differentiation
CDC14A	Cell Division Cycle 14A
CDC25A	Cell Division Cycle 25A
CDC4A	Cell Division Cycle Associated Protein 4
CDC6	Cell Division Cycle 6
CDKN1A	Cyclin-Dependent Kinase Inhibitor 1A
Cdks	Cyclin-Dependent Kinases
cDNA	Complementary deoxyribonucleic Acid
CFSE	Carboxyfluorescein succinimidyl ester
CIA	Collagen-Induced Arthritis
CLSPN	Claspin
Con A	Concanavalin A
DCT1	Divalent Cation transporter 1
DFO	Desferoxamine
DFP	Deferiprone
DFX	Deferasirox
DI	De-Ionized

DLGAP5	Disks large-associated Protein 5
DMSO	Dimethyl Sulfoxide
DMT1	Divalent Metal transporter 1
DNA	Deoxyribonucleic Acid
dsDNA	double stranded DNA
ECL	Enhanced Chemiluminescent
ELISA	Enzyme- linked Immunosorbent Assay
EPO	Erythropoietin
FACS	Fluorescence activated cell sorting
FCS	Fetal calf serum
FDA	Food and Drug Association
Fe^{2+}	Ferrous iron
Fe^{3+}	Ferric iron
Fe-S	Iron-Sulphur clusters
GADD45G	Growth-Arrest and DNA Damage inducible Protein, Gamma
GAPDH	Glyceraldehyde 3-phosphate dehydrogenase
GINS3	GINS complex subunit 3
GINS4	GINS complex subunit 4
HCP1	Haem Carrier Protein 1
HFE	Human hemochromatosis protein
HIF 1α	Hypoxia-inducible Factor 1α
HJV	Haemojuvelin
HO	Haem Oxygenase
HPO	3-hydroxypyridine-4-one
HRP	Horseradish-peroxidase
IDA	Iron Deficiency Anaemia
IgG	Immunoglobulin G
IL( )	Interleukin
IRE	Iron Responsive Element
IREB2	Iron-responsive Element Binding Protein 2
IRP	Iron Regulatory Protein
IVT	in-vitro transcription
JAK	Janus Associated Kinase

JNK	c JUN N-terminal kinases
KIP	Kinase Inhibitor Proteins
LPS	Lipopolysachharide
LSM	Lymphocyte separation medium
MAPK	Mitogen-Activated Protein Kinase
mg/lt	milligram per litre
miRNAs	MicroRNAs
ml/lt	millitre per litre
mRNA	messenger RNA
MS	Multiple Sclerosis
NAA35	N(Alpha)-Acetyltransferase 35
NF-AT	Nuclear Factor of Activated T cells
NF-kB	Nuclear Factor kappa beta
NO	Nitric Oxide
NSAID	Non-Steroidal anti-inflammatory drugs
NTBI	Non-Transferrin bound iron
OH^-	Hydroxyl
ORC	Origin Recognition Complex
PAGE	Polyacrylamide Gel Electrophoresis
PBMC	Peripheral blood mononuclear cells
PBS	Phosphate buffered saline
PCA	Principal Component Analysis
PCNA	Proliferating Cell Nuclear Antigen
PFA	Paraformaldehyde
PI	Propidium Iodide
PMA	Phorbol 12-myristate 13-acetate
pRb	Retinoblastoma Protein
PVDF	Polyvinylidene Flouride
qRT-PCR	Quantitative Reverse Transcriptase – Polymerase Chain Reaction
RA	Rheumatoid Arthritis
RBC	Red blood cell
RC	Replication Complex
RNA	Ribonucleic Acid

ROS	Reactive Oxygen Species
RR	Ribonucleotide Reductase
RRM1	Ribonucleotide Reductase subunit M1
SDS	Sodium Dodecyl Sulphate
SLE	Systemic Lupus Erythematosus
SMAD	Sma- and Mad related
STAT3	Signal Transducer and Activator of Transcription 3
STAT5	Signal Transducer and Activator of Transcription 5
TCR	T cell Receptor
Tf	Transferrin
TGFB1	Transforming Growth Factor, beta 1
TfR	Transferrin Receptor
TMB	Tetramethylbenzidine
TNFAIP2	Tumour Necrosis Factor Alpha-inducible Protein 2
Trx	Theoredoxin
UTR	Untranslated region

CHAPTER 1

GENERAL INTRODUCTION

CHAPTER 1

INTRODUCTION

1.1 General Introduction: Iron in Biological Processes

Iron, the most abundant metal by mass in earth's crust, is also the most abundant metal within the human body. In adult humans, approximately 40mg/kg of body weight is represented by Iron (Lieu *et al,* 2001). Approximately 60-70% of the body iron is found within the circulating erythrocytes and around 10% can be found within iron-containing proteins such as Myoglobin in the muscles and cytochromes. The remaining 20-30% of body iron is stored within storage molecules such as Ferritins and Haemosiderins found in hepatocytes and reticuloendothelial macrophages (Conrad *et al,* 1999).

The most significant and highest turning-over pool of iron within the body is that of the Transferrin - bound iron even though it amounts to less than 1% of total body iron. On average, Transferrin - bound iron turns over 25mg of iron per day in healthy individuals. 80% of this iron is used up by erythroid cells for synthesising haemoglobin within the bone marrow (Conrad *et al,* 1999). The majority of iron that is required to fulfil the daily requirement for haemoglobin synthesis comes from the iron recycled from senescent Red Blood Cells (RBCs). These RBCs are phagocytosed by macrophages of the reticuloendothelial system and haem molecules are released into the circulation (May *et al,* 1995).

Several prominent studies have highlighted the crucial role played by iron in cellular processes such as DNA, RNA and protein synthesis, cell growth, differentiation and proliferation, cellular respiration and electron transport, amongst others (Andrews *et al*, 1999; Boldt, 1999; Conrad *et al*, 1999; Wessling-Resnick, 1999). The transcription of certain genes that affect cell cycling and differentiation is also controlled by the levels of cellular iron (Boldt, 1999). Three prominent genes that are involved in this process and

are known to be iron dependent are Protein-kinase C-β, Tartare-resistant acid phosphatase and p21. Additionally, several cellular enzymes which include, oxidases, catalases, ribonucleotide reductase and peroxidases require iron for their proper functioning. These enzymes are not only essential for the proper functioning of cellular processes but a dysregulation of these enzymes and proteins can lead to the development of several serious disorders such as cancers and neurodegenerative diseases (Ponka, 1999). However, despite the large amount of literature highlighting the significant impact that iron has on key body functions, the molecular mechanisms underlying these cellular processes are not well defined (Lieu *et al*, 2001).

The unique chemistry of iron is responsible for its important physiological role. As a result of its ability to exist in both Ferrous (Fe^{2+}) and Ferric (Fe^{3+}) oxidation states, iron can act as an electron donor as well as an electron acceptor. This characteristic of iron makes it capable of participating in the oxidation-reduction reaction known as the Fenton Reaction, depicted below (Wessling-Resnick, 1999).

$$Fe^{3+} + \cdot O_2^- \longrightarrow Fe^{2+} + O_2$$

$$Fe^{2+} + H_2O_2 \longrightarrow .OH + OH^-$$

Due to the ability of iron to produce free oxygen radicals, it can prove to be extremely toxic if levels are not carefully controlled within the cells (McCord, 1998). The hydroxyl (OH^-) and superoxide ($\cdot O_2$) radicals produced in the Fenton reaction can quickly react with several molecules in living cells leading to DNA damage, altered cell proliferation and improper synthesis of proteins, lipids.

Apart from the Fenton reaction, free iron can also react with unsaturated fatty acids and produce lipid hydroperoxidases to form alkoxyl and peroxyl radicals which can also result in cell death (Gerlach *et al*, 1994). This toxic role of iron has been postulated to be responsible for carcinogenesis, atherosclerosis and also neurodegenerative diseases such as Alzheimer's and

Parkinson's. In order to keep these potentially toxic effects of iron under control the body has developed several specialised mechanisms that include specific molecules for acquisition, transport and storage of iron that help to meet the body's cellular iron requirements, while reducing the chances of toxicity. The process of regulating iron uptake and metabolism takes place most actively within the proximal small intestine, although excretion of iron by the body also plays an important role in maintaining iron balance (Dexter *et al*, 1991; Connar *et al*, 1992; Jenner *et al*, 2003).

1.2 Iron Regulation and Storage

Due to the importance of iron in several diverse cellular functions, the transport, storage and utilization of iron needs to be carefully maintained, especially since excessive iron can lead to extensive damage. In humans, as well as in several mammalian cells, many of the molecules that are essential for iron metabolism are closely regulated by a feedback mechanism based on intracellular iron levels (Kuhn *et al*, 1996; Haile, 1999). These are the Iron Regulatory Proteins 1 and 2 (IRP 1 and IRP2). Under conditions of iron deficiency, the IRPs bind to special stem-loop like structures called the Iron Responsive Elements (IREs) in the mRNA of the target gene. The IRPs regulate the post-transcriptional expression of the target gene by increasing mRNA stability or inhibiting the translation of the genes that contain the IREs (Hentze *et al*, 2004).

IRP1 can be found in all types of mammalian tissue however is highly expressed in the liver, kidneys and intestines (Guo *et al*, 1995). IRP2 has more than 50% homology to IRP1 and binds to IREs with similar affinity to IRP1. Additionally, just as IRP1, IRP2 can also be found on all mammalian tissue, but is often more scarcely expressed that the IRP1 (Henderson *et al*, 1993). One of the main differences between the two proteins is that IRP2 is rapidly degraded under conditions of excessive iron (Pantopoulos *et al*, 1995). Studies have showed that mice lacking IRP1 have no abnormalities in iron metabolism, suggesting that IRP2 may be capable of compensating for

the loss of IRP1 (Rouault and Klausner, 1997). However, IRP2-/- mice show abnormal distribution of body iron stores, along with neurodegenerative diseases (LaVaute *et al*, 2001; Galy *et al*, 2005). Furthermore, mice lacking both forms of the protein, show embryonic lethality highlighting the importance of iron regulation for survival (Smith *et al*, 2006).

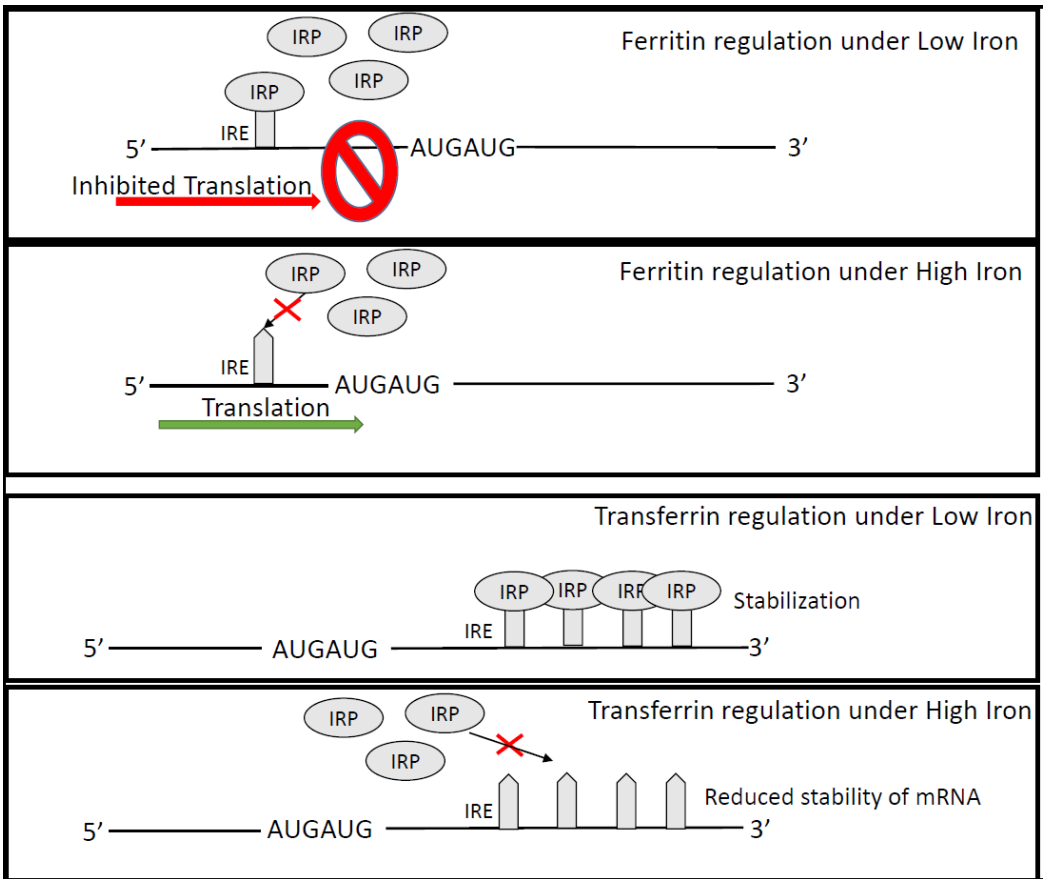

Figure 1.1: ***Post-transcriptional regulation of iron by Iron Regulatory Proteins and Iron Responsive Elements:*** Ferritin mRNA contains a single IRE in the 5' untranslated region whereas the Transferrin Receptor 1 mRNA contains 5 IREs in the 3' untranslated region. When intracellular iron levels are low, IRP binds to the IRE in the ferritin mRNA and prevents its translation. However, binding of IRP to the Transferrin Receptor 1 mRNA stabilizes the mRNA and increases synthesis. Contrary to this, under conditions of excess iron due to the absence of IRP and IRE binding Ferritin mRNA is efficiently translated and the translation of Transferrin receptor 1 is inhibited due to rapid degradation (Adapted from **Lieu *et al*, 2001).**

The sequence and structure of the IRE control the affinity and specificity with which the IRPs bind to these regions (Samaniego *et al*, 1994; Kim *et al*,

1995). Based on the location of the IRE within the mRNA sequence, these regions can either act as translational repressors or enhancers (Ponka *et al*, 1998). Genes such as the Ferritin light and heavy chains, iron exporter Ferroportin and mitochondrial aconitase have IREs in their 5' Untranslated region (UTR) whereas Transferrin receptor 1 and Nramp2 have IREs in their 3' UTR of their mRNA. Under conditions of iron deficiency, the binding of IRPs to the IREs within the 5' UTR of the mRNA sterically prevents the translation machinery from binding to the mRNA and hence inhibits the initiation of protein synthesis. However, when the IRPs bind to the IREs in the 3' UTR of the mRNA, it increases the stability of the mRNA and hence promotes translation and protein synthesis (Gray and Hentze, 1994; Muckenthaler *et al*, 1998a). On the other hand, when the concentration of intra-cellular iron is high, genes that have IREs in their 5' UTR get successfully translated whereas those with IREs in their 3' UTR are rapidly degraded due to unstable mRNA (Muckenthaler *et al*, 1998a) (Fig 1.1).

Another critical element that prevents free iron from producing reactive oxygen species and also forms the most important source of stored intracellular iron is the storage protein, Ferritin (Theil, 2003). It is made up of two subunits – a heavy chain and a light chain, that together form a protein shell that can store up to 4500 molecules of iron within it. As described above, Ferritin synthesis is induced when excessive iron is present and is suppressed in iron deficient conditions (Gdaniec *et al*, 1998; Ke *et al*, 1998). The synthesis of Ferritin is also controlled by inflammatory cytokine interleukin 1 (IL -1) in hepatic and endothelial cells. IL -1 causes a reduction in the levels of serum iron levels by increasing the synthesis of Ferritin. As a result of this mechanism, increased levels of Ferritin are often used as a diagnostic marker to help in detecting inflammation and other diseases (Gordeuk *et al*, 1992; Thomson *et al*, 1999).

1.3 Uptake of Dietary Iron

The main site for absorption of dietary iron is the small intestine. Iron from the diet is taken in from the brush border of the apical membrane and enters the circulation by passing though the basolateral membrane of the intestinal endothelial cells. Within the intestine, iron is present in both its oxidation states – that is as Fe^{2+} and Fe^{3+}. Most of the iron that is absorbed from the diet is in the form of Fe^{3+}, however due to the fact that it is insoluble at pH values of more than 3, Fe^{3+} is poorly absorbed by the intestine. On the other hand, Fe^{2+} is readily absorbed by intestinal endothelial cells. Hence, in order to facilitate the absorption of dietary iron Fe^{3+} must first be reduced to Fe^{2+} via the function of mucosal ferric reductase that are present in the apical membrane of the intestinal cells (Ekmekcioglu *et al*, 1996; Conrad *et al*, 1999)

1.3.1 Non-Haem iron uptake

The crypt cells of the duodenum and the jejunum in the small intestine are the main sites of haem as well as non-haem iron absorption. In order to enter the body circulation, the iron absorbed from the diet needs to successfully cross three cellular barriers – the apical membrane, translocate across the cytosol and lastly cross the basolateral membrane (Wood and Han, 1998). While in most cases, iron can enter the cell by Transferrin-receptor pathways, the cells in the apical membrane of the enterocytes lack the expression of transferrin receptors. As a result of this, the cells have to use different mechanisms in order to enter the cell cytosol (Pietrangelo *et al*, 1995). Therefore, the absorption of iron in these cells occurs via a specialist iron transporter known as the Divalent Cation transporter (DCT1, DMT1) also known as Nramp2 (Fleming *et al*, 1997).

Two isoforms of the protein are known to exist – Nramp2 isoform I and Nramp2 isoform II. The main difference between these 2 isoforms lies within the 3' UTR of their mRNA. In isoform I, this region contains an IRE, similar to that found in the 3' UTR of the transferrin mRNA. Isoform II, however, lacks this IRE region (Tandy *et al*, 2000). This suggests that in the condition

of iron deficiency, the expression of only isoform I of Nramp2 is increased leading to greater up take and absorption of iron, whereas isoform II is not affected (Fleet, 1998).

Nramp2 has been implicated in transporting not only ferrous iron but is also involved in the transport of several other divalent cations such as $Zn^{2+,}$ Mn^{2+}, Co^{2+}, Cu^{2+}, Ni^{2+} and Pb^{2+} (Gunshin *et al*, 1997). Nramp2 is found to be more highly expressed in the duodenum as compared to other tissues in of body. It is also found to be expressed at the sub-cellular level, within vesicles such as the late endosomes and lysosomes (Gruenheid *et al*, 1999; Tabuchi *et al*, 2000). This sub cellular localization of Nramp2 is consistent with that of Transferrin, suggesting that Nramp2 may play a role in transporting Transferrin - bound iron across endosomal membranes as well (Su *et al*, 1998).

1.3.2 Haem - iron uptake

The second type of mechanism for the uptake of iron involves the absorption of haem bound - iron, which can be more efficient than inorganic iron (Parmley *et al*, 1981). Once in the intestinal lumen, haemoglobin is enzymatically digested leading to the release of haem molecules, which can then be absorbed by the enterocytes via haem-receptor mediated internalization (Mills and Payne, 1995). Following internalization, the enzyme Haem Oxygenase (HO) degrades haem and releases the iron into the cell cytosol. This iron can now either be stored with Ferritin molecules or be transported across the membrane by the action of Ferroportin1 (Hentze *et al*, 2004; Steinbicker and Muckenthaler, 2013).

So far, the only mechanism via which iron can cross the basolateral membrane of enterocytes is through the iron exporter Ferroportin1. As with most of the protein involved in iron regulation, Ferroportin also contains an IRE in its 5' UTR (Donovan *et al*, 2000). It is found to be highly expressed in the tissues of the placenta, liver, spleen and kidneys (McKie *et al*, 2000). Also, the localization of Ferroportin1 to the basolateral membrane of

duodenal enterocytes strongly indicates its involvement in the export of iron from the enterocytes (McKie *et al*, 2000; Donovan *et al*, 2000).

The efflux of iron via Ferroportin is suggested to require auxiliary feroxidase activity. The membrane resident Feroxidase, Hephaestin, along with Ceruloplasmin, which is present in the serum, are believed to be important in the functioning of Ferroportin1 (McKie *et al*, 2000). Their activity is essential for the release of iron into the blood and for loading it on to Transferrin, but do not play a role in the transport of iron out of the enterocytes (Harris *et al*, 1998).

1.3.3 Regulation of absorbed dietary iron

The first line of regulation involves the 'Dietary regulation' mechanism under which the enterocytes exhibit a 'mucosal block' which make them resistant to absorbing any additional iron for a few days after iron has been consumed in the diet. The mucosal block is believed to result from the accumulation of intra-cellular iron after body iron requirements have been met (Andrews, 1999).

The second mechanism involved in regulating dietary iron absorption is based on sensing the body's stored iron levels, rather than just looking at the levels of dietary iron intake. This 'Store's regulation' mechanism is influenced by the extent to which plasma transferrin is saturated with iron. Finally, the third mechanism that can regulate the absorption of dietary iron is the 'Erythropoietic Regulation'. This mechanism modulates iron absorption based on the requirements for erythropoiesis (Finch, 1994; Lieu *et al*, 2001).

1.4 Regulation via Hepcidin

A specialised peptide hormone that recognizes and responds to all the regulatory cues discussed above, is Hepcidin, encoded by the HAMP gene. Hepcidin first received attention when it was identified in human urine and plasma samples due to its structural similarity with anti-microbial peptides, Defensins, which play an important role in host defence. The bioactive form of Hepcidin, which is a 25-amino acid peptide, is generated primarily by the hepatocytes but also in smaller quantities by other cell types such as Macrophages (Nemeth *et al*, 2006).

The role of Hepcidin in iron homeostasis has been demonstrated in studies that have used Hepcidin knockout mice, which exhibit signs of iron overload. Additionally, iron overloaded mice have also show increased Hepcidin mRNA expression (Nicolas *et al*, 2001; Pigeon *et al*, 2001). Conversely, Hepcidin levels decrease under conditions of iron deficiency and hypoxia. Therefore, Hepcidin acts as a negative regulator of iron absorption and transport across the cell. It acts via its ability to bind to the exclusive iron export channel on mammalian cells, that is, Ferroportin1. When the amount of extra-cellular iron is high, Hepcidin is synthesised and binds to Ferroportin1 causing its internalization and lysosomal degradation, resulting in accumulation of iron within the cells. Similarly, when cells require iron, Hepcidin production is suppressed leading to the export of iron from the macrophages via Ferroportin to make it available for binding to Transferrin (Nemeth *et al*, 2006).

Lee *et al* (2004) suggested that Hepcidin synthesis can also be initiated by the IL -6 pathway after lipopolysaccharide (LPS) stimulation. This elevated level of Hepcidin reduces the amount of iron leaving the enterocytes and macrophages, therefore decreasing the amount of serum iron that is available to invading pathogens and growing tumour cells. However, the increased level of Hepcidin is responsible for hypoferremia and the associated Anaemia of Chronic Diseases (ACD) (Vyoral and Petrak, 2005).

1.5 Transport of Iron

1.5.1 Transferrin-receptor mediated uptake

Apart from the absorption, storage and utilization of iron, transport of iron within the body is an important aspect of iron-metabolism, as it is an important mechanism for controlling and reducing excessive iron-related toxicities (Hoefkens *et al*, 1996). In the plasma, the role of iron transporter is played by the protein Transferrin, which has a high affinity for ferric iron. Although, Transferrin is known to be involved in the transport of several other metals as well, such as Aluminium, Manganese, Copper and Cadmium (Moos *et al*, 2000). But, of these Transferrin has the highest affinity for iron, which is capable of displacing other metals bound to Transferrin. Within the plasma, Transferrin can exist in several forms namely Apotransferrin (iron-free form), Mono-ferric Transferrin (bound to one molecule of iron) or Di-ferric Transferrin (bound to two molecules of iron). The extent to which each is present in the plasma depends on the concentration of iron and transferrin in the plasma. For cells to be able to absorb the iron from Transferrin, it first needs to bind to Transferrin receptors present on the cell membrane. Two distinct types of Transferrin receptors known are – TfR1 and TfR2 (Munoz *et al*, 2009; Anderson and Wang, 2011).

TfR1 is found to be expressed on the cell membrane of all cells apart from mature erythrocytes. TfR2, which is a homologue of TfR1, is expressed specifically in the liver and more so, on the cell membrane of hepatocytes. Once transferrin, is bound to the TfR, it is internalized via the classical endocytic pathway and iron is released once the complex is within acidic endosomal compartments. The iron that enters the cell, forms a part of the cellular labile iron pool. This is then used for the synthesis of iron containing proteins or is stored within Ferritin. Once free of iron, Transferrin and its receptor are recycled back to the cell surface (Dautry-Varsat *et al*, 1983; Gkouvatsos *et al*, 2011).

The expression of TfR1 is found to be higher on rapidly dividing cells, as compared to other non-dividing cells. Tumour and cancer cells can express up to 100,000 molecules of TfR1on their surface whereas, non-proliferating cells have a considerably lower expression of TfR1, with some cell types lacking it all together (Inoue *et al*, 1993). The link between cell proliferation and high expression of Transferrin can be traced back to the high requirement for iron by the DNA synthesising enzyme ribonucleotide reductase (RR) (Jordan and Reichard, 1998). Apart from tumour cells, TfR1 expression is high on erythroid cells that have a high need for iron in order to synthesise haemoglobin (Ponka and Lok, 1999). Other cell types such as placental cells, ensure transfer of sufficient iron from the mother to the foetus by expressing high levels of Transferrin receptor on their surface (Gambling *et al*, 2001) and similarly the brain's requirement for iron for its metabolic processes as well as repair and regeneration, is met by the high levels of transferrin-receptors present on its cells (Moos and Morgan, 2000).

1.5.2 Non-Transferrin bound Iron (NTBI)

As described above, the body has several ways of ensuring that once inside the body iron is absorbed, stored and transported safely in order to minimize any potential toxic effects. Transferrin plays an important role in making certain that there is no free iron in the blood by binding to it in order to assist its transport. However, despite all these mechanisms, there are some physiological conditions under which free iron or non-Transferrin bound iron (NTBI) is found in the blood. This is common in iron overload disorders such as Haemochromatosis. NTBI is generated when the Transferrin in the blood has been completely saturated and through increased release of haem iron from catabolised haemoglobin (Beutler *et al*, 2003).

This NTBI has been associated with excessive iron loading in tissues as well as the generation of Reactive Oxygen Species (ROS), causing cell damage and cell death. Hepatocytes are known to readily take up NTBI from the blood stream and store it within a transient pool of low-molecular weight

iron. This uptake of NTBI by the liver continues even under conditions of iron overload as no mechanisms exist for NTBI regulation. The low molecular weight iron stored in the iron pools within the hepatocytes is more prone to produce ROS via the Fenton reaction (Richardson and Ponka, 1997).

The transport of NTBI is an elusive mechanism. It has been suggested that NTBI is transported to tissue by Transferrin-independent mechanisms. DMT1 has been implicated to be the main transporter for NTBI within the liver. The Zinc transporter Zip 14 and L-type voltage dependent calcium channels within the cardiomyocytes are also responsible for considerable amounts of NTBI uptake (Oudit *et al*, 2003; Gunshin *et al*, 2005; Liuzzi *et al*, 2006). The pools of NTBI are known to be readily chelatable and iron chelating compounds have been successful in reducing the amount of NTBI in the body and reducing its toxic effects (Reviewed in Gkouvatsos *et al*, 2011).

1.6 Disorders of Iron Transport and Metabolism

Due to its essential, but potentially toxic nature, the regulation of iron within the human body is very tightly controlled. However, at times a dysregulation in this system occurs which results in several serious disorders in humans (Munoz *et al*, 2011).

1.6.1 Iron Deficiency Anaemia (IDA)

Under healthy physiological conditions, iron absorption, transport and storage are closely balanced. However factors such as increased requirement, limited supply or blood loss can often upset this balance causing iron deficiency. The deficiency results from either the body iron stores getting depleted, or from the inability of the body to mobilize its iron stores. The physical manifestations of iron deficiency are linked to the general symptoms of anaemia which include pale colour of the skin, tiredness and an overall lack of energy and decreased work performance. The clinical symptoms of IDA include low haemoglobin, low levels of Transferrin saturation and low

Ferritin concentrations. This condition is often associated with cases where the dietary intake of iron is insufficient in meeting the demands of the body. Hence is common in children, who have a higher need for iron as compared to adults. It is also common in menstruating women due to the regular loss of blood from the body (Reviewed in Munoz *et al*, 2011).

The treatments currently being commonly used in conditions of IDA include replenishment of body iron by external supplementation. This includes oral administration of iron salts, often given complexed with sulphates to increase their absorption. Severe cases of IDA are treated with intravenous injections of Iron Dextran. The intra-venous supplementation helps the iron to be processed and loaded onto Transferrin quicker and therefore reducing the chances of any associated toxicity (Beard, 2001).

1.6.2 Anaemia of Chronic Disease (ACD)

Anaemia, apart from being a common symptom of iron deficiency, can also be a common complication in chronic inflammatory disorders such as Rheumatoid Arthritis, Cancer and Inflammatory Bowel Disorder (Munoz *et al*, 2011a). This type of iron metabolism disorder is known as Anaemia of Chronic Disease or Anaemia of Inflammation (AI). The clinical symptoms can often be similar to that of IDA such as low haemoglobin levels, low Transferrin saturation but high serum Ferritin concentration. Additionally, these symptoms are manifested in the presence of chronic inflammation (Beard, 2001; Munoz *et al*, 2011a,b).

Anaemia under chronic inflammation occurs due to the underlying over-activation of the immune system. The changes in iron homeostasis, proliferation of erythroid progenitor cells, life span of RBCs and Erythropoietin (EPO) production, all of which result in the development of Anaemia are caused by the cells and cytokines of the reticuloendothelial system. The disturbance of iron homeostasis is reflected by the retention and increased uptake of iron by the cells of the reticuloendothelial system. Instead

of being in the circulation, iron is diverted into the storage sites within these cells leading to limited availability of iron for erythropoiesis (Weiss and Goodnough, 2005).

Under conditions of chronic inflammation, there are two prominent pathways by which macrophages acquire iron. Firstly, by the process of phagocytosing senescent RBCs and secondly, via the transmembrane iron importer DMT1. Inflammatory stimulants such as LPS and cytokines such as IFN -γ and TNF -α have been shown to cause an upregulation in the expression of DMT1, leading to the increased uptake of iron by the macrophages. Secondly, these stimuli are also responsible for causing the downregulation of the iron exporter, Ferroportin, from the cells leading to the retention of iron within the macrophages (Andrews, 1999; Ludwiczek *et al*, 2003).

Hepcidin also plays an important role in the development of ACD. LPS and the inflammatory cytokine, IL -6 are known to stimulate the production of Hepcidin. Once IL -6 binds to its receptor, the complex further binds to glycoprotein 130, which activates the downstream signalling pathway causing Signal Transducer and Activator of Transcription 3 (STAT3) to bind to the regulatory region of the Hepcidin gene promoter. Another pathway for induction of Hepcidin, is via the regulator Haemojuvelin (HJV). HJV is an iron-specific ligand which binds to the Bone Morphogenetic Protein receptors (BMP). The interaction of the HJV and BMP receptors leads to the transcription of a group of specific proteins known as the Sma- and Mad related (SMAD) proteins. Binding of HJV to BMP, first induces SMAD4 which then further regulates SMAD 1, 5 and 8 (Babitt *et al*, 2006). The complexity of the pathway is further increased due to the involvement of another important protein, Human haemochromatosis protein (HFE). Along with TfR1 and TfR2, HFE protein plays a role in sensing the level of holotransferrin in the plasma. When iron content in the plasma is high, TfR1 binds with a stronger affinity to holotransferrin, due to which HFE binds to TfR2. This binding activates the BMP-SMAD signalling pathway and the synthesis of Hepcidin (Mollbrink *et al*, 2011; Pietrangelo *et al*, 2011).

Hepcidin controls the level of plasma iron by binding to the iron export channel Ferroportin, on the basal membrane of enterocytes and macrophages, causing its internalization and degradation. This prevents any iron from being exported out and thus accumulates within the cells (Weiss and Goodnough, 2005).

Apart from the accumulation of iron within the cells of the reticuloendothelial system, the signals provided by inflammatory cytokines are responsible for the impaired proliferation of erythroid progenitor cells. Interferon – α, β and γ cause the cytokine mediated apoptosis of these cells and also have a more direct toxic effect on the progenitor cells due to their ability to generate free radicals such as Nitric Oxide (NO) (Maciejewski *et al*, 1995).

The anaemia that results from chronic inflammation is responsible for the blunted responses of Erythropoietin. Inflammatory cytokine, IL -1, has been implicated in inhibiting Erythropoietin expression by its ability to produce ROS that damages Erythropoietin-producing cells (Jelkmann, 1998). Finally, inflammation is responsible for reducing the half-life of erythrocytes by increased phagocytosis by circulating macrophages (Gasche *et al*, 2004).

Hence, the above described mechanism makes it evident that there is a close relationship between inflammation, inflammatory stimuli and iron homeostasis within the body.

1.7 Iron, Immunity and Inflammation

Anaemia of Chronic Disease serves as one of the best examples to visualize the relationship between Iron homeostasis, Immunity and Inflammation (Weiss and Goodnough, 2005).

Under normal physiological conditions, 95% of the body's need of iron, for erythropoiesis and other biological functions, is met by iron recycling by the macrophages (Hentze *et al*, 2010). However, inflammatory conditions lead to alteration of this process. Inflammatory cytokines and acute phase proteins affect the body iron homeostasis and macrophage iron metabolism leading to low levels of circulating iron and high levels of iron accumulated within storage proteins, Ferritin (Thomas and Thomas, 2005).

As discussed above, cytokines such as IL -1, IL -6, IL -22 as well as bacterial LPS, which are produced during autoimmune diseases such as cancer or infectious conditions, have been shown to induce the expression of Hepcidin (Nemeth *et al*, 2003). As a result of this, the export of iron into the circulation along with the absorption of iron from the diet is reduced. Furthermore, IL -6 and LPS stimulate macrophages to produce small amounts of Hepcidin that act in an autocrine manner to reduce iron egress. All of these mechanisms function as an immune strategy to restrict the availability of iron to extracellular pathogens (Theurl *et al*, 2009).

In addition to this, inflammatory cytokines have a Hepcidin - independent influence on iron homeostasis within the body (Weiss and Schett, 2013). TNF -α, IL -1, IL -6 and IFN -γ increase the uptake of transferrin bound and non-transferrin bound iron in the macrophage via their effect on the expression of Transferrin receptor and DMT1, further adding to the retention of iron within the macrophages (Ludwiczek *et al*, 2003). IFN -γ and LPS can directly influence Ferroportin expression inhibiting the export of iron from the macrophages (Yang *et al*, 2002). These effects have been attributed to the effect of Reactive Oxygen Species (ROS) and Reactive Nitrogen Species (RNS). The tissue damage that is caused due the production of ROS and RNS is responsible for anaemia of inflammation that limits the amount of iron in

the blood serum and increases the amount of intracellular stored iron. The accumulation of iron along with increase in ROS and RNS production that lead to more production of labile iron, further fuelling the vicious cycle of more ROS/RNS (Lehmann et al, 2015). Hence, the body has several mechanisms to control the levels of circulating iron, especially under conditions of infection and inflammation. While this is an important strategy to control the growth of extra-cellular pathogens, it can have harmful effects in certain other conditions. Olakanmi *et al* (2002) showed that *Mycobacterium tuberculosis* grew more slowly in patients with Hereditary Haemochromatosis as their macrophages showed lesser accumulation of iron, suggesting that iron-loaded macrophages play an important part in the growth of certain bacteria. Retention of iron within the macrophages, therefore impairs their ability to fight intra-cellular pathogens such as various bacteria, viruses and fungi via its inhibition of IFN -γ mediated and other anti-microbial effector pathways (Weiss, 2002b; Oexle *et a*l, 2003).

Parallel to this, iron has several positive effects on immune effector functions, such as differentiation and proliferation of immune cells such as antigen presenting cells and lymphocytes (Cairo *et al*, 2011). Therefore, since iron is used by pathogens to survive within the body and also used by the host to mount an effective immune response – the host must be able to effectively sequester iron from the pathogens while still being able to provide enough iron so as not to limit the responses of the immune system (Hershko, 1996).

1.7.1 Effect of Iron and Iron deficiency on Immunity

While few studies report otherwise, most experimental and clinical data suggests that iron deficiency negatively impacts immunity leading to increased risk of infection. It has been suggested that experimental iron deficiency can limit almost every immune effector response. It has been shown to be important for proper cell differentiation and growth, as a critical part of several enzymes that are needed for the functioning of immune cells, and also plays a part in production of several cytokines (Hershko, 1996). Iron

deficiency can impact non-specific immunity by reducing bactericidal activity of macrophages, reducing neutrophil activity by inhibiting the activity of the iron-containing enzyme Myeloperoxidase that plays an important part in intracellular pathogen killing (Spear and Sherman, 1993). Iron deficiency has also been shown to inhibit T lymphocyte blastogenesis and mitogenesis as well as have an effect on decreasing the number of T lymphocytes overall (Kuvibidila *et al*, 1999).

This effect of iron deficiency on the functioning of the immune system can be explained by several possible explanations. Firstly, due to its essential and rate limiting role in the cell proliferation process via the enzyme Ribonucleotide reductase. Secondly, not only cell proliferation but even differentiation of Th1 cells and B cells is under the control of iron homeostasis (Gasche *et al*, 2004). Lastly, Galan *et al* (1992) showed that iron deficiency can result in reduced IL -2 production from activated lymphocytes, which is an essential cytokine for cell proliferation and differentiation.

Iron has been implicated in the several immune related disorders, as a result of which iron chelation can be used as a potential therapy for several of these disorders. Accumulation of iron within the body has been implicated in the pathogenesis of atherosclerosis via its ability to cause vascular oxidative stress as well as initiating the inflammatory immune response (Yuan and Li, 2008). Studies in the past have shown that atherosclerotic lesions are often associated with high levels of iron. Additionally, use of DFO has been successful in delaying the onset of these lesions by reducing oxidative stress markers (Ishizaka *et al*, 2005; Ren *et al*, 2006).

An interesting, but not often discussed effect of iron on health includes its effect on obesity. Iron has the ability to contribute towards obesity by stimulating and activating adipocytes. DFO has once again been successful in reducing adiposity by reducing oxidative stress related signalling (Tajima *et al*, 2012).

Furthermore, iron has also been implicated in certain autoimmune diseases. Studies on mouse models of Systemic Lupus Erythematosus (SLE) show that iron supplementation leads to increased severity of renal disease and an increased rate of mortality. One of the reasons behind this effect could be the ability of iron to produce ROS leading to oxidative stress and damage under inflammatory conditions (Leiter *et al*, 1995). It has also been shown that iron has the ability to uniquely fragment auto-antigens such as in the case of Scleroderma, and often exposes cryptic epitopes in the periphery as seen in Goodpasture's Syndrome and Diabetes Mellitus I. This has been suggested to be responsible for the pathogenesis of autoimmunity (Casciola-Rosen *et al*, 1997; Kalluri *et al*, 2000). In the case of Diabetes, iron can result in the death of pancreatic beta cells via the oxidative stress due to uptake of non-transferrin bound iron (Masuda *et al*, 2014). Furthermore, the iron transporter NRAMP1 has been associated with several autoimmune diseases such as Rheumatoid Arthritis (RA), Juvenile RA, Multiple Sclerosis (MS) and Diabetes. Certain alleles in the NRAMP1 promoter are associated with increased susceptibility to both infectious diseases such as Tuberculosis, as well as autoimmune diseases such as RA (Bowlus, 2003).

Finally, one of the main role that iron plays is binding of oxygen via Haemoglobin, which implies that the level of oxygen in tissue depends on the amount of iron that is available. Therefore, reduced oxygen content leads to increase in erythropoiesis, similarly, reduced iron results in hypoxia like conditions. Use of iron chelators such as DFO has been shown to result in hypoxic conditions, even under physiological normoxia, by inducing the Hypoxia inducible factor (HIF) 1α. DFO has been shown to bring about stabilization and increased transcription of HIF 1α (Triantafyllou *et al*, 2007). Peyssonnaux *et al* (2007) showed that iron deficient mice have increased expression of HIF 1α. Additionally, they also showed that HIF 1α and hypoxia result in reduced Hepcidin gene expression as well, suggesting a connection between HIF and iron metabolism. Hypoxia is also responsible for apoptosis via the activation of the tumour suppressor p53, that regulates several genes involved in growth arrest and apoptosis (Suzuki *et al*, 2001).

1.7.2 Iron and T Lymphocytes

While iron is important for all cell types, it is particularly important for metabolically active and proliferating cells such as thymocytes and activated T lymphocytes. Studies on T cells illustrate the relationship between the need for iron and cell proliferation. The presence of transferrin receptor on the cell surface is recognized as a marker for cell activation, as resting T cells lack transferrin receptor expression. Initiation of cell division is accompanied by an increase in the expression of transferrin receptor on the surface of T cells (Kuvibidila *et al*, 1983; Bowlus, 2003).

Of the several immunological functions affected by iron deficiency, cell-mediated immunity is one of those most notably affected. It shows a reduction in the number of circulating T lymphocytes along with a reduction in the blastogenic response to mitogens. This reduction in T cells has been attributed to thymic Atrophy. Several studies on rodent models have shown that iron deficiency leads to thymic atrophy and significantly reduces the number of circulating peripheral T cells. Alternatively, the effect of iron overload on immune functions and T cells is not well characterised and relatively controversial. While some studies suggest increase in the number of circulating CD8+ T cells, others have shown blunted T cell responses after iron overload, decreased CD4+ T cell and CD4/CD8 T cell ratios (Kuvibidila *et al*, 1990; Kuvibidila *et al*, 2001).

1.8 Cell Cycle and the Role of Iron

The role of iron as an essential nutrient has been well established. It forms a part of several enzymes and proteins involved in cell growth and replication, a common example being ribonucleotide reductase (RR) (Lieu *et al*, 2001). The enzyme is responsible for conversion of ribonucleotides to deoxyribonucleotides. One of the two sub-units that make up the RR enzyme contains four non-haem iron molecules. In cases where there is not a constant supply of iron to this second sub-unit, a loss in function of RR is seen. Iron molecules help to stabilize the tyrosyl radical that is present at the core of the second sub-unit and hence are critical for the functioning of the enzyme and therefore also in the process of DNA synthesis and cell replication (Jong *et al*, 1998; Kayyali *et al*, 2001).

Several studies over the past few years have indicated that depletion of cellular iron can result in inhibition of cell cycle progression, cell growth and division. A block at various stages of the cell cycle has also been demonstrated as a result of iron deprivation. Also, removal of iron from cells has been shown to have significant anti-tumour activity. Previously, some studies have shown the involvement of iron transport and regulatory proteins to be involved in the cell cycle. Kawabata *et al* (1999) showed that while TfR1 is regulated by intracellular iron levels, TfR2 is regulated as a function of the cell cycle. They showed that TfR2 is expressed highly in the late G1 phase of the cycle but is completely lacking in the G0/G1 phase of the cell cycle. Also, the expression of TfR1 has been shown to be increased several fold during the S phase of the cell cycle. This increase has been attributed to the high need for iron by RR during the synthesis of DNA (Nyholm *et al*, 1993; Yu *et al*, 2007). A study by Sanchez *et al* (2006) proved the presence of an IRE in the 3' UTR of a cell cycle protein, Cell Division Cycle 14A (CDC14A). This further attested the involvement of iron within the regulation of the cell cycle. Despite the knowledge that iron plays a very important role in the cell cycle, little is known on how it can be regulated by iron. Hence it is evident that the study of the cell cycle and the role of iron in its regulation merits our attention. The following section will discuss the cell

cycle, specifically focussing on the role played by iron in its progression and regulation.

1.8.1 Overview of the mammalian cell cycle

Several studies have demonstrated that deprivation of iron could prevent the proliferation of cells by arresting them in specific phases of the cell cycle and halting its progression (Le and Richardson, 2002; Fu and Richardson, 2007; Yu *et al*, 2007; Gharagozloo *et al*, 2008). The success of iron deprivation as a potential therapeutic mechanism for the control of tumour and neoplastic growths further emphasizes the important role played by iron in the cell cycle. A typical cell will go through four different phases of the cell cycle. Gap1 or G1 Phase, where the cell begins to prepare of DNA synthesis. This is followed by the S Phase, where the synthesis of DNA takes place. The Gap2 or G2 phase sees the cell preparing for cell division. And finally, the Mitosis or M Phase where the cell division takes place (Fig 1.5) (Black and Black, 2013).

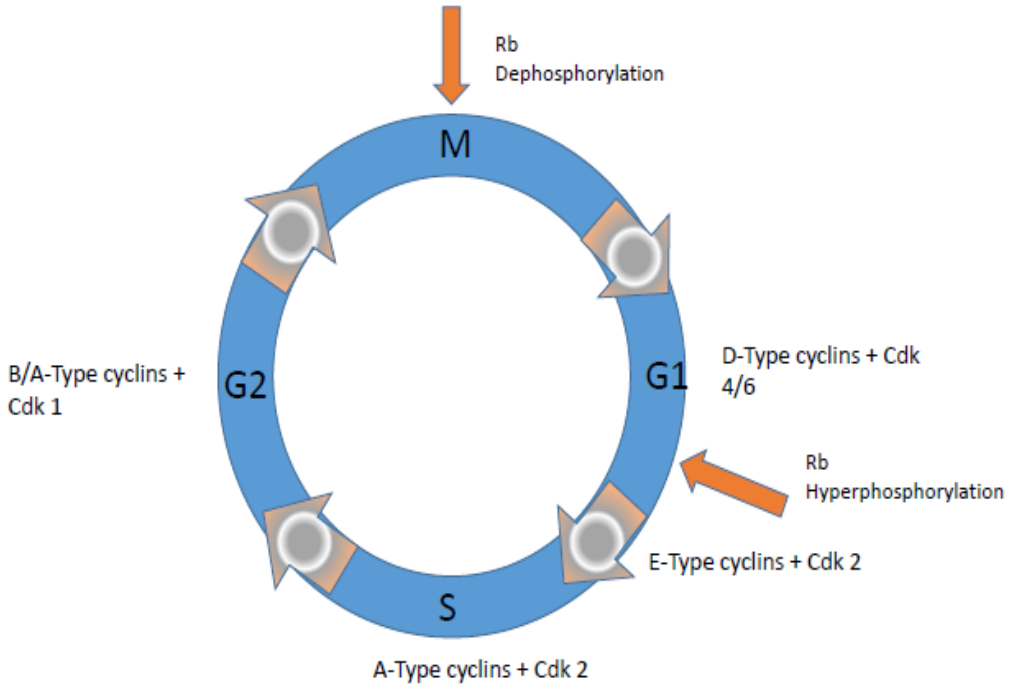

Figure 1.5: ***The various stages of the cell cycle controlled by the interaction of different cyclin-cdk complexes*** **(Adapted from Le and Richardson, 2002)**

The transition of a cell from these four stages of the cell cycle is tightly regulated and controlled by specific cell cycle proteins, cyclins, which are believed to be positive regulators of the cell cycle. Different types of cyclins are known to regulate different stages of the cell cycle. The main role of cyclins is to function as regulatory sub-units for the Cyclin-Dependent Kinases (cdks), a family of serine/threonine kinases. Progression through each phase of the cell cycle is controlled by the activity of specific cyclin-cdk partner complexes. Entry and transition through the G1 phase of the cell cycle is controlled by D type cyclins. Three kinds of D type cyclins are known, cyclin D1, D2 and D3. Each of these is found in varying degrees in different tissues and in order to become active they need to complex with cdk4/cdk6. Movement through the late stages of G1 and entry into the S phase is controlled by cyclin E and cdk2 complexes. Transition through the S phase requires cyclin A and cdk2 complexes to be actively present. Cyclin A and cdk1 complexes are also important in the transition through the S phase,

but are implicated more strongly in the movement from the end stages of S phase and the entry into the G2 phase. The final two phases of the cell cycle, that is the progression through the G2 and M phase, is governed by cyclin B/A and cdk1 complexes (Liu *et al*, 2012).

The expression of these critical molecules is however controlled by the level of intracellular iron. Experimental studies have shown that deprivation of iron from neoplastic cells as well as normal T lymphocytes reduces the expression of cyclin D as well as cyclin A from these cells. A more prominent reduction is seen in the expression of the three D-type cyclins as compared to the effect seen on both A and B type cyclins (Kulp *et al*, 1996; Black and Black, 2013). The mechanism behind the reduction in the level of cyclin D1 has been identified to be by proteasomal degradation of the protein, as no changes in the mRNA expression of cyclin D1 have been noticed under conditions of iron deprivation. Unlike normal ubiquitin-dependent degradation of the cyclin, the degradation in this case is induced by an Ubiquitin – independent mechanism. Further, the involvement of iron in this reduction has been confirmed via experiments where under iron-replete conditions the reductions in cyclin D1 can be reversed. Therefore, under conditions of iron deprivation, the reduction in cyclin D1 results in the G1/S phase arrest of the cells. The regulation at this restriction point is important as in the S phase the cell has a greater need for iron in order to allow for RR enzyme to be able to synthesise DNA. The excessive expression of cyclin D1 leads to over-activation of the cell cycle and releases the cells from the normal control of the G1/S phase restriction point, and thus acts as an oncogene. The control of cyclin D1, especially by iron deprivation, is a potential therapeutic anti-tumour mechanism. Apart from cyclin D, iron deprivation has a direct effect on the reduction of cdk2 and cdk4, further resulting in the G1/S phase arrest of the cell cycle progression (Golias *et al*, 2004).

Another cyclin that is modulated by the levels of intracellular iron is cyclin E. However, unlike the above described cyclins, cyclin E expression is increased under conditions of iron deprivation. This increase in expression is

believed to be an attempt from the cell to continue the progression of the cell cycle and push the cell into S Phase. However, cyclin E needs to complex with cdk2 to be activated, but due to the reductions in cdk2 levels under iron-deplete conditions the increase in cyclin E is unable to overcome the G1/S phase block (Chaston *et al*, 2003).

Iron deprivation is usually seen to result in a G1/S phase block of the cell cycle. However, in certain cell types and experimental conditions a block in G2/M phase has also been seen. This can be attributed to the reductions in the level of cdk1, along with changes in cyclin A/B levels, after iron deprivation (Reed, 1997; Golias *et al*, 2004).

An important role played by the cdks in the regulation of the cell cycle is the phosphorylation of the Retinoblastoma Protein (pRb). This molecule is involved in assisting the cell to transit from the G1 phase to the S phase of the cell cycle (Sherr, 2000). pRb and the pocket proteins that are associated with it, namely p107 and p130, serve as the main targets of the cyclin D-cdk4 complex (Cobrinik, 2005). Under normal conditions of the hypophosphorylated state, the pocket proteins p107 and p130 act as transcriptional repressors by binding to E2F transcription factor on the promoter region of the growth genes. These proteins are responsible for actively blocking the transcription of the genes that are required for DNA synthesis and cell cycle progression. Phosphorylation of these pocket proteins drives the expression of E2F-dependent genes such as cyclin E which are essential for the continuation of the cell cycle. In the initial stages of the G1 phase, the cell requires a mitogenic signal in order to promote the phosphorylation of pRb and the transcription of cyclin E and other cell cycle genes (DeGregori *et al*, 1995). However, over time, when sufficient amounts of cyclin E have been produced and accumulated, it is capable of driving its own production. At this point, the cell is ready to exit the G1 phase check point and proceed to the next phase of the cell cycle. In contrast, if mitogenic signal is lost before sufficient amounts of cyclin E have been accumulated to drive their own expression, the cell is unable to cross the first check point and the cell cycle is halted and cell goes into a quiescent stage or G0 stage (Sherr,

2000; Classon and Dyson, 2001). Since the Cyclin– cdk complexes during the G1/S phase are required for the phosphorylation of pRb, reduction caused by iron in the level of these cyclins and cdk is also responsible for the hypophosphorylation of pRb further leading to the inhibition at the G1/S phase (Gao and Richardson, 2001). The hypophosphorylated pRb prevents the release of the transcription factor E2F1, which is essential for the transcription of other cell cycle progression genes such as Cyclin A and E (Muller and Helin, 2000).

1.8.2 Cell Cycle Regulation

One of the most important regulators of the cell cycle that has several molecular targets and is an important player in the G1/S restriction point is p53. The p53 protein is activated under conditions of cellular stress and DNA damage and functions by either triggering DNA repair mechanisms or apoptotic pathways (Yu *et al*, 2007).

Under conditions of iron deprivation, levels of p53 are increased post-transcriptionally. That is, the level of p53 is increased only at the protein level and no changes in mRNA level have been studied. There are 4 distinct mechanisms that control the activation of the p53 pathway in response to reduced intracellular iron levels. Firstly, the increase in the level of p53 protein is believed to be the main factor leading to activation of the DNA damage pathway. Secondly, the decrease in iron levels is believed to be responsible for converting dormant p53 into its active DNA-binding form. Following this, an increase in the phosphorylation of p53 has been witnessed in response to iron deprivation. This phosphorylation helps to stabilize the protein and prevent its proteasomal degradation. Finally, increase in other transcriptional molecules, such as Hypoxia-Inducible Factor 1α (HIF 1α), have also been implicated in the increased activation of the p53 pathway after iron deprivation (Fukuchi *et al*, 1997; Ashcroft *et al*, 2000; Liang and Richardson, 2003).

Furthermore, apart from its role in activation of the p53 pathway, iron deprivation has also been shown to have an important effect of the downstream targets of p53, such as $p21^{CIP1/WAF1}$.

Control and regulation of the activity of cyclin– cdk complexes, that are essential for the progression of the cell cycle, is carefully monitored by specific proteins belonging to two families of cdk inhibitors (CKI). These two inhibitor families are the INK4 inhibitors and the Kinase Inhibitor Proteins, CIP/KIP.

The CIP/KIP family of inhibitory proteins consists of three main members, namely $p21^{WAF1/CIP1}$, $p27^{KIP1}$ and $p57^{KIP2}$. These proteins are best known for their negative regulation of the cell cycle. These molecules are capable of preventing the progression of the cell cycle via their ability to directly bind to the cyclin– cdk complexes and thereby inhibiting their activity.

$p21^{CIP1/WAF1}$ is an important cdk inhibitor of the CIP/KIP family that plays an essential role in the regulation and control of the cell cycle and is present in low levels throughout the different stages of the cell cycle. It is usually induced as a consequence of cellular stress and DNA damage via a p53-dependent pathway, but it can also be induced via a p53-independent pathway using other transcription factors such as AP-2 (Wajapeyee *et al*, 2003; Yu *et al*, 2007). At low expression levels, p21 acts as a promoter of the cell cycle and is required for the assembly of the cyclin D/cdk complexes that help in G1/S phase transition. However paradoxically, when p21 expression is increased it acts as a potent inhibitor of the cell cycle (Weiss, 2003). High levels of p21 are responsible for binding to cyclin E - cdk2 complexes and therefore interfering with the phosphorylation of pRb, thereby halting the cell cycle progression. Additionally, at high levels p21 also acts on transcriptional factors such as E2F1 and c-myc to regulate cell cycle, and has also been shown to inhibit DNA replication (Luo *et al*, 1995; Kitaura *et al*, 2000, Yu *et al*, 2007).

Similar to p53, the expression of p21 mRNA and protein levels is controversial under conditions of iron depletion. Several studies have

demonstrated that p21 mRNA levels are increased in response to low levels of intracellular iron. However, protein expression of p21 is reduced under the low iron conditions due to ubiquitin-independent proteasomal degradation of the protein along with low levels of nuclear translocation of p21 mRNA into the cytosol. The inhibition of p21 protein expression is an important mechanism for keeping its anti-apoptotic properties under control and hence is a novel anti-tumour target (Fu and Richardson, 2007).

$p27^{KIP1}$ is a potent cdk inhibitor, that is regulated by body iron levels. It controls the progression of the cell cycle by modulating cyclin– cdk binding affinities by phosphorylation of the other KIP inhibitors, making them inactive (Wang *et al*, 2000; Wang *et al*, 2004). Unlike its other CIP/KIP family members, p27 mRNA and protein levels are both up-regulated on exposure to iron-deplete conditions (Wang *et al*, 2000). Increase in p27 protein is responsible for inhibition of the cyclin D– cdk4/6 complex formation and therefore blocking the cell cycle in the G1/S restriction point (Cheng *et al*, 1999). The de-phosphorylation of p27 which is responsible for causing the cell cycle block has been suggested to be caused due to a cell cycle molecule known as CDC14A. The 3'UTR of the mRNA of CDC14A has an IRE that binds to IRP to control its expression levels. Under iron deprivation, the transcription of CDC14A mRNA is increased, which has the ability to dephosphorylate p27 as well as cyclin E therefore restricting the cell in the G1 phase (Kaiser *et al*, 2002; Sanchez *et al*, 2006).

However, the regulation by CIP/KIP proteins is not limited to their inhibitory properties. Several studies have been able to show that CIP/KIP proteins are in fact, an essential component along with the cyclin D – cdk4/6 complexes ensuring the progression of the G1 phase of the cell cycle (Blain *et al*, 1997; Cheng *et al*, 1999; Alt *et al*, 2001). It has been demonstrated that the CIP/KIP molecules play a role in the assembly, nuclear accumulation and stabilization of the cyclin– cdk complexes. Furthermore, p21 and p27 are also believed to play a part in the hyperphosphorylation of pRb in the presence of cyclin E – cdk2 complex during mid-G1 phase of the cell cycle (LaBaer *et al*, 1997).

The second family of cdk inhibitors that regulate the cell cycle is the INK4 proteins, which include $p15^{INK4B}$, $p16^{INK4A}$, $p18^{INK4C}$ and $p19^{INK4D}$. The inhibitory effects of these molecules has been found to be limited to only cdk4 and cdk6 molecules, and hence their main role is restricted to arresting the cell in the G1/S phase of the cell cycle (Ruas *et al*, 1998).

In addition to the different molecules and mechanisms described above there are several others mechanisms of cell cycle regulation that are affected in response to modulation of intra-cellular iron levels. Figure 1.6 summarises some of the main mechanisms, including those discussed above, by which iron depletion can influence normal cell cycle (Yu *et al*, 2007).

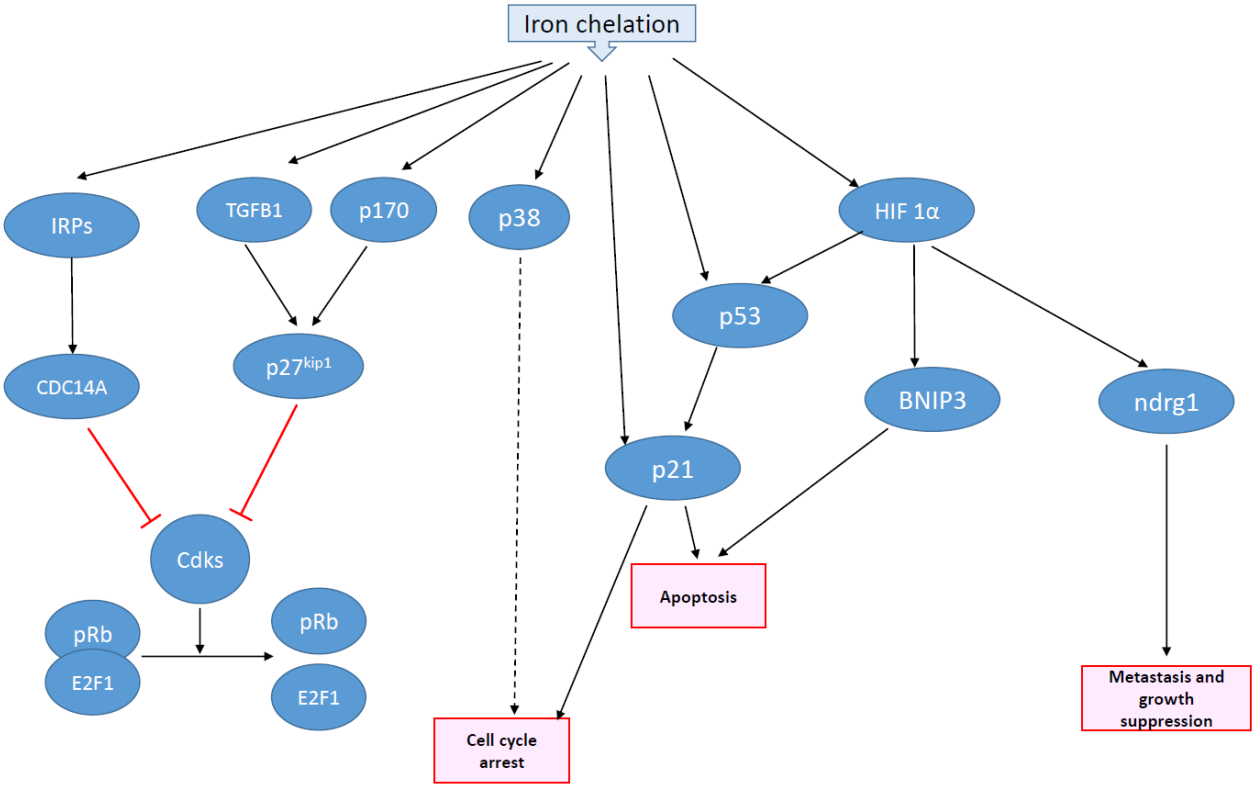

Figure 1.6: ***Effects of iron deprivation on the cell cycle:*** Iron deprivation can cause cell cycle arrest, apoptosis as well as suppression of cell growth and metastasis by increasing IRP activity, upregulating TGFB1 signalling leading to inhibition of cdks via KIP1, activating p38 MAPK, activating inhibitors such as p53 and p21 and finally stimulating the HIF-1α pathway. (Adapted from Yu *et al*, 2007).

1.9 Iron Chelation

The damage caused by excessive iron accumulation to the heart, liver and other organs of the human body is well established. The inability of the human body to physiologically excrete iron highlights the need to develop a cheap yet effective iron chelator, which can bind and eliminate excess iron from the circulation (Siddique and Kowdley, 2012).

Development of parenterally administrable iron chelators such as DFO was predominantly to treat patients with severe chronic anaemias, β-thalassemia and sickle-cell disease. These individuals are given regular blood transfusions which eventually leads to transfusional siderosis. Since phlebotomy is not an option for these patients, iron chelators were developed to reduce the iron overload. Currently, iron chelation as a therapy is being used extensively in patients with thalassaemia major as well as sickle cell anaemia (Kontoghiorghes *et al,* 2000; Flaten *et al,* 2012). Chelators are also a common form of therapy for Hereditary Haemochromatosis, however, their long term use is often limited due to the associated toxicities (Kontoghiorghes *et al,* 2005).

With the tremendous advancements in latest technology to quantify tissue and body iron levels, there has been a more specific and targeted approach towards the use of iron chelating compounds for treating disorders of iron metabolism (Kalinowski and Richardson, 2005). From being restricted to iron-overload disorders such as Hereditary Haemochromatosis, iron chelation as a therapy is now being used in a myriad of disorders such as Rheumatoid Arthritis (Blake *et al*, 1985), Cancer and tumorogenesis (Becton and Roberts, 1989), malaria (Gordeuk *et al*, 1992) and its use is even being studied in AIDS/HIV research (Sappey *et al*, 1995; Richardson, 1999). Especially over the last decade, iron chelation as a therapy has undergone drastic changes. Until very recently, Desferrioxamine (DFO) was the only clinically approved iron chelator for humans, but now within the last 10 years, the US Food and Drug Authority (FDA) has approved two new iron chelators – Deferasirox (DFX) and Deferiprone (DFP) for human use. Apart from these, several other novel chelators are currently being tested in different stages of clinical trials

and will be available for clinical use in the upcoming years. This heightened interest in iron chelation highlights the great potential it offers as a new form of therapy for a range of disorders (Richardson, 1999).

Table 1.1, adapted from from Poggiali *et al* (2012), provides a comparison between the three licensed iron chelators and CP655

Property	Deferoxamine	Deferiprone	Deferasirox	CP655
Stoichiometry	Hexadentate (1:1)	Bidentate (3:1)	Tridentate (2:1)	Bidentate (3:1)
Route	Subcutaneous, intravenous	Oral or solution	Tablets for oral suspension	Orally active
Usual Dose	20-40 mg/kg/day over 8-24 hours, 5 days a week	75-100 mg/kg/day in 3 doses daily	20 - 40 mg/kg/day	Not tested
Excretion	Urinary, Faecal	Mainly urinary	Faecal	Unknown
Half-life	20-30mins	3-4 hours	8-16 hours	Unknown
Adverse effects	Local Skin Reaction Ophthalmological Auditory Allergic reactions Growth retardation Bone abnormalities Pulmonary (at high doses) Neurological (at high doses)	Gastrointestinal Agranulocytosis/neutropenia Arthralgia Elevated liver enzymes	Gastrointestinal Rash Rise in creatinine Proteinuria Ophthalmological Auditory Elevated liver enzymes	Unknown Use in mouse models of Collagen-Induced Arthritis (CIA) do not show any adverse effects on total iron levels, anaemia or weight loss (Lloyd-Jones and Collins, unpublished data)
Challenges	Adherence to parenteral administration; need for yearly ophthalmology and auditory examination	Need for weekly blood count monitoring; not commercially available in all countries; limited data in children; variable efficacy in removal of hepatic iron.	Cost, especially at higher doses; gastrointestinal side effects may limit dosing; Need for monthly monitoring of creatinine, transaminases; bilirubin, complete blood count for renal or hepatic failure and/or gastrointestinal haemorrhage	Orally active, hence can reduce challenges associated with administration and adherence; high permeability allows for small doses thus reducing cost
Status	Licensed	Licensed in USA and Europe	Licensed in USA and Europe	Not licensed

Indications	Treatment of chronic iron overload due to transfusion-dependent anaemias (and for treatment of acute iron intoxication)	Treatment of iron overload in thalassemia major when DFO is contraindicated or inadequate	USA - Treatment of chronic iron overload due to transfusion-dependent anaemias in individuals aged 2 years and older Europe - Treatment of transfusional iron overload in beta-thalassaemia major patient, 6 years and older, and approved for use when DFO is inadequate or contraindicated in patients with other anaemias, patients 2-5 years, and patients with non-transfusion-dependent thalassaemia	Could be used for treatment of diseases showing excessive T cell proliferation, neurological disorders, cancers and transplantation

Table 1.1: Overview of Iron Chelators (Poggiali *et al*, 2012)

1.9.1 Desferrioxamine (DFO)

DFO was the first chelator to be approved for human use and has been in use for the last 40 years (Sheth, 2014).

DFO is a bacterial siderophore obtained from *Streptomyces pilosus*. Structurally, it is made up of one molecule of acetic acid, two molecule of succinic acid and three molecules of 1-amino-5hydroxylamino-pentane. It has a molecular weight of 597Da, which is heavier in comparison to several of the novel iron chelators under trial and development (Fig 1.7). It is a hexadentate molecule that can bind one molecule of Fe^{3+} in a stable conformation (Keberle, 1964, Kalinowski and Richardson, 2005).

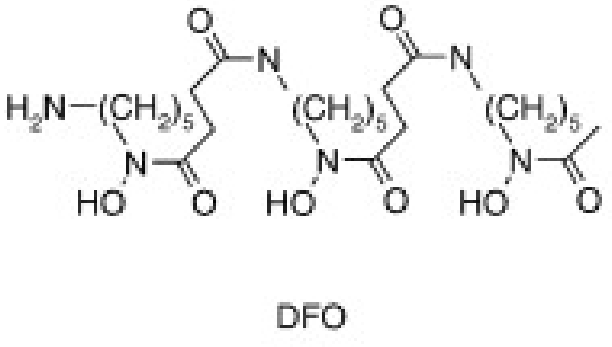

Figure 1.7: Structure of DFO (Kalinowski and Richardson, 2005)

Although DFO has a higher specificity for Fe^{3+} than any other metal ion, it is still capable of binding to ions such as Cu^{2+}, Zn^{2+}, Co^{2+} and Al^{2+}. Apart from not being specific to Iron, there are certain disadvantages and drawbacks associated with the use of DFO. Its high molecular weight and hydrophilic nature reduces its cellular permeability, as a result of which is enters the cell more slowly than its novel counterparts. Additionally, DFO as well as its iron-complexed form, have a net positive charge. This limits the ability of these compounds to get freely distributed within the cell and DFO gets restricted to the cell cytosol, hence highlighting the need to develop new iron chelators for clinical use (Hoyes *et al*, 1993).

Several clinical trials have attested the effectiveness of DFO as a therapeutic approach towards treating iron-overload disorders and improving survival. However, there have been several reports of toxic side effects that cannot be ignored. Due to the poor absorption of DFO by the body, it cannot be administered orally and hence has to be given to patients parenterally. Furthermore, since DFO is rapidly excreted from the body, prolonged infusion of the drug is needed in order to elicit the desired therapeutic effect. This prolonged and cumbersome method of administration, limits compliance in patients. All these effects along with the high cost of the drug make it impractical to use to several parts of the developing world, where it is needed the most (Blake *et al*, 1985; Brittenham, 1992; Kalpatthi *et al*, 2010; Algren, 2010; Poggiali *et al*, 2012).

In addition to the above drawbacks relating to the administration and absorption of the DFO, the drug by itself has been linked to severe biological side effects. A trial conducted by Blake *et al* (1985) used DFO to treat patients with Rheumatoid Arthritis. While some improvements in the clinical assessment of the patients were seen with regards to their RA, the trial had to be halted due to potentially serious cerebral and ocular toxicities. These were linked due to DFO binding to metals ions, specifically copper, in addition to Fe^{3+} and due to the ability of DFO to produce Nitric oxide free radicals.

All of these factors, highlight the need to develop more specific and orally active iron chelators to succeed DFO.

1.9.2 HPO Family chelators

The 3-hydroxypyridine-4-one (HPO) family is a bidentate iron chelator group known for its high affinity, selectivity and specificity to intracellular iron (III) (Fakih *et al*, 2009). These compounds have relatively lower molecular weights as compared to many of the previously used iron chelators. Additionally, the presence of a neutral charge in both iron-free and iron complexed forms, provides them the ability to easily cross cellular membranes. This helps them to distribute more evenly and freely within the intra-cellular compartments (Hoyes *et al*, 1992). As a result of these properties of HPO chelators, they are considered to be one of the main candidates for the development of orally active iron chelators (Ma *et al*, 2004). Another advantage of the HPO iron chelators is their ability to be used as chemosensors to determine the labile iron pool. Most of the existing methods to determine the distribution of labile iron were unsuitable to be used for living cells as they perturbed the nature and extent of the pool. Hence over the last few years, HPO iron chelators have been used to measure this chelatable iron pool within lymphocytes by making use of fluorescent probes (Fakih *et al*, 2009). The fluorescent probes are attached to HPO

chelators, which retain their iron binding capacity, and the fluorescent probes in turn undergo quenching when the compound interacts with intracellular iron. The fluorescence of the probe is increased under low/reduced iron conditions, whereas the fluorescence is decreased in the presence of excessive intracellular iron (Ma *et al*, 2007). Amongst the several different kinds of iron chelators, *7-diethylamino-N-((5-hydroxy-6-methyl-4-oxo-1,4-dihydropyridin-3-yl)methyl)-N-methyl-2-oxo-chromen-3-carboxamide (CP655)* is considered to be the most sensitive to intracellular iron levels.

After generation of the HPO chelating moiety, the fluorescence is added by coupling the compound to an activated Coumarin acid. By itself, Coumarin, is not a fluorescent compound however addition of electron donating substituents result in enhancing its fluorescence intensity. Also, in comparison to previously used fluorescent dyes such as Calcein and Fluorescein, these novel probes are more selective sensors for iron (III). Furthermore, in contrast to Calcein, these Coumarin labeled probes are not prone to oxidative damage even in the presence of ferrous labile iron (Ma *et al*, 2006).

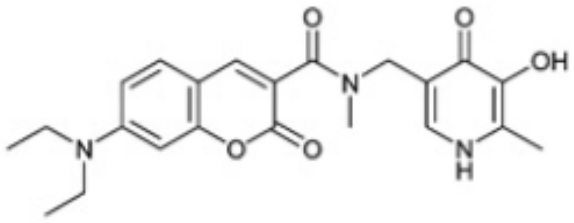

CP655

Figure 1.8: Structure of CP655 (Ma *et al*, 2006)

In the process of synthesis of CP655, the last step involves the removal of a protective methyl group by treatment with BCl_3 (Ma *et al*, 2006). The presence of the protective methyl group renders the compound incapable of binding with iron, and hence can function as a fluorescent non-chelator. Due to its structural similarity but opposite effect to CP655, this compound has been used as a control compound in the experimental set-ups.

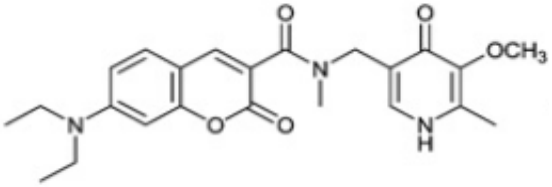

Figure 1.9: Structure of Methylated CP655 (CP655OMe) (Adapted from Ma *et al*, 2006)

1.10 Hypothesis, Aims and Objectives

Having highlighted the essential, yet potentially toxic, role played by iron within the human body it is evident that iron metabolism must be very carefully regulated. With several diseases resulting due to the iron-overload conditions, iron chelators have been the therapy of choice for several years. However, with only a handful of chelators approved for human use, there is need to develop new iron chelators with higher efficiency and reduced toxicities and side effects.

The hypothesis for this study was based on Evans et al (2009) who showed that synovial fluid and synovial membrane monocytes from patients with RA were capable of skewing the phenotype of CD4+ T cells cultured with them, by causing them to produce increased amounts of IL-17 and IFN γ as compared to CD 4+ T cells cultured with peripheral blood monocytes. It is well established in the literature that synovial fluid and synovial membrane monocytes of RA patients, those showing signs of Anaemia of Chronic Disease, have increased accumulation of iron suggesting that this excessive iron accumulation could be responsible for inflammation. Therefore, based on this, it was hypothesised that the use of iron chelators could reduce the inflammatory response shown by monocytes and the CD4 + T cells.

The main aim of this study was:

1. To test the effect of a novel class of HPO iron chelators on reducing inflammatory cytokine production and proliferation of primary human cells.

2. Establish the mechanism behind their action.

In order to achieve this, the main objectives of the study are detailed below:

1. To test the panel of different iron chelators to determine the most suitable iron chelator for use in humans.

2. To identify the main target cell for the chelator and to assess associated toxicities

3. To conduct micro-array analysis in order to isolate specific pathways being targeted by the chelator
4. To confirm results of the micro-array by RT-PCR and Western Blots
5. To establish mechanisms of action of the chelator

CHAPTER 2

MATERIALS AND METHODS

CHAPTER 2

MATERIALS AND METHODS

2.1 Peripheral blood mononuclear cell isolation

Blood samples of 60mls were routinely obtained from healthy volunteers after obtaining ethical approval and also obtaining consent from each of the donors. A list of all donors used along with age, gender and ethnicity has been provided in Table 2.1. Peripheral blood mononuclear cells (PBMCs) were isolated by density gradient centrifugation using Lymphocyte separation medium (LSM, PAA Austria). Blood was diluted 1:1 with sterile Dulbecco's PBS (PAA, Austria) and 30mls of diluted blood was layered on top of 15mls of Lymphocyte Separating Medium. The tubes were centrifuged at 800 x*g* for 20 minutes, with no brake. The buffy layer, which contains the mononuclear cells, is found at the interphase of the plasma and the LSM due to its density. The mononuclear cell layer was aspirated using Pasteur pipettes and diluted 1:1 with PBS. The cell suspension was centrifuged twice at 300 x*g* for 10 minutes at 4°C to remove any remaining LSM, plasma or platelets. The mononuclear cells were counted and then used for CD4+ and CD14+ isolation.

Donor		Age	Gender	Ethnicity
1		48	F	Caucasian
2		52	M	Caucasian
3		52	F	Asian
4		30	M	Asian
5		40	F	Caucasian
6		40	M	Caucasian
7		32	M	Caucasian
8		28	F	Caucasian
9		32	F	Caucasian
10		32	F	Caucasian
11		23	F	Asian
12		23	F	Asian
13		22	F	Asian
14		27	M	Caucasian
15		29	M	Caucasian
16		30	F	Asian
17		31	M	Caucasian
18		31	M	Asian
19		27	M	Asian
20		27	F	Caucasian
21		30	M	Caucasian
22		30	F	Caucasian
23		28	F	Caucasian
24		36	F	Hispanic
25		32	F	African
26		34	M	Caucasian
27		35	F	Caucasian
28		27	F	Asian
29		28	F	Caucasian
30		42	M	Caucasian
31		60	F	Caucasian
32		24	M	Asian
33		22	F	Caucasian
34		29	M	Caucasian

Table 2.1: Demographics of blood donors used throughout study

2.1.1 CD14+ cell isolation from peripheral blood mononuclear cells

CD14+ cells were positively selected using LS isolation columns (Miltenyi Biotec). $1x10^7$ PBMCs were resuspended in 1ml of cold MACS buffer (Recipe in Appendix) and 10µl of CD14 microbeads (Miltenyi Biotec) were added per 10^7 cells. The reagents were scaled up or down according to the number of PBMCs obtained. The cells were resuspended by pipetting several times and incubated at 4°C for 15 minutes, following which, 10mls of cold MACS buffer was added to the cell suspension, and centrifuged at 300 x*g* for 10 minutes at 4°C. During this time, the LS column was placed in the magnetic field by attaching it to the MACS separators. The columns were prepared by adding 3mls of cold MACS buffer and allowed to drip through. Once the cells were pelleted, they were resuspended in 500µl of cold MACS buffer and added to the LS column. The cells dripping through the column were depleted of CD14+ cells, which were retained in the column. The columns were washed three times with 3mls of MACS buffer while still attached to the magnetic separator. This CD14- fraction was used for isolation of CD4+ cells. Purity of the cells were assessed for each experiment and only isolations where purity was greater than 90% were used for experimental procedures.

The CD14+ cells were eluted by first removing the column from the magnetic separator and then plunging 5mls of MACS buffer to flush out the CD14+ cells. The cells were counted and diluted to the required concentrations with RPMI 1640 (GIBCO, New Zealand) supplemented with 2mM L-Glutamine (Lonza, Belgium), 100units/ml of Penicillin + 0.1mg/ml Streptomycin (Lonza, Belgium) and 10% FCS (GIBCO, UK).

2.1.2 CD4+ cell isolation from CD14- cell fraction

CD4+ cells were negatively isolated from the CD14- cell fraction using LD columns and CD4+ T cell isolation kit (Miltenyi Biotec). CD14- cells were centrifuged at 300 x*g* for 10 minutes and the pellet resuspended in 40µl of cold MACS buffer and 10µl of CD4+ T cell biotin-antibody cocktail per 10^7 cells and incubated at 4°C for 10 minutes. Following this, 30µl of cold

MACS buffer and 20µl of CD4+ T cell microbead cocktail (Miltenyi Biotec) was added per 10^7 cells. Cells were mixed well and incubated for a further 15 minutes at 4°C. Cells were washed with 10mls of cold MACS buffer. The LD column was placed in the magnetic separator and prepared by washing with 3mls of MACS buffer. The labelled cell pellet was resuspended in 500µl of MACS buffer and applied to the column and then washed again with 3mls of MACS buffer. The flow-through unlabelled cells were collected as the enriched CD4+ T cells. Cells were counted and diluted to the required concentration with RPMI 1640 (GIBCO, New Zealand) supplemented with 2mM L-Glutamine (Lonza, Belgium), 100 units/ml of Penicillin + 0.1mg/ml Streptomycin (Lonza, Belgium) and 10% FCS (GIBCO, UK).

2.2 *In vitro* stimulation of primary human CD4+ T cells

$0.5x10^6$ CD14+ cell and $1.0x10^6$ CD4+ cells were cocultured in 1ml RPMI 1640 (GIBCO, New Zealand) supplemented with 2mM L-Glutamine (Lonza, Belgium), 100units/ml of Penicillin + 0.1mg/ml Streptomycin (Lonza, Belgium) and 10% FCS (GIBCO, UK) in 48-well tissue culture plates, in a ratio of 1:2. For some of the experiments, cell cultures were stimulated with Tetanus Toxoid (kindly provided by Dr. L. Taams, KCL) in either the presence or absence of the chelator CP655 (5µM) or the control CP655OMe (5µM) (All chelators kindly provided by Prof. R. Hider, KCL). Cells were incubated at 37°C, 5% CO_2 in a humidified atmosphere, for six days. Following this, the cells were stimulated with 750 ng/ml Ionomycin (SIGMA-Aldrich, Poole, UK) and 50ng/ml PMA (SIGMA-Aldrich, Poole, UK) for four hours, supernatants were harvested and used to measure cytokines by ELISA. The above protocol was adopted from Walter *et al*, 2013 where double stimulation with PMA and Ionomycin was used to measure cytokine production from cultured CD4+ and CD14+ cells.

Alternatively, in some experiments CD14+ cells and CD4+ cells were incubated separately overnight either with or without CP655 at 37°C, 5% CO_2 in a humidified atmosphere. The following day, they were washed with

RPMI (supplemented as above) to remove the chelator and the cells were cocultured in different combinations in the absence or presence Tetanus Toxoid and further incubated at 37°C for six days. Following this, cells were stimulated with 750ng/ml Ionomycin and 50ng/ml PMA for four hours after which supernatants were harvested and cytokines measured by ELISA.

For experiments conducted specifically on CD4+ T cells, purified 1 x 10^6 CD4+ T cells were cultured in 1ml RPMI 1640 (GIBCO, New Zealand) supplemented as above in 48-well tissue culture plates. Cells were stimulated with anti-CD3/CD28 beads (Invitrogen, UK) in a ratio of 1:20 (Bead: CD4+ T cells) and treated with or without iron chelator CP655 (5µM) or control compound CP655OMe (5µM) for various time points ranging from 18 hours to six days post treatment.

Routinely for all of the experiments, 100µl of cells from each culture condition were transferred onto a U-bottom plate (VWR, Lutterworth, UK) and incubated with tritiated thymidine for measuring proliferation as described below (Section 2.5.1). Carboxyfluorescein succinimidyl ester (CFSE) staining was used to assess cell proliferation in some experiments as described below (Section 2.5.2).

2.3 Culturing Jurkat cells

The human T lymphocyte cell line, Jurkat (kindly provided by Dr. Susan John, KCL), were used for analysing cell cycle and molecular studies such as Western blots. 10 x 10^6 cells were resuspended in 10mls of RPMI 1640 (GIBCO, New Zealand) supplemented with 2mM L-Glutamine (Lonza, Belgium), 100 units/ml of Penicillin + 0.1mg/ml Streptomycin (Lonza, Belgium) and 10% FCS (GIBCO, UK). Cells were centrifuged at 300 *x*g for 10 minutes and the pellet was resuspended in 15mls of RPMI (as supplemented above) and seeded into 75cm^2 tissue culture flasks. Cells were maintained at 37°C in a 5% CO_2 humidified incubator. Cells were split into

three flasks 2-3 times a week. At the time of experimentation, cells were pelleted and counted before the desired cell density was used.

2.4 Supernatant ELISA

Cytokines were measured using Human ELISA Ready-Set-Go kits (eBioscience, San Diego, USA).

96-well NUNC Immunosorb plates (Maxisorp immunoplates, NUNC, Denmark) were coated with 100µl of pre-titrated capture antibody diluted 1/250 using coating buffer (10x PBS ELISA coating buffer, eBioscience, San Diego, USA). Plates were incubated overnight at 4°C. Plates were washed, 5 times, with ELISA wash buffer (PBS + 0.05% Tween-20) and blotted on absorbent paper before use. One part 5X assay diluent (eBioscience, San Diego, USA) was diluted with 4 parts of De-Ionized (DI) water and plates were blocked with 200µl of 1x Assay diluent and incubated for 1 hour at room temperature. After washing 5 times, the standard curve was set up using recombinant human cytokines (eBioscience, San Diego, USA). Starting concentration of the standard was 500pg/ml and serial doubling dilutions were made in 1x Assay diluent. 100µl of the sample supernatants were added, in triplicates, to the respective wells. The plate was incubated for 2 hours at room temperature before again being washed 5 times with ELISA wash buffer. The biotin labelled pre-titrated detection antibody was diluted 1/250 with 1x assay diluents, and 100µl of the solution was added to the wells and incubated for 1 hour at room temperature. The plates were washed 5 times with ELISA wash buffer. Detection enzyme, Avidin-HRP (eBioscience, San Diego, USA) was diluted 1/250 with 1x Assay diluent and 100µl was added to the wells and plate incubated for 30 minutes at room temperature. Plates were washed 7 times with wash buffer and 100µl of the Substrate, Tetramethylbenzidine (TMB) solution was added to the wells. Once the reaction was fully developed, 50µl of 2N H_2SO_4 was used to stop the reaction. Plates were read on MRX II ELISA plate reader (Dynex Technologies) at 450nm. The sensitivity of the ELISA kits was 4pg/ml.

2.5 Proliferation Assays

2.5.1 ^{3}H Thymidine Proliferation assay

100µl of cultured cells were transferred to 96 well U-bottomed plates (VWR, Lutterworth, UK) and pulsed with 0.5µCi/well of ^{3}H Thymidine and incubated for 24 hours at 37°C, 5% CO_2. The plates were harvested using a Tomtec harvester and the glass fibre filter mats (PerkinElmer, MA, USA) were left to dry for at least 24 hours. The filter mats were treated with liquid scintillation fluid (Scintillant-Beta plate scint, Wallac) and then counted using a Wallac Scintillation counter to measure proliferation.

2.5.2 CFSE incorporation Proliferation assay

1 x 10^6 CD4+ cells were resuspended in PBS and stained with 5µM Carboxyfluorescein succinimidyl ester (CFSE) (Sigma-Aldrich, UK), by incubating for 5 minutes in the dark at room temperature. The cells were then washed twice with PBS containing 10% FCS by centrifuging at 300 x*g* for 10 minutes at 4°C. The cell pellet was finally resuspended in RPMI media and cultured as above. Routinely, 10,000 cells were acquired and CFSE incorporation was analysed on the FL1 channel on the FACS calibur (Becton Dickinson) using CellQuest software and the data was analysed using the FlowJo software.

2.6 Cell Cycle Analysis

After 24, 48 and 72 hours of culture with or without anti-CD3/CD28 beads in the presence of absence of either the iron chelator CP655 (5µM) or control compound CP655OMe (5µM), 2 x 10^6 cells were lysed with 3mls of cold absolute ethanol for at least one hour at 4°C. Cells were washed with cold PBS before staining with 50µg/ml Propidium Iodide (PI) (Sigma, Catalogue number: P4864) and 0.1mg/ml Ribonuclease A (Sigma-Aldrich, UK) in PBS for 20 minutes at 37°C, 5% CO_2 in a humidified atmosphere. After incubation, the cells were resuspended in the same solution and 10,000 cells

were acquired immediately by FACS Canto flow cytometer (Becton Dickinson). The data was acquired as a Histogram on a linear scale where the x-axis represented the DNA content and the y-axis showed the relative cell number. Analysis was conducted using the FlowJo software and the histogram was divided into G_0/G_1, S and G_2/M phase based on the amount of DNA content.

2.7 Sodium Dodecyl Sulphate – Polyacrylamide Gel Electrophoresis (SDS-PAGE)

Primary human CD4+ T cells, as cultured above (Section 2.2) were mixed with 5x SDS sample loading buffer boiled at 95°C for 10 minutes. The samples were then further boiled at 95°C for 5 minutes and the lysates were used for western blotting (Section 2.8).

8-16% Pre-cast Tris-glycine protein gels (NuSep) were loaded into the electrophoresis tank along with 1x Running Buffer (Recipe given in Table 2.1). Samples were boiled for 5 minutes and then 15-20µl of the samples was loaded into the respective wells. To determine the molecular weight, the Precision Plus Dual-Colour protein standard (Bio-Rad, UK) was run along with the samples. The electrophoresis system was run at 135V for approximately 2 hours. The protein samples on the gel were transferred on to a Polyvinylidene fluoride (PVDF) membrane (GE Healthcare, UK) and used for western blotting as described in the section below.

2.8 Western Blotting

The gel was washed in transfer buffer following which it was stacked between layers of scotch pads, 3mm Whatmann filter paper and a PVDF membrane which had been activated by washing with 100% methanol before use. The stack was placed inside the transfer tank and filled with 1x transfer buffer with 20% methanol (Recipe given in Table 2.2). The tank was kept cool using distilled water and ice packs. A current of 400mA and 35V was applied for 1.5hours and once the transfer was complete the membrane was

blocked in 5% dried milk in PBS with 0.1% tween (Thermo-Scientific, UK), with constant shaking for 1 hour at room temperature. The membrane was then transferred to primary antibody in 5% milk in PBS + 0.1% tween overnight at 4°C. The membrane was washed 3 times in PBS+0.5% tween and then incubated for 1 hour at room temperature in Horseradish-peroxidase (HRP) conjugated IgG antibody. The membrane was again washed three times in PBS+0.5% tween-20.

Detection of HRP conjugated antibodies was carried out using SuperSignal West Femto ECL Western Blotting system (ThermoScientific,, USA). The membrane was incubated in the enhanced chemiluminescent (ECL) reagents for 2-3 minutes at room temperature, wrapped in a plastic sheet and immediately imaged using Bio-Rad Chemi-Doc XRS Molecular imager.

10 x Running Buffer	35 mM SDS (10.08 g) 250 mM Tris (30.3 g) 1.92 M glycine (144 g)
20% Methanol Transfer Buffer	25 mM Tris (3.03 g) 192 mM glycine (14.4g) In 800 mL final volume of water. Add 200 mL of methanol 100%

Table 2.2: Running Buffer and Transfer Buffer recipe

Antibody (Clone)	Manufacturer	Dilution
Rabbit anti-human p21 mAb (12D1) (Primary)	Cell Signalling, UK	1:1000
Rabbit anti-human pSTAT5 mAb (4694) (Primary)	Cell Signalling, UK	1:5000
Rabbit anti-human GAPDH mAb (9485) (Primary)	AbCam	1:2000
HRP Goat Anti-Rabbit IgG (84369) (Secondary)	Jackson ImmunoResearch	1:10000

Table 2.3: List of western blot antibodies

2.9 RNA isolation from CD4+ T cells

Isolated CD4+ cells were either left unstimulated or stimulated with anti-CD3/CD28 beads (1:20 bead:cells ratio) and treated with or without CP655 (5µM) or CP655OMe (5µM) for 18 hours. RNA from these cells was isolated using Qiagen RNeasy Microkit (Qiagen, UK) following the manufacturers instructions. Briefly, at various time points, $5x10^5$ cells were pelleted and homogenized using 350µl of Buffer RLT. Following this, an equal volume of 70% ethanol was added and mixed well by pipetting several times. The sample was then transferred to the RNeasy MinElute spin column and centrifuged at 8000 x*g* for 15 seconds and the flow through was discarded. 350µl of RW1 buffer was added to the column which was centrifuged at 8000 x*g* for 15sec and the flow through was discarded. 70µl of buffer RDD was mixed with 10µl of DNase I stock solution, 80µl of this mixture was added to the membrane of the RNeasy MinElute spin column and incubated at room temperature (20-30°C) for 15mins. Following this, 350µl of RW1 buffer was once again added to the columns before centrifuging at 8000 x*g* for 15sec and the columns were placed in a new 2ml collection tube,

provided along with the Qiagen kits. 500µl of buffer RPE was added to the spin column and centrifuged at 8000 x*g* for 15sec, the flow through was discarded, and 500µl of 80% ethanol was added to the column and centrifuged at 8000 x*g* for 2mins. The collection tube was replaced with a new one and the column was centrifuged with the lid open at 15000 x*g* for 5mins to dry the membrane. Finally, the column was placed into a 1.5ml collection tube, 14µl of RNase-free water was added to the spin column membrane and centrifuged at 15000 x*g* for 1 min to elute the RNA. The RNA was stored at -80°C till further use.

2.10 Quantitative Reverse Transcriptase – Polymerase Chain Reaction (qRT-PCR)

RNA isolated using Qiagen RNeasy microkit (Qiagen, UK), as described above (Section 2.9) was quantified using the NanoDrop 1000 Spectrophotometer (Thermo Scientific) and the quality of the RNA was assessed using Agilent 2100 Bioanalyser (Agilent technologies). For cDNA synthesis, 0.4µg of Random Hexamers were added to 100ng of RNA in a final volume of 22µl with RNA-free water. This was incubated at 70°C for 5 minutes and then transferred to ice following which, 16µl of the Master Mix, described below, was added to each of the samples.

Master Mix	**Volume**
5 x RT Reaction Buffer	8 µl
dNTPs (25mM)	1.6 µl
Riboblock RNase inhibitor (40U/ µl)	1 µl
RNase free water	5.4 µl
Total	**16 µl**

Samples were incubated at room temperature for 5 minutes. Following this, 400U of Revert-Aid Reverse Transcriptase enzyme (Life technologies, UK) were added to each sample, to obtain a final volume of 40µl. This was first incubated for 10 minutes at room temperature, then for 1 hour at 42°C and lastly at 70°C for 10 minutes to inactivate the Reverse Transcriptase enzyme. cDNA was diluted to 10x by adding 360µl of RNase free water and stored at -80°C till further use.

The cDNA was used for qRT-PCR with a TaqMan® detection system on a ViiA™ 7 Dx Real-Time PCR instrument (Life technologies). Each reaction contained 1.5µl of previously prepared cDNA and 8.5µl of the Master Mix described below.

Master Mix	Volume
2 x TaqMan PCR Master mix	5 µl
Gene of interest	0.33 µl
18srRNA (Housekeeping gene)	0.17 µl
RNase free water	3 µl
Total	**8.5 µl**

Relative expression of each of the target genes was calculated by normalizing it to the relative expression of the house-keeping gene 18s in the same sample.

Pre-designed TaqMan primers for the genes of interest were used (Table 2.4):

Gene of Interest	Catalogue number	Supplier
CDC6	Hs00154374_m1	Life technologies
CDKN1A	Hs00355782_m1	Life technologies
RRM1	s01040698_m1	Life technologies
GADD45G	Hs00198672_m1	Life technologies
ANAPC1	Hs00224096_m1	Life technologies

Table 2.4: List of RT-PCR primers

2.11 Flow Cytometry

1 x 10^6 cells were washed twice with FACS buffer (PBS + 1%BSA + 0.1%NaN_3) by centrifuging them at 300 x*g* for 5 minutes. Cell pellet was resuspended in 100µl of the FACS buffer and either left unstained or stained with the respective FACS antibodies, on ice for at least 40 minutes. 3mls of cold FACS buffer was added to the cells after the incubation period and the cells were again washed by centrifugation at 300 x*g* for 5 minutes. Following this, cells were resuspended in 500µl of cold FACS buffer and 2% Paraformaldehyde (PFA) (Alpha Aesar). Routinely, 10,000 cells were acquired by the FACS Calibur (Becton Dickinson) using CellQuest software and analysed using the FlowJo software.

Antibody (Clone)	Manufacturer	Amount used (µl/test)
Human anti-CD4-PerCP-Cy5.5 (L200)	BD	2 µl/test
Human anti CD14-AlexaFluor647 (61D3)	eBiosciences	1 µl/test

Table 2.5: List of FACS antibodies

2.12 Micro-array analysis of CD4+ Cells

CD4+ T cells were isolated as per the protocol above (Section 2.1). Isolated cells were stimulated with either anti-CD3/CD28 beads in a ratio of 1:20 bead:cells or left unstimulated in the presence or absence of CP655 or CP655OMe for 18 hours following which, RNA was extracted (Section 2.9) and Affymetrix Gene 1.0 ST array was performed as per Ambion's and Affymetrix's instructions, which have been briefly described below. The experiments were conducted in collaboration with Dr. Matthew Arno (Genomics Centre, KCL).

2.12.1 Synthesizing 1st Cycle cDNA

RNA was prepared as per the protocol described above using RNeasy Microkit (Qiagen, UK) (Section 2.9). Control RNA that is 1 mg/ml total RNA from HeLa cells (provided with kit), was used to normalize the samples and reagents used. Quality and quantity of RNA was determined using NanoDrop1000 spectrophotometer (Thermo Scientific). RNA used for the experiment was considered to be of good quality when it demonstrated a A_{260}/A_{280} ratio between the range of 1.7 to 2.1, as determined by the spectrophotometer. The integrity of the RNA was further assessed using the Agilent 2100 Bioanalyzer using the LabChip Kit. Assessing the integrity of

the RNA helps to establish the proportion of the sample that is full length. This is essential as reverse-transcribing partially degraded RNA can produce cDNA that is lacking part of the coding region. Following this, first strand cDNA was synthesized from the experimental RNA as well as the control RNA, using the First-Strand master mix that was provided along with the kit. The single-stranded cDNA was converted into a double-stranded cDNA, to act as a template for transcription. DNA polymerase and RNase H were used to degrade the RNA and simultaneously generate the second cDNA strand. This was done by using the second-strand Master mix provided along with the kit.

2.12.2 Synthesizing cRNA and 2nd Cycle cDNA

The second strand cDNA was used to synthesize the antisense cRNA, which was then amplified by in-vitro transcription (IVT), the master mix for which was supplied along with the kit. cRNA was purified according to the procedure described in the Affymetrix protocol and the yield was assessed using the NanoDrop1000 spectrophotometer (Thermo Scientific). Following this 10µg of cRNA was then used to synthesize sense-strand cDNA by reverse-transcription using random primers. 2nd cycle Master mix was used to generate the cDNA and RNase H was used to degrade the cRNA and produce single stranded cDNA. In order to prepare the cDNA for further fragmentation and labelling, the cDNA was purified to remove any incorporated salts, enzymes and unincorporated dNTPs, as per the protocol defined by Affymetrix. The quality and yield of the cDNA was reassessed by the NanoDrop1000 spectrophotometer (Thermo Scientific). The Affymetrix GeneChip® WT Terminal Labeling Kit (Part no. 900671) was used for the fragmentation and labeling of the cDNA.

2.12.3 Terminal labelling, Hybridization and Processing

The cDNA samples were used for fragmentation using the Fragmentation Master Mix and then were labelled using the GeneChip® WT Terminal Labeling Kit. The labeling reagents produced using the Master Mix provided were added to the fragmented DNA samples, which were then used for hybridizations for the cartridge arrays. Once the hybridization was set-up the arrays were stained as per the GeneTitan Setup protocol for Gene 1.1 ST Array Plates and processed on the GeneTitan® Instrument. The entire procedure is represented in the schematic below (Fig 2.1).

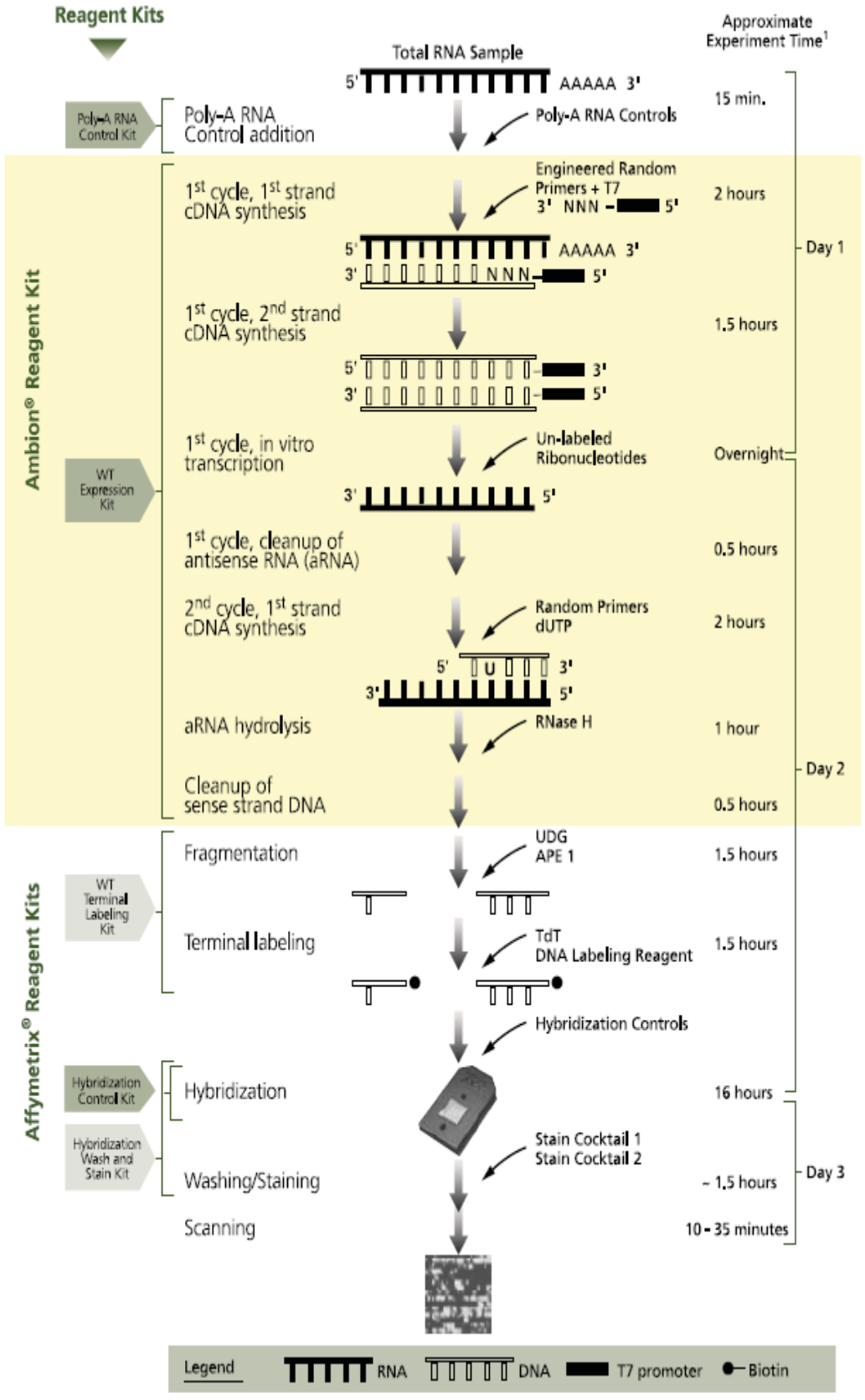

Figure 2.1: Assay Schematic For Generating Whole Transcript Sense Target
(Affymetrix User Manual)

2.13 Iron Chelators

The 3-hydroxypyridine-4-one (HPO) chelators (kindly provided by: Prof. R. Hider, KCL) were dissolved in Dimethyl Sulfoxide (DMSO) (Sigma-Aldrich, UK) and stored at a concentration of 50µM at -20°C. The chelators were diluted to the respective concentrations with RPMI media before use. The structures of the chelators used in this study are given below in Fig 2.2.

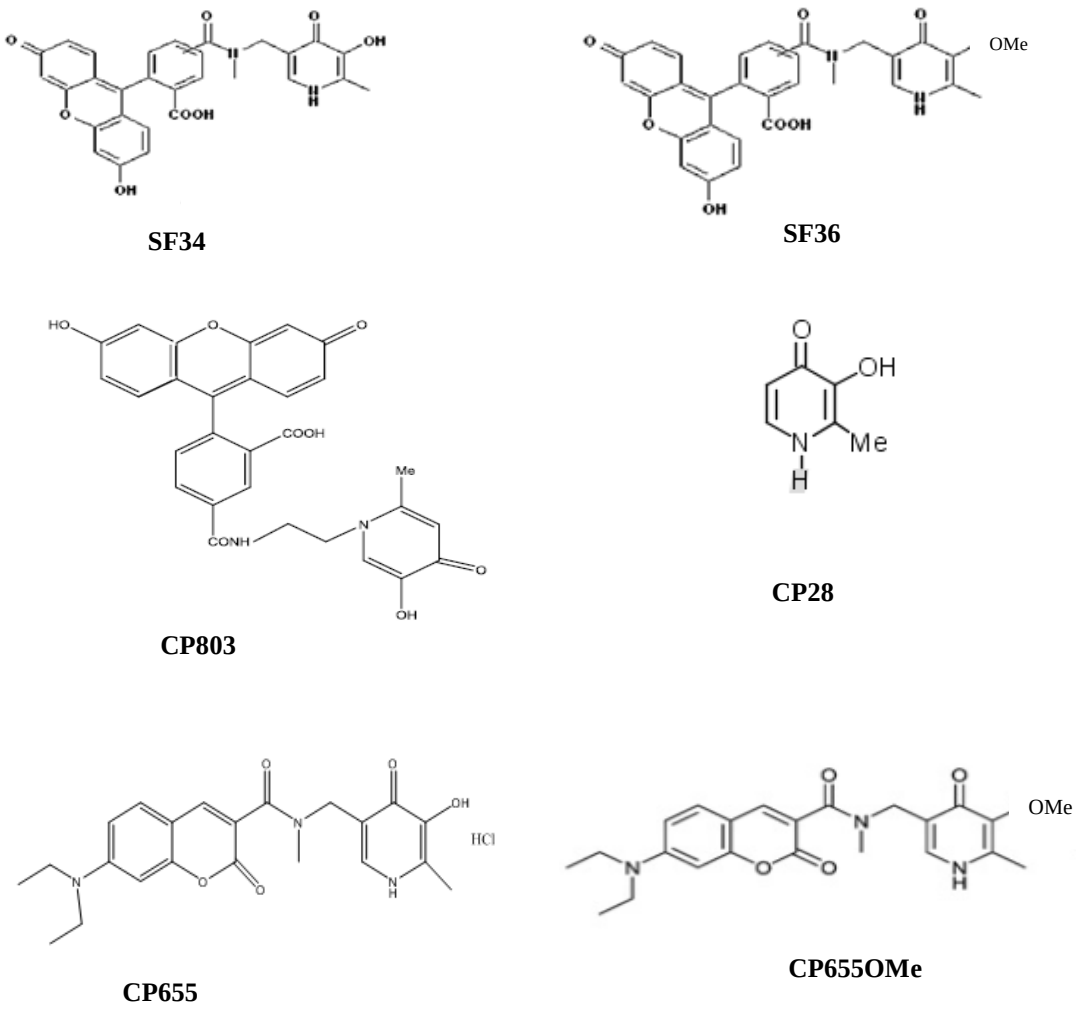

Figure 2.2: ***Structure and Molecular weights of iron chelators used in this study*** *(Ma et al, 2006; Fakih et al, 2009)*

2.14 Statistical Analysis

The results have been represented as Mean ± SEM for the stated number of replicates. Statistical differences between the data have been calculated using Graphpad Prism 5 software using the appropriate statistical tests as described in the respective figure legends.

CHAPTER 3

DETERMINING THE EFFECT OF IRON CHELATION ON HUMAN CD4+ AND CD14+ CELLS

CHAPTER 3

RESULTS

DETERMINING THE EFFECT OF IRON CHELATION ON HUMAN CD4+ AND CD14+ CELLS

3.1 INTRODUCTION

HPO iron chelators, SF34 and CP28, were previously used in our laboratory to test their effect on a mouse model of collagen-induced arthritis. It was observed that both SF34 and CP28 were able to significantly reduce CD4+ T cell proliferation and production of pro-inflammatory cytokine, such as IFN-γ and IL-17, in response to collagen stimulation *in vitro*. This ability of the chelators to modulate inflammatory responses was seen in response to antigen stimulation, but was not observed when cells were stimulated with the mitogen, Concanavalin A (Con A). Further experiments to identify the target cell indicated that the chelators were exerting their effects on murine CD4+ T cells (Lloyd-Jones and Collins, unpublished observations). This was contrary to the initial hypothesis where it was suggested that the main target of the iron chelators would be the CD14+ monocytes. This was based on the observation that in chronic inflammatory conditions, Anaemia of Chronic Disease is a common underlying problem. Patients with ACD have been shown to have accumulation of iron within the monocytes of the reticuloendothelial system, which drives inflammation in these individuals. Hence our original hypothesis proposed that the use of iron chelators would be able to reduce this accumulation of iron and thereby reduce the inflammatory conditions associated with sequestered iron.

Additionally, SF34 and CP28, were tested in an *in-vivo* collagen-induced Arthritis (CIA) disease model. When given prophylactically, both chelators were able to significantly delay the onset of arthritis as compared to the control groups which were given either PBS or the control compound SF36, which is similar in structure to SF34 but does not chelate iron. However, when the chelators were given as a therapy to test their effect on established disease, only CP28 was able to significantly reduce the mean clinical disease score as compared to the control

groups, whereas SF34 did not show any significant effect (Lloyd-Jones and Collins, unpublished observations) (Fig 3.1).

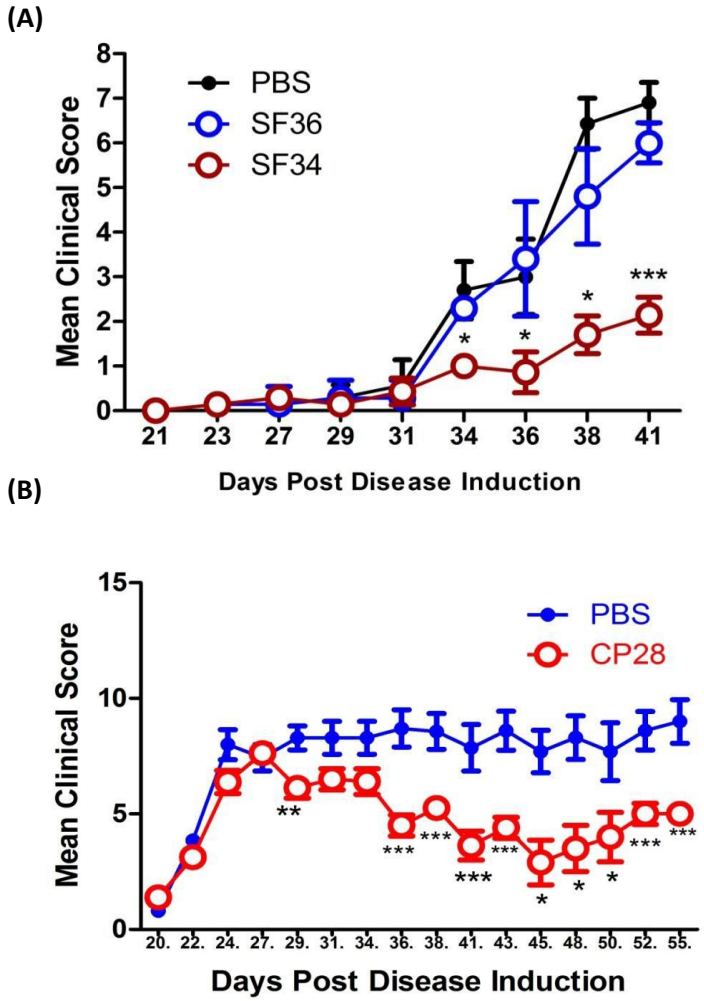

Figure 3.1: ***In-vivo prophylactic and therapeutic effect of iron chelation on disease score:*** A) C57Bl/6 mice were given either SF34 in 200µl at 250µM or control compounds SF36 and PBS i.p on Day -1, Day 0, Day 1 and twice per week from disease induction for 2 weeks. Disease was induced by i.d injections of chicken collagen in CFA. B) C57Bl/6 mice had disease induced as above. When symptoms became visible, 22 days post disease induction, mice were treated with either chelator CP28 or PBS twice weekly till the end of the trial. Mean clinical disease was assessed by visual scoring 3 times a week until the end of the trial. Data represented as Mean ± SD. n=7 for each group, *p<0.05, **p<0.01 and ***p<0.001 calculated using Wilcoxon non-parametric test

In the following chapter, I examined a panel of novel HPO chelators for their effect on human antigen stimulated or T- cell receptor (TCR) stimulated cells. I began by analysing the effect of different HPO chelators, namely CP655, CP28, CP803 and SF34, on Tetanus toxoid stimulated human CD4+ and CD14+ cells. Once the most effective chelator was identified, I conducted a titration to determine the appropriate concentration that the chelator should be used at. This was followed by conducting viability and purity assays to ensure that the chelator had no adverse effects on the cell population. Finally, experiments were conducted to find out the target cell of the iron chelator.

3.2 CHAPTER OBJECTIVES

Based on the discussion above, the specific aims for this chapter are as listed below:

a. Determining the effect of a panel of HPO chelators on cultures of human CD4+ and CD14+ cells
b. Identifying the most effect HPO chelator to be used for all future experiments
c. Identifying most suitable dose of chelator chosen for experimentation
d. Analysing effect of chelator on cell viability
e. Identifying target cell for chelator's action

3.3 RESULTS

3.3.1 Purity of CD14+ and CD4+ cells after PBMC isolation from fresh blood

For each of the experiments conducted, CD14+ monocytes and CD4+ T cells were isolated from freshly isolated human PBMCs by MACS separation protocols and their purity was assessed by flow cytometry in order to ensure that a pure population of CD14+ and CD4+ cells were used for the experiments. Figure 3.2 depicts the flow cytometry analysis for assessing CD4+ cell purity (Fig 3.2 A) and CD14+ purity (Fig 3.2 B) from one donor. Obtaining a high purity was essential since one of the main aims of the project included identifying the target cell of the chelator.

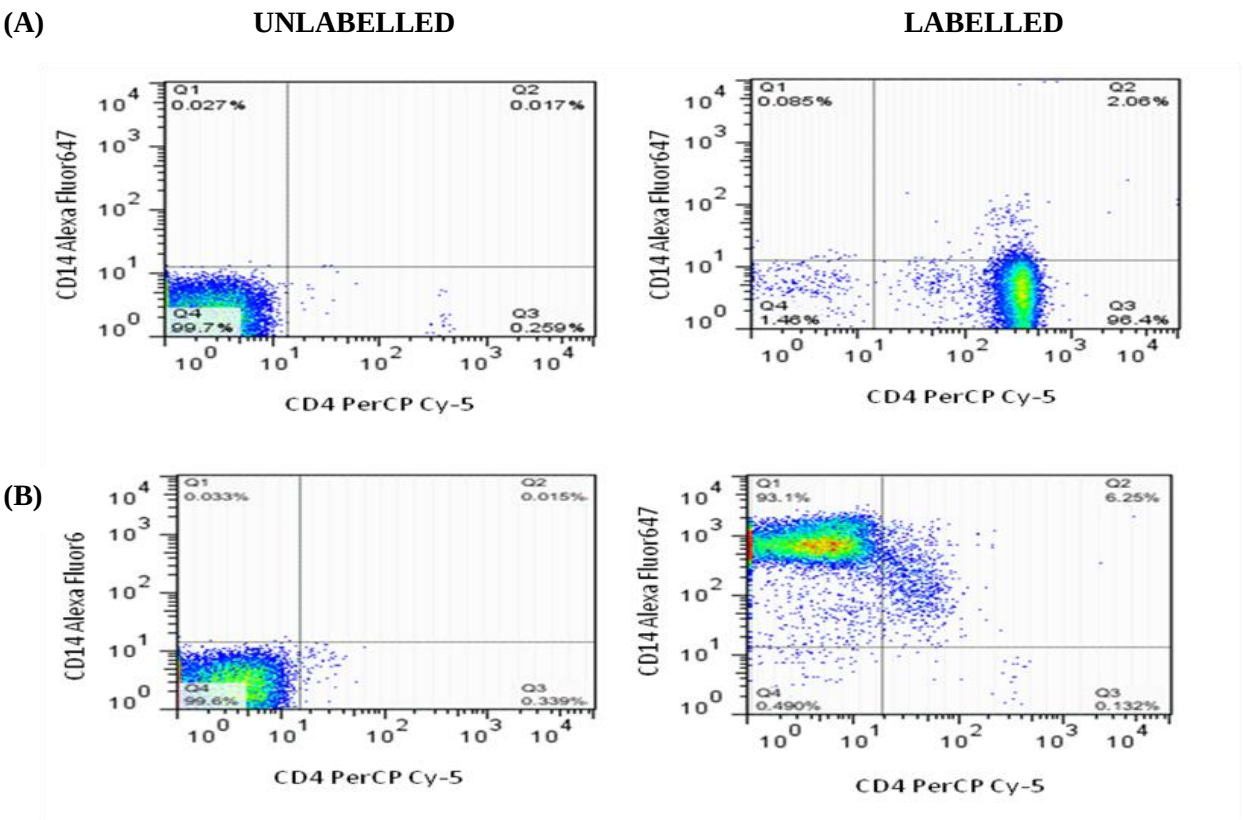

Figure 3.2: ***CD4+ and CD14+ cells purity:*** Cells were isolated from fresh PBMCs using Magnetic columns as per the MACS separation protocol. $1x10^6$ cells were stained with the respective FACS antibody and then analysed by flow cytometry. (A) Purity of isolated CD4+ T cells. (B) Purity of isolated CD14+ monocytes. Unlabelled = control cells; Labelled = Cells stained with antibody. Results representative of 1 donor.

In all of the following experiments, purity of both subsets was consistently greater than 85%. The average purity of CD4+ cells was 96.23% (n=19) and average purity of CD14+ cells was 88.75% (n=8).

3.3.2 The effect of HPO iron chelators on human CD4+ and CD14+ co-cultures.

Several different kinds of HPO chelators have been synthesised to date. While most of the chelators have a similar structure, the main difference lies in the varying specificities and affinities of these chelators to intracellular iron. In order to establish which analogue was most effective on human cell cultures, several chelators were tested on a co-culture of human CD4+ and CD14+ cells stimulated with Tetanus toxoid. The concentration of Tetanus toxoid to be used was determined by conducting a titration of the antigen, tetanus toxoid (Fig 3.3).

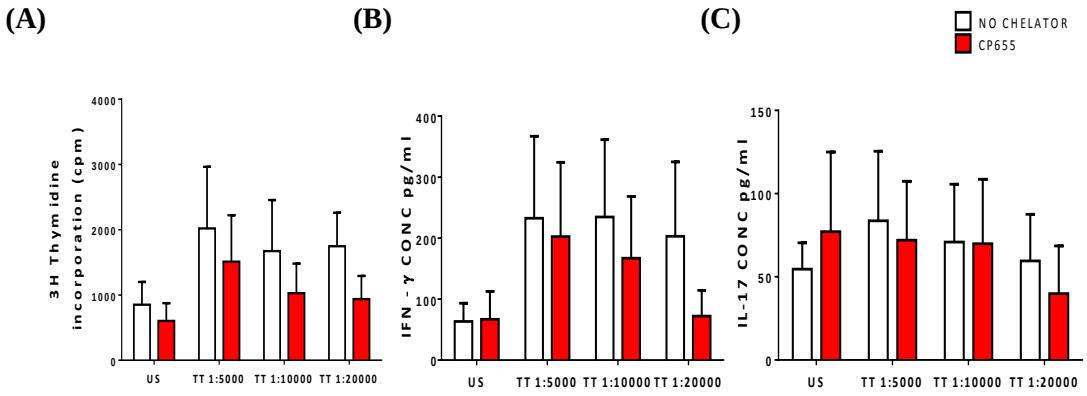

Figure 3.3*: Titration of Tetanus toxoid on human CD4+ and CD14+ cells:* CD4+ and CD14+ cells were isolated from fresh blood of healthy donors. Cells were mixed in a ratio of 2:1, stimulated with or without Tetanus Toxoid at either 1:5000, 1:10000 or 1:20000 dilution and treated with or without iron chelator CP655. After 6 days of incubation, cells were stimulated with 750ng/ml Ionomycin and 50ng/ml PMA for four hours. (A) Proliferation was measured by incorporation of ^{3}H thymidine. (B, C) Cytokines were measured by ELISA. Results depicted as Mean $\pm$ SEM, n=3 individual donors. CONC = concentration.

Based on the results of this experiment, it was decided to use the antigen at a concentration of either 1:20000 or 1:10000 dilution. Both concentrations were tested in each of the following experiments, and results where strongest stimulation was observed, were used for analysis.

The panel of chelators which were tested for their effect on proliferation, IFN-γ and IL-17 production from CD4+ and CD14+ cells stimulated with Tetanus Toxoid, consisted of CP655, CP28, CP803 and SF34. Results shown below are from tetanus concentrations at which maximum response was seen, 1:20000 for the majority of donors.

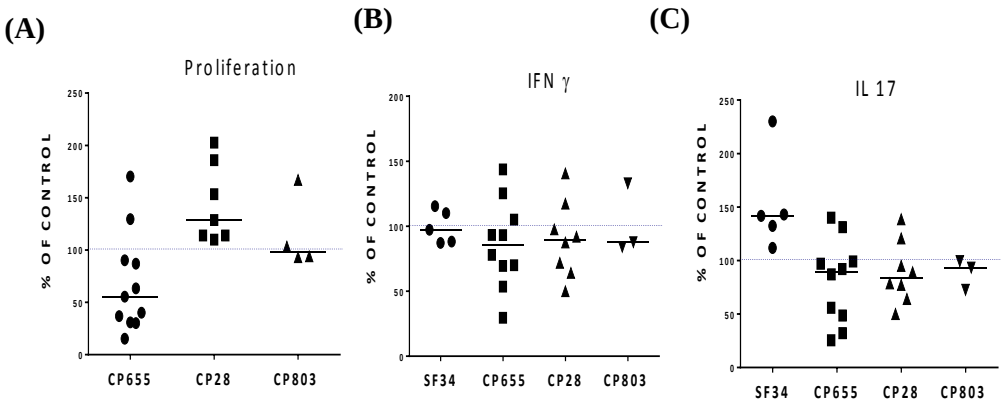

Figure 3.4*: Effect of chelators on human T cell proliferation and cytokine production:* CD4+ and CD14+ cells were isolated from fresh blood of healthy donors. Cells were mixed in a ratio of 2:1, stimulated with or without Tetanus Toxoid at either 1:10000 or 1:20000 dilution and treated with or without chelators. After 6 days of incubation, cells were stimulated with 750ng/ml Ionomycin and 50ng/ml PMA for four hours. (A) Proliferation was measured by incorporation of ^{3}H thymidine. (B,C) Cytokines were measured by ELISA. Cumulative results from donors tested shown as a percentage of cells from untreated cultures. Each symbol represents individual donor. Dotted line represents untreated control cells. Horizontal bar in A, B and C indicates the Median value.

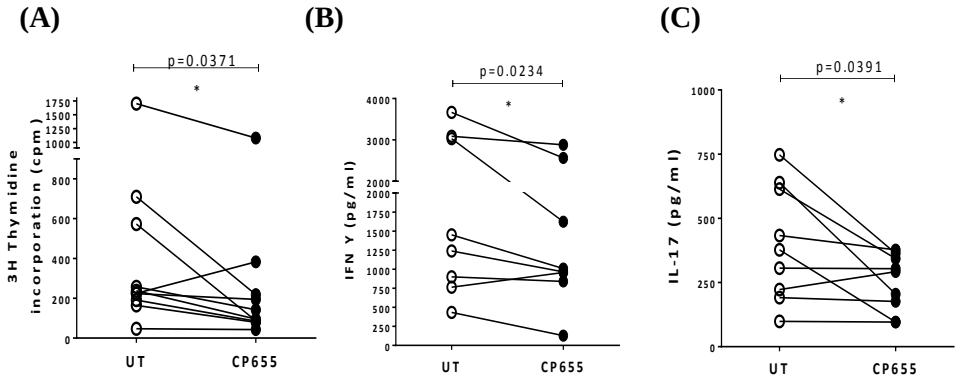

Figure 3.5: *Effect of CP655 on human T cell proliferation and cytokine production:* CD4+ and CD14+ cells were isolated from fresh blood of healthy donors. Cells were mixed in a ratio of 2:1, stimulated with or without Tetanus Toxoid at either 1:10000 or 1:20000 dilution and treated with or without chelators. After 6 days of incubation, cells were stimulated with 750ng/ml Ionomycin and 50ng/ml PMA for four hours. (A) Proliferation was measured by incorporation of ^{3}H thymidine. (B,C) Cytokines were measured by ELISA. Individual raw data for donors tested only with CP655. Each symbol represents an individual donor. UT = Untreated cells. * indicates $p<0.05$ between cultures with absence and presence of CP655 calculated using Wilcoxon nonparametric matched pairs test.

Out of all the chelators tested, only CP655 significantly reduced cell proliferation, in response to tetanus toxoid stimulation to approximately 50% of untreated control cells in 7 out of the 11 donors tested (Fig. 3.4 A). Moreover all the chelators tested were successful in reducing, IFN-γ and IL-17, production by the cells, although to varying degrees (Fig. 3.4 B, C). However, CP655 was noted to be most consistent and significantly reduced IFN-γ to 85% of control and IL-17 to 90% of control group.

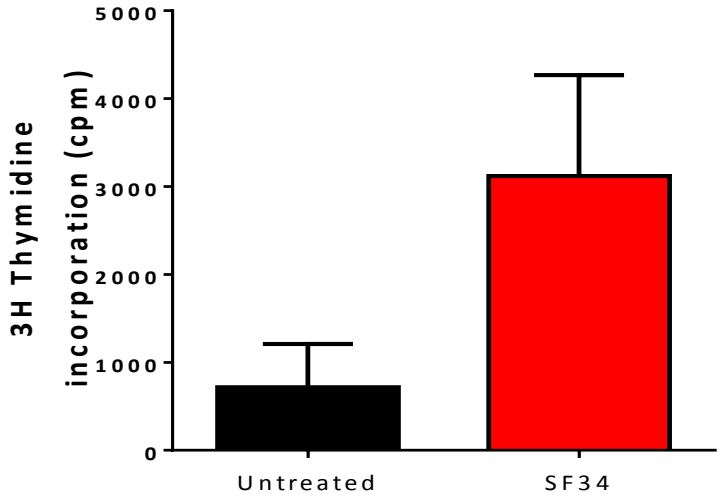

Figure 3.6*: Effect of SF34 on proliferation:* CD4+ and CD14+ cells were isolated from fresh blood of healthy donors. Cells were mixed in a ratio of 2:1, stimulated with or without Tetanus Toxoid at either 1:10000 or 1:20000 dilution and treated with or without SF34. After 6 days of incubation, cells were stimulated with 750ng/ml Ionomycin and 50ng/ml PMA for four hours. Proliferation was measured by incorporation of ^{3}H thymidine. Data represented as Mean ± SEM from n=3 individual donors.

In contrast to previous data obtained from murine cells, SF34 did not have any effect on reducing proliferation in response to antigenic stimulation of the cells. In fact, proliferation after SF34 treatment was found to be four times more than that of the untreated groups (Fig 3.6). Cytokine production after treatment with SF34 was also found to be consistently higher than after treatment with any other chelator (Fig 3.4 B, C).

3.3.3 Titration of CP655

As seen in the section above, the HPO chelator CP655 was found to be more effective than any of the other chelators tested in reducing cell proliferation and inflammatory cytokine production. In fact, CP655 has been previously shown to be the most sensitive to the presence of iron amongst all other HPO chelators (Ma *et al*, 2007). Therefore, based on those results it was decided to use CP655 in all of the future experiments. The next step required ascertaining the right concentration at which CP655 must be used in order to avoid any potential toxicity while still retaining the strong suppressive results.

Once again isolated human CD4+ and CD14+ cells were stimulated in culture with tetanus toxoid antigen in the presence of absence of varying concentrations of CP655 (Fig 3.7).

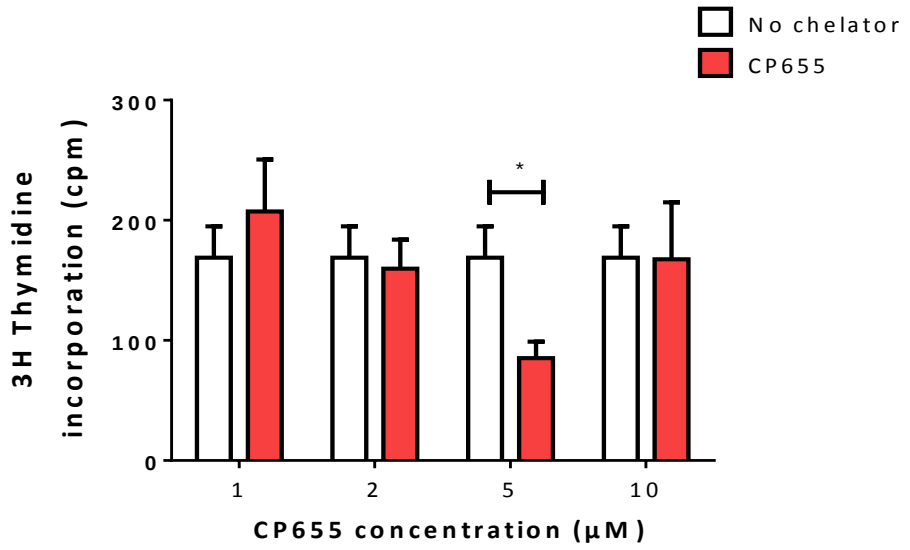

Figure 3.7: ***Dose titration for CP655:*** CD4+ and CD14+ cells were isolated from fresh blood of healthy donors. Cells were mixed in a ratio of 2:1, stimulated with or without Tetanus Toxoid at either 1:10000 or 1:20000 dilution and treated with or without CP655 at concentrations ranging from 1µM to 10µM. After 6 days of incubation, cells were stimulated with 750ng/ml Ionomycin and 50ng/ml PMA for four hours. Proliferation was measured by incorporation of ^{3}H thymidine. * indicates $p<0.05$ between cultures with absence and presence of CP655 calculated using students paired t-test. Data represented as Mean $\pm$ SEM from n=3 individual donors.

As seen in figure 3.7, the ability of CP655 to suppress proliferation of cells was best noticed when CP655 was used at 5µM concentration. Hence, based on these results all further experiments use CP655 at 5 µM concentration.

3.3.4 Measuring viability with CP655

Having established CP655 as the main chelator of choice, it was essential to ensure that it is not responsible for any unexplained cell death and excessive toxicity that can influence the interpretation of the data. To confirm this, isolated CD4+ and CD14+ human cells were treated with varying concentrations of CP655 in the presence of tetanus toxoid to maintain the same experimental conditions, and then viability of the cells were analysed after treatment with Propidium Iodide (PI) (Fig 3.8).

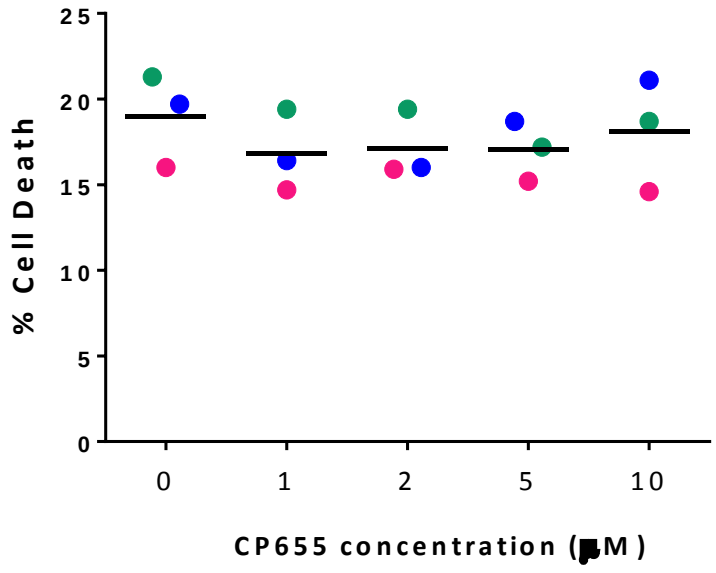

Figure 3.8: ***Viability of CD4+ and CD14+ cells:*** CD4+ and CD14+ cells were isolated from fresh blood of healthy donors. Cells were mixed in a ratio of 2:1, stimulated with or without Tetanus Toxoid at either 1:10000 or 1:20000 dilution and treated with or without CP655 at concentrations ranging from 1µM to 10µM. After 6 days of incubation, cells were stimulated with 750ng/ml Ionomycin and 50ng/ml PMA for four hours. Cells were stained with Propidium Iodide and viability was assessed by Flow Cytometry. Graph represents percentage of dead cells. Solid line represents Mean from n=3 individual donors.

Results indicated that treatment with the iron chelator, at all the concentrations tested, did not cause any statistically significant cell death. In fact, lower concentrations of the chelator ranging from 1µM to 5µM showed reduced cell death as compared to cells that were not treated with CP655 (Fig 3.8). These results confirmed the use of 5µM of CP655 for all experimental set-ups.

3.3.5 To determine iron-dependent effect on suppression caused by CP655

In order to confirm that the effect of the chelators is iron dependent, that is, the effect is based on the ability of the compound to chelate iron from cell cultures, a non-iron chelating compound CP655OMe was developed and tested in the same experimental set-up as CP655.

However, before this could be tested, the concentration of CP655OMe to be used in future experiments was determined. Similar to the set-up in Section 3.3.3, isolated human CD4+ T cells and CD14+ monocytes were stimulated with Tetanus Toxoid in the presence or absence of varying concentrations of the control compound CP655OMe and proliferation was measured by tritiated thymidine incorporation (Fig 3.9).

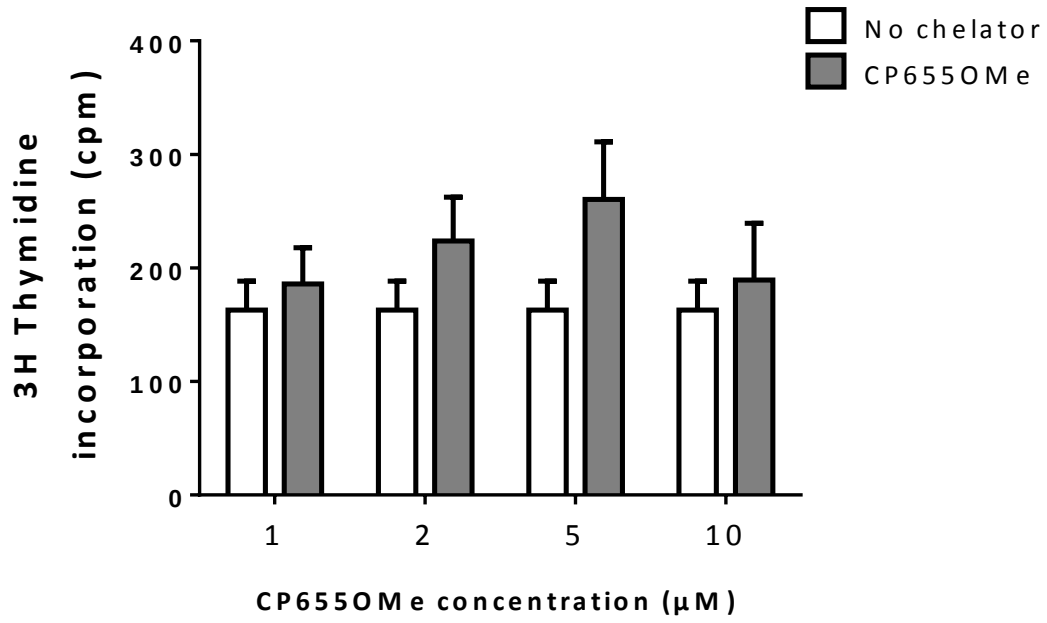

Figure 3.9: ***Dose titration for CP655Ome:*** CD4+ and CD14+ cells were isolated from fresh blood of healthy donors. Cells were mixed in a ratio of 2:1, stimulated with or without Tetanus Toxoid at either 1:10000 or 1:20000 dilution and treated with or without CP655Ome at concentrations ranging from 1µM to 10µM. After 6 days of incubation, cells were stimulated with 750ng/ml Ionomycin and 50ng/ml PMA for four hours. Proliferation was measured by incorporation of ^{3}H thymidine. Data represented as Mean $\pm$ SEM from n=3 individual donors.

The results indicated that at all concentrations of CP655Ome, no inhibition of proliferation was seen. Therefore, to maintain consistency it was decided to use CP655OMe at the same concentration as CP655, which is at 5µM in all further experiments.

Once again, before CP655OMe was used in further experiments, the effect of the compound of cell viability was assessed. Varying concentrations of CP655OMe were added to cultures containing isolated CD4+ and CD14+ cells stimulated with Tetanus toxoid antigen. Cell viability was measured after staining with Propidium Iodide (Fig 3.10).

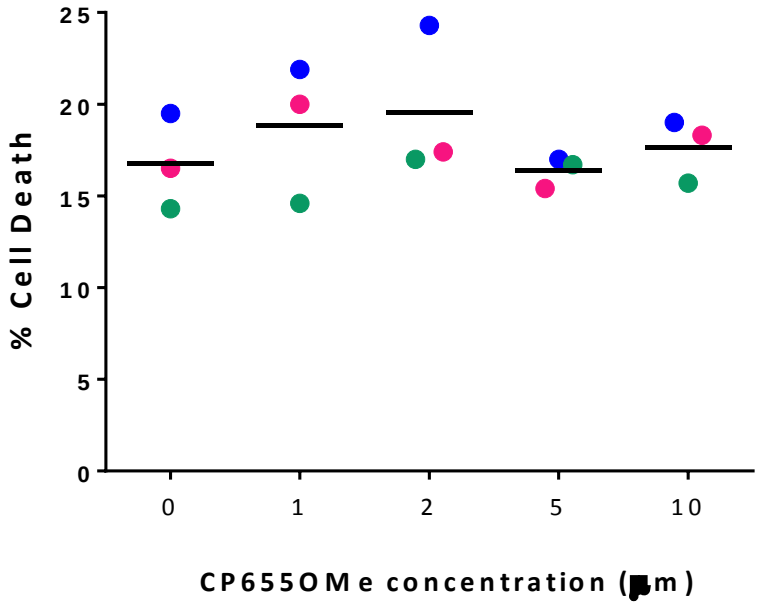

Figure 3.10: ***Viability of CD4+ and CD14+ cells:*** CD4+ and CD14+ cells were isolated from fresh blood of healthy donors. Cells were mixed in a ratio of 2:1, stimulated with or without Tetanus Toxoid at either 1:10000 or 1:20000 dilution and treated with or without CP655OMe at concentrations ranging from 1µM to 10µM. After 6 days of incubation, cells were stimulated with 750ng/ml Ionomycin and 50ng/ml PMA for four hours. Cells were stained with Propidium Iodide and viability was assessed by Flow Cytometry. Graph represents percentage of dead cells. Solid line represents Mean from n=3 individual donors.

Results indicated that CP655OMe treatment did not have any statistically significant effect on cell death as compared to cells that had not been treated with the chelator. At the previously decided concentration of 5µM, cell death seen was same as that caused in the absence of any treatment (Fig 3.10). Therefore, the concentration of CP655OMe to be used was also confirmed at 5µM for all experimental set-ups.

Following on, to confirm that the suppression caused by the chelator is due to its iron binding abilities both CP655, as well as, the control CP655OMe were tested for their effect on cell proliferation. Isolated human CD4+ T cells and CD14+ monocytes were stimulated with Tetanus Toxoid in the presence or absence of either CP655 or the control CP655OMe and proliferation was measured by tritiated thymidine incorporation (Fig 3.11).

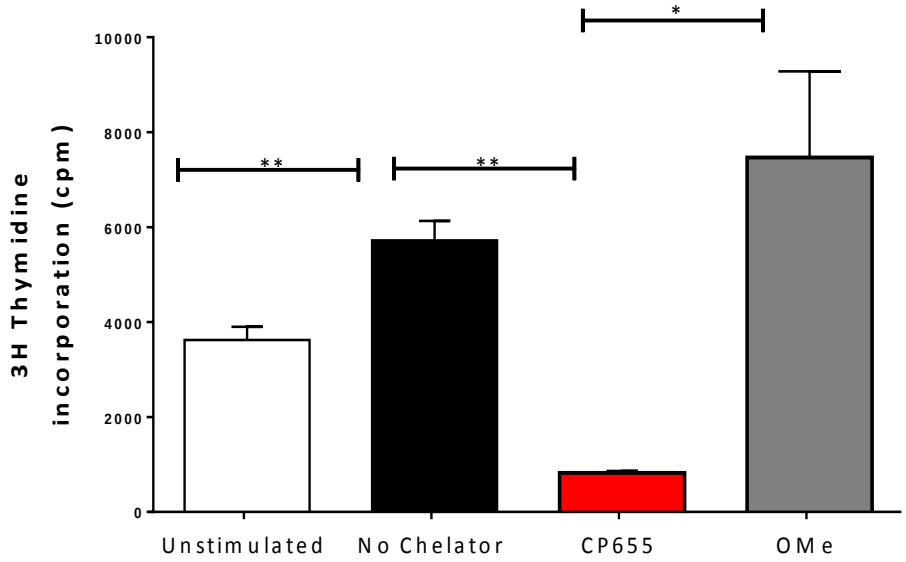

Figure 3.11: ***Iron dependent effect of CP655 on human CD4+ T cell proliferation:*** CD4+ and CD14+ cells were isolated from fresh blood of healthy donors. Cells were mixed in a ratio of 2:1, stimulated with or without Tetanus Toxoid at 1:10000 dilution and treated with or without CP655 (5µM) or the control compound CP655Ome (5µM). After 6 days of incubation, cells were stimulated with 750ng/ml Ionomycin and 50ng/ml PMA for four hours. Proliferation was measured by incorporation of ^{3}H thymidine. * $p<0.05$, ** $p<0.01$ between cultures with absence and presence of CP655 or CP655OMe calculated using paired t-test. Data represented as Mean $\pm$ SEM from n=3 individual donors.

Experiments on three individual donors confirmed that while treatment with CP655 was able to significantly reduce proliferation of the cell cultures, treatment with the non-iron chelating compound, CP655OMe, had no effect on the proliferation of the cells. This confirmed that the inhibition of proliferation is caused due to the chelation of iron from the cell cultures (Fig 3.11).

Therefore, due to the higher effectiveness of CP655 as demonstrated above, it was the main chelator tested in all of the following experiments. Along with CP655, the methylated non-iron chelating compound CP655OMe was also used in all the following experiments.

3.3.6 Identifying the target cell for CP655

Once CP655 was established as the most effective chelator in reducing pro-inflammatory responses, we next determined the cell that is the main target for the action of CP655. Our initial hypothesis proposed that sequestration of iron within Antigen Presenting Cells (APCs) was responsible for driving the inflammatory response that is seen in ACD. Hence in order to address this, we examined whether treatment of either the CD14+ monocytes or the CD4+ T cells separately with the chelator could reduce proliferation and IFN-γ and IL-17 production. CD14+ and CD4+ cells were isolated as described above and were incubated separately with or without the chelator for 24 hours. Following this, cells were washed out of the chelator and mixed in various combinations of either chelator treated monocytes, chelator treated T cells or both (Fig 3.12).

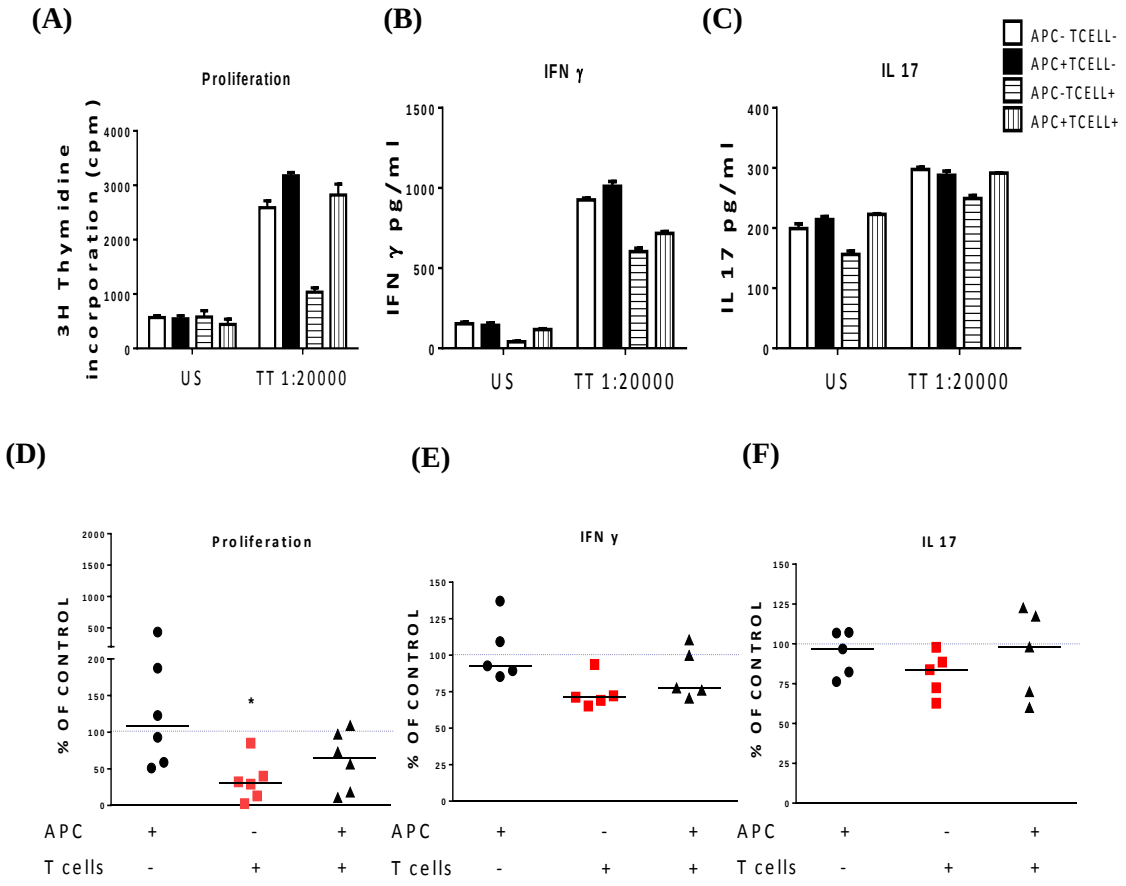

Figure 3.12: ***Effect of CP655 on CD4+ cells versus CD14+ cells*****:** CD4+ and CD14+ cells were isolated from blood of healthy donors. Cells were incubated separately with or without CP655 for 24 hours. The cells were then mixed in different combinations, stimulated with or without Tetanus Toxoid at either 1:10000 or 1:20000 dilution. After 6 days of incubation, cells were stimulated with 750ng/ml Ionomycin and 50ng/ml PMA for four hours. (A,D) Proliferation was measured by incorporation of ^{3}H thymidine. (B,C,E,F) Cytokines were measure by ELISA. Upper Panel: Results representative of 1 donor. Lower Panel: Cumulative results from individual donors. US = Unstimulated cells TT=Tetanus Toxoid stimulated cells. Each symbol represents an individual donor. Horizontal bars indicate the Median values. Dotted line represents control cultures were both CD4+ and CD14+ cells were untreated. * $p < 0.05$ calculated using Wilcoxon non-parametric test.

Contrary to the initial hypothesis, when the CD14+ monocytes were treated with CP655 prior to culture with CD4+ T cells, there was no reduction in cell proliferation in response to tetanus toxoid. In fact, an increase in proliferation was seen as compared to the control group (Fig. 3.12 A, D). However, a pronounced reduction in proliferation was consistently seen when the CD4+ cells were treated overnight with CP655. This reduction was even more prominent than the one seen when both CD4+ and CD14+ cells were treated

with the chelator overnight (Fig. 3.12 A, D). A similar pattern was observed with the production of the pro-inflammatory cytokines. Treatment of CD4+ T cells with CP655 overnight led to a marked reduction in IFN-γ and IL-17 production in all of the donors. In comparison, cultures where the CD14+ monocytes had been individually treated overnight with CP655 did not show a similar consistent reduction in cytokine production (Fig. 3.12 B, C, E, F).

Hence, these results indicated that the cell type that is specifically targeted by CP655 is in fact the CD4+ T cells and not the CD14+ monocytes as hypothesized.

To reconfirm and establish that the suppressive effects caused by CP655 are indeed due its ability to chelate iron, the experimental set-up explained above was repeated in the presence of the non-iron chelating control, CP655OMe (Fig. 3.13).

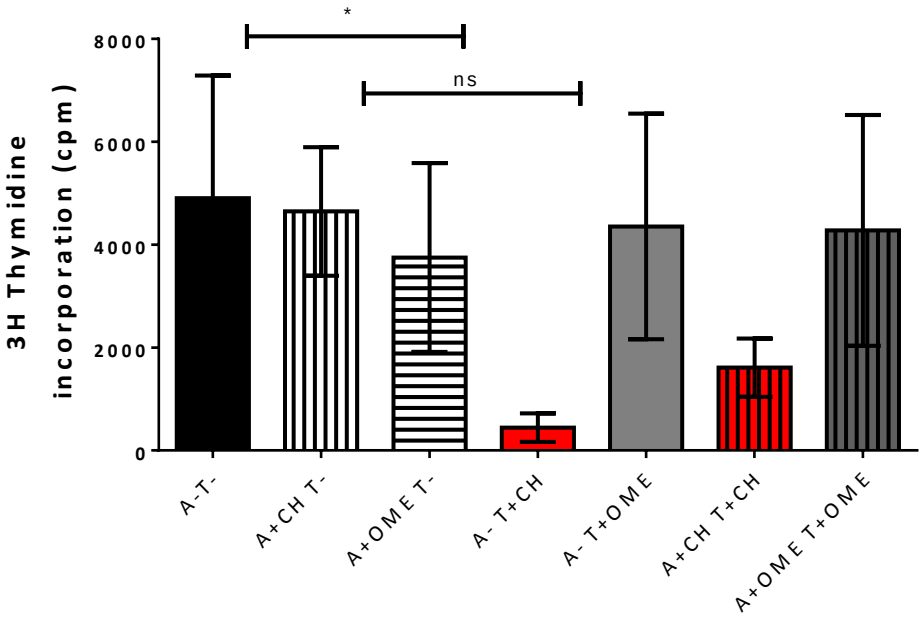

Figure 3.13: ***Iron-dependent effect of CP655 on CD4+ cells versus CD14+ cells:*** CD4+ and CD14+ cells were isolated from fresh blood of healthy donors. Cells were incubated separately with or without CP655 or CP655OMe for 24 hours. The cells were then washed out of the treatment and mixed in different combinations, stimulated with or without Tetanus Toxoid at 1:10000 dilution. After 6 days of incubation, cells were stimulated with 750ng/ml Ionomycin and 50ng/ml PMA for four hours. Proliferation was measured by incorporation of ^{3}H thymidine. A=CD14+cell, T=CD4+ cells, CH=CP655, OME= CP655OMe. * $p<0.05$ calculated using paired t-test. Results represented as Mean ± SEM from n= 3 individual donors.

In agreement with the previous results, a reduction in proliferation was only observed in cultures where the CD4+ T cells had been pre-treated with the iron chelator (Solid red column, Fig 3.13). No significant reduction was seen in the cultures where CD14+ monocytes were pre-treated with CP655. Treatment of the T cells with the control compound had no effect, with proliferation comparable to the untreated control cell cultures. Additionally, cell cultures where both CD14+ cell and CD4+ cells were pre-treated with CP655 a non-significant but consistent reduction in proliferation was seen (Fig 3.13). Treatment of only the CD14+ monocytes with either the chelator or the control compound did not show any differences as compared to the untreated cell cultures. These results were in accordance to data generated previously from murine experiments in our laboratory, where CD4+ T cells were also indicated to be the main target cells of SF34 and CP28 chelators.

3.3.7 Identifying the concentration of anti-CD3/CD28 beads for optimal stimulation of CD4+ T cells

Once experiments revealed that the target for CP655 were CD4+ T cells rather than the previously hypothesized CD14+ monocytes, purified CD4+ T cells were used for further experiments to identify the mechanism of action of the iron chelator.

Therefore, to determine the stimulation required to activate CD4+ T cells in the absence of the CD14+ monocytes, they were stimulated with a range of bead:cell ratios in the presence of either CP655 or the control compound CP655OMe (Fig 3.14).

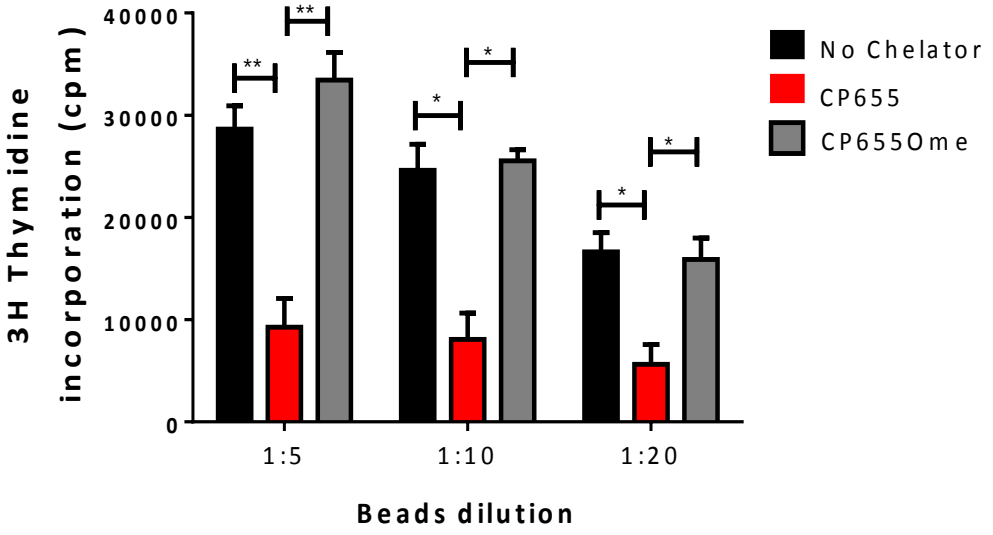

Figure 3.14: ***Titration of anti-CD3/CD28 beads on CD4+ cells:*** CD4+ cells were isolated from fresh blood of healthy donors. Cells were stimulated with anti-CD3/CD28 beads in ratios 1;5, 1;10 and 1:20 in the presence of 5µM CP655and 5µM CP655OMe 24 hours of culture proliferation was measured by incorporation of ^{3}H thymidine. **p<0.02, * p<0.05 calculated using paired t-test. Results represented as Mean $\pm$ SEM from n=5 individual donors.

A dose-dependent effect on proliferation was seen on stimulating with varying concentration of anti-CD3/CD28 beads. Results showed that the level of stimulation had no significant effect on the extent of suppression caused by the chelator on the CD4+ T cells. Approximately 75% inhibition was seen after treatment with CP655 with all three concentrations of the anti-CD3/CD28 beads. The amount of stimulation also had no effect on the action of the control, CP655OMe, as its results were comparable to the untreated control cells in all three titrations.

Hence, in line with this data, it was decided to use the lowest concentration of the anti-CD3/CD28 beads for stimulating CD4+ T cells that is 1:20 bead: CD4+ T cells ratio.

3.3.8 Titration of CP655 and CP655OMe to identify most effective dose

In order to maintain consistency of data and experimental set-up, titrations of CP655 and CP655OMe concentration were conducted once again, but this time in the presence of anti-CD3/CD28 stimulated CD4+ T cells to ensure that CP655 continued to inhibit CD4+ T cell proliferation in the absence of CD14+ monocytes.

CD4+ cells were isolated from freshly isolated PBMCs using the MACS protocol described above. The cells were stimulated with anti-CD3/CD28 beads in a ratio of 1:20 and treated with varying concentrations of CP655 and CP655OMe, ranging from 1µM to 20 µM. 24 hours after incubation the cells were incorporated with Tritiated thymidine and used to measure cell proliferation.

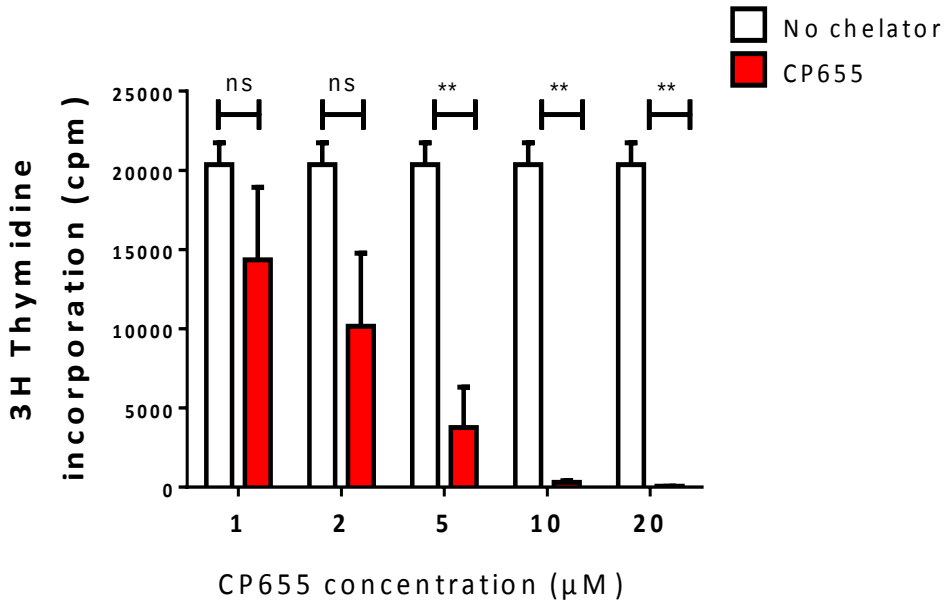

Figure 3.15: ***Dose titration of CP655:*** CD4+ cells were isolated from fresh PBMCs using Magnetic columns as per the MACS separation protocol. $1x10^6$ cells were treated with 1:20 anti-CD3/CD28 beads in the presence or absence of the chelator concentrations ranging from 1µM to 20µM. After 24 hours of culture, proliferation was measured by incorporation of ^3H thymidine. ns= non significant, ** $p<0.01$ calculated using paired t-test. Results represented as Mean ± SEM from n= 3 individual donors.

A dose dependent effect of CP655 was seen on the suppression of proliferation of anti-CD3/CD28 stimulated CD4+ T cells (Fig 3.15). At the lowest concentrations of 1µM and 2 µM, non-significant reductions in proliferation of the CD4+ T cells were observed. However, on increasing the concentration to 5 µM, a highly significant inhibition of proliferation, of almost 80% was observed. Further increasing the concentration to 10 µM and 20 µM showed a dose-dependent significant increase in suppression of proliferation in response to the chelator. At the highest concentration of 20µM, an almost 100% inhibition was noticed.

Based on the above titration of the chelator, the lower concentrations of 1µM and 2µM were ruled out due to insignificant effects. The higher concentrations of 20µM were also not used as it was associated with non significant, but slightly higher cell death as compared to cells not treated with chelator (See Fig 3.17). Therefore, for future experiments, the median dose of 5µM was chosen as the appropriate dose for testing.

Similarly, isolated CD4+ T cells were treated with varying concentrations of CP655OMe after stimulation with anti-CD3/CD28 beads and proliferation was measured using Tritiated thymidine incorporation (Fig 3.16).

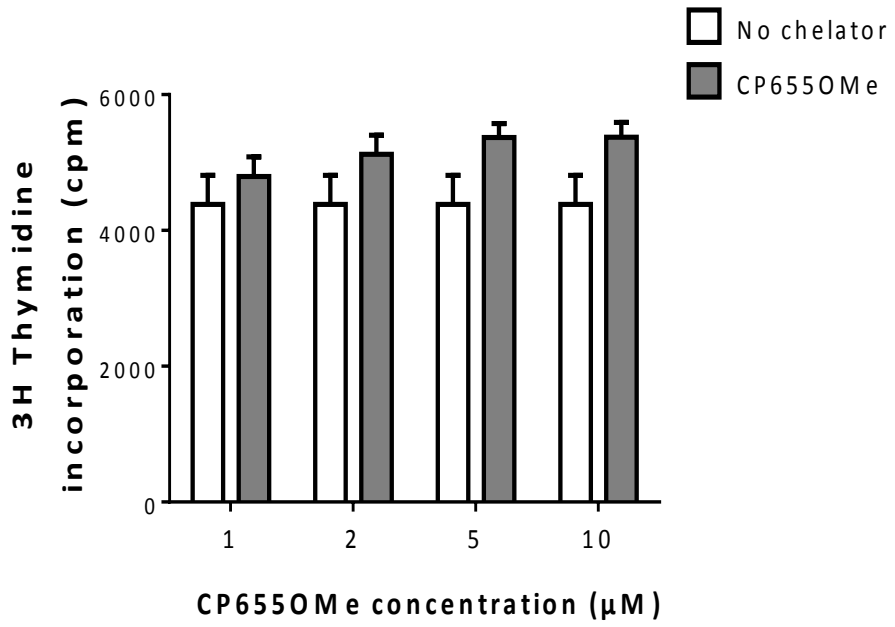

Figure 3.16: ***Dose titration of CP655OMe:*** CD4+ cells were isolated from fresh PBMCs using Magnetic columns as per the MACS separation protocol. $1x10^6$ cells were treated with 1:20 anti-CD3/CD28 beads in the presence or absence of CP655OMe, concentrations ranging from 1µM to 10µM. After 24 hours of culture, proliferation was measured by incorporation of ^3H thymidine. Calculated using paired t-test. Results represented as Mean $\pm$ SEM from n= 3 donors.

The varying concentrations of CP655OMe had no significant effect on the level of cell proliferation observed. In each of the cases, a slight non-significant increase in proliferation as compared to the untreated cells was seen (Fig 3.16). To maintain consistency with previously conducted experiments, it was decided to continue using 5µM concentration of CP655OMe in all further experiments.

3.3.9 Measuring viability of CD4+ T cells post CP655 and CP655OMe treatment

In order to ensure that treatment with both the compounds CP655 and CP655OMe did not cause cell death, viability of the cells was established after treatment with varying concentrations of the compounds in the presence of anti-CD3/CD28 beads. Additionally, this also helped to confirm that the ability of the chelator to inhibit cell proliferation and inflammatory cytokine production, was not a by product of any toxicity or cell death.

CD4+ T cells were isolated as per the protocol described earlier. The cells were stimulated with 1:20 anti-CD3/CD28 beads and treated for 24 hours with either CP655 or CP655OMe, ranging from 1uM to 20uM (Fig 3.17). Propidium Iodide staining was used to determine the percentage of dead cells.

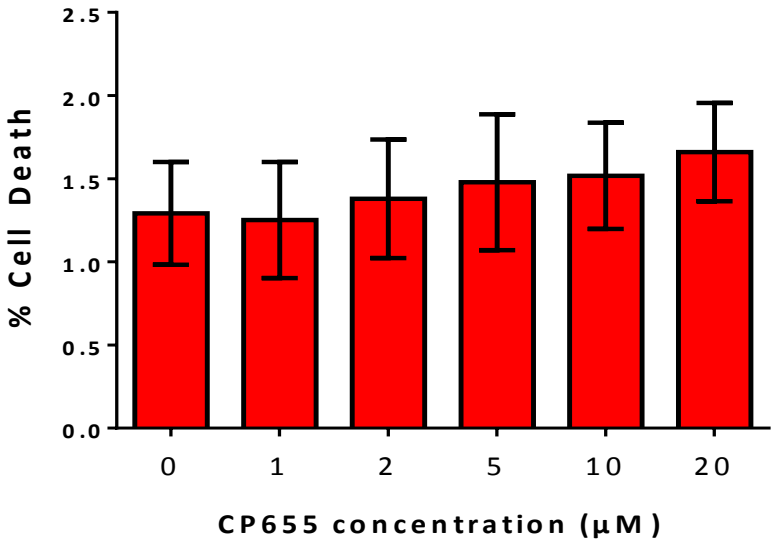

Figure 3.17: ***Viability of CD4+ T cells post CP655 treatment:*** CD4+ cells were isolated from fresh PBMCs using Magnetic columns as per the MACS separation protocol. $1x10^6$ cells were treated with 1:20 anti-CD3/CD28 beads in the presence or absence of the chelator concentrations ranging from 1µM to 20µM. After 24 hours of culture, cells were stained with Propidium Iodide and viability was assessed by Flow Cytometry. Graph represents percentage of dead cells as Mean $\pm$ SEM from n=4 individual donors.

Approximately 1.3% cell death was seen in an average of four experiments where CD4+ T cells had not been treated with the chelator. Treatment with 1µM of CP655 led to a slight decrease in percentage of dead cells. Following this, small but statistically insignificant dose dependent increases in the percentage of dead cells was seen with increasing concentrations of CP655 iron chelator. The highest amount of cell death, 1.66%, was observed after treatment with the highest concentration tested (20µM). Therefore, the effects demonstrated by CP655 cannot be attributed to cell death and toxicity but are in fact specific effects due to iron chelating properties of the compound. Therefore based on these, CP655 was used at a concentration of 5µM for all the following experiments.

Finally, the last check was to ensure viability of CD4+ T cells stimulated with anti-CD3/CD28 beads and treated with varying concentrations of the control compound, CP655OMe (Fig 3.18).

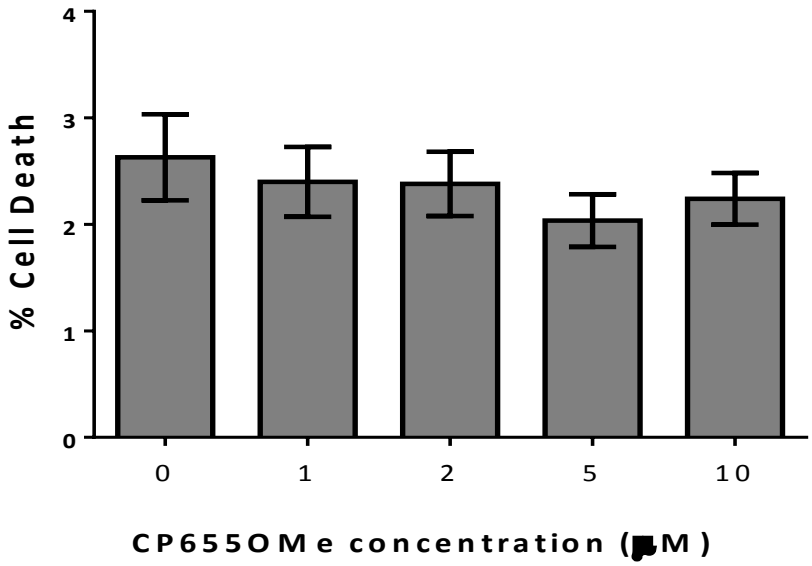

Figure 3.18: ***Viability of CD4+ T cells post CP655OMe treatment:*** CD4+ cells were isolated from fresh PBMCs using Magnetic columns as per the MACS separation protocol. $1x10^6$ cells were treated with 1:20 anti-CD3/CD28 beads in the presence or absence of CP655OMe concentrations ranging from 1µM to 10µM. After 24 hours of culture, cells were stained with Propidium Iodide and viability was assessed by Flow Cytometry. Graph represents percentage of dead cells as Mean ± SEM from n=4 individual donors.

Similar to the results obtained previously, no significant cell death was seen at any of the concentrations of CP655OMe used. The average cell death seen in the absence of any treatment was 2.5% and at all other concentrations the percentage of dead cells was found to be lower than this. The cell death seen on treatment with 5µM of CP655OMe was around 1.9%, and was lower than that seen at any other concentration of CP655OMe used.

Therefore, keeping in line with all previous experiments and results, CP655OMe was also used at a final concentration of 5µM.

3.3.10 Confirmation of CD4+ T cell proliferation by CFSE staining

So far, the proliferation of CD4+ T cells had been measured using Tritiated Thymidine (^{3}H) incorporation. However, since ^{3}H measures DNA replication via its ability to be incorporated within the DNA, it is therefore not a true measure for actual cell division (Lašt'ovička *et al*, 2009). In order to confirm the results obtained so far by ^{3}H thymidine incorporation, another method for measuring cell proliferation was adopted. CD4+ cells were labelled with 5µM CFSE and the dilution of the dye was measured to determine the amount of proliferating CD4+ cells (Fig 3.19).

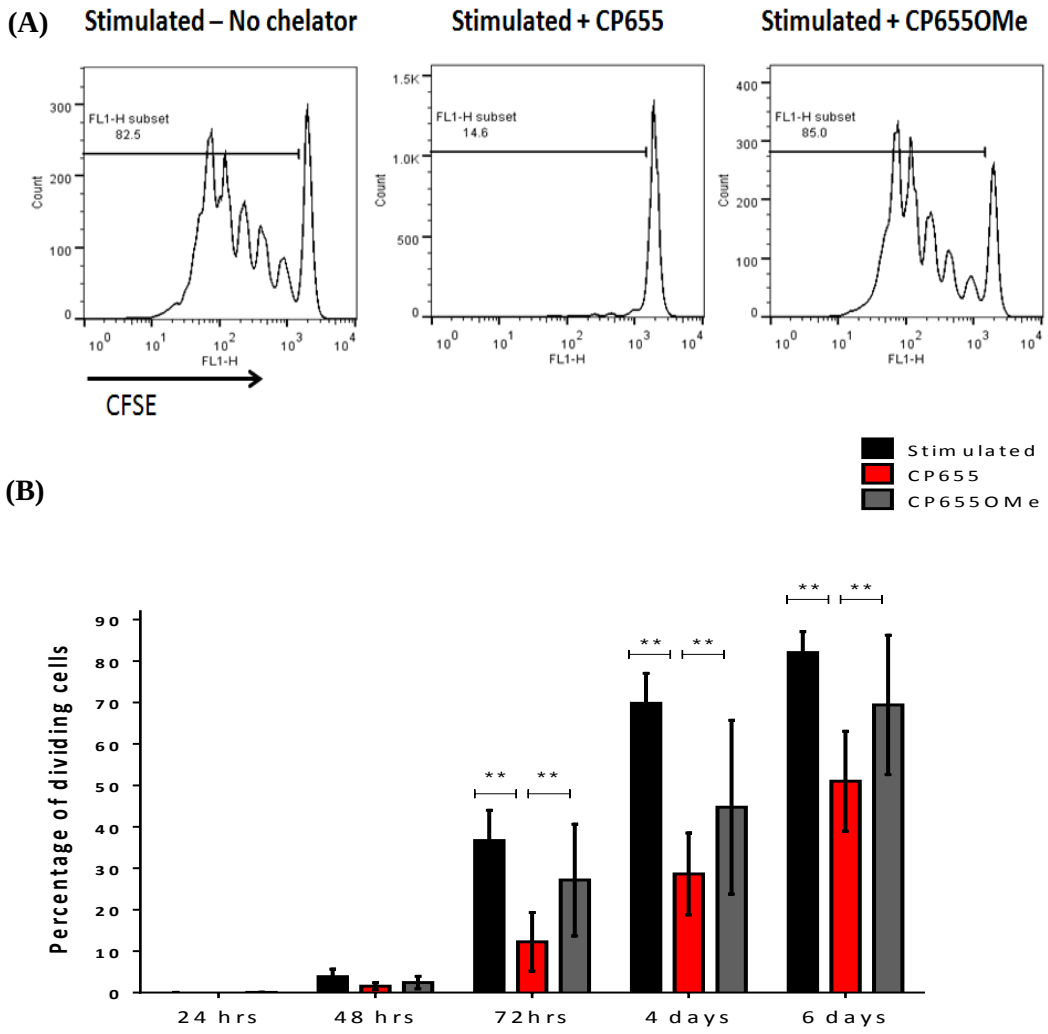

Figure 3.19: ***Proliferation of CD4+ cells by CFSE:*** CD4+ cells were isolated from fresh blood of healthy donors. Cells were stimulated with anti-CD3/CD28 beads in the ratio of 1:20 in the presence of 5µM CP655 or CP655OMe. Proliferation was measured by coating the surface of the cells by 5µM CFSE and measuring dilution of the dye by flow cytometry. (A) Results from one representative donor after 4 days of culture. (B) Cumulative results from n=3 individual donors Results shown as Mean ± SEM. ** $p<0.01$ calculated using Mann-Whitney non-parametric test.

CFSE dye dilution confirmed the tritiated thymidine proliferation results. Results verified that treatment with CP655 is able to inhibit CD4+ T cell proliferation by 40-50%, whereas the control compound CP655OMe has no effect on the proliferation of the cells. Results also showed that the inhibitory effect of the chelator was maintained up till 6 days post stimulation of the cells in culture.

However, in contrast to the previously conducted proliferation assays using ^{3}H thymidine, cell proliferation was only seen from 48 hours after stimulation of the CD4+ cells with anti-CD3/CD28 beads. A significant impact of CP655 on inhibition of proliferation was visible only 72 hours post stimulation of the cells (Fig. 3.19 B). However, using ^{3}H thymidine as a measure of cell proliferation, the effect of CP655 on the inhibition of this proliferation was visible from as early as 12 hours post stimulation.

In order to maintain consistency with previous experiments, tritiated thymidine incorporation was used to measure proliferation in all further experiments.

3.4 DISCUSSION AND CONCLUSION

The aim of this first chapter was to establish the basic effect of HPO chelators on freshly isolated human lymphocytes.

Bi-dentate 3-hydroxypyridine-4-one (HPO) iron chelators were developed in order to overcome the short comings and drawbacks of previously used iron chelators and are currently are the best alternative candidates to DFO (Liu and Hider, 2002). Studies in the past have suggested that DFO can cause toxicities in cells leading to apoptosis, cell shrinkage and chromatin fragmentation (Pan *et al*, 2004). In comparison to DFO, HPO iron chelators display greater selectivity, specificity for iron and have not known to be associated with any cellular toxicities. Additionally due to their lower molecular weight and neutral charge, they exhibit quicker diffusion across the cell membrane and diffuse more freely and within the cell (Hoyes *et al*, 1992). Their greater cell permeability and the ability to cross the blood-brain barrier has made it possible to use them in treating neuro-degenerative diseases that are associated with iron deposition in the brain. Zorzi *et al*, 2011 showed that treatment of patients with pantothenate kinase–associated neurodegeneration with Deferiprone resulted in a significant reduction in the iron deposition in the brain as determined by MRI scans, although no significant changes were seen in the clinical symptoms of the disease. However, a previous study by Forni *et al*, 2008 showed improvements in clinical symptoms and amelioration of disease in a patient suffering from neuro-degeneration after Deferiprone treatment for 10 months. This led to an on-going Phase II clinical trial to test the effect of Deferiprone on patients with Parkinsons Disease (Forni *et al*, 2012).

In order to investigate the effects of novel HPO chelators, four different analogues SF34, CP28, CP655 and CP803 were tested on human lymphocytes. CD4+ T cells and CD14+ monocytes, isolated from healthy donors, were activated by stimulating them with Tetanus toxoid in order to mimic an inflammatory condition. These cells were treated with each of the

HPO chelator analogues and cytokine production from and proliferation of these cells was analysed. The experiments revealed that although all the compounds were analogues they differed in the effects that they exerted on cells due to their varying specificities for intracellular iron. It was found that 7-diethylamino-N-((5-hydroxy-6-methyl-4-oxo-1,4-hydropyridine-3-yl)methyl)-N-methyl-2-oxo-*2H*-chromen-3-carboxamide (CP655) consistently and significantly reduced cell proliferation with a concomitant decrease in IFN-γ and IL-17 production from cell cultures. This was consistent with other studies conducted by Ma *et al* (2004) where the fluorescent iron chelators were used as iron sensors, and demonstrated that out of several HPO chelators tested, CP655 demonstrated the maximum sensitivity to intra-cellular iron. In another study by Ma *et al* (2006), CP655 was found to be the most effective chelator for hepatocytes due to its ability to most effectively reach the chelatable labile iron pool. This was due to the greater permeability displayed by CP655 in comparison to the previously used iron chelators.

Previously iron chelation has been shown to cause cell death due to their ability to promote cellular apoptotic pathways. Therefore, in order to ensure that the suppression caused after CP655 treatment was not associated with increased cell death, the viability of CD4+ and CD14+ cell cultures was assessed after treatment with CP655. Staining with Propidium Iodide confirmed that CP655 was not responsible for any excessive cell death when compared to cells that had not been treated with the chelator. In fact, treatment with lower concentrations of CP655 (1µM - 5 µM) seemed to be protective in nature to the cells, as there was a trend towards increased cell viability when compared to untreated cells. This is consistent with other reports where it has been suggested that iron chelation does not lead to increased apoptosis of cells, and in some cases as also been shown to inhibit TRAIL-mediated apoptosis (Bowlus, 2003; Moon *et al*, 2015).

Having established that the reduced cytokine production and reduced proliferation was not as a result of excessive toxicity or cell death, it was essential to prove that these effects were due to the iron chelating ability of

CP655 and not caused due to any structural or chemical effects of the compound. CP655OMe was developed on special request (Kindly provided by: Robert C.Hider, King's College London) to act as a control compound to CP655. The two compounds are similar in structure, however the main iron binding moiety in CP655 has been masked by methylation in CP655OMe, making it incapable of chelation iron (R.C. Hider, personal communication). Therefore, CP655OMe was used as a control in parallel with to CP655 in order to confirm that the effects of CP655 were due to its ability to chelate iron and not any other structural or physiological property of the chemical compound. The use of CP655OMe in cultures of stimulated CD4+ and CD14+ cells showed that it had no effect on cell proliferation, which was maintained at the same level as the stimulated but untreated cells. These results, along with the results of the viability experiments, made it evident that the significant and consistent inhibition in proliferation and cytokine production after treatment with CP655 was as a result of its ability to chelate intra-cellular iron and cannot be attributed to toxicity or physiological/structural properties of the compound being used.

While the results from experiments so far had provided an insight into the range of effects caused by the novel iron chelator, CP655, they had not provided an indication towards the mechanism that was responsible for the visible effects. It was decided that the first step towards identifying the mechanism of action of the chelator would be to identify and isolate the cell type on which it had its most prominent effect.

CD4+ T cells and CD14+ monocytes were treated separately with CP655 overnight before being mixed in culture and stimulated using tetanus toxoid. The aim of these experiments was to determine the main target cell of CP655. Results consistently suggested that treating CD4+ T cells, rather than CD14+ monocytes, with CP655 exhibited a stronger effect on inhibition of proliferation as well as cytokines production. In fact, treatment of CD14+ monocytes with CP655 led to a small increase in proliferation of cells and had no effect on IFN-γ and IL-17 production as compared to untreated cells. Whereas, cultures where only CD4+ T cells were treated with CP655 showed

a pattern similar to previous experiments, with significant reductions in proliferation of more than 50% and reductions in cytokine production of 25%-30%. These findings were consistent with murine experiments, which also implicated CD4+ T cells to be the main targets of chelator treatment.

Hence it was evident that the main target cells of CP655 treatment were CD4+ T cells. Several studies have highlighted the significant role played by iron in cellular proliferation, however this need for iron is more prominent in rapidly dividing, metabolically active cells such as lymphocytes (Golding and Young, 1995; Mullick *et al*, 2006). When lymphocytes are given a stimulus to proliferate, most of them respond to the stimulus by up-regulating the expression of TfR1 on their surface in order to acquire enough iron to fuel their proliferation. But, the increase in the expression of Transferrin receptors on the surface of T cells is more rapid and of greater magnitude than any other lymphocyte sub-sets (Neckers and Cossman, 1983; Brock, 1989; Seligman *et al*, 1992). In another study by Kumagai *et al* (1988) a comparison between B cells and T cells once again confirmed that T cells express increased levels of Transferrin receptor mRNA after a proliferative stimulus indicating their greater dependence on iron (Bowlus, 2003). Whitley *et al* (1993) also demonstrated that the effect of iron deficiency on host immunity is pre-dominantly due to the effects on functions and migratory patterns of T lymphocytes. Therefore, the literature clearly highlights the high dependence of T cells on iron for growth, differentiation and functioning. Based on this, it is evident that upon depletion of intra-cellular iron CD4+ T cells will be significantly affected, as described by the results discussed above.

So far, the proliferation of cells in all of the experiments was measured by incorporation of Tritiated thymidine into the cells. Tritiated thymidine incorporation into DNA is one of the most commonly used methods for measuring cell proliferation, and often considered the gold standard for proliferation assays (Bading and Shields, 2008). ^{3}H-thymidine is taken up by the cell, and with each cell division this radio-labelled DNA precursor gets replicated into the DNA strands. However, the problems associated with this

technique arise due to the fact that the extent of DNA synthesis does not always represent the exact extent of cell divisions (Maurer, 1981; Naito *et al*, 1987). As a result of these discrepancies, alternative methods of assessing cellular proliferation have been developed such as CFSE staining. CFSE is a non-fluorescent cytoplasmic dye that can track proliferation of lymphocytes by passively diffusing into their cytoplasm. Once inside the cell, specific esterases convert it into a fluorescent compound. With each cellular division, CFSE gets equally distributed to each of the daughter cells as a result of which the fluorescence of the dye is halved with each cell division. Hence, in comparison to ^{3}H-thymidine incorporation that measure DNA synthesis, CFSE staining assess actual cell division and proliferation (Weston and Parish, 1990).

To confirm the results that were obtained by ^{3}H-thymidine proliferation assays, CD4+ T cells stimulated with anti-CD3/CD28 beads and treated with either CP655 or CP655OMe, were stained with CFSE and proliferation was analysed by flow cytometry. In the absence of CD14+ cells to provide co-stimulation, anti-CD3/CD28 beads were used to stimulated CD4+ T cells. As expected, CP655 treated cells showed significantly reduced proliferation as compared to untreated or CP655OMe treated cells. Although the trend observed in both proliferation assays were similar, there was a stark difference in the kinetics. When ^{3}H-thymidine incorporation was used to measure cellular proliferation, significant inhibition of proliferation was observed from time points as early as 18hours post stimulation. However, when CFSE was used, cellular proliferation was visible only from 72 hours post stimulation, which was significantly inhibited following CP655 treatment and continued till up to six days post stimulation.

Furthermore, an observation made during these initial experiments was that while IFN-γ and IL-17 production from cell cultures after chelator treatment was reduced by 25%-35% on average, proliferation was consistently inhibited by 70%. This indicated that one of the key pathways that was being modulated by treatment with CP655 involved the proliferation of CD4+ T cells.

Therefore, based on these results the aim for the following chapter was to determine the mechanism of action behind the effect of CP655 on human CD4+ T cells.

CHAPTER 4

IDENTIFYING THE MECHANISM OF ACTION OF CP655 THROUGH MICRO-ARRAY ANALYSIS

CHAPTER 4

RESULTS

IDENTIFYING THE MECHANISM OF ACTION OF CP655 THROUGH MICRO-ARRAY ANALYSIS

4.1 INTRODUCTION

The results from the first chapter led to the identification of CP655 as the compound that was most potent in reducing inflammatory cytokine production from and proliferation of human CD4+ T cells, from the panel of different chelators that were tested. Additionally, we also determined that the main target cells of the chelator were CD4+ T cells rather than the previously hypothesised CD14+ monocytes.

From all the experiments that were conducted in the previous chapter, one of the observations that stood out was that while IFN-γ and IL-17 production were reduced by 25%-35% each time, proliferation was consistently suppressed by more than 75%. This observation, clearly suggested that the mechanism of action of CP655 may involve interfering or altering with pathways involved in cell proliferation and cell growth.

In order to further elucidate the mechanism of action of CP655, a whole-genome microarray analysis was conducted to identify specific genes or pathways that may be affected by CP655. Conducting a micro-array analysis is considered to be a useful approach when trying to identify changes in a large number of genes in response to treatment with either the chelator or control compound. The understanding of gene interactions and regulation can provide insights into the underlying mechanisms responsible for cellular effects of chelator treatment. The micro-array was conducted with the hope that it would help to identify novel target genes that were potentially involved in regulating CD4+ T cell responses after chelator treatment.

4.2 CHAPTER OBJECTIVES

Based on the discussion above, the specific aims addressed in this chapter are as follows:

a. Determining a suitable time point for conducting microarray experiment

b. Conducting microarray on RNA isolated from human CD4+ T cells

c. Identifying pathways and genes being differentially modulated after CP655 treatment based on analysis of microarray experiment

4.3 RESULTS

4.3.1 Determining ideal time point for microarray experiment

Results from the first chapter identified CD4+ T cells as the main target of the chelator, CP655. Therefore, in order to identify the main pathways and specific target molecules of the chelator, isolated CD4+ T cells were used for the microarray. In the absence of the CD14+ monocytes to provide co-stimulation to the cells, anti-CD3/CD28 microbeads were used to stimulate the cells.

In order to determine the time point most suitable for conducting the microarray, the kinetics, of the effect of CP655 and CP655OMe, were examined from 4 - 48 hours post stimulation (Fig 4.1).

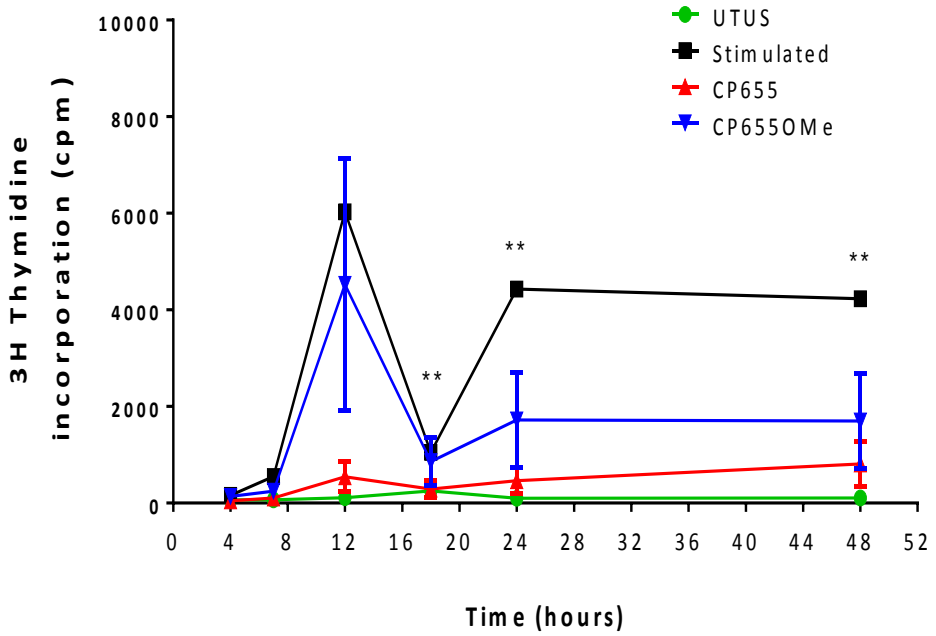

Figure 4.1: ***Kinetics of effect of CP655 on CD4+ T cells:*** CD4+ cells were isolated from blood of healthy donors. Cells were stimulated with anti-CD3/CD28 beads in a ratio of 1:20 in the presence or absence of either of 5µM CP655 or 5µM CP655OMe from 4 hours – 48 hours. At each time point proliferation was measured by incorporation of ^{3}H thymidine. **p<0.01, * p<0.05 calculated using paired t-test. Data represented as mean ±SEM from n=3 individual donors.

The results of the proliferation analysis revealed that while a trend in reduced proliferation of T cells was seen on treatment with the chelator as compared to the control or the untreated cells from as early as 4 hours post stimulation and treatment of the cells, the inhibition was not significant in the first three early time points, that is between 4 and 12 hours post stimulation. However, from 18 hours onwards a highly significant reduction in proliferation of CD4+ T cells was seen on treatment with CP655 in comparison to CP655OMe and untreated cells.

In order to elucidate the mechanism of CP655, a microarray was conducted at the earliest time point at which significant inhibition in proliferation was observed in all donors, that was, 18 hours post stimulation and treatment.

4.3.2 Confirming samples for micro-array analysis

Once the time point to conduct the microarray was determined, the next step was to ensure that the samples taken from the healthy controls for conducting the microarray show the same patterns of proliferation as had been observed so far in previous experiments. Therefore, before RNA was extracted from the cells and used for microarray, tritiated thymidine incorporation was used to measure proliferation for each of the samples (Fig 4.2)

.

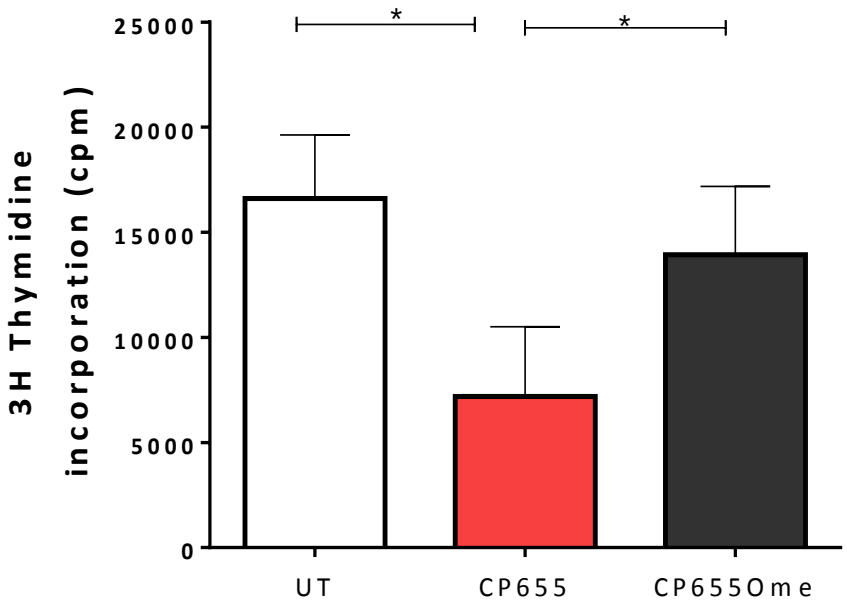

Figure 4.2: ***Proliferation of CD4+ T cell samples used for microarray.*** CD4+ T cells were isolated from PBMCs of healthy donors. Cells were stimulated with either anti-CD3/CD28 beads (1:20) and left untreated or treated with either CP655 (5µM) or the control CP655OMe (5µM) for 18hours. Proliferation was measured by ^{3}H thymidine incorporation. * $p<0.05$calculated using paired t-test. Data represented as mean $\pm$SEM from n=5 individual donors.

The proliferation results from the five donors chosen for micro-array analysis showed that, as before, CP655 significantly reduced CD4+ T cell proliferation as compared to untreated cells as well as CP655OMe treated control cells (Fig 4.2).

4.3.3 Quality analysis for isolated RNA

In order to ensure reliable and valid results of gene expression, good quality RNA was required throughout the experimental process to guarantee successful hybridization and reliable results, as a result of this the quality and quantity of the RNA being used was carefully assessed. The concentration and quality of the RNA sample was assessed by using the Agilent Bioanalyzer. RNA from each of the five samples was isolated as per the Qiagen protocol described earlier. The results from the Agilent Bioanalyzer were used to ascertain the quantity of RNA in each sample and also to maintain a consistent quality of the RNA before it was used for micro-array analysis (Fig 4.3).

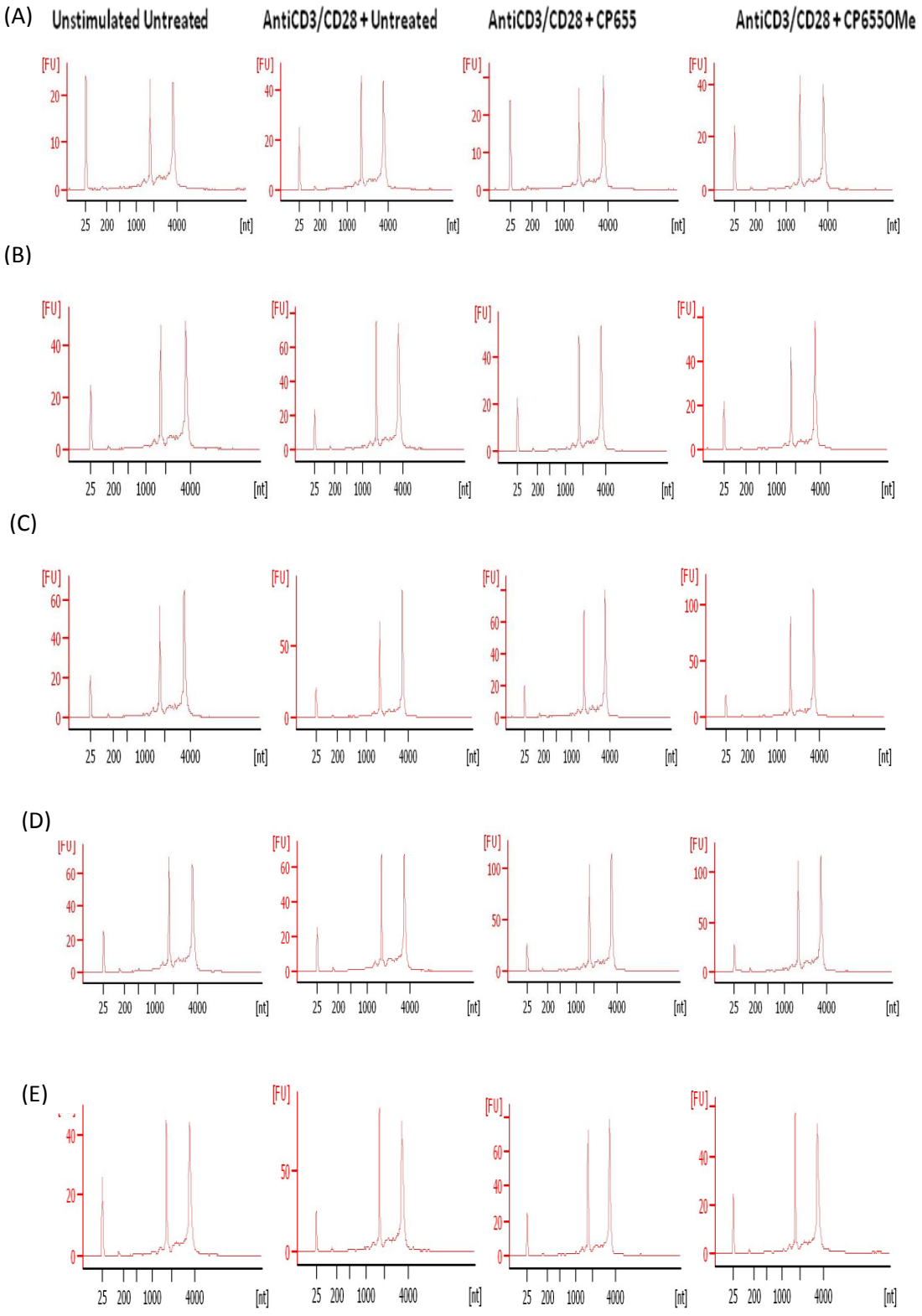

Figure 4.3: ***Quality Check of RNA for whole-genome micro-array.*** CD4+ cells were isolated from fresh blood of a healthy donor. Cells were left either unstimulated or stimulated with 1:20 anti-CD3/CD28 beads in the presence of absence of 5µM CP655 or 5µM CP655OMe. After 18hours of culture, RNA was extracted as per Qiagen protocol. Quality of RNA was assessed by Agilent Bioanalyzer. Each row indicates an individual donor (n=5).

The quality of the RNA was assessed using the RIN scores generated by the Bioanalyzer for each sample. The software provides a score between 1 to 10 for each sample, with 10 denoting good quality and fully intact RNA, and a score of 0 indicating inferior quality, degraded RNA.

The results for each sample used in this microarray showed a RIN score of greater than 9, indicating good quality and intact RNA, which was then used to conduct the micro-array.

4.3.4 Statistical significance testing

Since the aim of this experimental set-up was to assess whether treatment with CP655 or CP655OMe has any significant effect on the expression levels of various genes between 5 different individuals, it was decided to conduct a two-way analysis of variance (ANOVA) using Methods of Moments. This process helped in the identification of genes that were being differentially expressed when compared between CP655 treated, CP655OMe treated or the untreated cells. ANOVA compares the average gene expression level across all biological replicates of the chelator treated cells to the average gene expression level for control treated cells.

4.3.5 Selecting differentially expressed genes

For the experimental set-up described in this chapter, the genes that were classed as being differentially expressed were genes whose expression levels varied between cells treated with the chelator, CP655, as compared to cells treated with control compound, CP655OMe. Initially, genes showing a change of 1.2 folds, either up-regulated or down-regulated, with an unadjusted p value of less than 0.05 were selected, but these criteria produced a relatively limited list of 213 genes only. Additionally, several genes within this list were unknown genes. Therefore, in order to increase the scope of

genes being analysed, the criteria was expanded to include genes showing change in expression levels of 1.0 fold, either up-regulated or down-regulated and with a p value of less than 0.05.

Normally, biologically meaningful changes in expression levels is considered to be 2-fold or more in assays such as Western blot and RT-PCR. However, no such specification exists for micro-array data. Therefore, since fold changes observed overall in this experiment were low, it was decided to focus on genes that were significantly modulated after CP655 or CP655OMe treatment.

4.3.6 Heat Map and Principal Component Analysis (PCA)

The results obtained from the whole genome micro-array produced a list of 33297 genes in the first instance. The list of genes was generated based on the expression of differentially modulated genes following CP655 and CP655OMe treatment, with an unadjusted p value of less than 0.05 in each of the 5 donors tested.

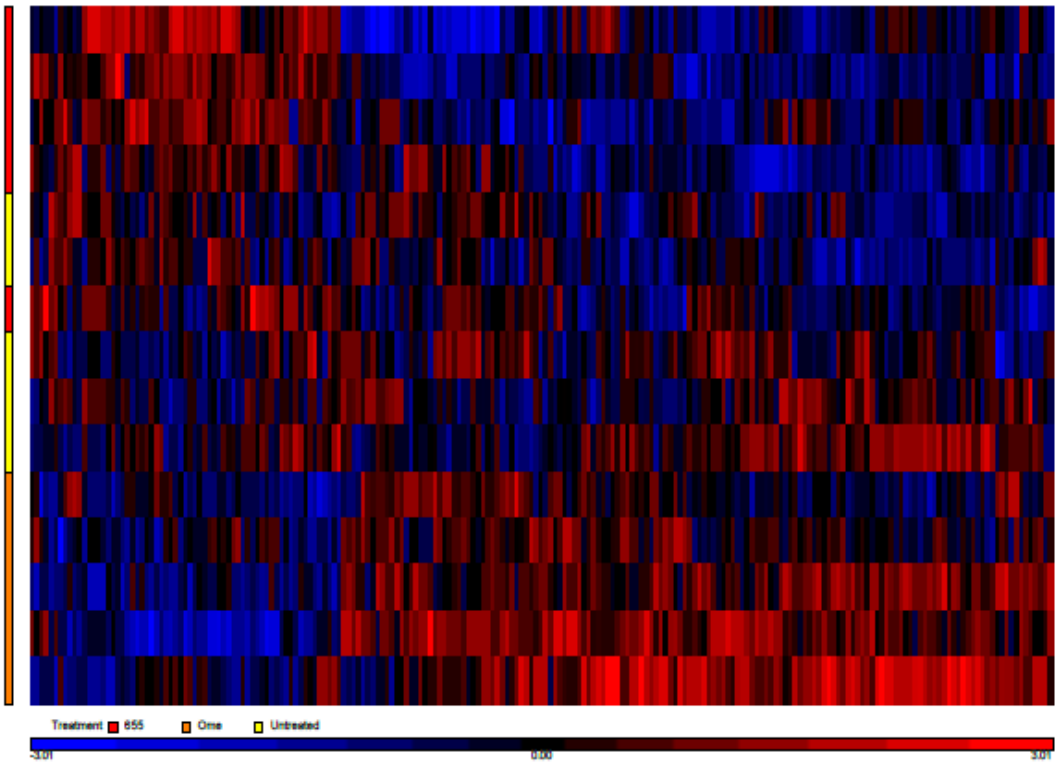

Figure 4.4: ***Hierarchical clustering for genes differentially changed (p<0.05) on treatment with CP655 in comparison to CP655OMe*****:** Cells from five individual donors were either left unstimulated or stimulated with anti-CD3/CD28 beads and left untreated or treated with eitherCP655 or CP655OMe for 18 hours. Extracted mRNA was used for microarray hybridization and analysis. Heat map prepared by GeneSpring Software shows hierarchical clustering using Pearson correlation. Each row represents results from an individual microarray chip (n=15) showing three treatment conditions for each of the five donors. Each column represents an individual gene. Genes have been clustered according to similarities in patterns of expression as shown by the horizontal axis, as well as, by treatment condition in the vertical axis. Treatment conditions are colour coded with red showing CP655 treated cells, Orange bar showing CP655OMe treated and yellow showing Untreated cells. Difference in expression level can be distinguished on the heat map based on colour with high expression genes in red, intermediate expression in black and low expression genes in blue.

Figure 4.4 represents a Heat map which is a visual presentation of the changes in gene expression based on specific treatments. A heatmap is prepared by clustering the data to identify patterns in expression of altered genes. The heatmap in the figure above was generated by unsupervised hierarchical clustering of data. This displays genes that have similar or co-ordinated expression patterns with respect to the specific treatments. Under hierarchical clustering genes are organized based on their similarities to each

other. This suggests that if the expression of two genes is altered at the same time due to the same treatment, their co-expression is probably required to observe the biological effect. The clustering used here was Agglomerative, using Euclidean dissimilarity and average linkage.

The coloured bar on the left side of the heat map indicates the treatment that was provided and each row represents an individual donor. Each coloured column on the heat map represents an individual gene that was significantly modulated when comparing between CP655 and CP655OMe treated samples. The heat map in Figure 4.4 does not take into consideration the unstimulated CD4+ T cells. This was because there were too many differentially modulated genes when comparing between the unstimulated and the CD3/CD28 stimulated samples, as a result of which the effect of the chelator and the control was diminished. Therefore, in order to get a clearer picture showing the effect of CP655 it was decided to disregard the effect caused only due to stimulation of the cells.

Principal Component Analysis

The Principal Component Analysis (PCA) is a mathematical algorithm that is often used in Micro-array data analysis to illustrate and visually analyse the similarities and differences that exist between the samples being tested in order to group them together (Ringner, 2008). The algorithm assesses the direction along with maximum variation in the data is seen and then plots the sample on a 3-dimentional axis.

The PCA of the data set did not highlight any specific patterns that could be used to group the samples together. No specific clustering patterns were noticed with differing effects of treatment or even with stimulation.

However, one of the patterns that were identified showed clustering of the samples based on the age of the donors (Fig 4.5).

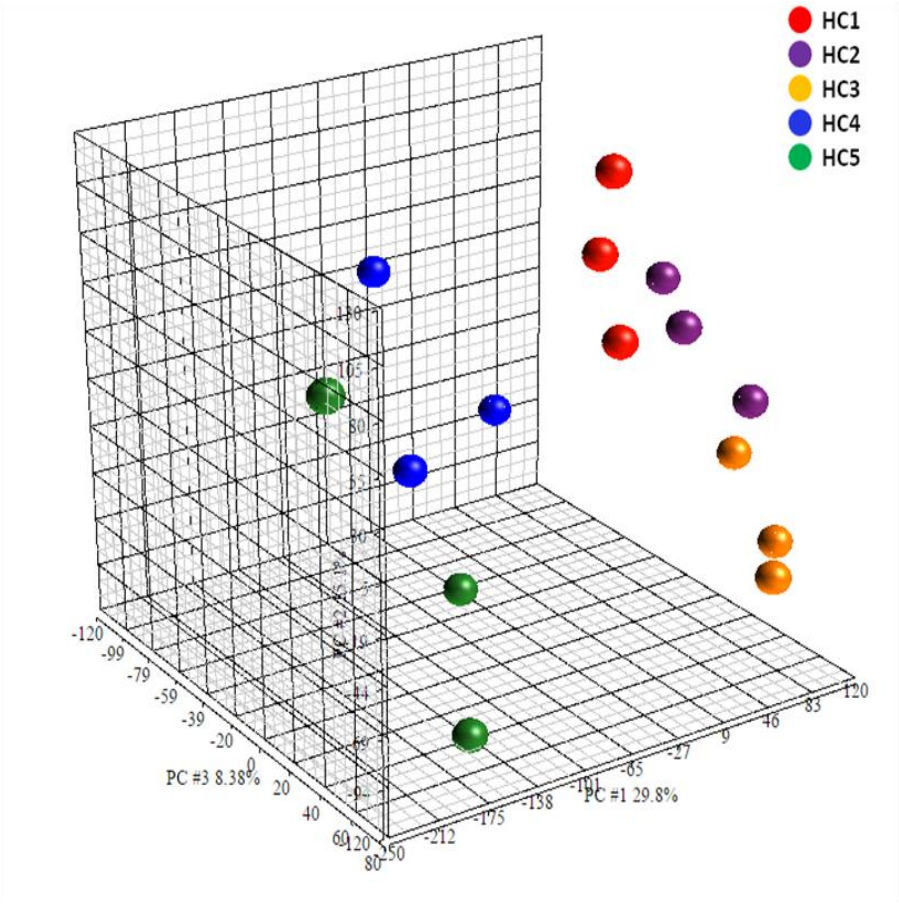

Figure 4.5: ***Principal Component Analysis based on donor differences*****:** mRNA from the CD4+ T cells of five healthy controls were used for microarray hybridization and analysis. Clustering based on donor-derived differences.

The three donors (HC1, HC2 and HC3) clustered together, all belonged to a similar age group (40years - 50years) and were significantly older than the two other donors (HC4 and HC5) who belonged to the 20 years – 25 years age group.

Based on the results of the PCA, previous proliferation data was reanalysed in order to confirm whether there was a correlation between age of the donor and the effect on CP655 treatment on the cells. Proliferation results from 12 of the donors used previously in the first result chapter, grouped according to age, were used to conduct a correlation analysis (Fig 4.6). The donors were grouped according to age, with six donors over the age of 40 and six donors under the age of 40. Correlation between age and the percentage of inhibition

of proliferation after treatment with CP655 was analysed using Spearman's Correlation.

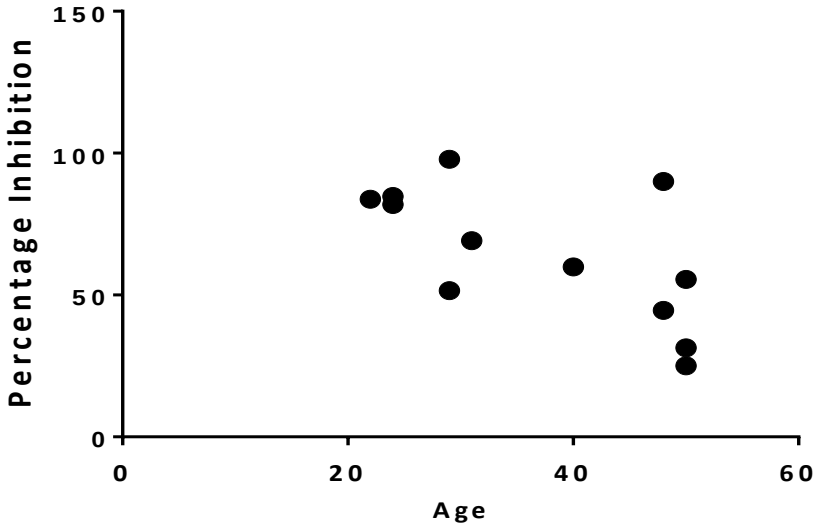

Number of XY Pairs	12
Spearman r	-0.6372
95% confidence interval	-0.8909 to -0.08050
P value (two-tailed)	0.0258
P value summary	*
Exact or approximate P value?	Exact
Is the correlation significant? (alpha=0.05)	Yes

Figure 4.6: ***Effect of CP655 based on age of donor (Age-Proliferation Correlation):*** CD4+ cells were isolated from fresh blood of healthy donors. Cells were left either unstimulated or stimulated with 1:20 anti-CD3/CD28 beads in the presence of absence of 5µM CP655 for 24 hours. Proliferation was measured by ^{3}H thymidine incorporation. Spearman's correlation was conducted between age of each donor and percentage of proliferation inhibition for each donor. Each dot represents an individual donor (n=12).

The analysis revealed that there was a significant negative correlation between age and level of inhibition caused by the chelator. Therefore, with increasing age the extent of CD4+ T cell inhibition caused by the chelator was reduced. The average inhibition of proliferation seen in donors below the age of 40 was 78.16% (Standard deviation $\pm$ 15.93%) and that in donors above the age of 40 was 51.06% (Standard deviation $\pm$ 23.34%).

4.3.7 Pathway Analysis and Identifying genes of Interest

The list of genes that was generated after the first unsupervised clustering and analysis of data contained a large number of unknown genes. This has been reported earlier by Yu and Richardson (2011) where they show that microarray results after chelation using Dp44mT reveal large number of unknown genes on human whole-genome micro-array assays.

Therefore, in order to uncover specific signalling pathways that may have been affected due to the treatment with CP655 or the control CP655OMe, Partek and GeneGo software were used to conduct pathway analysis of the data generated. However, while there were highly significant changes in gene expression when comparing between chelator and control treated cells, the fold change values were small. This prevented the software from clearly highlighting specific pathways that may have been altered by the treatment process (Fig 4.7).

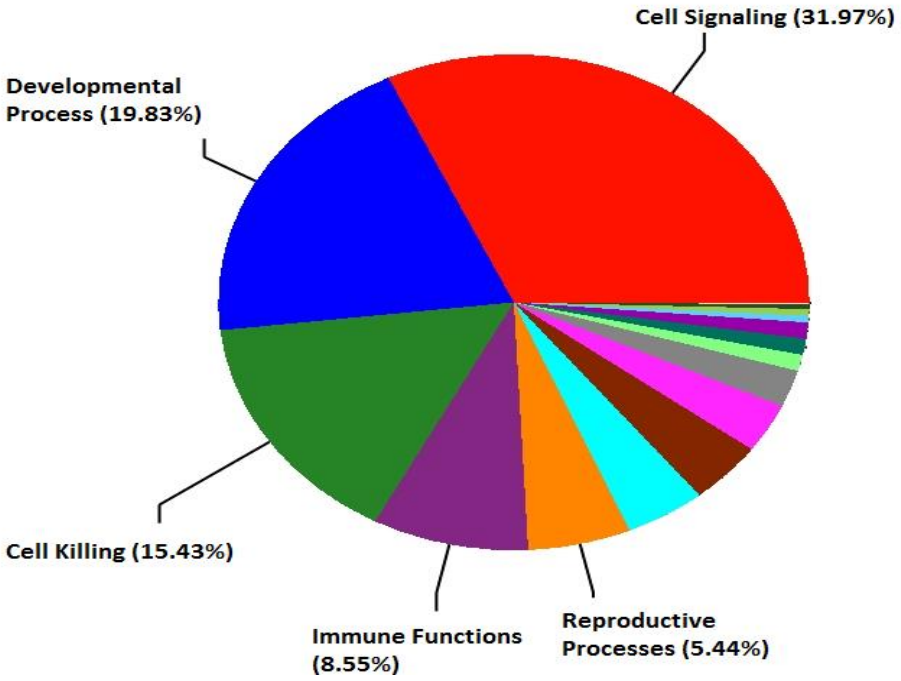

Figure 4.7: ***Pie-chart illustrating the most differentially modulated cellular pathways between CP655 and CP655OMe treatments*****:** GO-ontology software was used to determine pathways to which most of the differentially modulated genes belonged. Maximum percentage of modulated genes belonged to Cell Signaling pathways (31.97%) followed by genes controlling developmental processes (19.83%). The top five pathways have been shown in the figure.

The initial results from the pathway analysis showed that the pathway most affected by the treatment with CP655 as compared to CP655OMe was the cell signaling pathway, comprising of almost 32% of the total pathways affected. The second and third most affected pathways were those controlling cell developmental processes and cell killing pathways respectively (Fig 4.7).

However, the analysis of the initial list of genes generated was unsuccessful in highlighting any statistically significant specific pathways. Therefore, the literature was consulted to uncover genes that may be modulated by altering intra-cellular iron levels using different iron chelators. A review of the literature on iron regulation and inflammation, and cross-linking it to the initial list of genes significantly modulated by chelator versus control treatment and fold change of 1.0, up-regulated or down-regulated, led to the identification of 20 genes of interest. These genes have been linked to iron

regulation, iron metabolism and inflammatory processes within the human body and were also found to be significantly changed in the results of our micro-array studies (Table 4.1 and 4.2). Heat map for these genes is shown in Figure 4.8.

Gene Symbol	Gene Name	Fold Change (CP655 vs CP655OMe)	Function
CDC6	Cell Division Cycle 6	-1.2298	Initiation of DNA replication and ensures complete replication of DNA before mitosis. It is found to be localized in the nucleus in G1 phase of the cell cycle. Interacts with 4, iron 4, sulphur clusters (Petrakis *et al*, 2012).
DLGAP5	Disks large-associated Protein 5	-1.1417	Plays a role in carcinogenesis by potentially regulating the cell cycle. Knockdown of DLGAP5 inhibits cell proliferation by increasing p53 (Kuo *et al*, 2012). Gene-Ontology Molecular functions includes iron binding (ncbi, gene database)
CLSPN	Claspin	-1.1209	Required for cell cycle progression and movement through S-phase (Broderick *et al*, 2013). Maintains replication fork rates and stability (Yoshimura *et al*, 2011).
GINS4	GINS complex subunit 4	-1.0741	Required for initiation and progression of DNA replication, by moving ahead of the replication fork and unwinding double stranded DNA (MacNeill, 2010).

IREB2	Iron-responsive Element Binding Protein 2	-1.0712	Required for cellular iron homeostasis. Binds to Iron-Responsive elements in the 5' and 3' UTR of Ferritin and Transferrin respectively (Kuhn, 2015).
CDC25A	Cell Division Cycle 25A	-1.0563	Required for the transition from G1 to S phase of the cell cycle by activating cell dependent kinase, CDC2 and other cell cycle proteins (Hong *et al*, 2012)
ANAPC1	Anaphase Promoting Complex 1	-1.0557	E3-ubiquitin ligase that controls the progression of cells through G1 phase of cell cycle by ubiquitination and degradation of target regulatory proteins (Pines, 2011).
NAA35	N(Alpha)-Acetyltransferase 35	-1.0547	Negative regulator of apoptotic processes. Inhibition of NAA35 causes p53-dependent apoptosis (Starheim *et al*, 2009).
SMAD1	SMAD family member 1	-1.0393	Regulates and mediates several signalling pathways of cell growth, apoptosis and immune responses in response to BMP1 (Liu *et al*, 2014).
MIR320A	MicroRNA 320a	-1.0314	Inhibits cellular proliferation and cancer cell metasis (Sun *et al*, 2012)
RRM1	Ribonucleotide Reductase subunit M1	-1.0277	Synthesis of deoxy-ribonucleotides from ribonucleotides, necessary for

			synthesis of DNA (Zhou *et al*, 2013). Dependent on iron for proper functioning (Kayyali *et al*, 2001).
GINS3	GINS complex subunit 3	-1.0245	Initiation of DNA replication and progression of DNA replication fork (MacNeill, 2010).

Table 4.1: List of genes significantly down-regulated on treatment with CP655 showing greater than 1.0 fold change.

Gene Symbol	Gene Name	Fold Change (CP655 vs CP655OMe)	Function
CACNB4	Calcium Channel, Voltage-dependent, beta 4 subunit	1.15305	Plays a role in Calcium channel functioning by controlling G protein inhibition (Subramanyam *et al*, 2009).
CDKN1A	Cyclin-Dependent Kinase Inhibitor 1A	1.15253	Blocks cellular proliferation by inhibiting cyclin-dependent kinase activity. At low concentrations promotes CyclinD-CDK4 complex formation and nuclear localization, but at high concentrations, inhibits CyclinD-CDK2/4 activity. Can selectively bind to metal ions (Yu *et al*, 2007)
GADD45G	Growth-Arrest and DNA Damage inducible Protein, Gamma	1.1182	Regulation of growth and differentiation via positive control of Apoptotic pathways. Gene expression up-regulated due to growth arrest after cellular stress and activates stress responses (Saletta *et al*, 2011).
TNFAIP2	Tumour Necrosis Factor Alpha-inducible Protein 2	1.11122	It is a retinoic acid target gene, whose expression is induced by TNF-alpha and promotes cellular migration

			in carcinomas (Chen *et al*, 2011).
TGFB1	Transforming Growth Factor, beta 1	1.06621	Mature protein regulates cellular proliferation, adhesion, migration and differentiation. Frequently up-regulated in several tumour cells (Xu *et al*, 2007).
CDCA4	Cell Division Cycle Associated Protein 4	1.03991	Regulation of cell division and cell proliferation via E2F/RB pathway. Organization of the spindle apparatus during pro-metaphase (Wang *et al*, 2008).
MIR503	Micro-RNA 503	1.03019	Increased expression associated with inhibition of proliferation and metastasis in Hepatocellular Carcinoma (Zhou *et al*, 2013).
MIR99A	Micro-RNA 99A	1.00657	Potentially involved in promoting myeloid leukemia by promoting proliferation and inhibiting apoptosis (Zhang *et al*, 2014). Also shown to act as a tumour suppressor by inhibiting proliferation in bladder cancer (Feng *et al*, 2014).

Table 4.2: List of genes significantly up-regualted on treatment with CP655 with greater than 1.0 fold change.

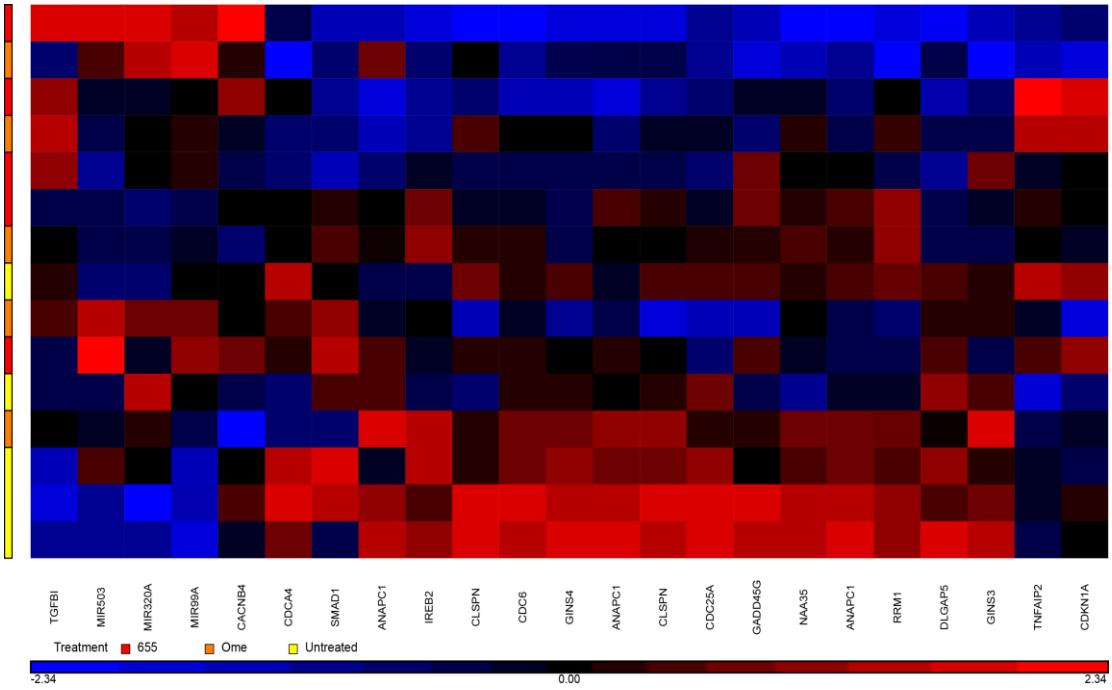

Figure 4.8: ***Hierarchical clustering for genes differentially changed (p<0.05) on treatment with CP655 in comparison to CP655OMe*****:** Cells from five individual donors were either left unstimulated or stimulated with anti-CD3/CD28 beads and left untreated or treated with eitherCP655 or CP655OMe for 18 hours. Extracted mRNA was used for microarray hybridization and analysis. Heat map prepared by GeneSpring Software shows hierarchical clustering using Pearson correlation. Each row represents results from an individual microarray chip (n=15) showing three treatment conditions for each of the five donors. Each column represents an individual gene. Genes have been clustered according to similarities in patterns of expression as shown by the horizontal axis, as well as, by treatment condition in the vertical axis. Treatment conditions are colour coded with red showing CP655 treated cells, Orange bar showing CP655OMe treated and yellow showing Untreated cells. Difference in expression level can be distinguished on the heat map based on colour with high expression genes in red, intermediate expression in black and low expression genes in blue.

The new list of 20 genes indicated that a large proportion of genes that were being differentially modulated were genes controlling for cell proliferation, growth and differentiation. Several cell cycle proteins, cyclinsand cdk inhibitors were amongst the genes significantly modulated by CP655 treatment. These results were in accordance to the data discussed in the previous chapter where it was seen that the most prominent effect of chelator treatment was on inhibition and suppression of cell proliferation.

Even though, the genes identified in this list showed a relatively modest fold change after treatment with CP655, the changes across the five donors tested were highly significant on treatment with CP655.

Based on the indications provided by the microarray data, functional studies to look at the cell cycle block caused by CP655 in purified CD4+ T cells were conducted, and some of genes short-listed from this microarray data were validated by RT-PCR.

4.4 DISCUSSION AND CONCLUSION

The main objective of this chapter was to use microarray analysis to identify specific pathways and genes that may be the target of CP655 and play a role in its mechanism. A microarray analysis on purified CD4+ T cells stimulated with anti-CD3/CD28 beads and treated with either the chelator, CP655 or the control compound, CP655OMe was considered to be ideal for discerning the specific genes or pathways that are getting modulated differentially due to treatment.

To begin with, it was essential to identify the time point that would be most suitable for conducting the microarray and in which the most constructive results could be obtained. Stimulated CD4+ T cells with either CP655 or CP655OMe were kept in culture for various time points from 4 hours to 48 hours. At each of the time points, proliferation was assessed by ^{3}H-Thymidine incorporation. The results indicated that, although a trend towards reduced proliferation after CP655 treatment began to emerge from as early as 4 hours post stimulation and treatment, significant levels of proliferation and differences between treatments were observed only 18 hours onwards. Therefore, based on this 18 hours was chosen as the time point to conduct the microarray analysis on CD4+ T cells.

The initial analysis of the micro-array results revealed that while there were highly significant changes in differentially expressed genes, the extent of the change that is indicated by the fold change were small. Another observation that was made during the initial analysis of the results was that there were a large number of unknown genes, and pseudo genes of no known function that appeared in the list of significantly modulated genes. A similar problem was reported by Yu and Richardson (2011) in a microarray conducted to study the role of cellular iron depletion using Dp44mT iron chelator. They showed that the majority of the genes significantly altered after treatment with Dp44mT were of unknown functions and they were unable to identify their molecular interactions. Several other studies in the past studying the effect on iron

chelation on various cellular and molecular processes via microarray analysis have revealed that the majority of the genes that are up-regulated on treatment with chelators are of unknown origin (Ducey *et al*, 2005; Saletta *et al*, 2010; Hernandez-Prieto *et al*, 2012).

With the reassurance that the presence of large number of unknown genes in the list of differentially expressed genes was not an anomaly with the data, Principal Component Analysis (PCA) and pathway analysis was conducted to identify any overlying patterns and trends in the data. The pathway analysis showed that genes most significantly modulated belonged to cell signalling and cellular developmental pathways. A further analysis by KEGG pathway analysis and Gene-GO analysis revealed that the three most modulated pathways were Immune responses via the NKG2D signalling pathway, the Pyruvate metabolism pathway and the Immune responses in T cells pathway. However, due to the extremely low levels of fold change in the data set, none of these analyses revealed any significant patterns or pathways that could provide a concrete indication regarding the mechanism of the iron chelator. Therefore, from the initial list of genes a new list was generated that included only those genes that were significantly modulated between CP655 and CP655OMe treated samples with a fold change of at least 1 fold or more. This time instead of relying on pathway analysis software, it was decided to conduct a manual search on the genes and the various pathways that they belonged to and correlate them to a review of the literature to identify genes of interest.

The main role played by iron in cellular signalling processes is concentrated around its control of the cell cycle and apoptotic pathways (Lewis *et al*, 1998; Darnell and Richardson, 1999; Deb *et al*, 2009). Saletta *et al* (2011) compared the effect of two different iron chelators and also demonstrated that the main pathways that seem to be differentially modulated by iron chelation were those controlling cellular proliferation, cell cycle and apoptosis. These results were encouraging as they corroborated the effect on inhibition of proliferation that had been observed in experiments conducted in this study. A review by Templeton and Liu (2003) suggested that due to the essential

role played by iron in cellular processes, changes in intracellular concentration of iron can result in a large number of changes in cellular, metabolical and physiological pathways. Although there is increasing evidence to suggest that the changes in cell cycle and cellular proliferation are one of the most prominent effects of cellular iron depletion. Gao and Richardson (2001) compared the effects of two iron chelators, DFO and 311, on a human neuroepithelioma cell line and showed that both were able to cause significant alterations in the expression of cell cycle regulators such as cyclin D1, D2, D3, cyclin A, cyclin B1, and phosphorylation of Rb. Also, they showed an increase in mRNA levels of p21 and GADD45G. Le and Richardson (2002) reviewed the various studies conducted on the role of iron in cell proliferation and division and concluded that the regulation of critical cell cycle molecules such as p21, p53, N-myc and c-myc by intra-cellular iron levels makes iron chelators a vital and effector anti-tumour tool.

Another observation that was made while comparing the data to the literature on microarray analysis after iron chelation showed that several studies conducted the microarray at least 24 hours after the cells had been stimulated and treated with their respective iron chelators (Saletta *et al*, 2010; Yu and Richardson, 2011). Therefore, it was possible that the 18 hour time point chosen to conduct the microarray in this study was too early to visualize any significant changes in the expression of the genes of interest. Additionally, as seen in the previous chapter, the time point at which significant suppression of proliferation was observed varied based on method that was used. This discrepancy with the time point could be a reason for why the fold changes seen in the microarray experiment were smaller than expected.

A review of the list of genes differentially modulated between CP655 and CP655OMe showed that out of the 20 most significantly modulated genes, 5 genes were of unknown function, and out of the remaining 15 genes, 8 genes (CUL3, CENPO, TNFAIP2, ANAPC1, MAP3K8, MCM3, C10orf90 and DNMT3A) belonged to various pathways controlling cell cycle, DNA replication and cell proliferation. Additionally, it was also observed that there were several cyclins (cyclin F, cyclin B3, cyclin E1, cyclin B1), Cell

Division Cycle proteins (CDC25A, CDCA5, CDC16, CDC6) and CDK proteins (Cdk20, Cdk1, Cdk5) that were in the list of highly significantly modulated genes. This reinforced the information gathered from the literature suggesting the essential requirement of iron for cell cycle progression and its subsequent inhibition following iron depletion.

In order to move ahead with the analysis, a list of 20 genes, 12 down-regulated and 8 up-regulated genes was prepared, based on the literature and indications from the data so far. This list consisted of cell cycle proteins (CDC6, CDC25A, ANAPC1, CDKN1A, NAA35 and CDCA4), miRNAs (miRNA 320A, miRNA 99A and miRNA 503), genes involved in DNA replication (RRM1, GINS3, GINS4, CLSPN), genes involved in carcinogenesis and tumorigenesis (DLGAP5, GADD45G, TGFB1, TNFAIP2).

Since it was beyond the scope of this study to analyse each of the 20 genes identified in order to determine which of these might be a potential target of the chelator CP655 and help point out a mechanism of action for the chelator, it was decided to further narrow down this list of genes and validate their expression by other techniques such as RT-PCR and Western Blotting. The genes chosen for RT-PCR and their biological validation in discussed in the following chapter.

CHAPTER 5

BIOLOGICAL VALIDATION OF MICROARRAY DATA

CHAPTER 5

RESULTS

BIOLOGICAL VALIDATION OF MICROARRAY DATA

5.1 INTRODUCTION

Iron is essential for cell proliferation and viability and it is well established that disrupting the iron uptake and metabolism of cells can be harmful for the cells, causing cell cycle arrest (Bowlus, 2003). This indispensable role played by iron in cell growth and division has been exploited by the use of iron chelators whose anti-proliferative activity has been found to be beneficial for treating not only iron overload diseases but also for controlling tumour growth and excessive cell proliferation (Yu *et al*, 2006; Munoz *et al*, 2009)

The following chapter aims to identify the mechanism of action of the iron chelator CP655. The results of the previous chapter highlighted that the main pathways as well as the main molecular targets of CP655 treatment were those controlling various aspects of the cell cycle. The chapter will begin by confirming the results of the microarray by conducting functional studies for assessing cell cycle progression in the presence of CP655. Genes that will be shortlisted from the microarray will then be validated by RT-PCR.

As the most prominent effect of CP655 treatment was seen on the inhibition of proliferation, this chapter will then examine the effect of CP655 on one of the main pathways that control cell proliferation and growth – the IL-2 pathway. The chapter will aim to determine the effect that addition of exogenous IL-2 can have on CP655 or CP655OMe treated cells, in order to determine whether inability to respond to IL-2 stimulus could be one of the possible mechanisms of action of CP655. Following this, the effect of iron chelation on the down-stream molecules of the IL-2 pathway, STAT5, will be examined as another potential mechanism of action for CP655.

5.2 CHAPTER OBJECTIVES

Based on the discussion above the specific aims for this final results chapter are as below:

(a) Conducting functional analysis of cell cycle progression in CD4+ T cells
(b) Validating genes short-listed after micro-array analysis and cell cycle studies
(c) Elucidating potential mechanisms for CP655 action
    (i) Mechanism 1 – Effect of CP655 on cell cycle proteins
    (ii) Mechanism 2 – Effect of CP655 on IL-2 pathway and downstream signalling molecules

5.3 RESULTS

5.3.1 Effect of CP655 on cell cycle of Jurkat and human CD4+ T cells

Analysis of the results obtained from the previous chapter highlighted that the genes which were most significantly modulated by CP655 treatment mostly belonged to pathways controlling cell cycle progression. In order to confirm the results obtained from the micro-array, it was essential to be able to replicate the results in a functional cell cycle assay.

To begin with based on a study by Gharagozloo *et al* (2008) analysing the effect of iron chelator Silybin on cell cycle, Jurkat cells were cultured from 24 hours - 72 hours either untreated or in the presence of CP655 or the control compound CP655Ome. At each time point, the nuclear material was stained with Propidium Iodide and analysed on the flow cytometer. After 24 hours of culture, there was no difference in the cell cycle profile of the untreated or the chelator and control treated cells. The G1, S and G2/M phase of the cell cycle had the same percentage of cells under all the three treatment conditions (Fig 5.1 A, Fig 5.2 A).

However, after 48 hours of culture, treatment with CP655 perturbed the normal cell cycle of the Jurkat cells. The percentage of cells in the G1 stage was significantly reduced in the cultures that were treated with CP655 but not in those that were treated with CP655OMe. Also, the percentage of cells in the S stage was significantly and consistently enhanced in the chelator treated cultures as compared to both the untreated and the control treated cells. A similar pattern was also observed 72 hours after culture (Fig 5.1 B, C; Fig 5.2 B, C).

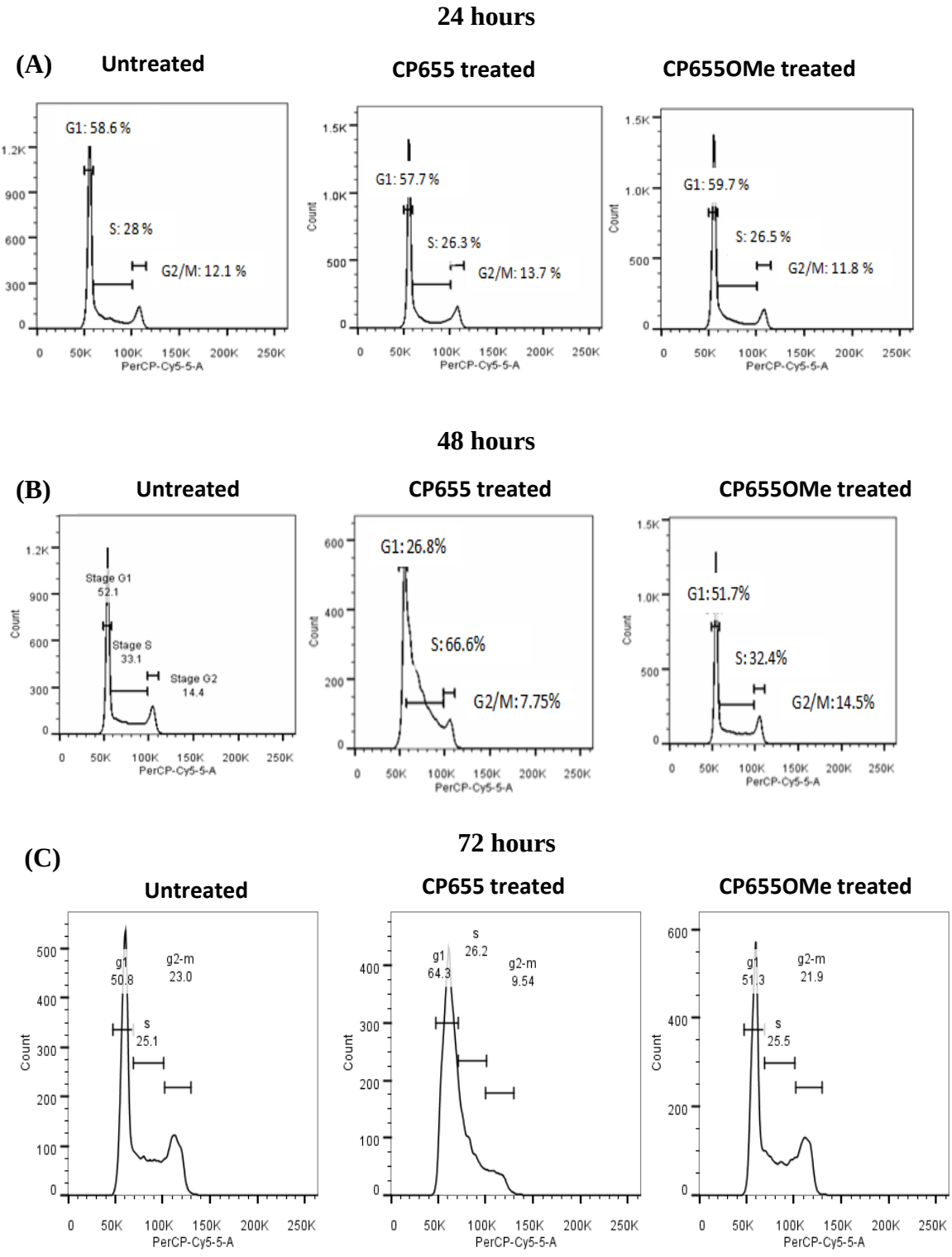

Figure 5.1: ***Cell cycle arrest of Jurkat cells*****:** Jurkat cells were either left untreated or treated with either 5µM CP655 or CP655OMe from 24 hours – 72 hours. Cells were lysed with cold 100% ethanol and stained with Propidium Iodide and Ribonuclease A, before analysing the cells by flow cytometry. (A) 24 hours post cell culture. (B) 48 hours post cell culture. (C) 72 hours post cell culture. FACS results from one representative experiment.

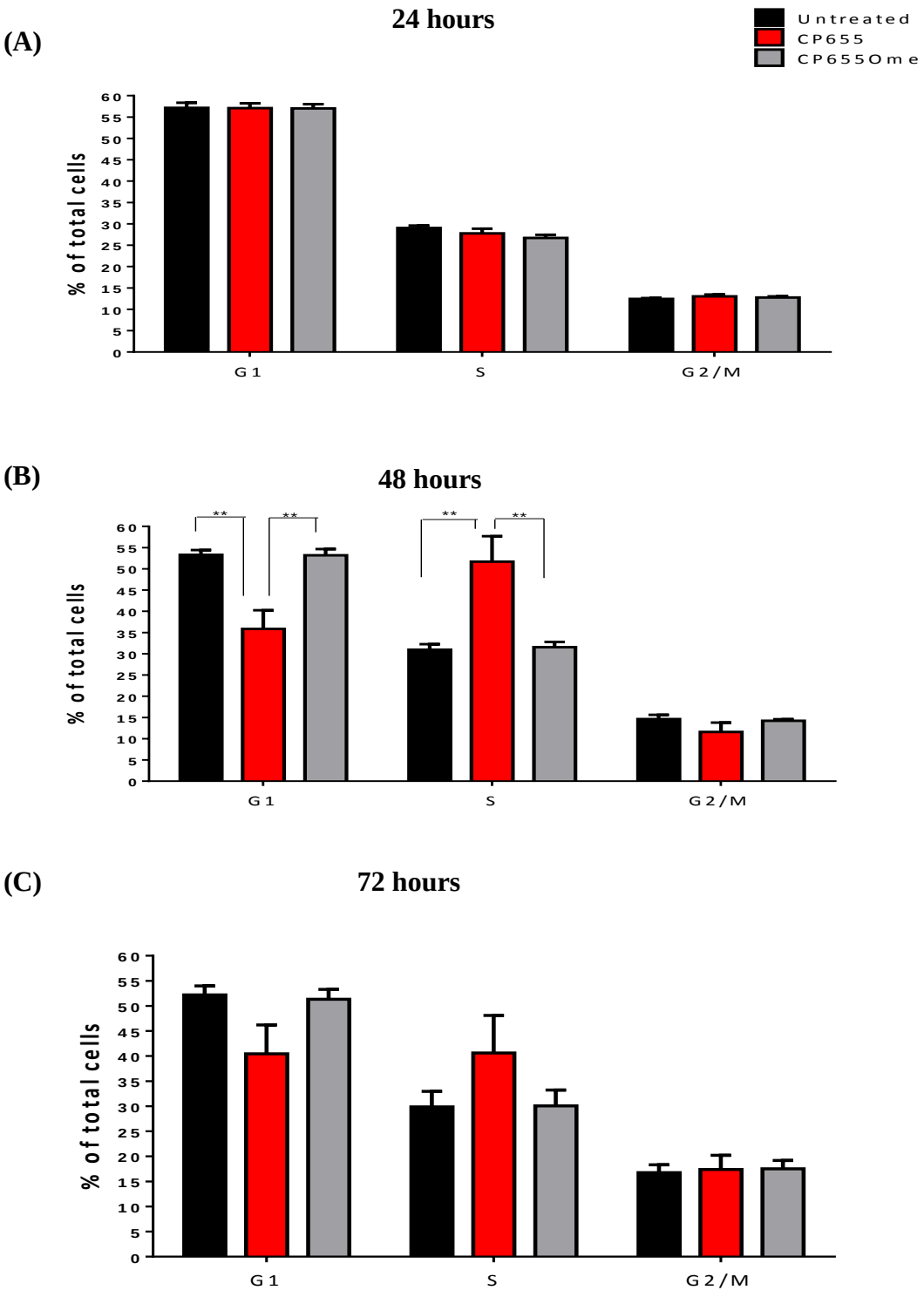

Figure 5.2: ***Cumulative data showing cell cycle arrest of Jurkat cells:*** Jurkat cells were either left untreated or treated with either 5µM CP655 or CP655OMe from 24 hours – 72 hours. Cells were lysed with cold 100% ethanol and stained with Propidium Iodide and Ribonuclease A, before analysing the cells by flow cytometry (A) 24 hours post cell culture. (B) 48 hours post cell culture. (C) 72 hours post cell culture. ** $p<0.01$ calculated using paired t-test. Results shown as Mean $\pm$ SEM from n=4 individual cultures.

Having successfully shown the effect of CP655 on altering cell cycle of Jurkat cells, the next step was to replicate the results using primary CD4+ T cells isolated from PBMCs of healthy donors to confirm whether a similar effect of the chelator can be seen in primary human cells. 24 hours after stimulation of cells with anti- CD3/CD28 beads, no cycling cells were visible via flow cytometry (Fig 5.3 A; Fig 5.4 A). However, after 48 hours of culture, cycling cells were visible. Approximately 50% of the stimulated CD4+ cells were seen in the G1 phase of the cell cycle. In the cell cultures that had been treated with CP655, it was seen that there was a consistent trend showing an increase in the percentage of cells arrested in the G1 phase. This led to a reduction in the percentage of cells entering the S phase, and a subsequent significant reduction in the percentage of cells present in the G2/M phase of the cell cycle. As previously seen, this effect was found only in cell cultures that had been treated with the iron chelator CP655 and not with the control compound CP655OMe, which consistently showed a profile similar to that of the untreated cells (Fig 5.3 B; Fig 5.4 B). The same trend was visible 72 hours post cell culture as well (Fig 5.3 C; Fig 5.4 C).

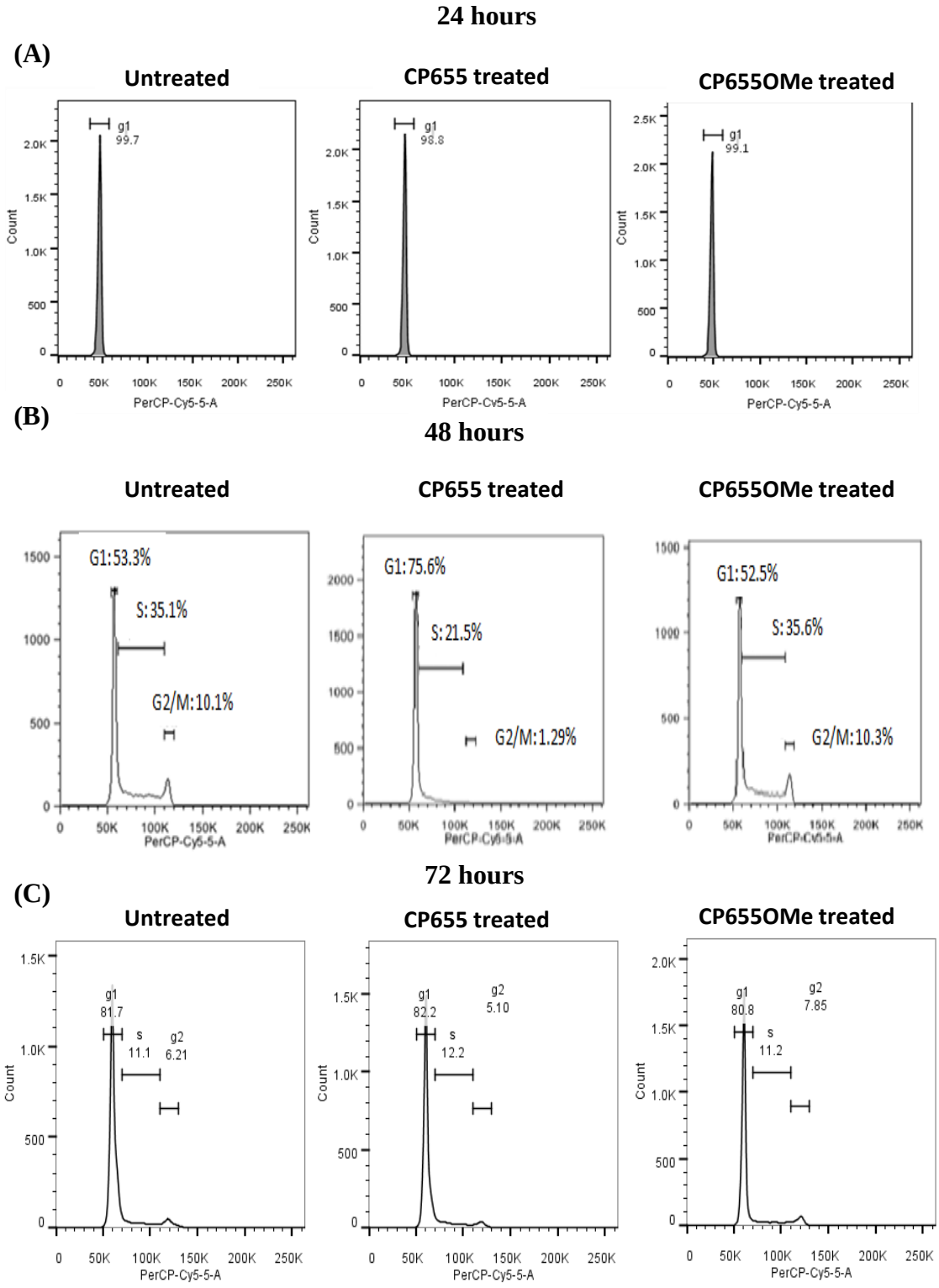

Figure 5.3: ***Cell cycle arrest of primary CD4+ T cells:*** CD4+ T cells were isolated from fresh PBMCs of healthy donors. Cells were either left unstimulated or stimulated with 1 : 5 bead: cells ratio of anti-CD3/CD28 beads in the presence or absence of either CP655 (5µM) or CP655OMe (5µM). Cells were lysed with cold 100% ethanol and stained with Propidium Iodide and Ribonuclease A, before analysis by flow cytometry. (A) 24 hours post cell culture. (B) 48 hours post cell culture. (C) 72 hours post cell culture. Graphs represent FACS results from one representative experiment.

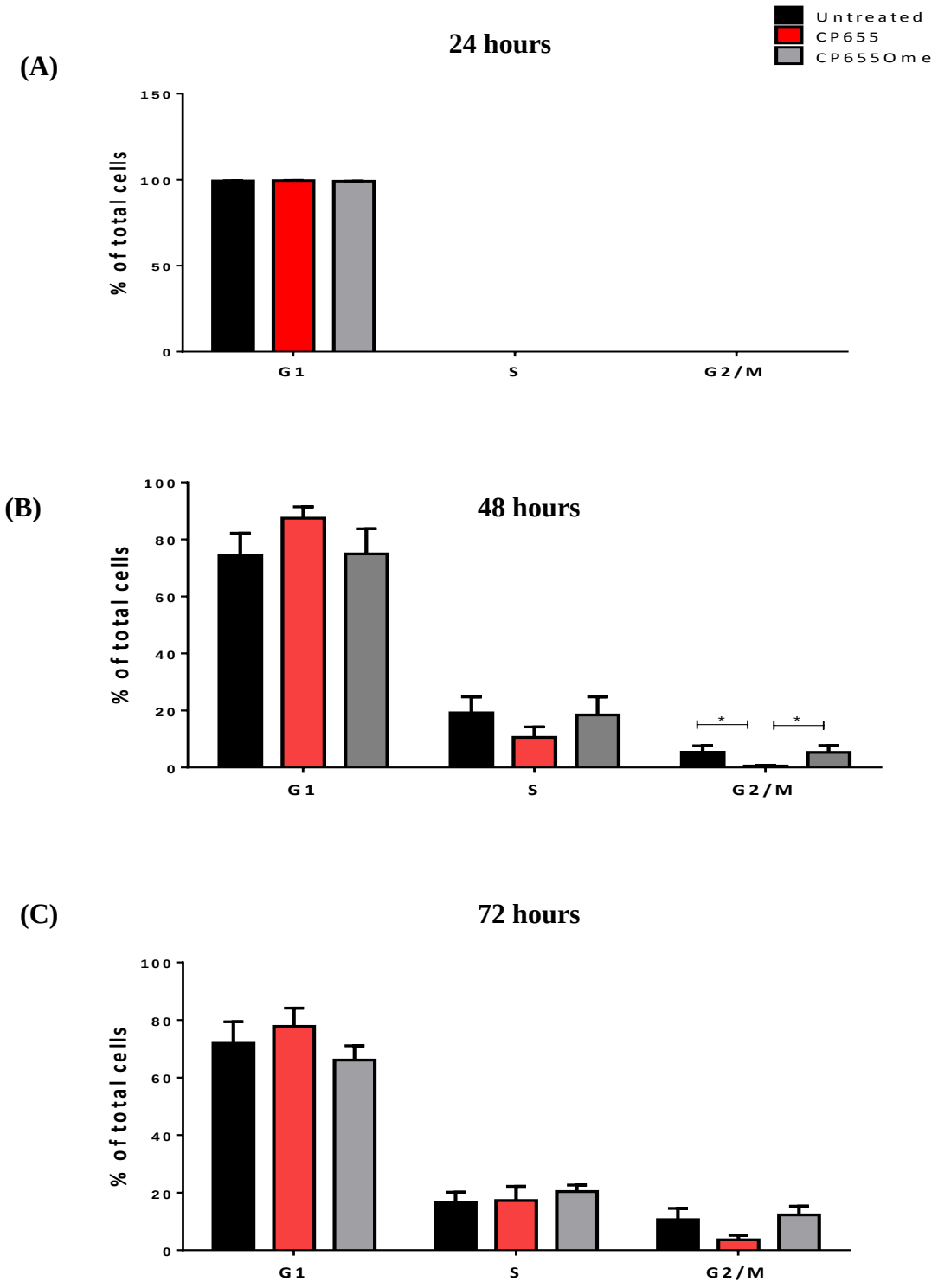

Figure 5.4: ***Cumulative data showing cell cycle arrest of primary CD4+ T cells:*** CD4+ T cells were isolated from fresh PBMCs of healthy donors. Cells were either left unstimulated or stimulated with 1:5 bead: cells ratio of anti-CD3/CD28 beads in the presence or absence of either CP655 (5µM) or CP655OMe (5µM). Cells were lysed with cold 100% ethanol and stained with Propidium Iodide and Ribonuclease A, before analysis by flow cytometry Cumulative results from n=4 donor. (A) After 24hours of culture. (B) After 48 hours of culture. (C) After 72 hours of culture. * $p<0.05$ calculated using paired t-test. Results shown as Mean $\pm$ SEM from n=4 individual donors.

These results corroborated the indications that were provided by the microarray data, confirming that CP655 treatment was indeed interfering with the normal progression of the cell cycle. The analysis revealed that CP655 was causing a block in the G1/S phase of the cell cycle. In order to decipher the mechanism that CP655 was using to cause this block it was decided to once again conduct a detailed review of the literature and correlate the findings with the list of 20 genes developed at the end of microarray analysis. Following this, genes that have been previously implicated in the literature for causing a G1/S phase block would be identified and used for further validation by RT-PCR.

5.3.2 Quantitative Reverse-Transcription PCR to confirm Micro-array Data

To begin with, based on the list of significantly down-regulated and up-regulated genes compiled in the previous chapter (Table 4.1 and Table 4.2), the genes those were chosen for RT-PCR have been detailed in Table 5.1. The genes were chosen based on either fold change following CP655 treatment or on the level of significance of differentially modulated genes. These were then correlated with literature and five genes were short-listed for analysis by RT-PCR.

The five genes highlighted for detailed analysis were CDC6, ANAPC1, RRM1, CDKN1A and GADD45G (Table 5.1). The table highlights the detailed functions of each of the five genes selected for further analysis. The main pathways that are linked to each of the genes have also been indicated. It is evident that all the genes that were selected belonged to the same cellular pathway, which was Cell Cycle and DNA replication processes.

GENE SYMBOL	NAME	FUNCTION	PATHWAY (KEGG Pathway Database)
CDC6	Cell Division Cycle 6	1. Initiation of DNA replication 2. Ensures complete replication of DNA before mitosis	1. Cell cycle 2. Regulation of DNA replication 3. Cell division
CDKN1A	Cyclin-Dependent Kinase Inhibitor 1A (a.k.a p21)	1. Blocks cellular proliferation by inhibiting cyclin-dependent kinase activity 2. At low concentrations promotes CyclinD-CDK4 complex formation and nuclear localization 3. At high concentrations, inhibits CyclinD-CDK2/4 activity 4. Can selectively bind to metal ions	1. Cell cycle 2. p53 Signalling 3. Cellular senescence
ANAPC1	Anaphase Promoting Complex 1	1. E3-ubiquitin ligase that controls the progression of cells through G1 phase of cell cycle by ubiquitination and degradation of target proteins	1. Cell Cycle 2. Ubiquitin-mediated proteolysis 3. Oocyte meiosis and maturation
RRM1	Ribonucleotide Reductase subunit M1	1. Synthesis of deoxy-ribonucleotides from ribonucleotides, necessary for synthesis of DNA	1. DNA replication 2. Metabolic pathways 3. Purine and Pyrimidine metabolism
GADD45G	Growth-Arrest and DNA Damage inducible Protein, Gamma	1. Regulation of growth and differentiation via positive control of Apoptotic pathways 2. Gene expression up-regulated due to growth arrest after cellular stress and activates stress responses	1. Cell Cycle 2. MAPK Signalling 3. p53 Signalling

Table 5.1: Genes for validation by RT-PCR

One of the possible explanations regarding why the micro-array experiment yielded small fold-change levels was that the time point chosen for analysis, 18 hours, may have been either too early or too late due to which the peak of gene expression had not been captured in the single experiment. In order to ensure that the changes over time can be identified, RT-PCR experiments were conducted over several different time points.

Five individual donors were selected to conduct the RT-PCR analysis, out of which one of the donors was the same as that used in the initial microarray analysis. The isolated cells were either left unstimulated or stimulated with anti-CD3/CD28 beads for 4-48 hours in the presence of either CP655 or CP655OMe and RNA extracted from the cells as previously described. The quality and quantity of the RNA extracted was assessed using Nanodrop, and was reconfirmed by checking the RIN score obtained from the Agilent 2100 Bioanalyzer. The RNA is given a score of between 1 to 10 for each sample, with 10 denoting good quality and fully intact RNA, and a score of 0 indicating bad quality, degraded RNA. Score for all the samples used in this experiment showed a RIN score of greater than 9, indicating good quality and intact RNA

Once the quality and quantity of RNA was established it was converted into cDNA by the procedure described earlier (Section 2.12). The cDNA was used for RT-PCR on a TaqMan based detection system on a ViiA™ 7 Dx Real-Time PCR instrument (Life technologies). The relative levels of mRNA expression for each target gene were calculated by normalizing it to the relative expression of house-keeping gene, 18s mRNA levels in the respective sample.

Initially, RT-PCR was conducted on the time points ranging from 4 -12 hours post stimulation (Fig. 5.5).

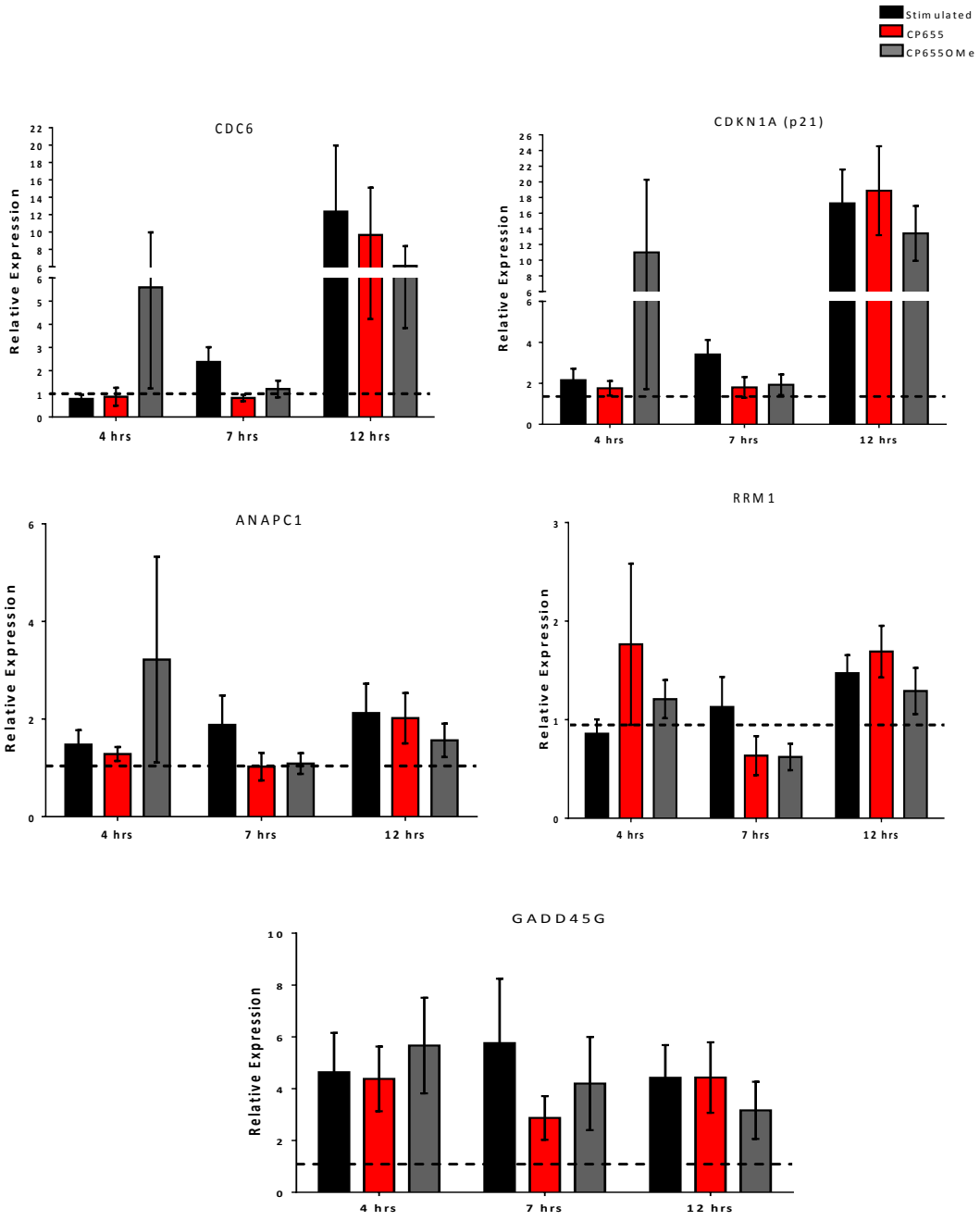

Figure 5.5: ***Effect of CP655 and CP655OMe on mRNA expression levels of genes:*** CD4+ T cells were isolated from fresh PBMCs of healthy donors. Cells were either left unstimulated or stimulated with 1:20 bead: cells ratio of anti-CD3/CD28 beads in the presence or absence of either CP655 (5µM) or CP655OMe (5µM) for 4 hours, 7 hours or 12 hours. At each time point, RNA was extracted from the cells and used for RT-PCR. Gene expression levels were normalized to 18s mRNA level. The results represent fold change in expression level relative to control (Dotted line), which is the untreated, unstimulated CD4+ T cell RNA. Graph represents the Mean $\pm$ SEM from n=5 individual donors.

The results were normalized to the samples that were not stimulated with anti-CD3/CD28 beads and had been left untreated. The relative change in mRNA expression was calculated by taking mRNA expression of the control samples as 1. The results indicated that each of the genes chosen for analysis showed a wide range of expression levels, over the different time points tested, as well as between individual donors. It was also evident that there were large inter-sample variations in the expression levels of the chosen targets, which can be seen by the large range of the Standard Error of Mean (SEM) (Fig 5.5). As a result of this, no significant changes were seen on treatment with either the chelator or the control compounds. The low levels of fold change of each of the genes can be attributed to the low levels of proliferation that are visible during the first 12 hours of cell culture. As shown by the proliferation data in the previous chapter, a significant effect of CP655 on cell proliferation becomes visible only 18 hours post stimulation and treatment.

Since no significant observations were made in the initial three time points the analysis of the target genes was continued at the three later time points that is from 18 hours - 48 hours (Fig 5.6).

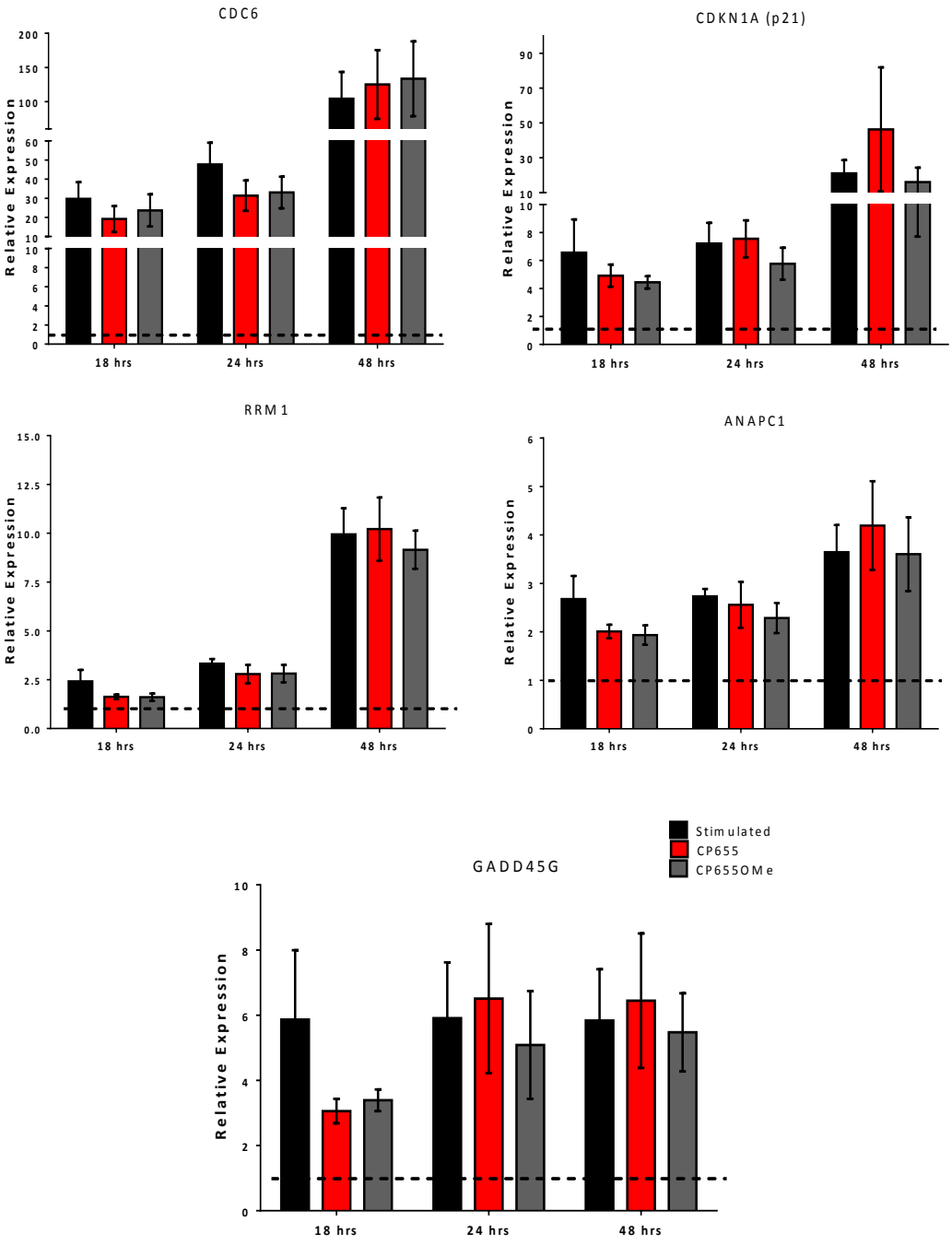

Figure 5.6: ***Effect of CP655 and CP655OMe on mRNA expression levels of genes:*** CD4+ T cells were isolated from fresh PBMCs of healthy donors. Cells were either left unstimulated or stimulated with 1:20 bead: cells ratio of anti-CD3/CD28 beads in the presence or absence of either CP655 (5µM) or CP655OMe (5µM) for 18 hours, 24 hours or 48 hours. At each time point, RNA was extracted from the cells and used for RT-PCR. Gene expression levels were normalized to 18s mRNA level. The results represent fold change in expression level relative to control (Dotted line), which is the untreated, unstimulated CD4+ T cell RNA. Graph represents the Mean $\pm$ SEM from n=5 individual donors.

The results indicated that the mRNA expression levels for CDC6 showed a consistent increase through all the time points, even in cultures that were treated with CP655. Similarly, RRM1 mRNA expression levels were also increased and did not support the data so far. As compared to the relative expression of mRNA levels for CDKN1A at the earlier time points, there was a gradual increase in the mRNA levels at the three later time points measured. In fact, the last time point of 48 hours showed more than 5-time increased fold change in CDKN1A mRNA expression. However, as previously noticed, no significant differences in mRNA levels were seen on treatment with either the chelator or the control. Although, it was observed that while most of the target genes showed a gradual increase in mRNA expression levels, CDKN1A was the only candidate where expression levels were dramatically increased from 24 hours to 48 hours for each of the treatment conditions. Furthermore, at 48 hours, the most prominent increase in CDKN1A mRNA expression was observed in the group that had been treated with the chelator CP655 as compared to the untreated as well as the CP655OMe treated conditions.

ANAPC1 and GADD45G mRNA expression levels were similar to those observed in the earlier 4 hour – 12 hour time points, and no significant patterns or trends were observed.

Therefore, keeping in mind the previous results obtained from micro-array analysis along with the results of the RT-PCR, the gene that had so far been most consistent in its expression trend was CDKN1A (p21). As a result of this, it was decided to focus further analysis on this gene in order to determine whether this could be one of the molecular targets of CP655.

5.3.3 Effect of CP655 on cell cycle inhibitor, CDKN1A (p21)

Based on the results of the microarray and RT-PCR, the protein that has so far been consistently modulated by CP655 was the cell-dependent kinase inhibitor CDKN1A (p21). Therefore, in order to confirm whether CP655 was able to modify the expression of p21 at the protein level the protein expression was analysed by western blot.

Initially Jurkat cells were used to look at the protein expression of p21. This was based on the proviso that since Jurkat cells are continuously dividing cancer cell lines, their expression of cell cycle proteins will be prolonged in comparison to primary cells which show cell cycle protein expression following stimulation and only for short periods of time. Jurkats were either left untreated or treated with either the chelator or the control for 1-48 hours before being lysed and used for western blot analysis (Fig 5.7).

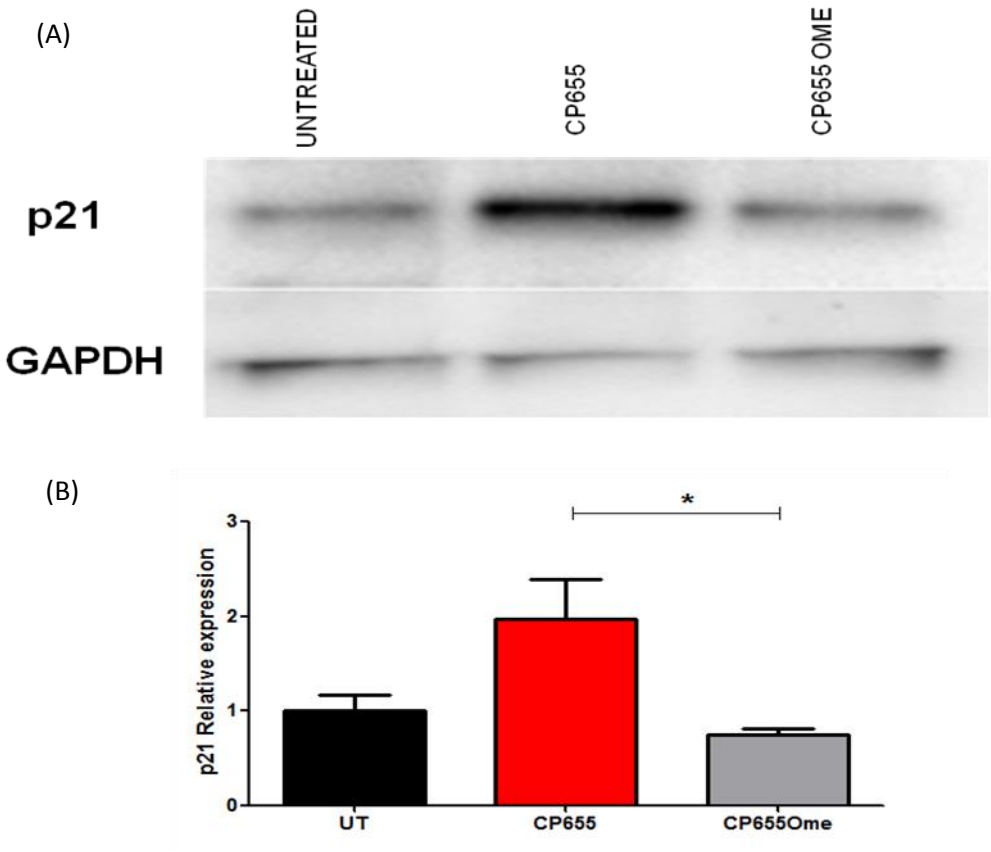

Figure 5.7: ***Effect of CP655 treatment on p21 protein expression in Jurkat cells*****:** Jurkat cells were either left untreated or treated with CP655 (5µM) or CP655OMe (5µM). After 4hours of culture, p21 expression was analysed by western blot. (A) Results from one representative experiment. (B) *p<0.05, calculated using student's paired t-test. Results represented as Mean ± SEM from n=3 different cultures.

The western blot experiments clearly demonstrated that CP655 was successful in significantly up-regulating proteins expression of p21 in RNA from jurkat cells. This was in accordance to the microarray as well as RT-PCR data, showing increased expression of p21 mRNA. Although, Fu and Richardson (2007) show that iron chelation decreases p21 protein levels, due to ubiquitin-independent degradation pathways, the results of this study were able to consistently demonstrate significantly increased p21 protein expression after iron chelation.

The next step was to replicate the above results on primary CD4+ T cells and determine the effect of CP655 treatment the expression level of p21 in these cells (Fig 5.8).

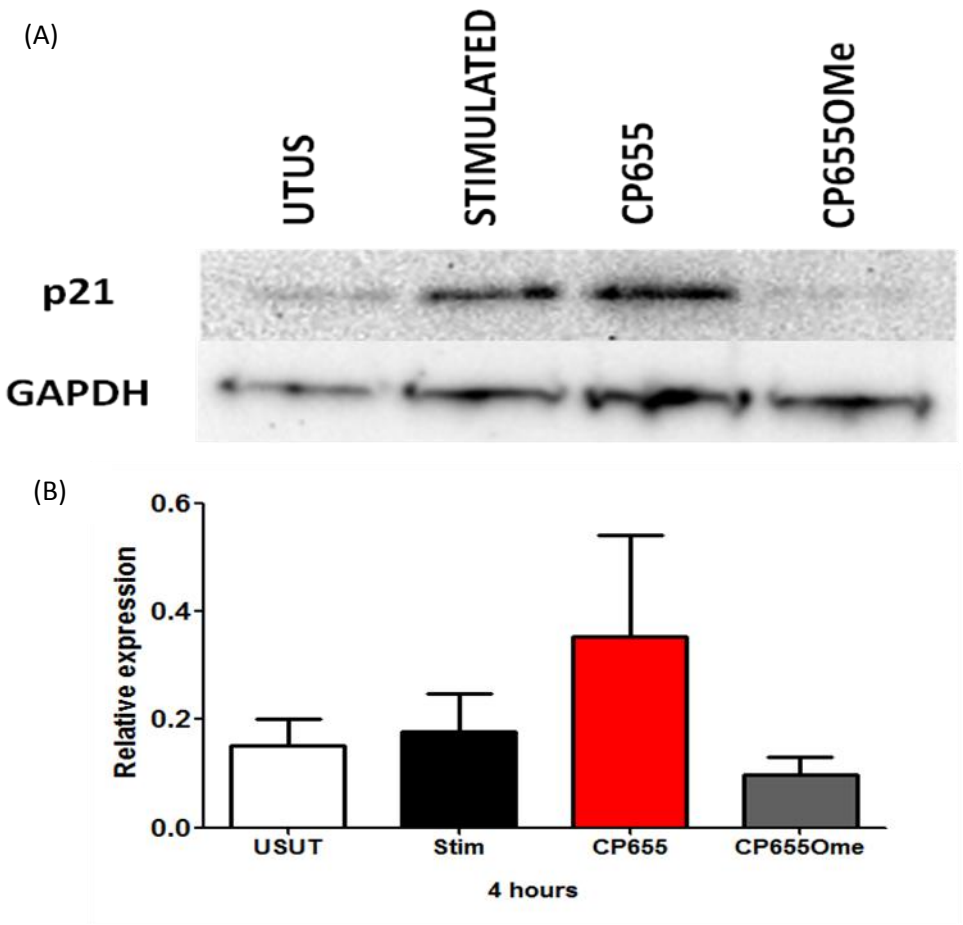

Figure 5.8: ***Effect of CP655 treatment on p21 protein expression in primary cells:*** CD4+ T cells were isolated from PBMCs of healthy donors and either left unstimulated (USUT) or stimulated with anti-CD3/CD28 beads (1:20) in the presence or absence of either CP655 (5µM) or CP655OMe (5µM). After 4hours of culture, p21 expression was analysed by western blot. (A) Results from one representative experiment. (B) Results represented as Mean ± SEM from n=4 individual donors.

Similar to the observations made using Jurkat cells, treatment of primary CD4+ T cells with CP655 also resulted in an increased expression of p21 protein at 4 hours post treatment. The increase was not found to be significantly more than the control CP655OMe treated or the untreated cells, but this may be due to the wide spread of expression level between donors and the presence of inter-sample variations.

Therefore, based on the results of the western blot experiments it was confirmed that one of the mechanisms via which CP655 was exerting its anti-proliferative effects on CD4+ T cells, was its ability to up-regulate the cell cycle inhibitor, p21, hence causing a block in the cell cycle at the G1/S phase as demonstrated.

5.3.4 Effect of CP655 and CP655OMe treatment on IL-2 pathway and its downstream target molecules

The results obtained so far show that the main effect of the chelator was on inhibition of proliferation. This was further confirmed in the previous section where it was demonstrated that an increased expression of p21 was responsible for the G1/S block of the CD4+ T cells.

In order to uncover other mechanisms that could be used by CP655 to cause a block in cell proliferation it was decided to look into the IL-2 pathway, which is one of the main pathways controlling cell proliferation. The cytokine IL-2 is essential for T cell development and proliferation and is produced mostly by CD4+ cells that have been activated by antigen stimulation. An important aspect of IL-2 is its ability to upregulate the expression of its own receptors by signalling in a positive feedback loop, which is essential for the differentiation of activated cells. Hence, not only is the production of IL-2 important for the proliferation of cells, but the ability of these cells to respond to IL-2 is also important for them to be able to differentiate (Busse *et al*, 2010).

To begin with, the ability of the antigen activated CD4+ T cells to respond to exogenous IL-2 in the presence or absence of the iron chelator CP655 was analysed. CD4+ and CD14+ cells were isolated from PBMC's of healthy donors. The cells were co-cultured in a ratio of 2:1 (CD4+:CD14+), and either left unstimulated or stimulated with the antigen, Tetanus Toxoid. The co-cultures were then left untreated or treated with either CP655, CP655 along with recombinant human IL-2 or just recombinant human IL-2 by

itself. Proliferation and cytokine production was measured from these cells after 6 days of culture (Fig 5.9).

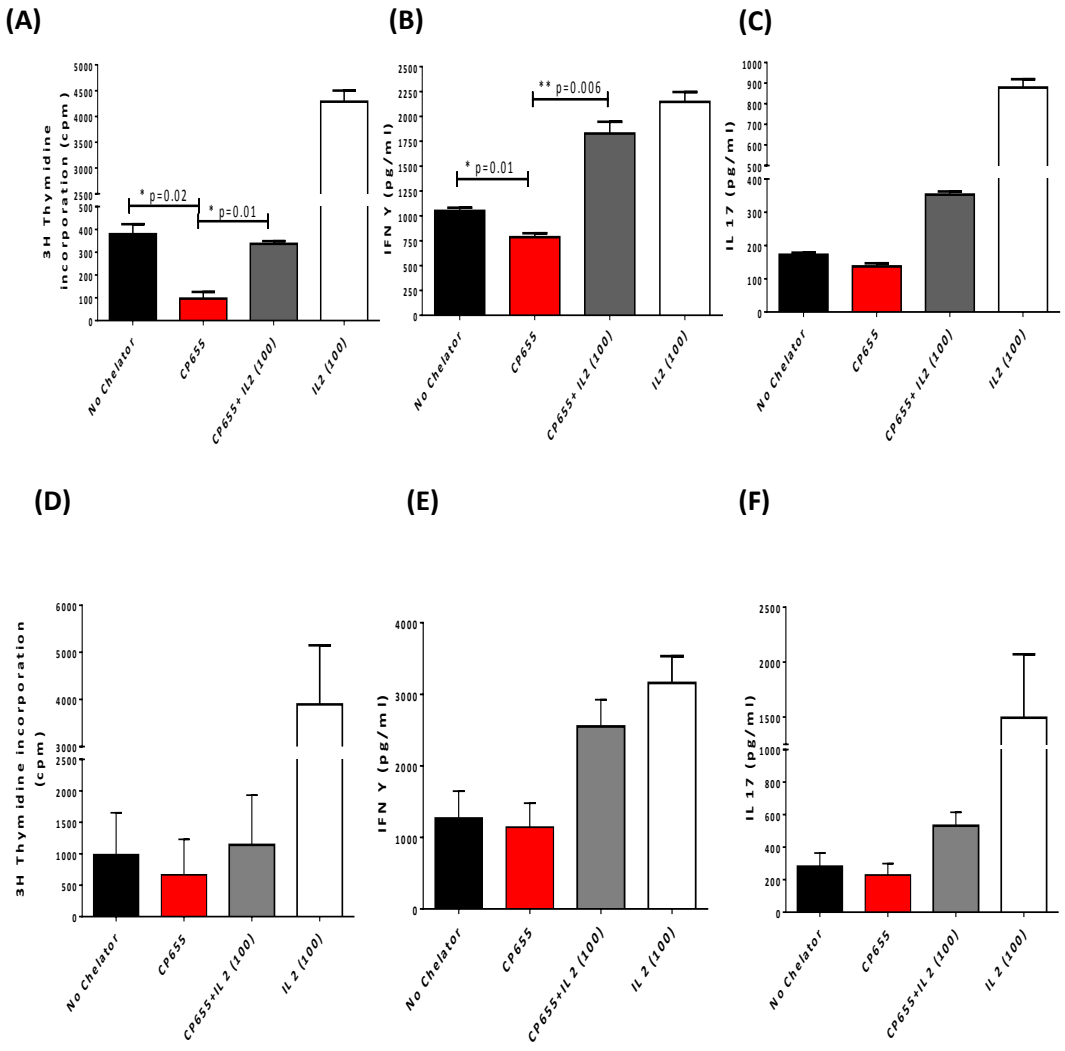

Figure 5.9: ***Effect of exogenous IL-2 on CP655 treatment:*** CD4+ T cells and CD14+ monocytes were isolated from fresh PBMCs of healthy donors. Cells were stimulated with Tetanus Toxoid in the presence or absence of either CP655 (5µM), CP655 with 100IU of rhIL-2 or just 100IU of rh IL 2. After 6 days of culture, proliferation was measured by tritiated thymidine incorporation and cytokine production by ELISA. (A-C) Results from one representative donor after 6 days of culture. (D-F) Cumulative data from n=5 individual donors. *p<0.05 and ** p<0.01, calculated using student's paired t-test. Results represented as Mean + SEM.

Results indicated that treatment of the cells with CP655 led to reduced proliferation and inflammatory cytokine production from the cell cultures as previously seen. The addition of exogenous recombinant-human IL -2 was able to overcome the suppression caused by CP655, and in fact in some of the donors tested, the cytokines produced were almost as high as those produced by cell cultures stimulated only by tetanus toxoid and IL-2. The experimental set-up described above was then repeated in the presence of the control compound CP655OMe (Fig 5.10).

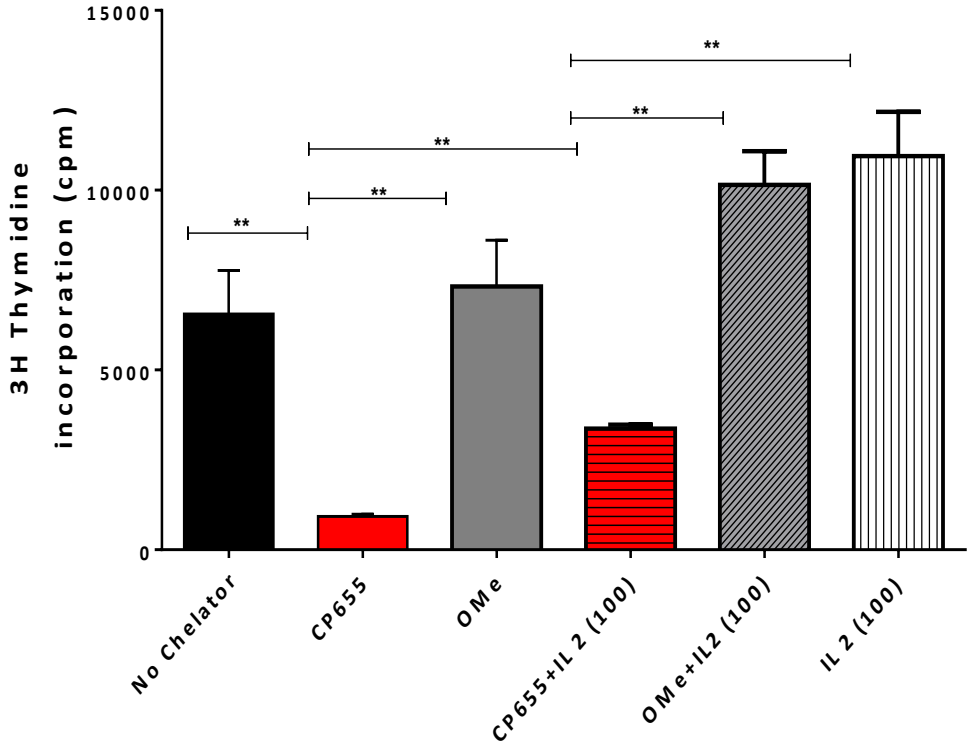

Figure 5.10: ***Effect of exogenous IL-2 on CP655 and CP655OMe treatment*****:** CD4+ T cells and CD14+ monocytes were isolated from fresh PBMCs of healthy donors. Cells were stimulated with Tetanus Toxoid in the presence or absence of either CP655 (5µM), CP655OMe (5µM), CP655 with 100IU of rhIL-2 or just 100IU of rh IL 2. After 6 days of culture, proliferation was measured by tritiated thymidine incorporation. Results shown as Mean ± SEM from n=3 individual donors. ** $p<0.01$ calculated using paired t-test.

As seen previously, treatment with CP655 led to a significant decrease in the proliferation of cells as compared to untreated cells as well as the cells treated with CP655OMe. Addition of exogenous IL-2 to cells treated with CP655 was able to significantly overcome the inhibition of proliferation. Exogenous IL-2 added to CP655OMe containing cells further increased their proliferative response. These results suggested that treatment with CP655 does not alter the ability of cells to respond to exogenous IL-2, but may be interfering with their ability to produce IL-2. Also, this supported the previous claim that treatment with the iron chelator does not cause any toxicities in the cell cultures and the cells retain their ability to mount a response to exogenous stimuli.

However, it was interesting to observe that when the same experimental set-up was repeated with only CD4+ T cells stimulated using anti-CD3/CD28 beads, the addition of exogenous IL-2 was unable to overcome the suppression caused by CP655 in these cell cultures (Fig 5.11)

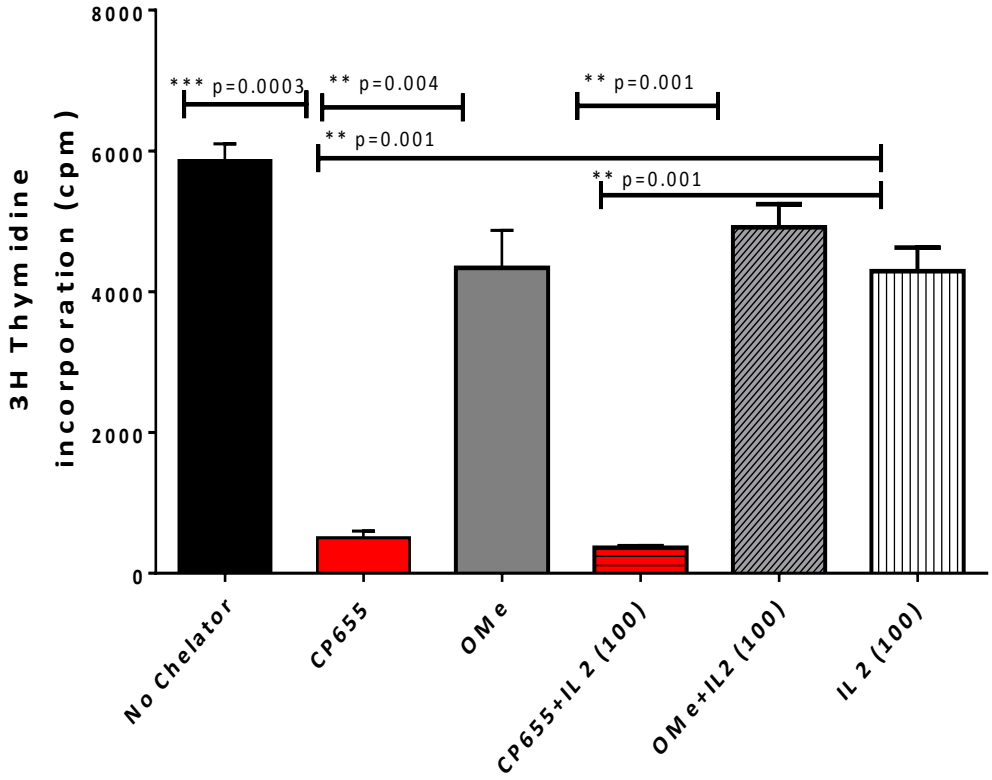

Figure 5.11: ***Effect of exogenous IL-2 on CP655 and CP655OMe treatment:*** CD4+ T cells were isolated from fresh PBMCs of healthy donors. Cells were stimulated anti-CD3/CD28 beads in a ratio of 1:20, in the presence or absence of either CP655 (5µM), CP655OMe (5µM), CP655 with 100IU of rhIL-2 or just 100IU of rh IL 2. After 24hours of culture, proliferation was measured by tritiated thymidine incorporation. Results shown as Mean ± SEM from n=3 individual donors. ** $p<0.01$, ***$p<0.001$ calculated using paired t-test.

The reason behind this could be the presence of CD14+ monocytes in the previous cell culture. Monocytes can be activated by IL-2, therefore it is possible that the revival of proliferation seen is due to the CD14+ monocytes being activated on exogenous IL-2 addition. Additionally, this study has previously shown that CD14+ monocytes are not affected by CP655 treatment, the main targets of which are CD4+ T cells. Therefore, when only CD4+ T cells were present in culture (Fig 5.11), the addition of exogenous IL-2 was unable to overcome the block in proliferation of these cells. This demonstrated that CP655 may be interfering with the IL-2 signalling pathway as another potential mechanism of its action.

To confirm this, the effect of the chelator on the downstream signalling molecules of the IL-2 pathway were determined. Aberrations in the signalling of IL-2 can affect transcription of several genes that are important for T cell activation and proliferation.

Binding of IL-2 to its receptor leads to the activation of several signalling pathways. One of these is the JAK3-STAT5 pathway which has been implication to play an important role in diseases such as Rheumatoid Arthritis (Walker and Smith, 2005). STAT5 plays a role in the transcription of genes such as NF-kB, NF-AT and AP-1 (Bromberg and Darnell, 2000). Hence, the next set of experiments looked at the effect of CP655 treatment on the phosphorylation of STAT5 in stimulated CD4+ T cells. CD4+ T cells were isolated from blood of healthy controls. The cells were stimulated with anti- CD3/CD28 beads either in the presence or absence of the chelator CP655, or the control CP655OMe for three different time points, starting from 24 hours - 72 hours. The protein expression for pSTAT5 was normalized to the expression of GAPDH in the cell lysates. Results showed that there was a small but consistent reduction in the phosphorylation of STAT5, 48 hours after stimulation in cells that had been treated with CP655 as compared to the untreated samples as well as those treated with CP655OMe (Fig. 5.13). No significant changes or discernible patterns were observed in the other two points (Fig 5.12; Fig 5.14).

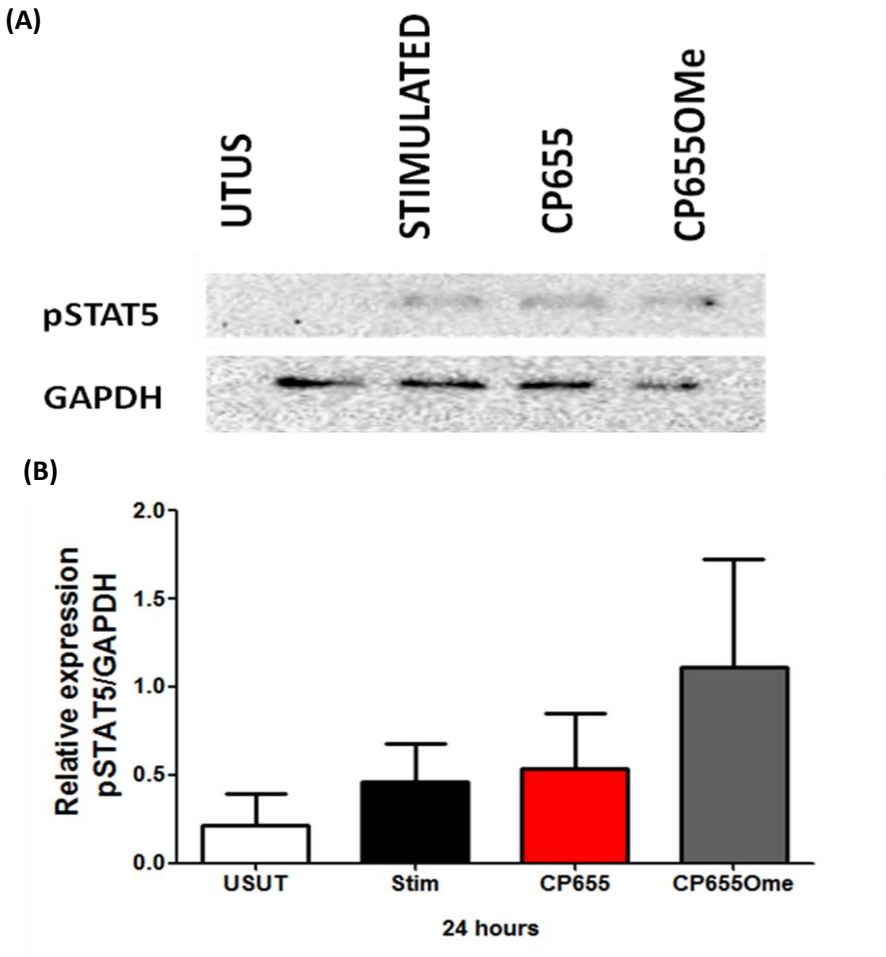

Figure 5.12: ***Effect of CP655 treatment on pSTAT5 expression 24 hours post stimulation:*** CD4+ T cells were isolated from fresh PBMCs of healthy donors. Cells were either left unstimulated (USUT) or stimulated with anti-CD3/CD28 beads in the presence or absence of CP655 (5µM) or CP655OMe (5µM). After 24 hours of culture, pSTAT5 expression was analysed by western blot. (A) Results from one representative donor. (B) Data represented as Mean ± SEM from n=3 individual donors.

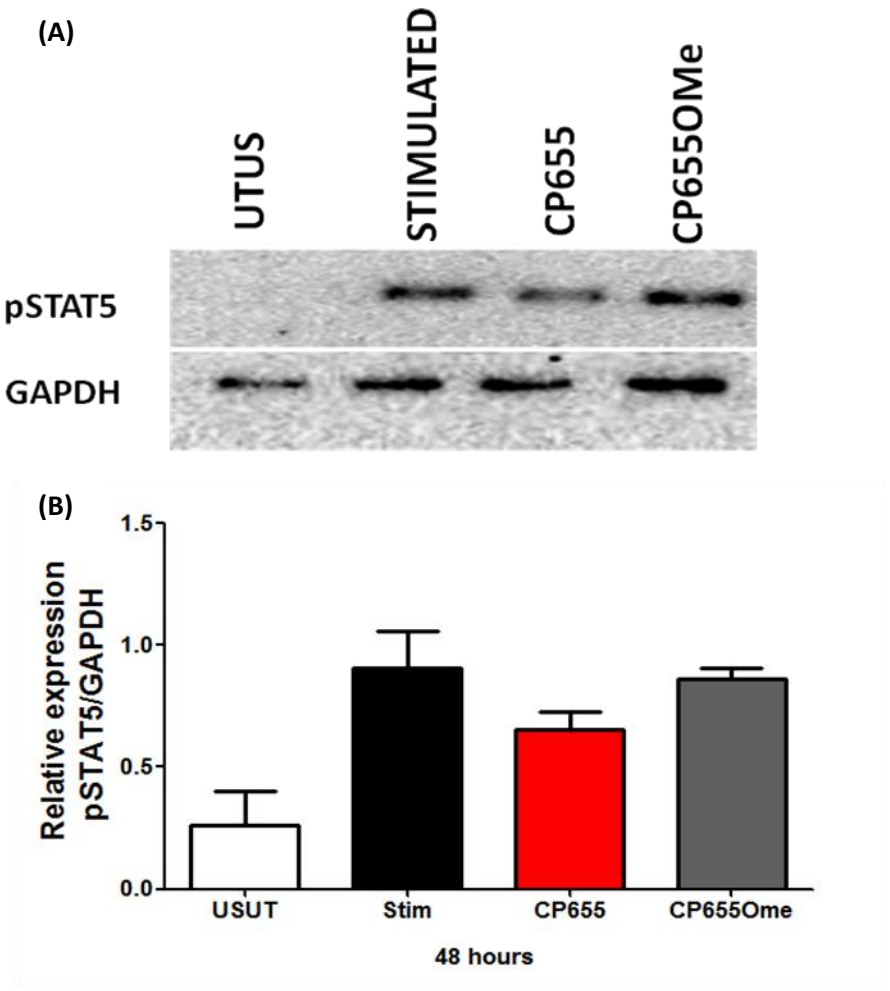

Figure 5.13: ***Effect of CP655 treatment on pSTAT5 expression 48 hours post stimulation*****:** CD4+ T cells were isolated from fresh PBMCs of healthy donors. Cells were either left unstimulated (USUT) or stimulated with anti-CD3/CD28 beads in the presence or absence of CP655 (5µM) or CP655OMe (5µM). After 48 hours of culture, pSTAT5 expression was analysed by western blot. (A) Results from one representative donor (B) Data represented as Mean ± SEM from n=3 individual donors.

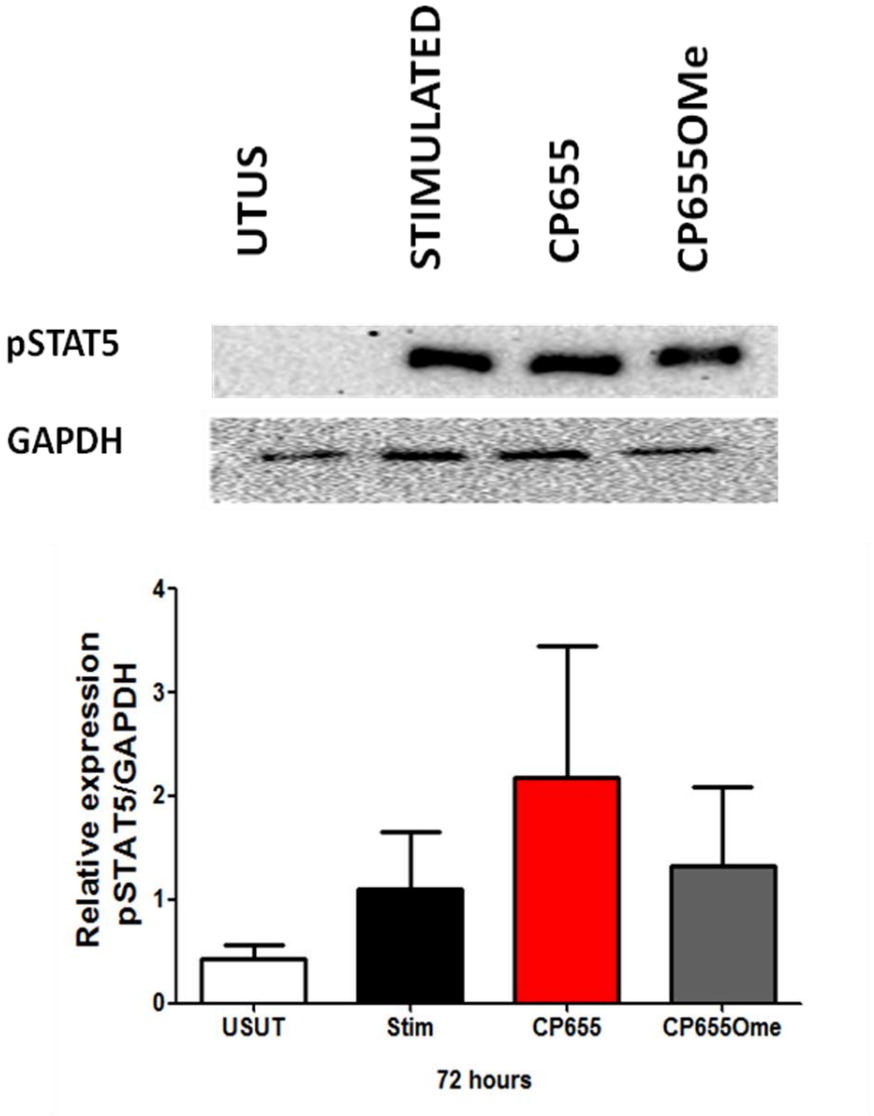

Figure 5.14: Effect *of CP655 treatment on pSTAT5 expression 72 hours post stimulation*: CD4+ T cells were isolated from fresh PBMCs of healthy donors. Cells were either left unstimulated (USUT) or stimulated with anti-CD3/CD28 beads in the presence or absence of CP655 (5µM) or CP655OMe (5µM). After 72 hours of culture, pSTAT5 expression was analysed by western blot. (A) Results from one representative donor. (B) Data represented as Mean $\pm$ SEM from n=3 individual donors.

These results suggested that the inability of the cells to respond to IL-2 in the presence of CP655 as seen in Fig 5.11 could be due to the effect of the iron chelator on downstream signalling molecules of the IL-2 pathway such as the phosphorylation of STAT5.

The dysregulated STAT5 signalling in CD4+ T cells, as a result of treatment with CP655 is suggested to be another possible mechanism used by the chelator to cause inhibition of cell proliferation.

5.3.5 Kinetic Analysis of CP655 and CP655OMe treatment

An important question while trying to identify the mechanism of action of the iron chelator is to determine the most appropriate time point at which the cells must be exposed to the chelator for it to exert the effects observed so far.

In order to address this two different sets of kinetic experiments were set-up. In the first set of experiments, isolated CD4+ T cells were pre-treated with either the chelator or the control compound for varying lengths of time starting from 2 hours - 48 hours. After each time point, the cells were washed out of their respective treatments and were then stimulated with anti-CD3/CD28 beads for an additional 24 hours (Fig. 5.15 A). Additionally, parallel experiments were set up where the cells were not washed out of the treatment, but after each treatment time point, anti-CD3/CD28 bead stimulation was added directly into the cell cultures for 24 hours (Fig. 5.15 B). In each experiment, proliferation was measured by ^{3}H thymidine incorporation.

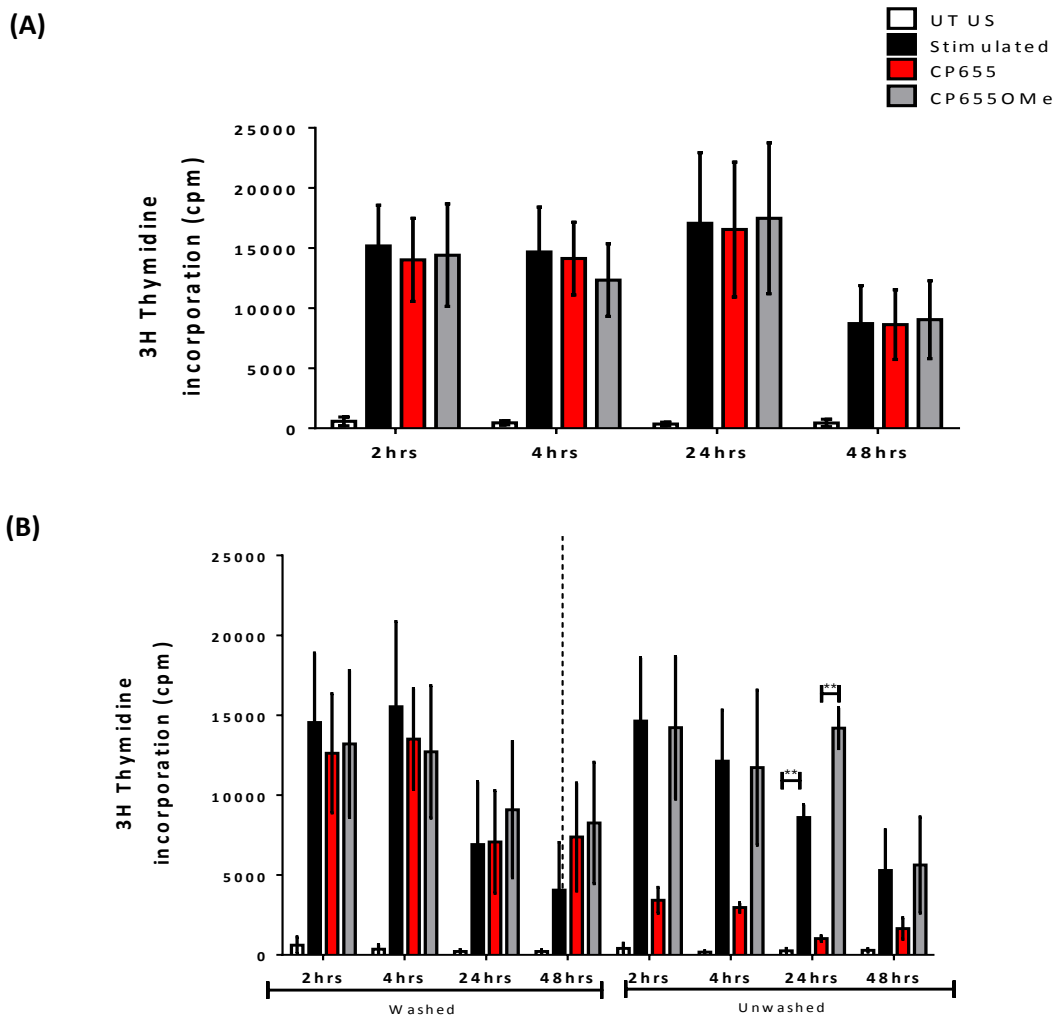

Figure 5.15: ***Kinetics of CP655 Pre-treatment:*** CD4+ T cells were isolated from PBMCs of healthy donors. Cells were pre-treated with either CP655 or the control CP655OMe for the indicated time. (A) After each time point, cells were washed and either left unstimulated (UTUS) or stimulated with anti-CD3/CD28 in a 1:20 bead: cells ratio for 24 hours (n=4). (B) In parallel experiments, cells were either washed out of the treatment or left unwashed for each of the time points and then left unstimulated or stimulated with anti-CD3/CD28 bead for 24hours. Proliferation was measured by 3H thymidine incorporation. Results are expressed as Mean $\pm$ SEM from n=3 individual donors. ** $p<0.01$ calculated using paired t-test.

Results showed that when the iron chelator CP655 and the control compound CP655OMe were washed out after pre-treatment in each of the time points, no effect on the proliferation of CD4+ T cells was visible. However, in contrast, when the cells were not washed out of their respective treatments and were directly stimulated with the anti CD3/CD28 beads in the presence

of the chelator or the control, the effect on inhibition of proliferation was maintained as seen previously following CP655 treatment.

These results indicated that it is essential for the chelator to be present at the time of stimulation of the cells for it to be able to exert its effects.

In order to confirm this, a second set of kinetic experiments were conducted where isolated CD4+ T cells were first stimulated with anti-CD3/CD28 beads in the ratio of 1:20 for different time points, ranging from 2 hours - 48 hours. At the end of each time point, either CP655 or the control CP655OMe was added to the cell culture and left for an additional 24 hours. Proliferation was measured by ^{3}H thymidine incorporation at the end of the 24 hours of treatment (Fig 5.16).

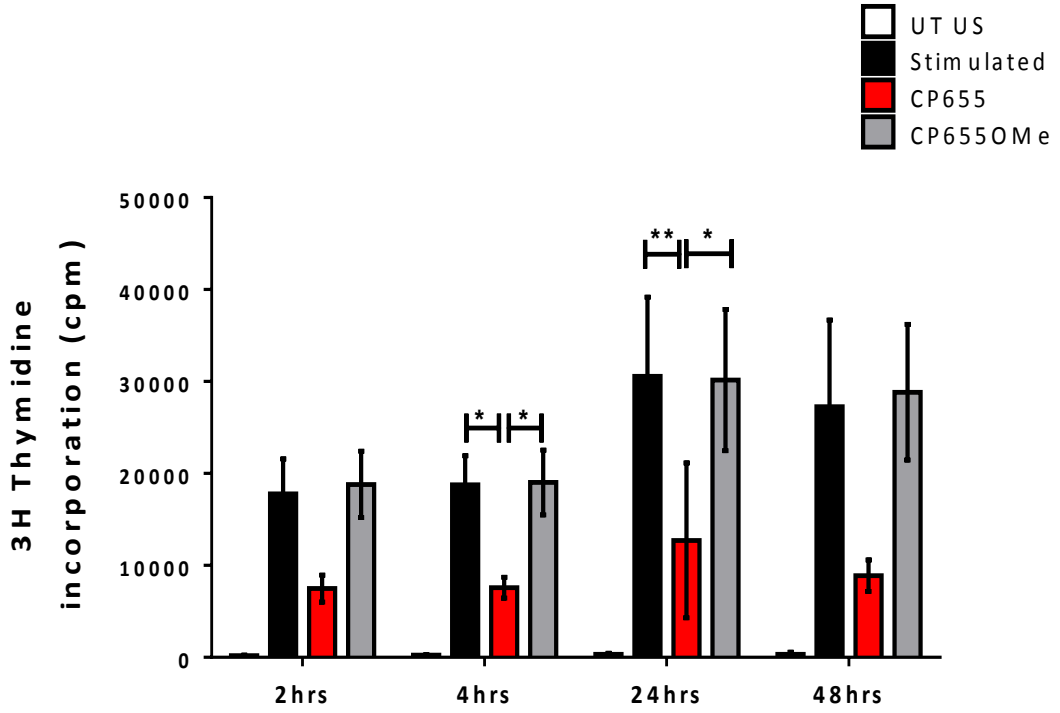

Figure 5.16: ***Kinetics of CP655 after pre-stimulation with anti-CD3/CD28 beads:*** CD4+ T cells were isolated from fresh PBMCs of healthy donors. Cells were stimulated with either anti-CD3/CD28 beads (1:20) for time points ranging from 2 hours to 48 hours. After each time point, cells were either left untreated or treated with either the control or the chelator CP655 for 24 hours. UT US = Untreated, unstimulated cells. Proliferation was measured by 3H thymidine incorporation. Results are expressed as Mean $\pm$ SEM from n=3 individual donors.** $p<0.01$ calculated using paired t-test.

Results showed that addition of the iron chelator after stimulation of the cells was effective in reducing proliferation of the CD4+ T cells. Even cultures where the cells had been stimulated for 48 hours before being treated with CP655 and CP655OMe showed significantly reduced proliferation after 24 hours of CP655 treatment and no effect after CP655OMe treatment.

This further confirmed the results obtained from the initial set of kinetic experiments. The results indicated that another mechanism via which CP655 could be exercising its effect is by interfering with signalling through the T-cell receptor. This justified the need for the chelator to be present in the cell cultures at the time when the signalling events, post stimulation of the cells, are taking place for it to be able to interfere with specific signalling pathways. Signalling via the TCR is essential for transcription and production of proliferative cytokines such as IL-2. Therefore, the inhibition of proliferation of CD4+ T cells could also be attributed to the reduction in IL-2 production due to aberrant TCR signalling. This also provides support to previous experiments which showed that addition of exogenous IL-2 can restore normal cell proliferation and cytokine production.

5.4 DISCUSSION AND CONCLUSION

Since review of the literature and analysis of the microarray data discussed in the previous chapter revealed that the pathways being affected most by CP655 treatment were those controlling for various aspects of the cell cycle, it was decided to conduct a functional cell cycle analysis of the effect of CP655 on primary human CD4+ T cells as well Jurkat cells. This was essential especially in order to help narrow down the list of 20 genes short-listed from the microarray data and identify genes that could be further validated by RT-PCR and western blotting.

To begin with, the effect of CP655 on Jurkat cells was determined, by using Propidium Iodide (PI) staining of the DNA to determine cell cycle profile of the cultured cells. Using PI to analyse cell cycle is based on the understanding that cells in the S phase of the cell cycle have more DNA than the cells in the G1 phase of the cell cycle and hence they absorb more PI and have a brighter fluorescence. Similarly, cells in the G2 phase will have twice as much DNA as the G1 phase since the cells would have doubled their DNA content by this phase. Therefore, the cell cycle profile is based on the number of cells and the DNA content of the cells to determine their phase (Shapiro, 1988). The analysis was conducted at three different time points, 24 hours, 48 hours and 72 hours post treatment with CP655 and CP655OMe, to help resolve the issue of the most appropriate time point of visualizing modulations in gene and protein expression of the cells. Also, a kinetic analysis of the effect of iron chelation was essential to establish whether the effect of the treatment is permanent or diminishes over time. The results revealed that after 24 hours of culture of Jurkats, a very small percentage of cycling cells were present, and most of the cells were still in the G1 phase of the cell cycle. 48 hours post culture a definite cell cycle profile of the cells became visible. Under untreated conditions, around 50% of the cells were in G1 phase, 35% cells in S phase and around 15% of total cells in G2 phase of the cell cycle. However, the cell cycle profile was dramatically altered on treatment with CP655. The transition from G1 to S phase was unclear, and majority of the cells seemed to be arrested in between the two stages, or arrested in the S phase.

Once again, in accordance with the previous results CP655OMe treatment had no effect on the cell cycle profile of the Jurkat cells, which looked the same as the untreated control cells. Consistently results showed that CP655 treatment led to a block in the G1/S phase of the cell cycle and an arrest of the cells in the S phase preventing them from completing their proliferation. Another interesting observation that was made was that the effect of the iron chelation was not permanent, and the effects began to wear off by 72 hours. Even though, the trend and pattern in the cell cycle profile was visible, the results were no longer as prominent or significant.

Previously, experiments using different iron chelators on Jurkat cells showed that, although they were all capable of causing a significant block in the cell cycle, but they affect different stages of the cell cycle. Also, the effect was seen to be dose-dependent. Gharagozloo *et al* (2008) showed that treatment of Jurkat cells with Silybin, a plant flavanoid with iron chelating properties, arrested the cells in the S phase of the cell cycle. However, when they treated Jurkat cells with DFO, at higher concentrations (200µM - 400µM) the cells were arrested in the G1 phase, but treatment with lower concentrations of DFO (50µM - 100µM) led to accumulation of cells in the S phase of the cell cycle. Others have also shown that treatment of Jurkat cell lines with iron chelator results in two separate blocks of the cell cycle – one in the early G1 phase and the second one in the S phase (Siriwardana and Seligman, 2013).

Moving on from Jurkat cells, the same experimental set-up was used to analyse purified human CD4+ T cells. Similar to what was seen with Jurkat cells, no cycling cells were seen in the first 24 hours of culture and most of the cells were in the G1 phase. But by 48 hours post stimulation, 60-70% of the cells were in G1 phase, around 20% in the S phase and the remaining 10-15% in the G2 phase. Treatment with CP655 once again significantly altered the cell cycle profile of the cells. In contrast to the Jurkat cells, most of the CP655 treated cells could be clearly seen to be arrested in the G1 phase, with fewer numbers of cells entering the S phase and subsequently, a significantly lower number of cells reaching the G2 phase. The results from these functional experiments confirmed the indications that developed following the microarray data analysis. As seen

previously with Jurkat cells, the effect of the chelator was diminished by 72 hours, although the trend remained visible. The impact of intracellular iron depletion on the cell cycle has been described by few studies in the past. Several different iron chelators such as Mimosines, Dp44mT, DFO and Silymarin have been shown to be able to arrest cells at the boundary of the G1-S phase in various different cell types (Kulp and Vullient, 1996; Gao and Richardson, 2001; Clement *et al*, 2002; Szuts and Krude, 2004).

The aberrations in the cell cycle caused following iron chelation have been linked to the inhibition of the DNA synthesis enzyme Ribonucleotide Reductase (RR), which is dependent on iron for its proper functioning (Renton and Jeitner, 1996; Kayyali *et al*, 2001). Bi-dentate chelators such as the HPO chelators used in this study have been shown to inhibit the activity of RR faster, by quickly binding to the iron molecules in the core of the enzyme, as compared to larger hexadentate chelators such as DFO (Abeysinghe *et al*, 1996; Cooper *et al*, 1996). This can be attributed to the ability of HPO chelators to diffuse faster across cellular membranes due to their lower molecular weight and neutral charge (Hoyes *et al*, 1992). RR has become a popular target for anti-cancer drugs due to its central role in DNA synthesis and replication (Kolberg *et al*, 2004; Cerqueira *et al*, 2007; Zhou *et al*, 2013). Ribonucleotide Reductase is made up of two subunits, the larger α subunit (RRM1) and the smaller β subunit (RRM2). Both of these subunits are required in equimolar concentrations for the enzyme to function effectively. Any alterations in either of the subunits can render the enzyme inactive (Larsson and Sjoberg, 1986; Richard, 1993). The data generated from the microarray conducted in this study had revealed that RRM1 was one of the genes that was significantly modulated ($p=0.02$) and was down-regulated by 1.02 fold on treatment with CP655 as compared to CP655OMe. Therefore, since the importance of this enzyme and its subunits had been clearly established in the literature, and it had been shown to be one of the main mechanisms by which iron chelation inhibits cellular proliferation, it was decided to short-list RRM1 as one of the final five genes that would be validated by RT-PCR.

Apart from their ability to inhibit RR enzyme, iron chelators have been shown to cause inhibition of the cell cycle by their ability to directly target various cell

cycle proteins in different stages of the cell cycle (Darnell and Richardson, 1999; Yu *et al*, 2007; Gharagozloo *et al*, 2008). Cyclins and CDKs are essential components of the cell cycle and it is the interplay between different cyclins, cdks and other proteins that control the transition between the different cell cycle stages (Kulp *et al*, 1996; Sherr and Roberts, 1999).

Chelation has been shown to affect several cyclins and cdk proteins (Simonart *et al*, 2000; Fu and Richardson, 2007). D-type cyclins, along with C- and E-type cyclins, are the main type of cyclin proteins that control the progression of the cell cycle through the G1 phase. Depletion of iron using iron chelators has been shown to reduce the expression of different D-type cyclins such as D1, D2 and D3. The D-type cyclins need to form complexes with cdk4 in order to become active and push the cell through the G1 phase (Malumbres and Barbacid, 2005). Studies have demonstrated that iron chelation can reduce expression of cdk4 and also inhibit the ability of Cyclin-D1 and cdk4 to form active complexes (Gao and Richardson, 2001). Although CyclinD1 was reduced in the microarray experiment, the reduction was not significant hence, despite being a good candidate for the mechanism of the chelator, it was decided not to conduct further examination of this protein. An interesting observation that was made from the microarray data was that the expression of cdk4 was significantly increased after treatment with CP655. This might be an attempt, albeit unsuccessful, from the cell to continue the progression of the cell cycle by increasing cdk4 expression in response to the reduced expression of cyclin D1. Terrada *et al* (1991) reported a similar pattern in the expression of cyclin E and cdk2, where cyclin E levels were elevated from iron chelation but were unable to over the block in the cell cycle due to reduced cdk2 expression. One cell division cycle protein (CDC6) is amongst the earliest proteins that initiate the process of DNA replication by binding with the Origin recognition complex (ORC) to form the Replication Complex (RC). The activation of this complex is responsible for initiating DNA replication and the movement of the cell from the G1 phase into the S phase (Krude, 2006). As a result of this, the expression of CDC6 is very tightly controlled throughout the progression of the cell cycle (Boronat and Campbell, 2006). The results from the microarray experiment in this study showed that

CDC6 was significantly (p=0.004) down-regulated by 1.22 fold after CP655 treatment. In fact, in the list of 20 genes generated after correlating the microarray results and the literature, CDC6 was on the top of the list of highly down-regulated genes. Due to its indispensible role in controlling cell cycle progression and its prominent down-regulation in the microarray analysis, it was decided to further validate the expression of CDC6 via RT-PCR.

Another gene that was of interest was the Anaphase Promoting Complex 1 (ANAPC1) gene. It is a E3-ubiquitin ligase that target cell cycle regulatory proteins for degradation and helps initiate Anaphase and subsequently the completion of the cell cycle. It has been shown to interact with several Cdk and cdc proteins (Kraft *et al*, 2003). Apart from being highlighted in the literature as being important for cell cycle regulation, ANAPC1 was of statistical importance to this study as it was one of the top 10 genes that were highly significantly and differentially down-regulated on treatment with CP655. Therefore, it was decided that the effect of CP655 on ANAPC1 would be further investigated by RT-PCR.

Another family of genes closely associated with maintaining normal cell cycle progression, regulating growth and development and also known to be influenced by changes in intra-cellular iron concentrations are the Growth Arrest and DNA Damage (GADD) family genes (Darnell and Richardson, 1999; Tamura *et al*, 2012). The GADD family is made up of three members GADD34, GADD45 and GADD153 each of which are involved in various stress responses in the body (Yu *et al*, 2007). GADD45 has been implicated to play an essential role regulating DNA repair, controlling cell cycle progression, apoptosis etc. It has been shown that GADD45 group of proteins play an essential role during the G2/M phase check point of the cell cycle (Zerbini and Libermann, 2005). The GADD45 proteins which are highly expressed during the G1 phase of the cell cycle, are immediately up-regulated following DNA damage and bring about an arrest of the cell cycle and are involved in various DNA repair mechanisms (Kearsey *et al*, 1995; Garcia *et al*, 2005).

The importance of GADD45 proteins can be visualized from their extensive use in several cancer therapeutic agents. In fact, it has been suggested that anti-cancer

drugs as well as certain Non-Steroidal anti-inflammatory drugs (NSAIDs) depend on up-regulating GADD45 to cause cell cycle arrest and apoptosis, as a mechanism of their action and effect (Zerbini *et al*, 2006). Studies using different iron chelators, on several different cell lines have shown significant accumulation and time-dependent increase in GADD45 concentration following treatment (Darnell and Richardson, 1999; Saletta *et al*, 2011). Proteins of the GADD45 family have been shown to interact with several cell cycle proteins such as cdc2, CyclinB1, p21 and p38MAPK. It is therefore suggested that the GADD45 mediated inhibition of the cell cycle caused following iron-depletion could be attributed to the changes in the expression level of its various interacting proteins such as cdc2 and CyclinB1 (Vairapandi *et al*, 2002; Lee *et al*, 2006). The results from the microarray in this study showed that GADD45γ levels were significantly ($p=0.002$) up regulated by 1.12 fold after CP655 treatment. Furthermore, this was supported by a subsequent down regulation of CyclinB1 levels by 1.1 fold after treatment with CP655 ($p=0.02$). Although levels of GADD45α and GADD45β expression levels were increased by around 1 fold after treatment with the chelator, the changes in expression were not significant and hence these genes were not considered for further analysis. Based on the close relation between GADD45 proteins and regulation of the cell cycle, as well as the effect of iron depletion on the expression of this protein it was decided to further analyse and validate the effect of CP655 on GADD45γ via RT-PCR.

While reviewing the literature on cell cycle regulation and the effect on iron chelators on progression of the cell cycle, a protein that was discussed in several studies due to its important role in different signaling pathways was $p21^{CIP1/WAF1}$ (CDKN1A). The Cdk Inhibitor, p21, is one of the most crucial molecules involved in regulating the cell cycle (Xiong *et al*, 1993; Harper *et al*, 1993). In most normal mammalian cells the cell cycle is controlled by a group of enzymes known as the cell-dependent kinases (cdk), which are in turn controlled by their regulatory sub-units, the cyclins. These are accompanied by the Proliferating Cell Nuclear Antigen (PCNA) and the p21 protein. Early studies showed that in several transformed cancerous cells, the PCNA and p21 proteins are lost from this quaternary structure as a result of which these cells show extensive,

uncontrollable proliferation. Therefore, the role of p21 was suggested to involve the inactivation of cyclin/cdk complexes leading to inhibition of proliferation and control of the cell cycle (Xiong *et al*, 1992; Zhang *et al*, 1993). p21 has been shown to arrest the cell cycle in the G1/S phase transition by inhibiting phosphorylation of pRb due to its ability to bind to the cyclin E/cdk2 complex and render it inactive (Vidal and Koff, 2000).

Apart from interfering with cyclin and cdk complexes, p21 also directly alters the expression of several transcription factors such as E2F1 and c-myc (Delavaine and La Thangue, 1999). The activation of p21 is controlled by two different signaling pathways, one is via the p53 pathway and the other in a p53-independent manner through its own transcription factors such as AP2 (Wajapeyee and Somasundaram, 2003). An important aspect of the p21-mediated regulation of the cell cycle is that it can have both positive as well as negative effects on the cell cycle. It has been shown that proper activation and cyclin-cdk complex formation requires low levels of p21 expression. However, the same protein in higher concentrations can inhibit the cyclin-cdk complex formation as well (Cheng *et al*, 1999).

Studies have demonstrated that depletion of intra-cellular iron can have contrasting effects on the expression of p21 mRNA levels and p21 protein levels. Iron chelators such as DFO and 311 have been shown to significantly increase p21 mRNA levels, in a p53 independent pathway leading to G1/S phase arrest of the cell cycle. However, other studies showed a decrease in p21 protein level after iron depletion (Fukuchi *et al*, 1999; Abeysinghe *et al*, 2001). It has been suggested that the decrease in p21 protein expression could be due to ubiquitin-independent proteasomal degradation of the protein (Fu and Richardson, 2007). Goldie *et al* (2013) showed that Deferasirox can inhibit the proliferation of lung cancer and neuroepithelioma cell lines by causing an up-regulation of p21mRNA levels. As p21 is one of the key molecules regulating cell cycle progression and since the changes in expression of p21 vary based on the type of chelator used, to the cell types etc it was decided to further investigate the effect of CP655 on p21 expression level and hence was chosen as the final gene for validation via RT-PCR.

Therefore, the functional experiments to analyse cell cycle aberrations following iron chelation were successful in assisting to short-list and identify five genes that could serve as potential targets for CP655. These genes Ribonucleotide Reductase, CDC6, ANAPC1, GADD45γ and CDKN1A were hence chosen for further validation by RT-PCR.

Finally, before moving ahead to the validation of the above genes, another important observation that came to light following the cell cycle analysis was that the time point at which the effects of the chelator became visible was in fact 48 hours, much later than what was previously hypothesized based on the results of the proliferation assays using Tritiated thymidine. But, still in accordance with the results of the CFSE-based proliferation assays. This further strengthened the view that the time point chosen to conduct the microarray was too early to visualize any significant effects relating to the effect of the chelation as discussed previously.

CDKN1A mRNA and protein levels up-regulated following iron depletion using CP655

Dallas *et al* (2005) showed that one of the best techniques for validating microarray results is by RT-PCR. Therefore, once the five genes had been identified, RT-PCR was carried out in order to establish whether the results of the microarray could be replicated at the mRNA level. Since it was believed that one of the reasons why the microarray did not reveal high fold change results was due to the time point of the experiment not being appropriate, it was decided to conduct the RT-PCR analysis of the chosen genes at several different time points, starting from as early as 4 hours post-stimulation until 48 hours post-stimulation. Additionally, the expression of various cell cycle proteins is cyclical and varies from time to time, depending on the phase of the cell cycle (Fitzgerald-Hayes and Reichsman, 2010). Therefore, in order to ensure that any changes in mRNA levels of the five chosen genes could be observed it was essential to have a wide time point range for analysis. Four out of the five genes that were examined, namely CDC6, RRM1, GADD45G and ANAPC1 did not

reflect the alterations in mRNA expression level as were predicted by the microarray analysis.

For genes such as RRM1 the mRNA expression patterns were the opposite of what was predicted by the microarray analysis. At all of the time points analysed, RRM1 mRNA was either unchanged or increased in comparison to the untreated as well as the CP655OMe treated cells. This was very surprising as RRM1, one of the two major sub-units of the DNA synthesis enzyme Ribonucleotide reductase, is responsible for causing and controlling cellular proliferation. So far, CP655 had been able to significantly inhibit proliferation by at least 50% but did not seem to have any effect on the mRNA levels of RRM1. One of the explanations for this could be that although the RRM1 sub-unit contains the main active site of the enzyme, it is the second sub-unit RRM2 that contains the Fe-core, hence making it more susceptible to iron chelation (Shao *et al*, 2013; Zhou *et al*, 2013). Therefore, while subtle changes in RRM1 were observed in the microarray, the changes were not substantial enough to elicit significant changes at the mRNA level.

Moving on, genes such as CDC6 and ANAPC1, which showed highly significant, albeit small, fold changes in expression level in the microarray did not illustrate any significant patterns in their mRNA profiles. Once again, similar to the results with RRM1, the mRNA levels were mostly unchanged in comparison to the untreated or the CP655OMe treated cells. Although, the literature had suggested that CDC6 and ANAPC1 are indispensible parts of the cell cycle machinery, there were no reports linking either of these proteins to iron chelation, nor were there any studies highlighting their dependence on iron for proper functioning. Hence, it may be possible that the changes seen in these genes in the microarray were in downstream effects of the chelator inhibiting other cell cycle controlling proteins. As a result of which no significant changes at the mRNA level were observed for these genes.

GADD45 family genes had been shown in the literature to be affected by iron chelation. This observation was supported by the result of the microarray, where GADD45G was significantly up-regulated after iron chelation. However, once

again similar to other results, this up-regulation was not reproduced in the RT-PCR. A pattern towards increased GADD45G mRNA was noticed in the 24 hours and 48 hours time point, but it was not found to be statistically significant. Further examination of the literature revealed that more than GADD45G, it was in fact GADD45A, which interacted with several cell cycle proteins such as p21 and was even shown to be affected by iron depletion (Darnell and Richardson, 1999).

Another observation that was made was that there was very high inter-sample variation while conducting the RT-PCR, as can be seen by the large error bars in the results. This was also one of the reasons why it was not possible to get significant differences in mRNA levels.

Finally, after several inconsistent and disappointing results, the only gene that maintained the same trend and pattern as that suggested by the microarray data was the tumour suppressor gene, CDKN1A (p21). As compared to the other genes, where expression levels seemed almost constant or showed small gradual increases over time, the mRNA expression of p21 showed a dramatic increase at 12 hours post stimulation and then once again at 48 hours post stimulation. Additionally, even though due to the large inter-sample variations the results were not significant the pattern in expression of mRNA was relatively clear. It was evident that at the 48 hour time point, there was an increase in p21 mRNA levels after treatment with CP655 as compared to the untreated or the CP655OMe treated cells. These results were encouraging, especially since there were a large number of studies implicating p21 as the protein responsible for causing cell cycle arrest following iron chelation.

In order to confirm the results obtained following the RT-PCR, Western Blotting was used to further confirm and validate the effect of CP655 on p21 expression levels.

The effect of iron chelation on the expression of p21 has been discussed in several studies and the discrepancy between mRNA and protein level expressions go on to suggest that p21 is regulated not only at a transcriptional level but also post-transcriptionally. Fu and Richardson (2007) showed that

depleting intra-cellular iron led to an increase in p21 mRNA, but this was not reciprocated at the protein level. In fact, p21 protein levels were reduced after iron chelation due to proteasomal degradation of the protein. In a previous study by Fukuchi *et al* (1998) they showed that using a DNA-damaging agent led to increase in p21 expression at both the mRNA as well as protein level, suggesting that DNA damage was important to illicit an increase in p21 protein levels. In this study, we analysed the effect of CP655 and the control CP655OMe on p21 protein levels from Jurkat cells as well as primary human CD4+ T cells. Western blot experiments for assessing p21 protein expression were conducted at different time points in order to ensure that the effect of CP655 can be visualized. The results showed that, contrary to other data so far, the only time point at which p21 protein expression was significantly affected was at 4 hours post treatment and culture. At this time point, a significant increase in p21 protein level was observed between CP655 treated cells and both the untreated as well as the CP655OMe treated cells.

Therefore, the consistent results obtained from the micro-array, RT-PCR and western blot experiments indicated that one of the target molecules for CP655, through which it exerts its effects on human CD4+ T cells, was the tumour suppressor Cell-Dependent Kinase Inhibitor, CDKN1A (p21).

Moving on to the second set of experiments, since the suppression of proliferation of CD4+ T cells by CP655 was the strongest phenotype observed in this study so far it was only logical to assess the impact of CP655 on signalling pathways that are directly related to cell proliferation such as the IL-2 pathway.

The IL-2 family of cytokines, which includes IL-4, IL-7, Il-9 and IL-15 apart from IL-2, play an essential role in the development of the immune system and immune responses. The expression of IL-2 receptor (IL-2R) on the surface of T cells is important for initiating proliferation. The receptor is made up of three chains – the α chain that binds IL-2 with low affinity, the β- and γ- chains that bind IL-2 with intermediate affinity, and a receptor made out of the combination of each of these three chains bind IL-2 with high affinity. Binding of IL-2 to the

intermediate or high affinity receptors provides the signal to initiate transition from G1 to the S phase of the cell cycle and begin the process of proliferation (Kim *et al*, 1993). In fact, IL-2 provides a signal strong enough to initiate proliferation of resting T-cells even in the absence of an antigen (Nakamura *et al*, 1991).

Binding of IL-2 to either the intermediate or the high-affinity receptor leads to dimerization and stabilization of the IL-2 receptor and initiates a cascade of downstream signalling events. The cytoplasmic tails of the β- and γ- receptor chains have docking sites for Janus-Associated Kinase (JAK) molecules as well as several tyrosine residues, phosphorylation of which leads to the recruitment of several signalling molecules. Activating the IL-2 receptor leads to a sudden increase in the recruitment of JAK1 and JAK3 to the receptor tails, which phosphorylate themselves and the receptor and attract other signalling molecules to the site. Phosphorylation of the tyrosine residues by JAK1 and JAK3 converts them into docking sites for other signalling molecules such as the Signal Transducers and Activators of Transcription 5a (STAT5a) and STAT5b. Once the STAT5a and STAT5b proteins are attracted to the phosphorylated tyrosine docking sites, they are phosphorylated and activated by the JAK1 and JAK3 proteins. The activated and phosphorylated STAT proteins dissociate from the receptor, dimerize and then translocate to the nucleus where they bind to the specific DNA binding sites to begin transcription of their target genes that cause cellular growth, development and proliferation (Lin and Leonard, 2000). In fact, the importance of the IL-2 signalling pathway via JAK3-STAT5 can be appreciated from the several studies that have highlighted this signalling pathway in T-cell driven chronic inflammatory diseases such as Rheumatoid Arthritis. JAK inhibitors have been in trial for treating people with RA, based on the hypothesis that JAK3 is essential for the activation, differentiation and proliferation of lymphocytes that drive the disease (Kremer *et al*, 2009; Patel *et al*, 2011).

There were two distinct aspects of the IL-2 pathway that we were interested in covering as a part of this study. First was to assess whether the cells cultured with CP655 were able to respond to exogenous IL-2, or was this ability

compromised after treatment. The second aspect was to determine whether CP655 treatment was affecting the downstream signalling events involved in the IL-2 signalling pathway.

To address the first aspect, exogenous IL-2 was added to CD4+ and CD14+ co-culture in the presence of CP655 and proliferation as well as cytokine production from these cells was measured. It was observed that while CP655 caused inhibition of proliferation and IFN-γ and IL-17 production as before, the addition of IL-2 was able to overcome the suppression caused by the chelation and these cells proliferated and produced cytokines at the same level as untreated and control cells. These results indicated that the inhibitory effects caused by CP655 were not permanent or damaging to the cells, as they still retained their ability to respond to exogenous IL-2. However, when only CD4+ T cells were treated with CP655, addition of exogenous IL-2 was unable to overcome the suppression caused by CP655 treatment. Since experiments during the initial part of this study showed that the main targets of CP655 treatment are the CD4+ T cells, it is suggested that the presence of CD14+ monocytes in the cell culture were responsible for the restoration of proliferative response on addition of exogenous IL-2. Additionally, IL-2 has been shown to be a strong activator of human CD14+ monocytes, causing them to produce large amount of growth factors and cytokines such as IL-6 and IFN-γ, which can in turn further activate the CD4+ T cells (Musso *et al*, 1992; Gusella *et al*, 1993; Bosco *et al*, 2000). Therefore, the inhibition caused by the treatment with CP655 cannot be overcome by the addition of exogenous IL-2 in CD4+ T cells, suggesting that CP655 may in fact, be interfering with the IL-2 signalling pathway as another possible mechanism of its action.

Therefore, in order to confirm this, the second aspect of the IL-2 pathway was addressed. It was decided to look at one of the most essential downstream signalling molecules of the IL-2 proliferation pathway, STAT5, and see if it was being affected by CP655 treatment. When the effect of the iron chelation was assessed on phosphorylation of STAT5, it was encouraging to see that CP655 was successful in reducing the phosphorylation of STAT5 in comparison to cells that did not receive the chelator, as well as those that received the control

compound, CP655OMe. Additionally, it was once again noticed that the time point at which the most prominent reduction in the phosphorylation of STAT5 was observed was 48 hours post stimulation and treatment, similar to what had been seen in previous experiments so far. This suggested that another reason why CP655 treatment was inhibiting proliferation of cells was due to its ability to inhibit phosphorylation of STAT5, which is important for cell proliferation.

Another set of interesting kinetic experiments set-up in this study revealed that pre-treating the CD4+ T cells with CP655 and then washing it out before the cells were stimulated with anti-CD3/CD28 beads did not affect the proliferation observed in the cells. However, if the cells were first stimulated with anti-CD3/CD28 beads and then treated with the chelator in the presence of the beads, led to the significant inhibition of proliferation as previously observed. These results suggested that it was important for the chelator to be present at the time the T-cell receptor was being stimulated in order to exert its effect on cell proliferation. Therefore, it can be hypothesized that CP655 may be interfering with some of the downstream signalling molecules of the T-cell receptor.

These results also linked in with the data showing reduced STAT5 phosphorylation, since the activation of the TCR is one of the main pathways for producing IL-2 in CD4+ T cells. Therefore, reduced IL-2 production due to aberrations in the T-cell signalling pathway could also be responsible for reduced phosphorylation of STAT5 that was previously observed. So, it can be suggested that apart from repressing the ability of CD4+ T cells to respond to IL-2 by reducing STAT5 phosphorylation, CP655 may potentially also be reducing the production of IL-2 due to aberrant TCR signalling.

Therefore, in conclusion, apart from directly affecting cell cycle proteins such as p21, CP655 can inhibit CD4+ T cell proliferation by affecting the IL-2 pathway and its downstream signalling molecule STAT5 and may also interfere with downstream signalling molecules of the T-Cell receptor.

CHAPTER 6

GENERAL DISCUSSION

CHAPTER 6

DISCUSSION

6.1 GENERAL DISCUSSION

The critical role played by iron in supporting life via its ability to promote cell growth, division and proliferation has been well established. The importance of iron for cellular processes can be judged by the various pathways that it plays a part in such as Electron transport, cellular respiration, DNA and RNA synthesis, cellular proliferation and regulation of gene expression. Additionally, several organs of the body are involved in iron metabolism such as the testis, brain, intestines and liver further highlighting the importance of its homeostasis (Boldt, 1999; Lieu *et al*, 2001; Koskenkorva-Frank *et al*, 2013). However the potentially toxic nature of iron and its ability to promote infectious diseases by aiding invading microorganisms cannot be ignored either. Microorganisms such as *Mycobacterium tuberculosis* and *Corynebacterium diphtheria*, have several mechanisms through which they source iron from the body and even steal it from iron storage sites such as Ferritin, in order to maintain a sufficient supply for survival and proliferation (Crouch *et al*, 2008; Cassat and Skaar, 2013). Therefore, it is evident that maintaining a balance in the availability of iron within the human body is of utmost importance (Lieu *et al*, 2001).

The importance of iron for metabolically active cells is pivotal, especially for thymocytes and activated T cells. Due to their high rate of metabolism and increased proliferation, their dependence on iron is greater than most other cell types in the human body (Kuvibidila *et al*, 2001). As a result of this iron forms an essential co-factor of the human immune system (Bowlus, 2003). Iron deficiency is believed to be one of the contributing factors responsible for thymic atrophy which results in reduced cell-mediated immunity due to reduction in the number of circulating T lymphocytes (Savino, 2002).

Therefore, whether it is carrying oxygen in haemoglobin, acting as an electron donor or acceptor in various enzymes or producing damaging free hydroxyl radicals and promoting microorganism growth, the impact of iron deficiency or iron overload can lead to several immune dysfunctions, disorders and even autoimmunity (Bowlus, 2003; Nairz *et al*, 2014).

One of the most frequently cited examples for understanding the relationship between Iron and immunity is that of the Anaemia of Chronic Disease (ACD). The main pathology of the disease stems from accumulation of iron within monocytes leading to impaired formation of the hormone Erythropoietin (Epo) and impaired proliferation of Erythroid progenitor cells. It is most commonly found in patients suffering from chronic inflammatory diseases such as Rheumatoid Arthritis (RA) and Cancers (Weiss and Goodnough, 2005).

Previously Blake *et al* (1985) used an iron chelator, Deferrioxamine (DFO) to investigate and elaborate on the role that iron accumulation plays in inflammatory diseases such as RA. This was based on previous observations from Muirden and Peace (1969) and Blake *et al* (1983), where DFO had been successful in reducing both acute and chronic inflammation in animal models of acute inflammation. Seven patients with RA were given DFO during this trial, however the study had to be terminated early due to adverse side effects, in the form of cerebral and ocular toxicities, caused due to the use of the chelator. However, these effects were attributed to the low specificity of DFO to iron and its ability to bind intra-cellular copper as well. While initial studies using DFO for treating inflammation in patients with RA had severe side effects, some of the trial patients did demonstrate good clinical responses to RA by showing a sharp reduction in the acute phase response (Blake *et al*, 1985).

DFO was the only iron chelator approved by the US Food and Drug Association (FDA) to be given parenterally to patients with iron overload. But in the past decade, the FDA has approved two more iron chelators for oral use in humans, Deferiprone and Deferasirox (Sheth, 2014). A lot of

advancements have been made in the field of iron chelation over the past few years. Several novel iron chelators have been developed and tested in various models of disease.

In this present study, I have investigated the effect of novel HPO iron chelator treatment on human CD4+ T lymphocytes. I have also explored the various mechanisms by which iron chelation exerts its effect on human CD4+ T cells. Implications of the findings of this study are discussed below. Having tested several different HPO iron chelators on mixed cultures of human CD4+ and CD14+ cells, it was evident that CP655 was most effective in reducing inflammatory cytokine production and proliferation of the cells. During the initial part of this study, it was also established that the main target cell of these HPO iron chelators, specifically CP655, are the purified CD4+ T cells. Furthermore, these experiments indicated that the main effect of iron chelation was on inhibition of proliferation of CD4+ T cells. In order to determine the mechanism of action of the iron chelators, all the subsequent experiments were conducted on human CD4+ T cells using CP655 as the main chelator.

6.1.1 *CP655 inhibits cellular proliferation by interfering with cell growth and development signalling pathways*

Having uncovered the first step towards identifying the mechanism of CP655 action by identifying CD4+ T cells as the main targets of chelation, the next aim was to try and identify the various pathways that may be altered after treatment with CP655. It was decided that conducting a whole genome microarray on anti-CD3/CD28 stimulated CD4+ T cells would help to identify novel genes and targets of chelation by CP655.

The microarray revealed a large number of unknown genes that were modulated by iron chelation. Additionally, most of the known genes that were highly significantly upregulated on treated with CP655 as compared to the untreated or the CP655OMe control treated cells showed only small fold changes in expression. As a result of this, it was difficult to identify clear patterns and trends in the data in order to highlight specific pathways that may be getting affected following chelator treatment. However, a manual review of the data indicated that majority of the genes that were significantly modulated by treatment with CP655 were those involved with MAPK signalling, cell proliferation and cell growth and division pathways. This was in correlation with the previous *in-vitro* results where inhibition of proliferation of the main phenotype being altered after treatment with chelator.

A further observation was that there were a large number of microRNAs, which appeared in the list of significantly modulated genes. MicroRNAs (miRNAs) are 20-25 nucleotides long, non-coding small RNAs that act as post-transcriptional regulators of gene expression by binding to 3'UTR of target mRNAs causing inhibition of translation and degradation (Lai, 2002; Qu *et al*, 2013). Several studies have highlighted the role of miRNAs in tumorigenesis, either in the form of oncogenes promoting tumour growths

and excessive cellular proliferation or in the form of tumour suppressors, inhibiting tumours and cellular proliferation (Bushati and Cohen, 2007; Budd *et al*, 2012; Zhang *et al*, 2012; Nadiminty *et al*, 2012). For instance, miRNA 503 has been found to be associated with hepatocellular carcinoma. It acts as a tumour suppressor and its expression results in blocking of the cell cycle, apoptosis and tumour suppression (Wang *et al*, 2014).

The microarray conducted in this study revealed a significantly increased fold expression of miRNA 503 after treatment with CP655. It has been suggested that miRNA 503 inhibits cellular proliferation by directly targeting two cell cycle proteins, cyclin D3 and E2F3 (Xiao *et al*, 2013). While there were other miRNAs such as miRNA 99A that was significantly upregulated in this study and the literature suggests several contradictory roles for this miRNA. Feng *et al* (2012) demonstrated that miRNA 99a acts as a tumour suppressor and inhibits proliferation in bladder cancer. Another study (Hu *et al*, 2014) showed that miRNA 99a inhibits proliferation by its ability to cause a cell cycle arrest via the m-TOR pathway. However, contradictory to this Chen *et al* (2015) suggest that in certain cancers such as Non-small cell lung cancer, miRNA 99A can promote proliferation and cell migration.

During this process of reviewing the literature, and correlating the findings to the results of the microarray experiment it became evident that even though software analyses did not show any significantly enriched pathway due to the small fold changes in the gene, most of the genes that were significantly modulated, belonged to a few common pathways. One of the drawbacks of microarray analysis is to decide where to put the cut-off point in terms of fold change for genes. If a low cut-off point is chosen such as 0.5 or 1.0 fold, it can increase the chances of false positive results. However, if a high cut-off is chosen it can lead to some important genes being left out of analysis. It has been suggested that there might be some genes that are crucial for specific pathways or processes to take place, but they often do not show large fold changes in expression (Chin and Moldin, 2001). Therefore, in order to move ahead with the analysis of the data generated it was decided to prepare a manual list of genes that were differentially modulated in the micro-array

following CP655 treatment after cross-linking and consultation with the literature. This list consisted of several cell cycle proteins, some microRNAs as well as those involved in carcinogenesis and tumorigenesis. Since it was not possible to validate each of these 20 genes by RT-PCR due to limited time and resources, a functional analysis of the effect of CP655 was conducted in order to further narrow down the list of prospective targets. This was done by conducting cell cycle analysis on CD4+ T cells, since most of these in the list were involved in controlling different aspects of the cell cycle.

6.1.2 *CP655 causes G1/S phase arrest of human CD4+ T cells and Jurkat cell lines*

Treatment of both Jurkat cells, and primary human CD4+ T cells with CP655 led to a functional block in the cell cycle progression of these cells. In both cases, the kinetics of the effect of treatment was maintained and significant block of the cell cycle was observed only 48hours after treatment with CP655. In Jurkat cells, the transition from the G1 to the S phase was significantly altered with most of the cells getting arrested between the two stages.

A similar pattern was observed in primary CD4+ T cells, although the results were not as prominent as those observed in the Jurkat cells. At 48 hours post treatment, most of the cells were arrested in the G1 phase of the cycle with significantly fewer cells entering the G2/M phase. These results were consistent with previous studies that have used several different types of iron chelators and shown similar results in several different cell types (Clement *et al*, 2002; Szuts and Krude, 2004; Gharagazloo *et al*, 2008).

The results from these functional studies helped to narrow down the list of 20 genes developed following the microarray to five genes that could potentially play a role in controlling the transition from G1 to S phase of the cell cycle.

6.1.3 *Potential mechanism of action for CP655 via increased CDKN1A expression*

The five genes short-listed for validation were CDC6, CDKN1A (p21), RRM1, GADD45G and ANAPC1. RT-PCR at various time points ranging from 4 hours to 48 hours post treatment. Results indicated that the only gene where mRNA expression correlated with the functional analysis so far was p21. This gene showed increased expression following treatment with CP655 at 12 hours and also at 48 hours post treatment. The increased expression of p21 was replicated in Western blot experiments were p21 protein expression was significantly increased in Jurkat cells, as well as primary CD4+ T cells following CP655 treatment. However, the time point continued to remain a point of concern, as increased protein expression was only observed at early time points of 4 hours post treatment.

The increased expression of CDKN1A (p21) can be attributed to two individual pathways – a p53 dependent pathway and a p53 independent pathway.

One of the suggested mechanisms through which iron chelation causes increased expression of p53 and hence p21, is via the JNK and p38 MAPK signalling pathways. It has been shown that iron chelation leads to the dissociation of the Apoptosis-Signal Regulating Kinase1 (ASK1) and Theoredoxin (Trx) complex. The dissociation of Ask1 and its increased phosphorylation leads to the initiation of a signalling cascade causing increased phosphorylation of the JNK and p38 MAPK pathways, which are tumour suppressor pathways having p53 as their immediate down-stream target (Yu and Richardson, 2011). In fact, p38 has been shown to cause increased phosphorylation and activation of p53, leading to G1/S phase arrest of the cell cycle via its downstream targets such as p21. JNK as well, has been shown to phosphorylate p53 leading to its activation (Wilkinson and Millar, 2000). Another more commonly discussed mechanism via which iron chelation leads to increased p53 expression, is through its interaction with the

Hypoxia-Inducible factor-1α (HIF-1α). Hypoxia caused due to iron chelation leads to increased concentration of HIF-1α, which directly binds to and stabilizes p53 and promotes p53-dependent activities (Suzuki *et al*, 2001).

p21 forms an integral part of the growth and cell cycle arrest pathways mediated by p53 (El-Deiry *et al*, 1994) and has been well established as a downstream target effector of p53 (Harper *et al*, 1993; Xiong *et al*, 1993). Therefore, one of the ways that CP655 inhibits cellular proliferation and causes a block in the G1/S phase of the cell cycle could be due to the activation of the p53 pathway, which leads to activation and over expression of p21 (Fig 6.1).

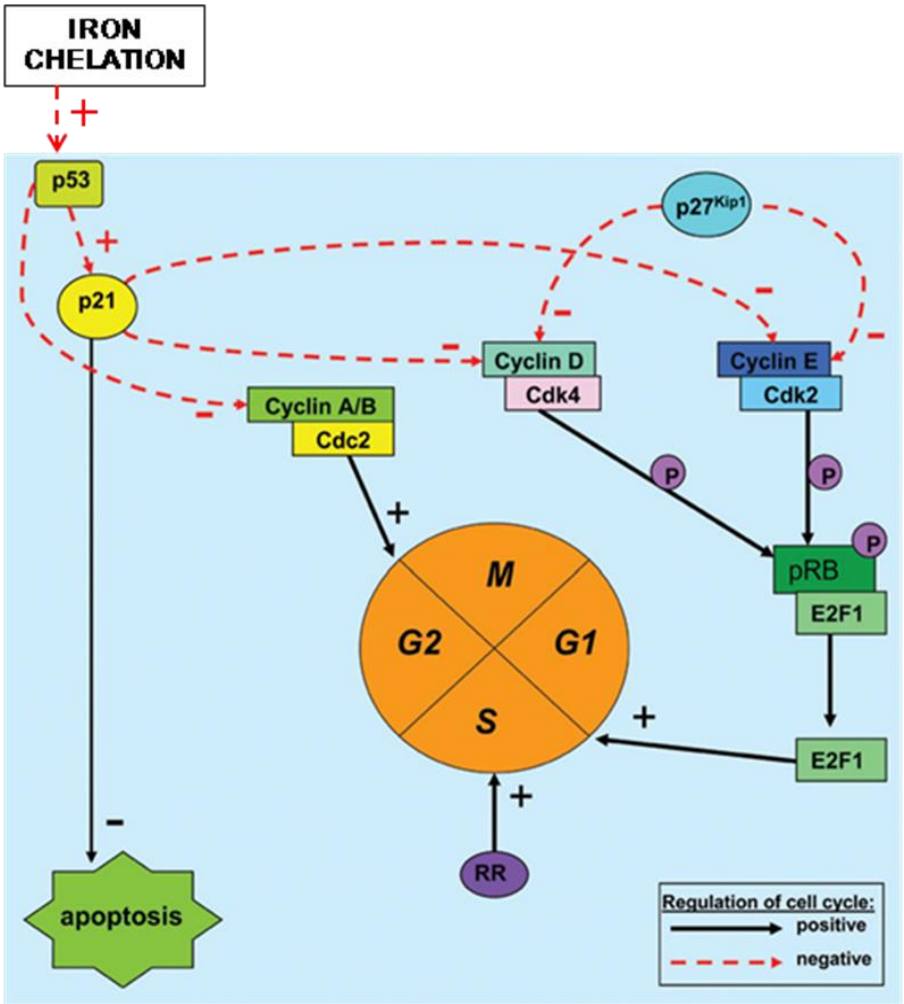

Figure 6.1: Effect of Iron chelation on cell cycle proteins.

(Adapted from Yu et al, 2007)

Apart from a p53-dependent pathway, p21 can also be upregulated in a p53-independent manner. There are several transcription factors, such as Activating Protein 2 (AP2), E2F1, Specificity Protein 1 (Sp1), that have DNA-binding sites within the promoter region of p21 suggested that these transcription factors may be responsible for the p53-independent up-regulation of p21. The tumour suppressor protein, BRCA1, has also been suggested to be one of the transactivators of p21 in a p53 independent manner (Gartel and Tyner, 1999).

SUGGESTED MECHANISM – 2

6.1.4 CP655 inhibits cellular proliferation by suppressing the IL-2 pathway and reducing STAT5 phosphorylation

It is well established in the literature that iron is essential for the proper functioning of the immune system, and iron deficiency or iron depletion can result in reduced or dysfunctional cell-mediated immunity. Additionally, as discussed previously iron deficiency affects the proper functioning of the Thymus and impaired proliferation of T cells. Therefore, reduced iron content may affect the production of IL-2 from T cells. A study on children with Iron-Deficiency Anaemia, reported that they also had low levels of IL-2 (Jason *et al*, 2001; Suega and Bakta, 2010). Another interesting study linking iron metabolism to the JAK2-STAT5 axis was conducted by Kerenyi *et al* (2008). In this study, they used mice completely lacking STAT5 (*STAT5-/-)* and showed that these animals suffered from microcytic anaemia. Additionally, the erythroid cells in these animals showed a marked reduction in the cell surface expression of TfR1, which they showed was due to the marked reduction in the expression of IRP2, a direct target of STAT5 transcription. They were successful in proving this relation between IRP2 and STAT5 by showing that the promoter region of the IRP2 gene had three

functional binding sites for STAT5 thereby suggesting that a reduction in phosphorylation of STAT5 would lead to impaired development and functioning of IRP2 and hence TfR1, upsetting the intracellular iron metabolism.

In a second set of mechanistic experiments, CP655 or control treated cells were supplemented with exogenous IL-2. CD4+ and CD14+ cells cultures treated with CP655 when supplemented with IL-2 were able to overcome the suppression of proliferation. However, when only CD4+ T cells were supplemented with IL 2 following CP655, the cells were unable to overcome the suppression suggesting that CP655 was interfering with the IL-2 signalling pathway. pSTAT5 western blot were conducted in order to elaborate on the mechanism by which CP655 was inhibiting the IL 2 pathway and thereby affecting proliferation in turn. CP655 was able to consistently reduce pSTAT5 expression in stimulated CD4+ T cells suggesting another possible route of affect.

The link between STAT5, proliferation and G1/S phase cell cycle transition has been elaborated upon by studies showing that several D-type cyclins that control progression through the G1 phase are direct targets of the transcription factor STAT5. Therefore binding of IL-2 to its receptor thus activating STAT5 transcription factor leads to cell proliferation due to activation of various cyclin proteins. In fact, cyclin E has also been suggested to be a target of STAT5 and up-regulated in response to IL-2 signalling (Moon and Nelson, 2001; Moon *et al*, 2004; Kerenyi *et al*, 2008). However, the role of STAT5a and STAT5b on the cell cycle has been contested, as there have been studies showing that these transcription factors negatively regulate the cell cycle, by activating and inducing the expression of inhibitors such as CDKN1A (Yu JH *et al*, 2010).

To summarize, it can be hypothesized that due to the impaired development and functioning of T cells, and the reduced phosphorylation of STAT5 following CP655 treatment, the ability of T cell to respond to IL-2 was compromised leading to repressed proliferation. Additionally, reduced

STAT5 phosphorylation could also be affecting the transcription of other cell cycle controlling genes such as cyclin D1 and cyclin E also leading to a block in the cell cycle.

6.1.5 *CP655 may interfere with signalling via the T-cell Receptor*

Previous studies have showed that iron chelation can influence T cell stimulation by down-regulating CD28 co-stimulatory molecule from the surface of the cell. Engagement of the CD3/TCR complex along with the CD28 co-stimulatory molecule is essential for proper TCR signalling and cell proliferation (Kuvibidila and Porretta, 2003). Another study conducted by Kuvibidila *et al* (1999) showed that iron chelation reduced Protein Kinase C-θ (PKC-θ) activity in murine lymphocytes which was responsible for altered proliferation of the cells. PKC-θ is an important serine/threonine kinase that is activated following signal from the TCR and the CD28 molecule, and it further activates transcription factors such as NF-κB, NF-AT and AP-1 which are responsible for T cell activation, differentiation and proliferation (Wang *et al*, 2012). Furthermore, some of these transcription factors, such as NF-AT and AP-1, have been implicated in the production of IL-2 (Chow *et al*, 1999).

Preliminary experiments using different kinetics of CP655 treatment of CD4+ T cells revealed that CP655 is required to be present along with the cells during the time of TCR stimulation. That is, pre-treating the cells with CP655 and removing it before stimulating the TCR did not show any effect on inhibition of proliferation. Therefore, a third possible mechanism of action of CP655 could involve its ability to interfere with proteins downstream of TCR signalling that affect the ability of T cells to proliferation. However, due to time constraints, no further work was done to elucidate this possible mechanism of CP655 and could potentially be one of the aspects to be looked at in future studies.

An interesting observation made during the course of these final experiments was that the strength of the stimulation provided to T cells could have an effect on the action of CP655. During the initial part of the study, when experiments were conducted to identify the target cell type for CP655, CD4+

T cells and CD14+ monocytes were treated separately with CP655 for 24 hours and then the chelator was washed out before the cells were cultured together and stimulated with the antigen, Tetanus Toxoid. In such as experimental set-up, CP655 was able to significantly inhibit cellular proliferation and IFN-γ and IL-17 production. However, the experiments discussed in this last section showed that when CD4+ T cells were pre-treated with CP655 and then stimulated with anti-CD3/CD28 beads after washing out the chelator, no effect of CP655 was seen. This suggested that there was a possibility that the strength of the signal provided to the CD4+ T cells following TCR stimulation with an antigen was not very strong and CP655 was able to cause a suppression of its effects. Whereas, stimulation using anti-CD3/CD28 beads may provide a much stronger signal for proliferation to CD4+ T cells, making it difficult for CP655 to overcome it and exert its effect. Therefore, in the case of a stronger stimulus, CP655 needs to be present at the time of TCR stimulation in order to maintain its effect on signalling molecules.

Nicholson *et al* (1997) and Murtaza *et al* (1999) showed that the strength of TCR stimulation as well as the strength of co-stimulation affect the differentiation as well as the proliferative ability of CD4+ T cells, that is, a stronger stimulus meant greater proliferative ability of the CD4+ T cells. Similar results were obtained in murine experiments conducted previously in our laboratory. CD4+ and CD14+ cells obtained murine spleen and lymph nodes were stimulated with Tetanus Toxoid and then treated with the iron chelator, which was able to successfully reduce proliferation and cytokine production from these cells. However, when these cells were stimulated with Concanavalin A (Con A), a strong mitogen, the chelators were unable to suppress both proliferation and cytokine production.

6.2 CONCLUSION

The essential role of iron within the human body has been known for years. The ability of iron to promote and up-hold cell mediated immunity, participate in various metabolical and physiological pathways along with its ability to cause toxicities and promote infection has been discussed in several studies. As a result of this crucial balance that is required by the body, various pathways involved in iron metabolism have been studied extensively. Iron has been implicated to play a role in several autoimmune inflammatory disorders such as Rheumatoid Arthritis, in several cancers and even in several neuro-physiological disorders such as Alzheimers and Multiple Sclerosis.

In this study, iron chelators have been used to modulate the function of human CD4+ T cells with the aim that these chelators could potentially be used to treat CD4 driven diseases characterised by excessive cellular proliferation and inflammation. The chelator used in this study, CP655, is a novel HPO chelator that has been shown to be more specific, and have higher affinity to intracellular iron as compared to previously used iron chelators such as DFO. The results have established that CP655 inhibits proliferation and inflammatory cytokine production from CD4+ T cells. This study was successful in demonstrating that the effect caused by CP655, in suppressing cell proliferation, was an iron dependent effect by using a structurally similar analogue to CP655 that does not chelate iron (CP655OMe). Additionally, this study suggests three individual, yet overlapping, mechanisms by which CP655 could potentially be exerting its effects on CD4+ T cells.

Firstly, this study demonstrated that CP655 was causing a block in the G1/S phase of the cell cycle which was responsible for the inhibition of proliferation observed by tritiated thymidine incorporation as well as CFSE staining. The block in the cell cycle was suggested by data generated from microarray studies and was further confirmed by functional studies by Propidium Iodide staining of the cells. Potential target proteins of the chelator were then identified after correlating results to the literature out of which one

protein, CDKN1A (p21) was found to be consistently affected by CP655 treatment. CDKN1A, which is a tumour suppressor, was upregulated in microarray analysis as well as in RT-PCR studies and was also confirmed by western blot analysis. Upregulation of this protein causes a block in the cell cycle, and is one of the mechanism by which CP655 could be affecting CD4+ T cells.

The second mechanism explored in this study was the effect of CP655 on the IL-2 pathway and its downstream signaling molecule, STAT5. Treatment with CP655 led to reduced phosphorylation of STAT5 which has been shown to be essential for causing proliferation of CD4+ T cells. STAT5 is also an essential factor for several other cell proliferation and cell cycle progression proteins such as D-type cyclins, cyclin E1 etc. This suggested that the reduced phosphorylation of STAT5 due to CP655 treatment could also lead to an aberration in the progression of the cell cycle.

Lastly, kinetic analysis of the effect of CP655 revealed that the chelator needs to be present in the cell during the time of TCR stimulation, suggesting that it may be acting on T cells by interfering with TCR signaling pathways. This potential mechanism was not analysed in this study, but could be an interesting option to explore in future studies.

The possible mechanisms by which CP655 inhibits cell proliferation are summarized in Figure 6.2.

This study clearly showed that the chelator was not responsible for any toxicities in the different cell types used. Hence, it can be an interesting therapeutic mechanism for treating several diseases resulting in ACD such as Rheumatoid Arthritis, diseases causing excessive cellular proliferation such as various cancers and diseases showing deposition of iron such as Parkinson's disease.

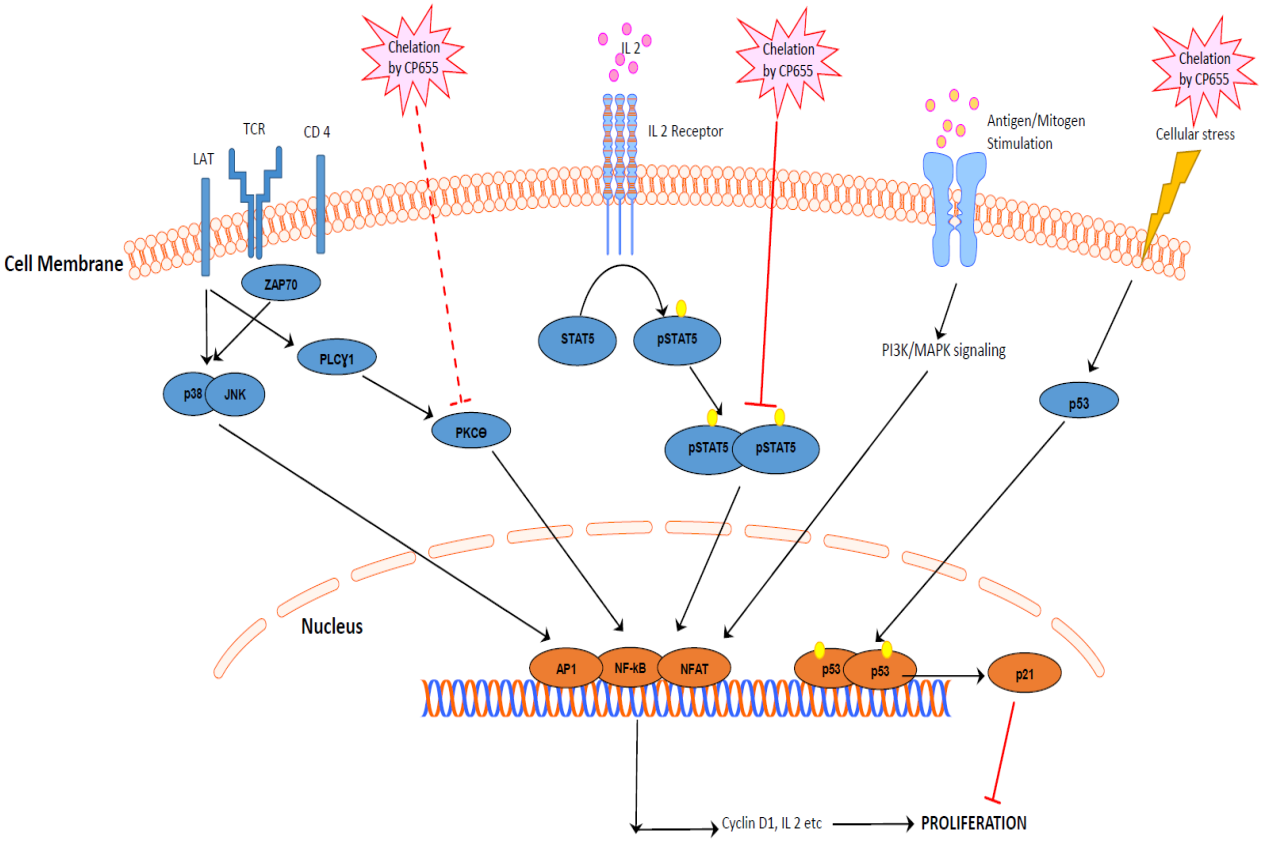

Figure 6.2: Possible mechanisms of action of CP655

6.3 LIMITATIONS AND FUTURE WORK

All the experiments in this study were done, *in vitro*, on cells isolated from healthy human controls or on cell lines. As a result of this, it is difficult to correlate the data to *in vivo* studies.

The initial experiments on CD4+ and CD14+ cell cultures were conducted using only Tetanus toxoid as the antigen for stimulation, or using anti-CD3/CD28 bead stimulation for purified CD4+ cell cultures. Future work could include using different stimulants such as PHA or other antigens in order to get a better idea on the mechanism of CP655 action.

One of the main limitations of this study is related to the microarray analysis that was conducted in order to understand the mechanism of the chelator. Due to time and financial constraints, the experiment could only be conducted once. Therefore, a specific time point had to be chosen which would provide the most relevant results for this study. The 18 hour time point chosen in this study may not have been most appropriate. Future work could include conducting a microarray at several different time points, using synchronized cells so as to get a better idea of how CP655 affects genes over time. Additionally, the cells used to conduct the microarray experiments had not been synchronized before being used. Use of synchronized cells may have provided more consistent and prominent results. Another limitation associated with this study is that it was unable to identify a specific time point around which the chelator shows the most prominent effect. While some assays reveal 48 hours post treatment to be the ideal time point to visualize the effect of CP655, other experiments such as the Western blots suggest that the changes take place as early as 4 hours post treatment with CP655. This problem can be overcome by using cell lines rather than primary cells to see more consistent effects and reduce any inter-donor variation that exists while using primary human cells.

Similar time and financial constraints were in place while conducting RT-PCR and western blot analysis on the short-listed genes. Under ideal conditions, there would have been several other genes and proteins that I would have liked to analyse but for this study it was decided that it would be better to focus on one specific gene/protein after consulting with the literature. The effect of CP655 on some other proteins involved in the cell cycle progression forms an important part of the future work that is required to follow this study. Several other genes belonging to the p21 pathway such as p53, pRb as well as other cell cycle controlling proteins such as Cyclin D1 could be analysed by western blot and RT-PCR in the future.

Another important aspect to be elucidated upon is identifying the location of the chelator within the cells. The fluorescent nature of CP655 can help to identify its localization within the cell by imaging.

Furthermore, the IL-2 and TCR signalling pathways are important for the proliferation of CD4+ T cells, this study has added to the literature regarding the effect that iron chelation can have on these pathways. However, there is still a lot of unanswered questions and studying the effect on different T cell signalling molecules may be an interesting option for conducting future studies. Zap 70 and PKC θ have previously shown to be modulated on treatment with iron chelators and could be important targets to look at following CP655 treatment. Also, as mentioned earlier, using different types of stimulus for the CD4+ T cells can help to identify specific target molecules. Lastly, experiments elucidating the different effects CP655 may have on antigen-stimulated cells versus anti-CD3/CD28 stimulated cell could also add to the literature on the effect of signal strength on T cell proliferation and activation.

The future therapeutic applications of this compound could include use in anti-cancer drugs due to its ability to significantly inhibit proliferation. Iron chelation has recently been used for the treatment of several neurological disorders such as Alzheimer's and Parkinson's, where studies have shown increased accumulation of iron in the brain. The small size and faster permeability could make CP655 a potentially beneficial therapeutic agent.

CHAPTER 7
REFERENCE LIST

CHAPTER 7
REFERENCE LIST

1. Abeysinghe, R. D., Roberts, P. J., Cooper, C. E., MacLean, K. H., Hider, R. C., & Porter, J. B. (1996). The environment of the lipoxygenase iron binding site explored with novel hydroxypyridinone iron chelators. *Journal of Biological Chemistry*, *271*(14), 7965-7972.
2. Algren, D. A. Review of Oral Iron Chelators (Deferiprone and Deferasirox) for the Treatment of Iron Overload in Pediatric Patients.
3. Alt, J. R., Gladden, A. B., & Diehl, J. A. (2002). p21Cip1 promotes cyclinD1 nuclear accumulation via direct inhibition of nuclear export. *Journal of Biological Chemistry*, *277*(10), 8517-8523.
4. Anderson, G. J., & Wang, F. (2012). Essential but toxic: controlling the flux of iron in the body. *Clinical and Experimental Pharmacology and Physiology*, *39*(8), 719-724.
5. Andrews, N. C. (1999). Disorders of iron metabolism. *New England Journal of Medicine*, *341*(26), 1986-1995.
6. Andrews, N. C., Fleming, M. D., & Levy, J. E. (1999). Molecular insights into mechanisms of iron transport. *Current opinion in hematology*, *6*(2), 61.
7. Ashcroft, M., Taya, Y., & Vousden, K. H. (2000). Stress signals utilize multiple pathways to stabilize p53. *Molecular and cellular biology*, *20*(9), 3224-3233.
8. Babitt, J. L., Huang, F. W., Wrighting, D. M., Xia, Y., Sidis, Y., Samad, T. A. & Lin, H. Y. (2006). Bone morphogenetic protein signaling by hemojuvelin regulates hepcidin expression. *Nature genetics*, *38*(5), 531-539.
9. Bading, J. R., & Shields, A. F. (2008). Imaging of cell proliferation: status and prospects. *Journal of Nuclear Medicine*, *49*(Suppl 2), 64S-80S.
10. Beard, J. L. (2001). Iron biology in immune function, muscle metabolism and neuronal functioning. *The Journal of nutrition*, *131*(2), 568S-580S
11. Becton, D. L., & Roberts, B. (1989). Antileukemic effects of deferoxamine on human myeloid leukemia cell lines. *Cancer research*, *49*(17), 4809-4812.
12. Beutler, E., Hoffbrand, A. V., & Cook, J. D. (2003). Iron deficiency and overload. *ASH Education Program Book*, *2003*(1), 40-61.

13. Black, A. R., & Black, J. D. (2012). Protein kinase C signaling and cell cycle regulation. *Frontiers in immunology*, *3*.
14. Blain, S. W., Montalvo, E., & Massagué, J. (1997). Differential interaction of the cyclin-dependent kinase (Cdk) inhibitor p27Kip1 with cyclinA-Cdk2 and cyclinD2-Cdk4. *Journal of Biological Chemistry*, *272*(41), 25863-25872.
15. Blake, D. R., Hall, N. D., Bacon, P. A., Dieppe, P. A., Halliwell, B., & Gutteridge, J. M. (1983). Effect of a specific iron chelating agent on animal models of inflammation. *Annals of the rheumatic diseases*, *42*(1), 89-93.
16. Blake, D. R., Winyard, P., Lunec, J., Williams, A., Good, P. A., Crewes, S. J. & Hider, R. C. (1985). Cerebral and ocular toxicity induced by desferrioxamine. *QJM*, *56*(1), 345-355.
17. Blow, J. J., & Gillespie, P. J. (2008). Replication licensing and cancer—a fatal entanglement?. *Nature Reviews Cancer*, *8*(10), 799-806.
18. Boldt D.H (1999). New perspectives on iron: an introduction. *American Journal of Medical Science*. 318. 207– 212
19. Boronat, S., & Campbell, J. L. (2007). Mitotic Cdc6 stabilizes anaphase-promoting complex substrates by a partially Cdc28-independent mechanism, and this stabilization is suppressed by deletion of Cdc55. *Molecular and cellular biology*, *27*(3), 1158-1171.
20. Bosco, M. C., Curiel, R. E., Zea, A. H., Malabarba, M. G., Ortaldo, J. R., & Espinoza-Delgado, I. (2000). IL-2 Signaling in Human Monocytes Involves the Phosphorylation and Activation of p59hck 1. *The Journal of Immunology*,*164*(9), 4575-4585.
21. Bowlus, C. L. (2003). The role of iron in T cell development and autoimmunity. *Autoimmunity reviews*, *2*(2), 73-78.
22. Brittenham, G. M. (1992). Development of iron-chelating agents for clinical use [editorial; comment]. *Blood*, *80*(3), 569-574.
23. Broderick, R., Rainey, M. D., Santocanale, C., & Nasheuer, H. P. (2013). Cell cycle-dependent formation of Cdc45–Claspin complexes in human cells is compromized by UV-mediated DNA damage. *FEBS Journal*, *280*(19), 4888-4902.
24. Bromberg, J., & Darnell Jr, J. E. (2000). The role of STATs in transcriptional control and their impact on cellular function. *Oncogene*, *19*(21), 2468-2473.

25. Budd WT, Weaver DE, Anderson J, Zehner ZE (2012) MicroRNA dysregulation in prostate cancer: network analysis reveals preferential regulation of highly connected nodes. *Chemical Biodiversity* 9:857–867
26. Bushati, N., & Cohen, S. M. (2007). microRNA functions. *Annual Review of Cell and Developmental Biology*, *23*, 175-205.
27. Cairo, G., Recalcati, S., Mantovani, A., & Locati, M. (2011). Iron trafficking and metabolism in macrophages: contribution to the polarized phenotype. *Trends in immunology*, *32*(6), 241-247.
28. Casciola-Rosen, L., Wigley, F., & Rosen, A. (1997). Scleroderma autoantigens are uniquely fragmented by metal-catalyzed oxidation reactions: implications for pathogenesis. *The Journal of experimental medicine*, *185*(1), 71-80.
29. Cassat, J.E.,andSkaar,E.P.(2013).Iron in infection and immunity. *Cell Host and Microbe* 13, 509–519.doi:10.1016/j.chom.2013.04.010
30. Cerqueira, N. M., Fernandes, P. A., & Ramos, M. J. (2007). Ribonucleotide reductase: a critical enzyme for cancer chemotherapy and antiviral agents. *Recent patents on anti-cancer drug discovery*, *2*(1), 11-29.
31. Chaston, T. B., & Richardson, D. R. (2003). Iron chelators for the treatment of iron overload disease: relationship between structure, redox activity, and toxicity. *American journal of hematology*, *73*(3), 200-210.
32. Chen, C., Zhao, Z., Liu, Y., & Mu, D. (2015). microRNA-99a is downregulated and promotes proliferation, migration and invasion in non-small cell lung cancer A549 and H1299 cells. *Oncology Letters*, *9*(3), 1128-1134.
33. Chen, L. C., Chen, C. C., Liang, Y., Tsang, N. M., Chang, Y. S., & Hsueh, C. (2011). A novel role for TNFAIP2: its correlation with invasion and metastasis in nasopharyngeal carcinoma. *Modern Pathology*, *24*(2), 175-184.
34. Cheng, M., Olivier, P., Diehl, J. A., Fero, M., Roussel, M. F., Roberts, J. M., & Sherr, C. J. (1999). The p21Cip1 and p27Kip1 CDK 'inhibitors' are essential activators of cyclinD-dependent kinases in murine fibroblasts. *The EMBO journal*, *18*(6), 1571-1583.

35. Chow, C. W., Rincón, M., & Davis, R. J. (1999). Requirement for transcription factor NFAT in interleukin-2 expression. *Molecular and cellular biology*, *19*(3), 2300-2307.
36. Classon, M., & Dyson, N. (2001). p107 and p130: versatile proteins with interesting pockets. *Experimental cell research*, *264*(1), 135-147.
37. Clement, P. M., Hanauske-Abel, H. M., Wolff, E. C., Kleinman, H. K., & Park, M. H. (2002). The antifungal drug ciclopirox inhibits deoxyhypusine and proline hydroxylation, endothelial cell growth and angiogenesis in vitro. *International journal of cancer*, *100*(4), 491-498.
38. Cobrinik, D. (2005). Pocket proteins and cell cycle control. *Oncogene*, *24*(17), 2796-2809.
39. Connor, S. L., Gustafson, J. R., Sexton, G., Becker, N., Artaud-Wild, S., & Connor, W. E. (1992). The Diet Habit Survey: a new method of dietary assessment that relates to plasma cholesterol changes. *Journal of the American Dietetic Association*, *92*(1), 41-47.
40. Conrad, M. E., Umbreit, J. N., & Moore, E. G. (1999). Iron absorption and transport. *The American journal of the medical sciences*, *318*(4), 213.
41. Cooper, C. E., Lynagh, G. R., Hoyes, K. P., Hider, R. C., Cammack, R., & Porter, J. B. (1996). The relationship of intracellular iron chelation to the inhibition and regeneration of human ribonucleotide reductase. *Journal of Biological Chemistry*, *271*(34), 20291-20299.
42. Crouch,M.L.,Castor,M.,Karlinsey,J.E.,Kalhorn,T.,andFang,F.C.(2008).Biosyn- thesis and Iron-dependent export of the siderophore salmochelin are essential for virulence of *Salmonella enterica* serovar *Typhimurium*. *Molecular Microbiology.* 67, 971–983. doi:10.1111/j.1365-2958.2007.06089.x
43. Dallas, P. B., Gottardo, N. G., Firth, M. J., Beesley, A. H., Hoffmann, K., Terry, P. A., ... & Kees, U. R. (2005). Gene expression levels assessed by oligonucleotide microarray analysis and quantitative real-time RT-PCR–how well do they correlate?. *BMC genomics*, *6*(1), 59.
44. Darnell, G., & Richardson, D. R. (1999). The potential of iron chelators of the pyridoxal isonicotinoyl hydrazone class as effective antiproliferative

agents III: the effect of the ligands on molecular targets involved in proliferation. *Blood*, *94*(2), 781-792.

45. Dautry-Varsat, A., Ciechanover, A., & Lodish, H. F. (1983). pH and the recycling of transferrin during receptor-mediated endocytosis. *Proceedings of the National Academy of Sciences*, *80*(8), 2258-2262.
46. Deb, S., Johnson, E. E., Robalinho-Teixeira, R. L., & Wessling-Resnick, M. (2009). Modulation of intracellular iron levels by oxidative stress implicates a novel role for iron in signal transduction. *Biometals*, *22*(5), 855-862.
47. DeGregori, J., Leone, G., Ohtani, K., Miron, A., & Nevins, J. R. (1995). E2F-1 accumulation bypasses a G1 arrest resulting from the inhibition of G1 cyclin-dependent kinase activity. *Genes & Development*, *9*(23), 2873-2887.
48. Delavaine, L., & La Thangue, N. B. (1999). Control of E2F activity by p21Waf1/Cip1. *Oncogene*, *18*(39), 5381-5392.
49. Dexter, D. T., Carayon, A., Javoy-Agid, F., Agid, Y., Wells, F. R., Daniel, S. E., ... & Marsden, C. D. (1991). Alterations in the levels of iron, ferritin and other trace metals in Parkinson's disease and other neurodegenerative diseases affecting the basal ganglia. *Brain*, *114*(4), 1953-1975.
50. Donovan, A., Brownlie, A., Zhou, Y., Shepard, J., Pratt, S. J., Moynihan, J., ... & Zon, L. I. (2000). Positional cloning of zebrafish ferroportin1 identifies a conserved vertebrate iron exporter. *Nature*, *403*(6771), 776-781.
51. Ducey, T. F., Carson, M. B., Orvis, J., Stintzi, A. P., & Dyer, D. W. (2005). Identification of the iron-responsive genes of Neisseria gonorrhoeae by microarray analysis in defined medium. *Journal of bacteriology*, *187*(14), 4865-4874.
52. Ekmekcioglu, C., Feyertag, J., Marktl, W., (1996). A ferric reductase activity is found in brush border membrane vesicles isolated from Caco-2 cells. *Journal of Nutrition*. 126, 2209±2217
53. El-Deiry, W. S., Harper, J. W., O'Connor, P. M., Velculescu, V. E., Canman, C. E., Jackman, J., ... & Vogelstein, B. (1994). WAF1/CIP1 is induced in p53-mediated G1 arrest and apoptosis. *Cancer research*, *54*(5), 1169-1174.
54. Fakih, S., Podinovskaia, M., Kong, X., Schaible, U. E., Collins, H. L., & Hider, R. C. (2009). Monitoring intracellular labile iron pools: A novel

fluorescent iron (III) sensor as a potential non-invasive diagnosis tool. *Journal of pharmaceutical sciences*, *98*(6), 2212-2226.

55. Feng, Y., Kang, Y., He, Y., Liu, J., Liang, B., Yang, P., & Yu, Z. (2014). microRNA-99a acts as a tumor suppressor and is down-regulated in bladder cancer. *BMC urology*, *14*(1), 50.
56. Finch, C. (1994). Regulators of iron balance in humans [see comments]. *Blood*, *84*(6), 1697-1702.
57. Fitzgerald-Hayes, M., & Reichsman, F. (2009). *DNA and Biotechnology*. Academic Press.
58. Flaten, T. P., Aaseth, J., Andersen, O., & Kontoghiorghes, G. J. (2012). Iron mobilization using chelation and phlebotomy. *Journal of Trace Elements in Medicine and Biology*, *26*(2), 127-130.
59. Fleet, J.C. *(*1998*)* Identification of Nramp2 as an iron transport protein: another piece of the intestinal iron absorption puzzle. *Nutrition Review* 56*:* 88–89.
60. Fleming, M. D., Trenor, C. C., Su, M. A., Foernzler, D., Beier, D. R., Dietrich, W. F., & Andrews, N. C. (1997). Microcytic anaemia mice have a mutation in Nramp2, a candidate iron transporter gene. *Nature genetics*, *16*(4), 383-386.
61. Forni, G. L., Balocco, M., Cremonesi, L., Abbruzzese, G., Parodi, R. C. and Marchese, R. (2008), Regression of symptoms after selective iron chelation therapy in a case of neurodegeneration with brain iron accumulation. *Movement Disorders*, 23: 904–907.
62. Forni, G. L. (2012). Ferrochelating treatment in patients affected by neurodegeneration with brain iron accumulation.
63. Fu, D., & Richardson, D. R. (2007). Iron chelation and regulation of the cell cycle: 2 mechanisms of posttranscriptional regulation of the universal cyclin-dependent kinase inhibitor p21CIP1/WAF1 by iron depletion. *Blood*, *110*(2), 752-761.
64. Fukuchi, K., Tomoyasu, S., Watanabe, H., Tsuruoka, N., & Gomi, K. (1997). G1 accumulation caused by iron deprivation with deferoxamine does not

accompany change of pRB status in ML-1 cells. *Biochimica et Biophysica Acta (BBA)-Molecular Cell Research*, *1357*(3), 297-305.

65. Galan, P., Thibault, H., Preziosi, P., & Hercberg, S. (1992). Interleukin 2 production in iron-deficient children. *Biological trace element research*, *32*(1-3), 421-426.
66. Galy, B., Ferring, D., and Hentze, M. W. (2005) *Genesis* 43, 181–188
67. Gambling, L., Danzeisen, R., Gair, S., Lea, R., Charania, Z., Solanky, N. & Mcardle, H. (2001). Effect of iron deficiency on placental transfer of iron and expression of iron transport proteins in vivo and in vitro. *Journal of Biochemistry 356*, 883-889.
68. Gao, J., & Richardson, D. R. (2001). The potential of iron chelators of the pyridoxal isonicotinoyl hydrazone class as effective antiproliferative agents, IV: the mechanisms involved in inhibiting cell-cycle progression. *Blood*, *98*(3), 842-850.
69. Gao, J., & Richardson, D. R. (2001). The potential of iron chelators of the pyridoxal isonicotinoyl hydrazone class as effective antiproliferative agents, IV: the mechanisms involved in inhibiting cell-cycle progression. *Blood*, *98*(3), 842-850.
70. Garcia, V., García, J. M., Pena, C., Silva, J., Domínguez, G., Rodríguez, R., & Bonilla, F. (2005). The GADD45, ZBRK1 and BRCA1 pathway: quantitative analysis of mRNA expression in colon carcinomas. *The Journal of pathology*, *206*(1), 92-99.
71. Gartel, A. L., & Tyner, A. L. (1999). Transcriptional regulation of the p21 (WAF1/CIP1) gene. *Experimental cell research*, *246*(2), 280-289.
72. Gasche, C., Lomer, M. C. E., Cavill, I., & Weiss, G. (2004). Iron, anaemia, and inflammatory bowel diseases. *Gut*, *53*(8), 1190-1197.
73. Gdaniec, Z., Sierzputowska-Gracz, H., & Theil, E. C. (1998). Iron regulatory element and internal loop/bulge structure for ferritin mRNA studied by cobalt (III) hexammine binding, molecular modeling, and NMR spectroscopy. *Biochemistry*, *37*(6), 1505-1512
74. Gerlach, M., Ben-Shachar, D., Riederer, P., & Youdim, M. B. H. (1994). Altered brain metabolism of iron as a cause of neurodegenerative diseases?. *Journal of neurochemistry*, *63*(3), 793-807.

75. Gharagozloo, M., Khoshdel, Z., & Amirghofran, Z. (2008). The effect of an iron (III) chelator, silybin, on the proliferation and cell cycle of Jurkat cells: a comparison with desferrioxamine. *European journal of pharmacology*, *589*(1), 1-7.
76. Gkouvatsos, K., Papanikolaou, G., & Pantopoulos, K. (2012). Regulation of iron transport and the role of transferrin. *Biochimica et Biophysica Acta (BBA)-General Subjects*, *1820*(3), 188-202.
77. Golding, S. and Young, S. P. (1995), Iron Requirements of Human Lymphocytes: Relative Contributions of Intra- and Extra-Cellular Iron. *Scandinavian Journal of Immunology*, 41: 229–236
78. Golias, C. H., Charalabopoulos, A., & Charalabopoulos, K. (2004). Cell proliferation and cell cycle control: a mini review. *International journal of clinical practice*, *58*(12), 1134-1141.
79. Gordeuk, V., Mukiibi, J., Hasstedt, S. J., Samowitz, W., Edwards, C. Q., West, G., ... & Brittenham, G. (1992). Iron overload in Africa. *New England Journal of Medicine*, *326*(2), 95-100.
80. Gordeuk, V., Thuma, P., Brittenham, G., McLaren, C., Parry, D., Backenstose, A., & Poltera, A. A. (1992). Effect of iron chelation therapy on recovery from deep coma in children with cerebral malaria. *New England Journal of Medicine*, *327*(21), 1473-1477.
81. Gray, N. K., & Hentze, M. W. (1994). Iron regulatory protein prevents binding of the 43S translation pre-initiation complex to ferritin and eALAS mRNAs. *The EMBO journal*, *13*(16), 3882.
82. Gruenheid, S., Canonne-Hergaux, F., Gauthier, S., Hackam, D. J., Grinstein, S., & Gros, P. (1999). The iron transport protein NRAMP2 is an integral membrane glycoprotein that colocalizes with transferrin in recycling endosomes. *The Journal of experimental medicine*, *189*(5), 831-841.
83. Gunshin, H., Fujiwara, Y., Custodio, A. O., DiRenzo, C., Robine, S., & Andrews, N. C. (2005). Slc11a2 is required for intestinal iron absorption and erythropoiesis but dispensable in placenta and liver. *Journal of Clinical Investigation*, *115*(5), 1258.

84. Guo, B., Brown, F. M., Phillips, J. D., Yu, Y., & Leibold, E. A. (1995). Characterization and expression of iron regulatory protein 2 (IRP2). Presence of multiple IRP2 transcripts regulated by intracellular iron levels. *Journal of Biological Chemistry*, *270*(28), 16529-16535.
85. Gusella, G. L., T. Musso, M. C. Bosco, I. Espinoza-Delgado, K. Matsushima, L. Varesio. 1993. IL-2 up-regulates but IFN-γ suppresses IL-8 expression in human monocytes. *Journal of Immunology.* **151**: 272
86. H. Gunshin, B. Mackenzie, U.V. Berger, Y. Gunshin, M.F. Romero, W.F. Boron, S. Nussberger, J.L. Gollan, M.A. Hediger, Cloning and characterization of a mammalian protein-coupled metal-ion transporter, *Nature* 388 (1997) 482–488.
87. Haile, D. J. (1999). Regulation of genes of iron metabolism by the iron-response proteins. *The American journal of the medical sciences*, *318*(4), 230.
88. Harper, J. W., Adami, G. R., Wei, N., Keyomarsi, K., & Elledge, S. J. (1993). The p21 Cdk-interacting protein Cip1 is a potent inhibitor of G1 cyclin-dependent kinases. *Cell*, *75*(4), 805-816.
89. Harris, Z. L., Klomp, L. W., & Gitlin, J. D. (1998). Aceruloplasminemia: an inherited neurodegenerative disease with impairment of iron homeostasis. *The American journal of clinical nutrition*, *67*(5), 972S-977S.
90. Henderson, B. R., Seiser, C., & Kühn, L. C. (1993). Characterization of a second RNA-binding protein in rodents with specificity for iron-responsive elements. *Journal of Biological Chemistry*, *268*(36), 27327-27334.
91. Hentze, M. W., Muckenthaler, M. U., & Andrews, N. C. (2004). Balancing acts: molecular control of mammalian iron metabolism. *Cell*, *117*(3), 285-297.
92. Hentze, M. W., Muckenthaler, M. U., Galy, B., & Camaschella, C. (2010). Two to tango: regulation of Mammalian iron metabolism. *Cell*, *142*(1), 24-38.
93. Hernández-Prieto, M. A., Schön, V., Georg, J., Barreira, L., Varela, J., Hess, W. R., & Futschik, M. E. (2012). Iron deprivation in Synechocystis: inference of pathways, non-coding RNAs, and regulatory elements from

comprehensive expression profiling. *G3: Genes| Genomes| Genetics*, *2*(12), 1475-1495.

94. *Hershko, C. (1996) Iron and infection. Iron Nutr. Health Dis. 22:231-238*
95. Hoefkens, P., De Smit, M. H., De Jeu-Jaspars, N. M., Huijskes-Heins, M. I., De Jong, G., & Van Eijk, H. G. (1996). Isolation, renaturation and partial characterization of recombinant human transferrin and its half molecules from Escherichia coli. *The international journal of biochemistry & cell biology*, *28*(9), 975-982.
96. Hong, H. Y., Choi, J., Cho, Y. W., & Kim, B. C. (2012). Cdc25A promotes cell survival by stimulating NF-κB activity through IκB-α phosphorylation and destabilization. *Biochemical and biophysical research communications*, *420*(2), 293-296.
97. Hoyes, K. P., & Porter, J. B. (1993). Subcellular distribution of desferrioxamine and hydroxypyridin-4-one chelators in K562 cells affects chelation of intracellular iron pools. *British journal of haematology*, *85*(2), 393-400.
98. Hu, Y., Zhu, Q., & Tang, L. (2014). MiR-99a antitumor activity in human breast cancer cells through targeting of mTOR expression. *PloS one*, *9*(3), e92099.
99. Inoue, T., Cavanaugh, P. G., Steck, P. A., Brünner, N., & Nicolson, G. L. (1993). Differences in transferrin response and numbers of transferrin receptors in rat and human mammary carcinoma lines of different metastatic potentials. *Journal of cellular physiology*, *156*(1), 212-217.
100. Jason, J., Archibald, L. K., Nwanyanwu, O. C., Bell, M., Jensen, R. J., Gunter, E. & Jarvis, W. R. (2001). The effects of iron deficiency on lymphocyte cytokine production and activation: preservation of hepatic iron but not at all cost. *Clinical & Experimental Immunology*, *126*(3), 466-473.
101. Jelkmann, W. (1998). Pro-inflammatory cytokines lowering erythropoietin production. *Journal of interferon & cytokine research*, *18*(8), 555-559.
102. Jenner, P. (2003). Oxidative stress in Parkinson's disease. *Annals of neurology*, *53*(S3), S26-S38.

103. Jong, A. Y., Yu, K., Zhou, B., Frgala, T., Reynolds, C. P., & Yen, Y. (1998). A simple and sensitive ribonucleotide reductase assay. *Journal of biomedical science*, *5*(1), 62-68.

104. Jordon, A. & Reichard, P. *(*1998*)* Ribonucleotide reductases. *Annual Review of Biochemistry,* 67*,* 71–98.

105. Kaiser, B. K., Zimmerman, Z. A., Charbonneau, H., & Jackson, P. K. (2002). Disruption of centrosome structure, chromosome segregation, and cytokinesis by misexpression of human Cdc14A phosphatase. *Molecular biology of the cell*, *13*(7), 2289-2300.

106. Kalinowski, D. S., & Richardson, D. R. (2005). The evolution of iron chelators for the treatment of iron overload disease and cancer. *Pharmacological reviews*, *57*(4), 547-583.

107. Kalluri, R., Cantley, L. G., Kerjaschki, D., & Neilson, E. G. (2000). Reactive oxygen species expose cryptic epitopes associated with autoimmune Goodpasture syndrome. *Journal of Biological Chemistry*, *275*(26), 20027-20032.

108. Kalpatthi, R., Peters, B., Kane, I., Holloman, D., Rackoff, E., Disco, D. & Abboud, M. R. (2010). Safety and efficacy of high dose intravenous desferrioxamine for reduction of iron overload in sickle cell disease. *Pediatric blood & cancer*, *55*(7), 1338-1342.

109. Kawabata, H., Yang, R., Hirama, T., Vuong, P. T., Kawano, S., Gombart, A. F., & Koeffler, H. P. (1999). Molecular cloning of transferrin receptor 2 A new member of the transferrin receptor-like family. *Journal of Biological Chemistry*, *274*(30), 20826-20832.

110. Kayyali, R., Porter, J. B., Davies, N. A., Nugent, J. H., Cooper, C. E., & Hider, R. C. (2001). Structure-function investigation of the interaction of 1-and 2-substituted 3-hydroxypyridin-4-ones with 5-lipoxygenase and ribonucleotide reductase. *Journal of Biological Chemistry*, *276*(52), 48814-48822.

111. Ke Y., Wu J., Leibold E. A., Walden W. E., Theil E. C. *(1998) Loops and bulge/ loops in IRE isoforms influence IRP binding. Journal of Biological Chemistry 273:23637–23640*

112. Kearsey, J. M., Coates, P. J., Prescott, A. R., Warbrick, E., & Hall, P. A. (1995). Gadd45 is a nuclear cell cycle regulated protein which interacts with p21Cip1. *Oncogene*, *11*(9), 1675-1683.

113. Keberle, H. (1964) The biochemistry of desferrioxamine and its relation to iron metabolism. *Annals of New York Academy of Science* 119:758-768

114. Kerenyi, M. A., Grebien, F., Gehart, H., Schifrer, M., Artaker, M., Kovacic, B. & Müllner, E. W. (2008). Stat5 regulates cellular iron uptake of erythroid cells via IRP-2 and TfR-1. *Blood*, *112*(9), 3878-3888.

115. Kim, H. P., Kelly, J., & Leonard, W. J. (2001). The basis for IL-2-induced IL-2 receptor α chain gene regulation: importance of two widely separated IL-2 response elements. *Immunity*, *15*(1), 159-172.

116. Kim, H. Y., Klausner, R. D., & Rouault, T. A. (1995). Translational repressor activity is equivalent and is quantitatively predicted by in vitro RNA binding for two iron-responsive element-binding proteins, IRP1 and IRP2. *Journal of Biological Chemistry*, *270*(10), 4983-4986.

117. Kitaura, H., Shinshi, M., Uchikoshi, Y., Ono, T., Tsurimoto, T., Yoshikawa, H., ... & Ariga, H. (2000). Reciprocal regulation via protein-protein interaction between c-Myc and p21 cip1/waf1/sdi1 in DNA replication and transcription. *Journal of Biological Chemistry*, *275*(14), 10477-10483.

118. Kolberg, M., Strand, K. R., Graff, P., & Andersson, K. K. (2004). Structure, function, and mechanism of ribonucleotide reductases. *Biochimica et Biophysica Acta (BBA)-Proteins and Proteomics*, *1699*(1), 1-34.

119. Kontoghiorghes, G. J., Pattichi, K., Hadjigavriel, M., & Kolnagou, A. (2000). Transfusional iron overload and chelation therapy with deferoxamine and deferiprone (L1). *Transfusion science*, *23*(3), 211-223.

120. Kontoghiorghes, G. J., Eracleous, E., Economides, C., & Kolnagou, A. (2005). Advances in iron overload therapies. Prospects for effective use of deferiprone (L1), deferoxamine, the new experimental chelators ICL670, GT56-252, L1NAll and their combinations. *Current medicinal chemistry*, *12*(23), 2663-2681.

121. Koskenkorva-Frank, T. S., Weiss, G., Koppenol, W. H., & Burckhardt, S. (2013). The complex interplay of iron metabolism, reactive oxygen species, and reactive nitrogen species: insights into the potential of various iron therapies to induce oxidative and nitrosative stress. *Free Radical Biology and Medicine*, *65*, 1174-1194.

122. Kraft, C., Herzog, F., Gieffers, C., Mechtler, K., Hagting, A., Pines, J., & Peters, J. M. (2003). Mitotic regulation of the human anaphase-promoting complex by phosphorylation. *The EMBO journal*, *22*(24), 6598-6609.

123. Kremer, J. M., Bloom, B. J., Breedveld, F. C., Coombs, J. H., Fletcher, M. P., Gruben, D., ... & Zwillich, S. H. (2009). The safety and efficacy of a JAK inhibitor in patients with active rheumatoid arthritis: Results of a double-blind, placebo-controlled phase IIa trial of three dosage levels of CP-690,550 versus placebo. *Arthritis & Rheumatism*, *60*(7), 1895-1905.

124. Krude, T. (2006). Initiation of chromosomal DNA replication in mammalian cell-free systems. *Cell Cycle*, *5*(18), 2115-2122.

125. Kühn, L. C. (2015). Iron regulatory proteins and their role in controlling iron metabolism. *Metallomics*, *7*(2), 232-243.

126. Kühn, L. C., Hallberg, L., & Asp, N. G. (1996). Control of cellular iron transport and storage at the molecular level. In *Proceedings of the Swedish Nutrition Foundation's 20th International Symposium and the Swedish Society of Medicine Berzelius Symposium XXXI, 24-27 August, 1995, Stockholm, Sweden.* (pp. 17-29). John Libbey and Co. Ltd..

127. Kulp, K. S., & Vulliet, P. R. (1996). Mimosine blocks cell cycle progression by chelating iron in asynchronous human breast cancer cells. *Toxicology and applied pharmacology*, *139*(2), 356-364.

128. Kumagai, N. A. O. K. I., Benedict, S. H., Mills, G. B., & Gelfand, E. W. (1988). Comparison of phorbol ester/calcium ionophore and phytohemagglutinin-induced signaling in human T lymphocytes. Demonstration of interleukin 2-independent transferrin receptor gene expression. *The Journal of Immunology*, *140*(1), 37-43.

129. Kuo, T. C., Chang, P. Y., Huang, S. F., Chou, C. K., & Chao, C. C. K. (2012). Knockdown of HURP inhibits the proliferation of hepacellular carcinoma cells via downregulation of gankyrin and accumulation of p53. *Biochemical pharmacology*, *83*(6), 758-768.

130. Kuvibidila, S. R., & Porretta, C. (2003). Iron deficiency and in vitro iron chelation reduce the expression of cluster of differentiation molecule (CD) 28 but not CD3 receptors on murine thymocytes and spleen cells. *British Journal of Nutrition*, *90*(01), 179-189.

131. Kuvibidila, S. R., Kitchens, D. & Baliga, B. S. (1999) In vivo and in vitro iron deficiency reduces protein kinase C activity and translocation in murine splenic and purified T cells. *Journal of Cellular Biochemistry 74:468-478*

132. Kuvibidila, S. R., Porretta, C., Baliga, B. S., & Leiva, L. E. (2001). Reduced thymocyte proliferation but not increased apoptosis as a possible cause of thymus atrophy in iron-deficient mice. *British Journal of Nutrition*, *86*(02), 157-162.

133. Kuvibidila, S., Dardenne, M., Savino, W., & Lepault, F. (1990). Influence of iron-deficiency anemia on selected thymus functions in mice: thymulin biological activity, T-cell subsets, and thymocyte proliferation. *The American journal of clinical nutrition*, *51*(2), 228-232.

134. Kuvibidila, S., Nauss, K. M., Baliga, B. S., & Suskind, R. M. (1983). Impairment of blastogenic response of splenic lymphocytes from iron-deficient mice: in vivo repletion. *The American journal of clinical nutrition*, *37*(1), 15-25.

135. LaBaer, J., Garrett, M. D., Stevenson, L. F., Slingerland, J. M., Sandhu, C., Chou, H. S. & Harlow, E. D. (1997). New functional activities for the p21 family of CDK inhibitors. *Genes & development*, *11*(7), 847-862.

136. Lai, E. C (200). Micro RNAs are complementary to 3 UTR sequence motifs that mediate negative post-transcriptional regulation. *Nature Genetics* 30, 363–364

137. Larsson, A., & Sjöberg, B. M. (1986). Identification of the stable free radical tyrosine residue in ribonucleotide reductase. *The EMBO journal*, *5*(8), 2037.

138. Lašťovička, J., Budinský, V., Špíšek, R., & Bartůňková, J. (2009). Assessment of lymphocyte proliferation: CFSE kills dividing cells and modulates expression of activation markers. *Cellular immunology*, *256*(1), 79-85.

139. LaVaute, T., Smith, S., Cooperman, S., Iwai, K., Land, W., Meyron-Holtz, E., Drake, S. K., Miller, G., Abu-Asab, M., Tsokos, M., Switzer, R., 3rd, Grinberg, A., Love, P., Tresser, N., and Rouault, T. A. (2001) *Nature Genetics* 27, 209–214

140. Le, N. T., & Richardson, D. R. (2002). The role of iron in cell cycle progression and the proliferation of neoplastic cells. *Biochimica et Biophysica Acta (BBA)-Reviews on Cancer*, *1603*(1), 31-46.

141. Lee, P., Peng, H., Gelbart, T., & Beutler, E. (2004). The IL-6-and lipopolysaccharide-induced transcription of hepcidin in HFE-, transferrin receptor 2-, and β2-microglobulin-deficient hepatocytes. *Proceedings of the National Academy of Sciences of the United States of America*, *101*(25), 9263-9265.

142. Lee, S. K., Jang, H. J., Lee, H. J., Lee, J., Jeon, B. H., Jun, C. D., ... & Kim, E. C. (2006). p38 and ERK MAP kinase mediates iron chelator-induced apoptosis and-suppressed differentiation of immortalized and malignant human oral keratinocytes. *Life sciences*, *79*(15), 1419-1427.

143. Leiter, L. M., Reuhl, K. R., Racis Jr, S. P., & Sherman, A. R. (1995). Iron status alters murine systemic lupus erythematosus. *The Journal of nutrition*, *125*(3), 474-484.

144. Lewis, T. S., Shapiro, P. S., & Ahn, N. G. (1998). Signal transduction through MAP kinase cascades. *Advances in cancer research*, *74*, 49-139.

145. Liang, S. X., & Richardson, D. R. (2003). The effect of potent iron chelators on the regulation of p53: examination of the expression, localization and DNA-binding activity of p53 and the transactivation of WAF1. *Carcinogenesis*, *24*(10), 1601-1614.

146. Lieu, P. T., Heiskala, M., Peterson, P. A., & Yang, Y. (2001). The roles of iron in health and disease. *Molecular aspects of medicine*, *22*(1), 1-87.

147. Lin, J. X., & Leonard, W. J. (2000). The role of Stat5a and Stat5b in signaling by IL-2 family cytokines. *Oncogene*, *19*(21), 2566-2576.

148. Liu, Y., Yang, T., Li, H., Li, M. H., Liu, J., Wang, Y. T., ... & Zou, Q. (2013). BD750, a benzothiazole derivative, inhibits T cell proliferation by affecting the JAK3/STAT5 signalling pathway. *British journal of pharmacology*, *168*(3), 632-643.

149. Liu, Z. D., & Hider, R. C. (2002). Design of iron chelators with therapeutic application. *Coordination chemistry reviews*, *232*(1), 151-171.

150. Liuzzi, J. P., Aydemir, F., Nam, H., Knutson, M. D., & Cousins, R. J. (2006). Zip14 (Slc39a14) mediates non-transferrin-bound iron uptake into cells. *Proceedings of the National Academy of Sciences*, *103*(37), 13612-13617.

151. Ludwiczek, S., Aigner, E., Theurl, I., & Weiss, G. (2003). Cytokine-mediated regulation of iron transport in human monocytic cells. *Blood*, *101*(10), 4148-4154.

152. Luo, Y., Hurwitz, J., & Massagué, J. (1995). Cell-cycle inhibition by independent CDK and PCNA binding domains in p21/Cip1. *Nature* **375**, 159 - 161

153. Ma, Y., de Groot, H., Liu, Z., Hider, R., & Petrat, F. (2006). Chelation and determination of labile iron in primary hepatocytes by pyridinone fluorescent probes. *Journal of Biochemistry*, *395*, 49-55.

154. Ma, Y., Liu, Z., Hider, R. C., & Petrat, F. (2007). Determination of the labile iron pool of human lymphocytes using the fluorescent probe, CP655. *Analytical chemistry insights*, *2*, 61.

155. Ma, Y., Luo, W., Quinn, P. J., Liu, Z., & Hider, R. C. (2004). Design, synthesis, physicochemical properties, and evaluation of novel iron chelators with fluorescent sensors. *Journal of medicinal chemistry*, *47*(25), 6349-6362.

156. Maciejewski, J. P., Selleri, C., Sato, T., Cho, H. J., Keefer, L. K., Nathan, C. F., & Young, N. S. (1995). Nitric oxide suppression of human hematopoiesis in vitro. Contribution to inhibitory action of interferon-gamma and tumor necrosis factor-alpha. *Journal of Clinical Investigation*, *96*(2), 1085.

157. MacNeill, S. (2010). Structure and function of the GINS complex, a key component of the eukaryotic replisome. *Journal of Biochemistry*, *425*, 489-500.

158. Malumbres, M., & Barbacid, M. (2005). Mammalian cyclin-dependent kinases. *Trends in biochemical sciences*, *30*(11), 630-641.

159. Maurer, H. R. (1981). Potential pitfalls of [3H] thymidine techniques to measure cell proliferation. *Cell Proliferation*, *14*(2), 111-120.

160. May, B.K., Dogra, S.C., Sadlon, T.J., Bhasker, C.R., Cox T.C. & Bottomley S.C. (1995). Molecular regulation of heme biosynthesis in higher vertebrates. *Progress in Nucleic Acid Research and Molecular Biology.* 51, 1-51.

161. McCord, J. M. (1998, January). Iron, free radicals, and oxidative injury. In *Seminars in hematology* (Vol. 35, No. 1, pp. 5-12).

162. McKie, A. T., Marciani, P., Rolfs, A., Brennan, K., Wehr, K., Barrow, D., ... & Simpson, R. J. (2000). A novel duodenal iron-regulated transporter, IREG1, implicated in the basolateral transfer of iron to the circulation. *Molecular cell*, *5*(2), 299-309.

163. Mills, M., & Payne, S. M. (1995). Genetics and regulation of heme iron transport in Shigella dysenteriae and detection of an analogous system in Escherichia coli O157: H7. *Journal of bacteriology*, *177*(11), 3004-3009.

164. Mirnics, K. (2001). Microarrays in brain research: the good, the bad and the ugly. *Nature Reviews Neuroscience*, *2*(6), 444-447.

165. Mollbrink, A., Holmström, P., Sjöström, M., Hultcrantz, R., Eriksson, L. C., & Stål, P. (2012). Iron-regulatory gene expression during liver regeneration. *Scandinavian journal of gastroenterology*, *47*(5), 591-600.

166. Moon, J. H., Jeong, J. K., & Park, S. Y. (2015). Deferoxamine inhibits TRAIL-mediated apoptosis via regulation of autophagy in human colon cancer cells. *Oncology reports*, *33*(3), 1171-1176.

167. Moon, J. J., & Nelson, B. H. (2001). Phosphatidylinositol 3-kinase potentiates, but does not trigger, T cell proliferation mediated by the IL-2 receptor. *The Journal of Immunology*, *167*(5), 2714-2723.

168. Moon, J. J., Rubio, E. D., Martino, A., Krumm, A., & Nelson, B. H. (2004). A permissive role for phosphatidylinositol 3-kinase in the Stat5-

mediated expression of cyclinD2 by the interleukin-2 receptor. *Journal of Biological Chemistry*, *279*(7), 5520-5527.

169. Moos T., Trinder D. *and* Morgan E. H. *(*2000*)* Cellular distribution of ferric iron, ferritin, transferrin and divalent metal transporter (DMT1) in substantia nigra and basal ganglia of normal and β2-microglobulin deficient mouse brain. *Cellular and Molecular Biology.* 46, 549–561

170. Moos, T., & Morgan, E. H. (2000). Transferrin and transferrin receptor function in brain barrier systems. *Cellular and molecular neurobiology*, *20*(1), 77-95.

171. Muckenthaler, M., Gray, N. K., & Hentze, M. W. (1998). IRP-1 binding to ferritin mRNA prevents the recruitment of the small ribosomal subunit by the cap-binding complex eIF4F. *Molecular cell*, *2*(3), 383-388.

172. Muirden, K. D., & Peace, G. (1969). Light and electron microscope studies in carragheenin, adjuvant, and tuberculin-induced arthris. *Annals of the rheumatic diseases*, *28*(4), 392-401.

173. Müller, H., & Helin, K. (2000). The E2F transcription factors: key regulators of cell proliferation. *Biochimica et Biophysica Acta (BBA)-Reviews on Cancer*, *1470*(1), M1-M12.

174. Mullick, S., Rusia, U., Sikka, M., & Faridi, M. A. (2006). Impact of iron deficiency anaemia on T lymphocytes & their subsets in children. *Indian Journal of Medical Research*, *124*(6), 647.

175. Muñoz, M., García-Erce, J. A., & Remacha, Á. F. (2011). Disorders of iron metabolism. Part 1: molecular basis of iron homoeostasis. *Journal of clinical pathology*, *64*(4), 281-286.

176. Muñoz, M., Villar, I., & García-Erce, J. A. (2009). An update on iron physiology. *World journal of gastroenterology: WJG*, *15*(37), 4617.

177. Murtaza, A., Kuchroo, V. K., & Freeman, G. J. (1999). Changes in the strength of co-stimulation through the B7/CD28 pathway alter functional T cell responses to altered peptide ligands. *International immunology*, *11*(3), 407-416.

178. Musso, T., Espinoza-Delgado, I. G. O. R., Pulkki, K. A. R. I., Gusella, G. L., Longo, D. L., & Varesio, L. (1992). IL-2 induces IL-6

production in human monocytes. *The Journal of Immunology*, *148*(3), 795-800.

179. Nadiminty, N., Tummala, R., Lou, W., Zhu, Y., Shi, X. B., Zou, J. X. & Gao, A. C. (2012). MicroRNA let-7c is downregulated in prostate cancer and suppresses prostate cancer growth. *PLoS One*, *7*(3), e32832.

180. Nairz, M., Haschka, D., Demetz, E., & Weiss, G. (2014). Iron at the interface of immunity and infection. *Frontiers in pharmacology*, *5*.

181. Naito, K., Skog, S., Tribukait, B., Andersson, L., & Hisazumi, H. (1987). Cell cycle related [3H] thymidine uptake and its significance for the incorporation into DNA. *Cell Proliferation*, *20*(4), 447-457.

182. Nakamura, Y., Nishimura, T., Tokuda, Y., Kobayashi, N., Watanabe, K., Noto, T. & Habu, S. (1991). Macrophage–T cell interaction is essential for the induction of p75 interleukin 2 (IL–2) receptor and IL–2 responsiveness in human CD4+ T cells. *Cancer Science*, *82*(3), 257-261.

183. Neckers, L. M., & Cossman, J. (1984). Transferrin receptor induction in mitogen-stimulated human T lymphocytes is required for DNA synthesis and cell division and is regulated by interleukin-2 (TCGF). In *Thymic Hormones and Lymphokines* (pp. 383-394). Springer US.

184. Nemeth, E., Preza, G. C., Jung, C. L., Kaplan, J., Waring, A. J., & Ganz, T. (2006). The N-terminus of hepcidin is essential for its interaction with ferroportin: structure-function study. *Blood*, *107*(1), 328-333.

185. Nemeth, E., Valore, E. V., Territo, M., Schiller, G., Lichtenstein, A., & Ganz, T. (2003). Hepcidin, a putative mediator of anemia of inflammation, is a type II acute-phase protein. *Blood*, *101*(7), 2461-2463.

186. Nicholson, L. B., Murtaza, A., Hafler, B. P., Sette, A., & Kuchroo, V. K. (1997). AT cell receptor antagonist peptide induces T cells that mediate bystander suppression and prevent autoimmune encephalomyelitis induced with multiple myelin antigens. *Proceedings of the National Academy of Sciences*, *94*(17), 9279-9284.

187. Nicolas, G., Bennoun, M., Devaux, I., Beaumont, C., Grandchamp, B., Kahn, A., & Vaulont, S. (2001). Lack of hepcidin gene expression and severe tissue iron overload in upstream stimulatory factor 2 (USF2) knockout mice. *Proceedings of the National Academy of Sciences*, *98*(15), 8780-8785.

188. Nyholm, S., Mann, G. J., Johansson, A. G., Bergeron, R. J., Gräslund, A., & Thelander, L. (1993). Role of ribonucleotide reductase in inhibition of mammalian cell growth by potent iron chelators. *Journal of Biological Chemistry*, *268*(35), 26200-26205.

189. Oexle,H.,Kaser,A.,Most,J.,Bellmann-Weiler,R.,Werner,E.R.,Werner-Felmayer, G., etal.(2003).Pathways for the regulation of interferon-gamma-inducible genes by iron in human monocytic cells. *Journal of Leukocyte Biology* 74, 287–294.doi: 10.1189/jlb.0802420

190. Olakanmi, O., Schlesinger, L.S., Ahmed, A., *and* Britigan, B.E. *(*2002*)* Intraphagosomal *Mycobacterium tuberculosis* acquires iron from both extracellular transferrin and intracellular iron pools. Impact of interferon-gamma and hemochromatosis. *Journal of Biological Chemistry* 277*:* 49727–49734.

191. Oudit, G. Y., Sun, H., Trivieri, M. G., Koch, S. E., Dawood, F., Ackerley, C. & Backx, P. H. (2003). L-type Ca2+ channels provide a major pathway for iron entry into cardiomyocytes in iron-overload cardiomyopathy. *Nature medicine*, *9*(9), 1187-1194.

192. Pan, Y. J., Hopkins, R. G., & Loo, G. (2004). Increased GADD153 gene expression during iron chelation-induced apoptosis in Jurkat T-lymphocytes. *Biochimica et Biophysica Acta (BBA)-Molecular Cell Research*, *1691*(1), 41-50.

193. Pantopoulos, K. O. S. T. A. S., Gray, N. K., & Hentze, M. W. (1995). Differential regulation of two related RNA-binding proteins, iron regulatory protein (IRP) and IRPB. *Rna*, *1*(2), 155.

194. Parmley, R. T., Barton, J. C., Conrad, M. E., Austin, R. L., & Holland, R. M. (1981). Ultrastructural cytochemistry and radioautography of hemoglobin—iron absorption. *Experimental and molecular pathology*, *34*(2), 131-144.

195. Patel, A. M., Lupash, D., Chew, D., Levesque, M. C., & Moreland, L. W. (2011). JAK inhibition in rheumatoid arthritis. *Current rheumatology reports*,*13*(5), 379-380.

196. Petrakis, T. G., Vougas, K., & Gorgoulis, V. G. (2012). Cdc6: a multi-functional molecular switch with critical role in carcinogenesis. *Transcription*, *3*(3), 124-129.

197. Pietrangelo, A., Caleffi, A., & Corradini, E. (2011, August). Non-HFE hepatic iron overload. In *Seminars in liver disease* (Vol. 31, No. 3, pp. 302-318).

198. Pietrangelo, A., Casalgrandi, G., Quaglino, D., Gualdi, R., Conte, D., Milani, S., & Cairo, G. (1995). Duodenal ferritin synthesis in genetic hemochromatosis. *Gastroenterology*, *108*(1), 208-217.

199. Pigeon, C., Ilyin, G., Courselaud, B., Leroyer, P., Turlin, B., Brissot, P., & Loréal, O. (2001). A new mouse liver-specific gene, encoding a protein homologous to human antimicrobial peptide hepcidin, is overexpressed during iron overload. *Journal of biological chemistry*, *276*(11), 7811-7819.

200. Pines, J. (2011). Cubism and the cell cycle: the many faces of the APC/C. *Nature Reviews Molecular Cell Biology*, *12*(7), 427-438.

201. Poggiali, E., Cassinerio, E., Zanaboni, L., & Cappellini, M. D. (2012). An update on iron chelation therapy. *Blood Transfusion*, *10*(4), 411.

202. Ponka, P. (1999). Cellular iron metabolism. *Kidney International*, *55*, S2-S11.

203. Ponka, P., & Lok, C. N. (1999). The transferrin receptor: role in health and disease. *The international journal of biochemistry & cell biology*, *31*(10), 1111-1137.

204. Ponka, P., Beaumont, C., & Richardson, D. R. (1998, January). Function and regulation of transferrin and ferritin. In *Seminars in hematology* (Vol. 35, No. 1, pp. 35-54).

205. Qu, F., Cui, X., Hong, Y., Wang, J., Li, Y., Chen, L. & Wang, Q. (2013). MicroRNA-185 suppresses proliferation, invasion, migration, and tumorigenicity of human prostate cancer cells through targeting androgen receptor. *Molecular and cellular biochemistry*, *377*(1-2), 121-130.

206. Reed, S. I. (1996). Control of the G1/S transition. *Cancer surveys*, *29*, 7-23.

207. Renton, F. J., & Jeitner, T. M. (1996). Cell cycle-dependent inhibition of the proliferation of human neural tumor cell lines by iron chelators. *Biochemical pharmacology*, *51*(11), 1553-1561.

208. Richardson, D. R. (1999). The therapeutic potential of iron chelators. *Expert opinion on investigational drugs*, *8*(12), 2141-2158.

209. Richardson, D. R., & Ponka, P. (1997). The molecular mechanisms of the metabolism and transport of iron in normal and neoplastic cells. *Biochimica Et Biophysica Acta (BBA)-Reviews on Biomembranes*, *1331*(1), 1-40.

210. Ringnér, M. (2008). What is principal component analysis?. *Nature biotechnology*, *26*(3), 303-304.

211. Rouault, T., & Klausner, R. (1996). Regulation of iron metabolism in eukaryotes. *Current topics in cellular regulation*, *35*, 1-19.

212. Ruas, M., & Peters, G. (1998). The p16 INK4a/CDKN2A tumor suppressor and its relatives. *Biochimica et Biophysica Acta (BBA)-Reviews on Cancer*, *1378*(2), F115-F177.

213. Saletta, F., Rahmanto, Y. S., Noulsri, E., & Richardson, D. R. (2010). Iron chelator-mediated alterations in gene expression: identification of novel iron-regulated molecules that are molecular targets of hypoxia-inducible factor-1α and p53. *Molecular pharmacology*, *77*(3), 443-458.

214. Saletta, F., Rahmanto, Y. S., Siafakas, A. R., & Richardson, D. R. (2011). Cellular iron depletion and the mechanisms involved in the iron-dependent regulation of the growth arrest and DNA damage family of genes. *Journal of Biological Chemistry*, *286*(41), 35396-35406.

215. Samaniego, F., Chin, J., Iwai, K., Rouault, T. A., & Klausner, R. D. (1994). Molecular characterization of a second iron-responsive element binding protein, iron regulatory protein 2. Structure, function, and post-translational regulation. *Journal of Biological Chemistry*, *269*(49), 30904-30910.

216. Sanchez, M., Galy, B., Dandekar, T., Bengert, P., Vainshtein, Y., Stolte, J., & Hentze, M. W. (2006). Iron Regulation and the Cell Cycle identification of an iron-responsive element in the 3′-untranslated region of

human cell division cycle 14a mRNA by a refined microarray-based screening strategy. *Journal of Biological Chemistry*, *281*(32), 22865-22874.

217. Sappey, C., BOELAERT, J. R., Legrand-Poels, S., Forceille, C., Favier, A., & Piette, J. (1995). Iron Chelation Decreases NF-k B and HIV Type 1 Activation due to Oxidative Stress. *AIDS research and human retroviruses*, *11*(9), 1049-1061.

218. Savino, W. (2002). The thymus gland is a target in malnutrition. *European journal of clinical nutrition*, *56*, S46-9.

219. Seligman, P. A., Moran, P. L., Schleicher, R. B., & David Crawford, E. (1992). Treatment with gallium nitrate: evidence for interference with iron metabolism in vivo. *American journal of hematology*, *41*(4), 232-240.

220. Shao, J., Liu, X., Zhu, L., & Yen, Y. (2013). Targeting ribonucleotide reductase for cancer therapy. *Expert opinion on therapeutic targets*, *17*(12), 1423-1437.

221. Shapiro, H. M. (1988). Parameters and probes. *Practical flow cytometry*, 273-410.

222. Sherman, A. R., & Spear, A. T. (1993). Iron and immunity. In *Nutrition and immunology* (pp. 285-307). Springer US.

223. Sherr, C. J. (2000). Cell cycle control and cancer. *Harvey lectures*, *96*, 73.

224. Sherr, C. J., & Roberts, J. M. (1999). CDK inhibitors: positive and negative regulators of G1-phase progression. *Genes & development*, *13*(12), 1501-1512.

225. Sheth S. (2014) Iron chelation: an update. *Current Opinion in Hematology* 21:179–185.

226. Siddique, A., & Kowdley, K. V. (2012). Review article: the iron overload syndromes. *Alimentary pharmacology & therapeutics*, *35*(8), 876-893.

227. Simonart, T., Degraef, C., Andrei, G., Mosselmans, R., Hermans, P., Van Vooren, J. P. & Heenen, M. (2000). Iron chelators inhibit the growth and induce the apoptosis of Kaposi's sarcoma cells and of their putative endothelial precursors. *Journal of investigative dermatology*, *115*(5), 893-900.

228. Siriwardana, G., & Seligman, P. A. (2013). Two cell cycle blocks caused by iron chelation of neuroblastoma cells: separating cell cycle events associated with each block. *Physiological reports*, *1*(7), e00176.

229. Smith, S. R., Ghosh, M. C., Ollivierre-Wilson, H., Hang Tong, W., and Rouault, T. A. (2006) *Blood Cells Molecules and Disease* 36, 283–287

230. Starheim, K. K., Gromyko, D., Velde, R., Varhaug, J. E., & Arnesen, T. (2009, August). Composition and biological significance of the human Nα-terminal acetyltransferases. In *BMC proceedings* (Vol. 3, No. Suppl 6, p. S3). BioMed Central Ltd.

231. Stein, J., Hartmann, F., & Dignass, A. U. (2010). Diagnosis and management of iron deficiency anemia in patients with IBD. *Nature Reviews Gastroenterology and Hepatology*, *7*(11), 599-610.

232. Steinbicker, A. U., & Muckenthaler, M. U. (2013). Out of Balance—Systemic Iron Homeostasis in Iron-Related Disorders. *Nutrients*, *5*(8), 3034-3061.

233. Su, M. A., Trenor III, C. C., Fleming, J. C., Fleming, M. D., & Andrews, N. C. (1998). The G185R mutation disrupts function of the iron transporter Nramp2. *Blood*, *92*(6), 2157-2163.

234. Subramanyam, P., Obermair, G. J., Baumgartner, S., Gebhart, M., Striessnig, J., Kaufmann, W. A. & Flucher, B. E. (2009). Activity and calcium regulate nuclear targeting of the calcium channel beta4b subunit in nerve and muscle cells. *Channels*, *3*(5), 343-355.

235. Suega, K., & Bakta, I. M. (2010). Influence of iron on plasma interleukin-2 and gamma interferon level in iron deficiency anemia. *Acta medica Indonesiana*, *42*(3), 147-151.

236. Sun, J. Y., Huang, Y., Li, J. P., Zhang, X., Wang, L., Meng, Y. L., ... & Zhang, R. (2012). MicroRNA-320a suppresses human colon cancer cell proliferation by directly targeting β-catenin. *Biochemical and biophysical research communications*, *420*(4), 787-792.

237. Suzuki, Y., Nakabayashi, Y., & Takahashi, R. (2001). Ubiquitin-protein ligase activity of X-linked inhibitor of apoptosis protein promotes proteasomal degradation of caspase-3 and enhances its anti-apoptotic effect

in Fas-induced cell death. *Proceedings of the National Academy of Sciences*, *98*(15), 8662-8667.

238. Szüts, D., & Krude, T. (2004). Cell cycle arrest at the initiation step of human chromosomal DNA replication causes DNA damage. *Journal of cell science*, *117*(21), 4897-4908.

239. Tabuchi, M., Yoshimori, T., Yamaguchi, K., Yoshida, T., & Kishi, F. (2000). Human NRAMP2/DMT1, which mediates iron transport across endosomal membranes, is localized to late endosomes and lysosomes in HEp-2 cells. *Journal of Biological Chemistry*, *275*(29), 22220-22228.

240. Tamura, R. E., de Vasconcellos, J. F., Sarkar, D., Libermann, T. A., Fisher, P. B., & Zerbini, L. F. (2012). GADD45 proteins: central players in tumorigenesis. *Current molecular medicine*, *12*(5), 634.

241. Tandy S., Williams M., Leggett A., Lopez-Jimenez M., Dedes M., Ramesh B., Srai S.K., Sharp P.(2000) Nramp2 expression is associated with pH-dependent iron uptake across the apical membrane of human intestinal Caco-2 cells. *Journal of Biological Chemistry 275:1023–1029*

242. Templeton, D. M., & Liu, Y. (2003). Genetic regulation of cell function in response to iron overload or chelation. *Biochimica et Biophysica Acta (BBA)-General Subjects*, *1619*(2), 113-124.

243. Terada, N. A. O. H. I. R. O., Lucas, J. J., & Gelfand, E. W. (1991). Differential regulation of the tumor suppressor molecules, retinoblastoma susceptibility gene product (Rb) and p53, during cell cycle progression of normal human T cells. *The Journal of Immunology*, *147*(2), 698-704.

244. Theil, E. C. (2003). Ferritin: at the crossroads of iron and oxygen metabolism. *The Journal of nutrition*, *133*(5), 1549S-1553S.

245. Theurl, I., Aigner, E., Theurl, M., Nairz, M., Seifert, M., Schroll, A., & Weiss, G. (2009). Regulation of iron homeostasis in anemia of chronic disease and iron deficiency anemia: diagnostic and therapeutic implications. *Blood*, *113*(21), 5277-5286.

246. Thomas, C., & Thomas, L. (2005). Anemia of chronic disease: pathophysiology and laboratory diagnosis. *Laboratory Hematology*, *11*(1), 14-23.

247. Thomson, A. M., Rogers, J. T., & Leedman, P. J. (1999). Iron-regulatory proteins, iron-responsive elements and ferritin mRNA translation. *The international journal of biochemistry & cell biology*, *31*(10), 1139-1152.

248. Vairapandi, M., Balliet, A. G., Hoffman, B., & Liebermann, D. A. (2002). GADD45b and GADD45g are cdc2/cyclinB1 kinase inhibitors with a role in S and G2/M cell cycle checkpoints induced by genotoxic stress. *Journal of cellular physiology*, *192*(3), 327-338.

249. Vidal, A., & Koff, A. (2000). Cell-cycle inhibitors: three families united by a common cause. *Gene*, *247*(1), 1-15.

250. Vyoral, D., & Petrák, J. (2005). Hepcidin: a direct link between iron metabolism and immunity. *The international journal of biochemistry & cell biology*, *37*(9), 1768-1773.

251. Wajapeyee N, Somasundaram K. Cell cycle arrest and apoptosis induction by activator protein 2alpha (AP-2alpha) and the role of p53 and p21WAF1/CIP1 in AP-2alpha-mediated growth inhibition. *Journal of Biological Chemistry* 2003; 278:52093-101.

252. Wajapeyee, N., & Somasundaram, K. (2003). Cell cycle arrest and apoptosis induction by activator protein 2α (AP-2α) and the role of p53 and p21WAF1/CIP1 in AP-2α-mediated growth inhibition. *Journal of Biological Chemistry*, *278*(52), 52093-52101.

253. Walker, J. G., & Smith, M. D. (2005). The Jak-STAT pathway in rheumatoid arthritis. *Journal of rheumatology*, *32*(9), 1650.

254. Walter, G. J., Evans, H. G., Menon, B., Gullick, N. J., Kirkham, B. W., Cope, A. P., & Taams, L. S. (2013). Interaction with activated monocytes enhances cytokine expression and suppressive activity of human CD4+ CD45RO+ CD25+ CD127low regulatory T cells. *Arthritis & Rheumatism*, *65*(3), 627-638.

255. Wang, G., Miskimins, R., & Miskimins, W. K. (2000). Mimosine arrests cells in G1 by enhancing the levels of p27 Kip1. *Experimental cell research*, *254*(1), 64-71.

256. Wang, G., Miskimins, R., & Miskimins, W. K. (2004). Regulation of p27Kip1 by intracellular iron levels. *Biometals*, *17*(1), 15-24.

257. Wang, L., Zhu, G., Yang, D., Li, Q., Li, Y., Xu, X., & Zeng, C. (2008). The spindle function of CDCA4. *Cell motility and the cytoskeleton*, *65*(7), 581-593.

258. Weiss, G., & Goodnough, L. T. (2005). Anemia of chronic disease. *New England Journal of Medicine*, *352*(10), 1011-1023.

259. Weiss, G., & Schett, G. (2013). Anaemia in inflammatory rheumatic diseases. *Nature Reviews Rheumatology*, *9*(4), 205-215.

260. Weiss, R. H. (2003). p21 Waf1/Cip1 as a therapeutic target in breast and other cancers. *Cancer cell*, *4*(6), 425-429.

261. Weiss,G.(2002).Iron and immunity: a double-edged sword. *European Journal of Clinical Investigation* 32(Suppl.1),70–78.

262. Wessling-Resnick, M. (1999). Biochemistry of iron uptake. *Critical reviews in biochemistry and molecular biology*, *34*(5), 285-314.

263. Weston, S. A., & Parish, C. R. (1990). New fluorescent dyes for lymphocyte migration studies: analysis by flow cytometry and fluorescence microscopy. *Journal of immunological methods*, *133*(1), 87-97.

264. Whitley, W. D., Hancock, W. W., Kupiec-Weglinski, J. W., DeSousa, M., & Tilney, N. L. (1993). Iron Chelation Suppresses Mononuclear Cell Activation, Modifies Lymphocyte Migration Patters, And Prolongs Rat Cardiac Allograft Survival In Rats. *Transplantation*, *56*(5), 1182-1187.

265. Wilkinson, M. G., & MILLAR, J. B. (2000). Control of the eukaryotic cell cycle by MAP kinase signaling pathways. *The FASEB Journal*, *14*(14), 2147-2157.

266. Wood, R. J., & Han, O. (1998). Recently identified molecular aspects of intestinal iron absorption. *The Journal of nutrition*, *128*(11), 1841-1844.

267. Xiao, L., Rao, J. N., Zou, T., Liu, L., Cao, S., Martindale, J. L., & Wang, J. Y. (2013). miR-29b represses intestinal mucosal growth by inhibiting translation of cyclin-dependent kinase 2. *Molecular biology of the cell*, *24*(19), 3038-3046.

268. Xiong, Y., Hannon, G. J., Zhang, H., Casso, D., Kobayashi, R., & Beach, D. (1993). p21 is a universal inhibitor of cyclin kinases. *Nature*, *366*(6456), 701-704.

269. Xu, Y., & Pasche, B. (2007). TGF-β signaling alterations and susceptibility to colorectal cancer. *Human molecular genetics*, *16*(R1), R14-R20.

270. Yang, J., Goetz, D., Li, J. Y., Wang, W., Mori, K., Setlik, D., & Barasch, J. (2002). An iron delivery pathway mediated by a lipocalin. *Molecular cell*, *10*(5), 1045-1056.

271. Yoshimura, A., Akita, M., Hosono, Y., Abe, T., Kobayashi, M., Yamamoto, K. I., & Enomoto, T. (2011). Functional relationship between Claspin and Rad17. *Biochemical and biophysical research communications*, *414*(2), 298-303.

272. Yu, J. H., Zhu, B. M., Wickre, M., Riedlinger, G., Chen, W., Hosui, A., & Hennighausen, L. (2010). The transcription factors signal transducer and activator of transcription 5A (STAT5A) and STAT5B negatively regulate cell proliferation through the activation of cyclin-dependent kinase inhibitor 2b (Cdkn2b) and Cdkn1a expression. *Hepatology*, *52*(5), 1808-1818.

273. Yu, Y., & Richardson, D. R. (2011). Cellular iron depletion stimulates the JNK and p38 MAPK signaling transduction pathways, dissociation of ASK1-thioredoxin, and activation of ASK1. *Journal of Biological Chemistry*, *286*(17), 15413-15427.

274. Yu, Y., Kovacevic, Z., & Richardson, D. R. (2007). Tuning cell cycle regulation with an iron key. *Cell cycle*, *6*(16), 1982-1994.

275. Zerbini, L. F., & Libermann, T. A. (2005). Life and Death in Cancer GADD45 α and γ are Critical Regulators of NF-κB Mediated Escape from Programmed Cell Death. *Cell Cycle*, *4*(1), 18-20.

276. Zerbini, L. F., Czibere, A., Wang, Y., Correa, R. G., Otu, H., Joseph, M., ... & Libermann, T. A. (2006). A Novel Pathway Involving Melanoma Differentiation Associated Gene-7/Interleukin-24 Mediates Nonsteroidal Anti-inflammatory Drug–Induced Apoptosis and Growth Arrest of Cancer Cells. *Cancer research*, *66*(24), 11922-11931.

277. Zhang, E. B., Kong, R., Yin, D. D., You, L. H., Sun, M., Han, L., ... & fei Chen, J. (2014). Long noncoding RNA ANRIL indicates a poor

prognosis of gastric cancer and promotes tumor growth by epigenetically silencing of miR-99a/miR-449a. *Oncotarget*, *5*(8), 2276.

278. Zhang, J., & Ma, L. (2012). MicroRNA control of epithelial–mesenchymal transition and metastasis. *Cancer and Metastasis Reviews*, *31*(3-4), 653-662.

279. Zhou, B., Su, L., Hu, S., Hu, W., Yip, M. R., Wu, J. & Yen, Y. (2013). A small-molecule blocking ribonucleotide reductase holoenzyme formation inhibits cancer cell growth and overcomes drug resistance. *Cancer research*, *73*(21), 6484-6493.

280. Zhou, J., & Wang, W. (2011). Analysis of microRNA expression profiling identifies microRNA-503 regulates metastatic function in hepatocellular cancer cell. *Journal of surgical oncology*, *104*(3), 278-283.

281. Zhu, J. K. (2009). Active DNA demethylation mediated by DNA glycosylases. *Annual review of genetics*, *43*, 143.

282. Zorzi, G., Zibordi, F., Chiapparini, L., Bertini, E., Russo, L., Piga, A., Longo, F., Garavaglia, B., Aquino, D., Savoiardo, M., Solari, A. and Nardocci, N. (2011), Iron-related MRI images in patients with pantothenate kinase–associated neurodegeneration (PKAN) treated with deferiprone: Results of a phase II pilot trial. *Movement Disorders*, 26: 1755–1759.

CHAPTER 8

APPENDIX

CHAPTER 8

APPENDIX

8.1 RECIPES AND BUFFERS

Cell Isolation MACS buffer

1xPBS (PAA, Austria) + 2mM EDTA (Lonza) + 0.5% FCS (PAA)

FACS Washing Buffer

1xPBS + 0.1% Sodium Azide (Sigma Aldrich)

FACS Staining Buffer

1xPBS + 0.1% Sodium Azide (Sigma Aldrich) + 2% BSA

10x Running Buffer for Western Blot

35 mM SDS (10.08 g)
250 mM Tris (30.3 g)
1.92 M glycine (144 g)

10x Transfer Buffer for Western Blot

25 mM Tris (3.03 g)
192 mM glycine (14.4g)

In 800 mL final volume of water. Add 200 mL of methanol 100%